

TE
662
.A3
no.
FHWA-
RD-
77-116

Report No. FHWA-RD-77-116

STUDIES ON FLEXIBLE HIGHWAYS OF INCREASED LEGAL VEHICLE WEIGHTS USING VESYS IIM



Dept. of Transportation
DEC 21 1978
Library

January 1978

Final Report

Document is available to the public through
the National Technical Information Service,
Springfield, Virginia 22161

Prepared for
FEDERAL HIGHWAY ADMINISTRATION
Offices of Research & Development
Washington, D. C. 20590

FOREWORD

This report provides results of a detailed study to estimate lifetime costs for flexible pavements as a function of legal axle limits using an improved version of FHWA Computer Program VESYS IIM.

VESYS IIM was modified to include capabilities for: 1) seasonal characterizations of pavement materials, 2) a discretized representation of axle load distribution, and 3) low-temperature cracking predictions.

A combined survey of the literature and laboratory testing program was conducted to define the variations in material permanent deformation parameters as important material characteristics vary seasonally with the environment. The resulting data and other information and experience were applied to arrive at input data that would yield realistic performance predictions.

A factorial of 64 solutions was obtained using the improved version of VESYS IIM and the input data developed to study the effects of truck traffic consistent with four levels of legal axle limits (18, 20, 22, and 24 kips), two levels of traffic, two levels of pavement section thickness and four environmental zones (Wet-Freeze, Dry-Freeze, Wet-No Freeze and Dry-No Freeze). Where failures were predicted, an overlay was applied and a new solution obtained until a pavement life of at least 20 years was attained. The initial and overlay costs were estimated and these costs for 20 years of pavement service were related to the legal axle limits.

Copies of the report, intended primarily for research and development audiences, are being distributed by transmittal memorandum to such individuals.



Charles F. Scheffey
Director, Office of Research
Federal Highway Administration

NOTICE

This document is disseminated under the sponsorship of the Department of Transportation in the interest of information exchange. The United States Government assumes no liability for its contents or use thereof.

The contents of this report reflect the views of Austin Research Engineers, Inc., which is responsible for the facts and the accuracy of the data presented herein. The contents do not necessarily reflect the official views or policy of the Department of Transportation.

This report does not constitute a standard, specification, or regulation.

The United States Government does not endorse products or manufacturers. Trademarks or manufacturers' names appear herein only because they are considered essential to the object of this document.

TE
 210-33662
 RD - FHWA -
 77-116

1. Report No. FHWA-RD-77-116		2. Government Accession No.		3. Recipient's Catalog No.	
4. Title and Subtitle EFFECTS ON FLEXIBLE HIGHWAYS OF INCREASED LEGAL VEHICLE WEIGHTS USING VESYS IIM				5. Report Date January , 1978	
				6. Performing Organization Code	
7. Author(s) J. B. RAUHUT, P. R. JORDAHL				8. Performing Organization Report No.	
9. Performing Organization Name and Address Austin Research Engineers Inc 2600 Dellana Lane Austin, Texas 78746				10. Work Unit No. (TRAIS) FCP 35D3122	
				11. Contract or Grant No. DOT-FH-11-9104	
12. Sponsoring Agency Name and Address U.S. Department of Transportation, Federal Highway Administration Office of Research Washington, D.C. 20590				13. Type of Report and Period Covered Final Report	
				14. Sponsoring Agency Code 50785	
15. Supplementary Notes FHWA Contract Manager: William J. Kenis (HRS-14)					
16. Abstract <p>This report provides results of a detailed study to estimate lifetime costs for flexible pavements as a function of legal axle limits using an improved version of FHWA Computer Program VESYS IIM.</p> <p>VESYS IIM was modified to include capabilities for: 1) seasonal characterizations of pavement materials, 2) a discretized representation of axle load distribution, and 3) low-temperature cracking predictions.</p> <p>A combined survey of the literature and laboratory testing program was conducted to define the variations in material permanent deformation parameters as important material characteristics vary seasonally with the environment. The resulting data and other information and experience were applied to arrive at input data that would yield realistic performance predictions.</p> <p>A factorial of 64 solutions was obtained using the improved version of VESYS IIM and the input data developed to study the effects of truck traffic consistent with four levels of legal axle limits (18, 20, 22 and 24 kips), two levels of traffic, two levels of pavement section thickness and four environmental zones (Wet-Freeze, Dry-Freeze, Wet-No Freeze and Dry-No Freeze). Where failures were predicted, an overlay was applied and a new solution obtained until a pavement life of at least 20 years was attained. The initial and overlay costs were estimated and these costs for 20 years of pavement service were related to the legal axle limits.</p>					
17. Key Words Flexible Pavement Analysis, legal axle limits, lifetime pavement costs, fatigue cracking, low-temperature cracking, rutting, slope variance, Present Serviceability Index, service life.			18. Distribution Statement No restrictions. This document is available to the public through the National Technical Information Service, Springfield, Virginia 22161		
19. Security Classif. (of this report) Unclassified		20. Security Classif. (of this page) Unclassified		21. No. of Pages 215	22. Price

Dept. of Transportation
 DEC 21 1978
 Library

PREFACE

This work was accomplished and this report prepared by a team of engineers and computer programmers including J. Brent Rauhut, Peter Jordahl, Jack C. O'Quin, W. R. Hudson, Thomas W. Kennedy, Phil Smith and Ben Greider.

Appreciation is extended to Ralph C. G. Haas, Professor of Civil Engineering, University of Waterloo; Fred N. Finn, Consultant; Robert Lytton, Texas Transportation Institute; Dale Peterson and Doug Anderson, Utah Department of Transportation; Larry L. Smith and Jatinder Sharma, Florida Department of Transportation; Byron Ruth, Professor of Civil Engineering, University of Florida; Michael I. Darter, Associate Professor of Civil Engineering, University of Illinois; Richard A. Lill, Trucking Associations, Inc.; Roger W. Sackett, Freightliner Corporation; Richard Barksdale, Professor of Civil Engineering, Georgia Institute of Technology; Herbert F. Southgate, Kentucky Bureau of Highways and others for the useful information and ideas that they have provided to the research team.

Support for this research effort was provided by the Federal Highway Administration, Offices of Research and Development, Contract No. DOT-FH-11-9104. We are grateful for the valuable technical coordination provided by Mr. William J. Kenis, FHWA Contract Manager.

J. Brent Rauhut
Peter R. Jordahl

COMMENTS BY FHWA

The improved VESYS structural subsystem generated in this research study, also referred to as VESYS A, was verified with comparisons of predicted and actual distresses in twelve flexible pavement test sections throughout the country. Four of these sections were subjected to an indepth analysis of the effect of increasing axle weights representing the following four different environmental zones:

FREEZE WET	Illinois IH-80, Section 38
FREEZE DRY	Utah IH-80
NO FREEZE WET	Florida I-10
NO FREEZE DRY	Texas IH-20

The lifetimes and costs generated for these environmental zones reflect the behavior of the four specific test sections only. These specific conditions should not be associated with conditions existing in other environmental zones.

The study demonstrates the usefulness of predictive type models for future planning of roadway systems. The criteria for overlay, costs, etc., are based on the best data available. However, additional information is required to provide a more precise estimate of pavement performance.

Research and development of VESYS A is continuing to expand its present analysis capability from three to seven layers. This will lead to development of the new generation of the VESYS system, VESYS III.

TABLE OF CONTENTS

	Page
List of Figures	vi
List of Tables	x
CHAPTER I. INTRODUCTION	1
Background	1
Program Modifications to VESYS IIM	2
Development of Input Data for Modified VESYS IIM	
Analyses	3
Relating Increased Legal Axle Loads to Flexible	
Pavement Life Cycle Costs	5
CHAPTER II. PROGRAM MODIFICATIONS TO VESYS IIM	6
Seasonal Characterizations of Pavement	
Materials	6
Discretized Representation of Axle Load	
Distributions	10
Low-Temperature Cracking Predictions	16
Subroutine to Save Static Solutions	19
Verification of Program Changes	21
CHAPTER III. SELECTION OF INTERSTATE HIGHWAYS FOR	
FOUR ENVIRONMENTAL ZONES	28
CHAPTER IV. DEVELOPMENT OF INPUT DATA FOR MODIFIED	
VESYS IIM ANALYSIS	31
Seasonal Pavement Temperatures	31
Seasonal Permanent Deformation Characterizations	33
Seasonal Layer Stiffness Characterizations	41
Low Temperature Cracking	43
Axle Load Distributions for the Four Legal Axle	
Loads	47
Fatigue Potential Characterizations	49
Pavement Structure, Truck Traffic and Other	
Input Values	52
CHAPTER V. CALIBRATION OF MODEL FOR REALISTIC	
PREDICTIONS	59
Comparisons to AASHO Road Test Measurements	60
Comparisons to Brampton Test Road Measurements	64
Analysis of Solutions for Four Interstate	
Pavements	67
Final Input Values for Solution Factorial	85

TABLE OF CONTENTS (Continued)

	Page
CHAPTER VI. FACTORIAL SOLUTIONS FOR INITIAL CONSTRUCTION AND OVERLAYS	86
Results from Initial Construction Solutions	86
Overlays to Restore Pavements and Their Simulation in VESYS A	86
Results from Overlay Construction Solutions	94
Overall Performance Results	94
CHAPTER VII. RELATIONSHIPS BETWEEN INCREASED LEGAL AXLE LOADS AND LIFE CYCLE COSTS FOR FLEXIBLE PAVEMENTS	113
Cost Evaluations and Relating Costs to Legal Axle Loads	115
Cost Relationships for New Pavements	116
Cost Relationships for Existing Pavements	126
CHAPTER VIII. SUMMARY	130
APPENDIXES-	
APPENDIX A. Permanent Deformation Parameters ALPHA(1) and GNU(1) for Asphalt Concrete as Functions of Temperature and Deviator Stress	133
APPENDIX B. Permanent Deformation Parameters ALPHA(2) and GNU(2) for Base Material As Functions of Density and Moisture Content	148
APPENDIX C. Permanent Deformation Parameters ALPHA(3) and GNU(3) for Subgrade as Functions of Moisture Content, Density and Deviator Stress	154
APPENDIX D. Evaluation of Corrected Hajek-Haas Model for Predicting Low Temperature Cracking for Flexible Pavement	175
APPENDIX E. Structure of the Saved Static Solution File	186

TABLE OF CONTENTS (Continued)

	Page
APPENDIX F. Variance of Cracking as a Function of Evaluation Frequency	187
APPENDIX G. Guide for Developing Input for Low Temperature Cracking Predictions	190
REFERENCES	198

LIST OF FIGURES

	<u>Page</u>
1. Examples of Curves Showing Distribution of Axle Weight by Vehicle Class from a Truck Weight Study (solid curves) (From Ref. 24)	48
2. Comparisons of Measured Rut Depths and those Predicted by VESYS IIM and VESYS A	62
3. Comparisons of Measured Responses and those Predicted by VESYS IIM and VESYS A, AASHO Section 470	63
4. Rut Depth Versus Time, Section 3	66
5. Rut Depth Versus Time, Section 4	68
6. Rut Depth Versus Time, Section 11	69
7. PSI Versus Time, Section 17	70
8. PSI Versus Time, Section 3	71
9. PSI Versus Time, Section 4	72
10. PSI Versus Time, Section 11	73
11. Rut Depth Versus Time, Section 17	74
12. Rut Depth Predicted After Seven Years Versus the Surface Layer Permanent Deformation Parameters for Section 3, Brampton Test Road	75
13. ALPHA(1) Versus GNU(1) for Summer Seasons and Four Solutions, Brampton Section 3	76
14. Predicted and Measured Rut Depths for a Section of IH-80N in Utah Between Snowville and the Idaho Border	78
15. Predicted and Measured Serviceability for a Section of IH-80N in Utah Between Snowville and the Idaho Border	79
16. Predicted and Measured Cracking Damage for a Section of IH-80N in Utah Between Snowville and the Idaho Border	80
17. ALPHA(1) Versus Temperature for the Four Interstate Highway Sections Considered	82

	<u>Page</u>
18. Comparative Plots of Percent of Rutting at the Surface Contributed by the Various Layers by Pavement Section and with Seasons Identified	83
19. Comparative Plots of Percent of Rutting at the Surface by Season and Pavement Section	84
20. Equivalent Surface Thickness to Represent Cracked Pavement and Overlay	92
21. Predicted Performance, Wet-Freeze Environment, Low Traffic and Thin Pavement Sections	97
22. Predicted Performance, Dry-Freeze Environment, Low Traffic and Thin Pavement Section	98
23. Predicted Performance, Wet-No Freeze Environment, Low Traffic and Thin Pavement Section	99
24. Predicted Performance, Dry-No Freeze Environment, Low Traffic, Thin Pavement Section	100
25. Predicted Performance, Wet-Freeze Environment, Low Traffic and Thick Pavement Section	101
26. Predicted Performance, Dry-Freeze Environment, Low Traffic and Thick Pavement Section	102
27. Predicted Performance, Wet-No Freeze Environment, Low Traffic Thick Pavement Section	103
28. Predicted Performance, Dry-No Freeze Environment, Low Traffic and Thick Pavement Section	104
29. Predicted Performance, Wet-Freeze Environment, High Traffic and Thin Pavement Section	105
30. Predicted Performance, Dry-Freeze Environment, High Traffic and Thin Pavement Section	106
31. Predicted Performance, Wet-No Freeze Environment, High Traffic and Thin Pavement Section	107
32. Predicted Performance, Dry-No Freeze Environment, High Traffic and Thin Pavement Section	108
33. Predicted Performance, Wet-Freeze Environment, High Traffic and Thick Pavement Section	109
34. Predicted Performance, Dry-Freeze Environment, High Traffic and Thick Pavement Section	110

	<u>Page</u>
35. Predicted Performance, Wet-No Freeze Environment, High Traffic and Thick Pavement Section	111
36. Predicted Performance, Dry-No Freeze Environment, High Traffic and Thick Pavement Section	112
37. Average Annual Cost by Environmental Zone for Low Traffic and Thin Pavement Section	123
38. Average Annual Cost by Environmental Zone for Low Traffic and Thick Pavement Section	123
39. Average Annual Cost by Environmental Zone for High Traffic and Thin Pavement	124
40. Average Annual Cost by Environmental Zone for High Traffic and Thick Pavement	124
41. Aggregate Grading Curve for Typical Asphalt Concrete Mix Used for Permanent Deformation Testing	135
42. Effects of Deviator Stress Level and Temperature on ALPHA(1)	138
43. Effects of Temperature and Deviator Stress Level on GNU(1)	139
44. Resilient Modulus for the Typical Asphalt Concrete Versus Temperature	140
45. Resilient Modulus Versus Stress for the Typical Asphalt	141
46. Permanent Strain After 100,000 Cycles of Load as a Function of Deviator Stress	142
47. Permanent Strain After 100,000 cycles of a load as a Function of Temperature	143
48. Plot of ALPHA(1) Versus Deviator Stress for Asphaltic Concrete	145
49. Plot of GNU(1) Versus Deviator Stress for Asphaltic Concrete	146
50. Plots of ALPHA(1) and GNU(1) Versus Temperature	147
51. Permanent Strain Versus Percent Moisture for a Gravel Base with Plastic Fines	150
52. Relationships Between ALPHA(2), GNU(2) and Permanent Strain for a Gravelly Sand After 100,000 Load Cycles Versus Deviator Stress with Lateral Pressure Constant at 10 psi (0.694 Kg/cm ²)	151

	<u>Page</u>
53. Relationship Between ALPHA(2), GNU(2) and Permanent Deformation for a Crushed Limestone After 100,000 Load Cycles Versus Lateral Pressure at Approximate Constant Deviator Stresses	152
54. Plots of Dry Density Versus Moisture Content	157
55. Plots of Dry Density Versus Compactive Blows Per Layer in the Specimen Mold	158
56. Factorial Experiment for Subgrade Soil	159
57. Variations in ALPHA(3) with Moisture Content and Dry Density	162
58. Variations in GNU(3) with Moisture Content and Dry Density	163
59. Relation Between ALPHA(3) and GNU(3) for Variations in Moisture Content and Dry Density	164
60. Variations in ALPHA(3) with Moisture Content and Dry Density from Data in Reference 48	166
61. Variations in GNU(3) with Moisture Content and Dry Density from Data in Reference 48	167
62. Variations in ALPHA(3), GNU(3) and Permanent Strain at 50,000 Cycles of Load as Functions of Moisture Content and Dry Density from Data in Reference 49	168
63. Permanent Strain at 10,000 cycles of Load Versus Deviator Stress	169
64. Resilient Strain Versus Deviator Stress	170
65. Relationship Between Freezing Index and Winter Design Temp.	192
66. Map of Canada Illustrating Freezing Indices	193
67. Freezing Index Map of the United States	194
68. McLeod's Chart for Estimating the P.I. of an Asphalt Cement	195
69. Suggested Modification of Heukelom's Version of Pfeiffer's and Van Doormal's Nomograph for Relationship Between Penetration, Penetration Index and base temp (After McLeod)	196
70. Suggested Modification of Heulelom's and Klomp's Version of Van Der Poel's Nomograph for Determining Modulus of Stiffness of Asphalt Cements (After McLeod)	197

LIST OF TABLES

	<u>Page</u>
1. Indexing Example	12
2. List of Keywords Removed from VESYS-A	25
3. New or Changed Keywords	27
4. Ratios of Seasonal Average Pavement Temperature to Air Temperature at 2 to 4 inches (5.1 to 10.2 cm) Below the Surface, Various Locations	34
5. Pavement Temperatures by Season	35
6. Seasonal Permanent Deformation Parameters, ALPHA and GNU	39
7. Seasonal Multipliers for Creep Compliance Arrays, Base and Subgrade	44
8. Creep Compliance in Constant Value Arrays for Base and Subgrade Layers	45
9. Input Data Developed for Low Temperature Cracking Predictions	46
10. Discretized Representations of Legal Axle Load Distributions by Percent of Total	49
11. Axle Load Distributions in Percent of Total Representing Different Single Axle Load Limits	50
12. Values of MPLITUD and Resulting Wheel Loads	51
13. Fatigue Life Potential Characterizations for the Four Environmental Zones and the Four Seasons	53
14. Truck Traffic in Axles per Day	55
15. Creep Compliance Arrays for LAYER1, Asphalt Concrete Surface Layer	56
16. Fixed Input Values	57
16. (Continued) Fixed Input Values	58
17. Predicted Values of Rut Depth for the Solution Factorial in Inches (1 cm = 0.394 inches)	87

	<u>Page</u>
18. Predicted Values of Present Serviceability Index for the Solution Factorial	88
19. Predicted Values of Fatigue Damage Index for the Solution Factorial	89
20. Predicted Values of Low-Temperature Cracking Indices and Average Crack Spacing	90
21. Equivalent Thickness for Single Layer Approximation to Overlay + Original Pavement, Inches (1 cm = 0.394 inches)	91
22. New Static Solutions for Overlays (1 cm = 0.39 inches)	93
23. Predicted Life of Pavement and Points in Time When Overlaid in Years	95
24. Estimates for Initial Construction Costs for Thin and Thick Pavement Sections	114
25. Cost Data in Dollars as a Function of Legal Axle Load, Environmental Zone, and Pavement Section for Low Traffic Cases	117
26. Cost Data in Dollars as a Function of Legal Axle Load, Environmental Zone, and Pavement Section for High Traffic Cases	118
27. Cost Data From Table 25 Normalized by Dividing All Values by the Corresponding 18-kip Legal Axle Limit Costs, Low Traffic Cases (1 - kip = 454 kg)	120
28. Cost Data From Table 26 Normalized by Dividing All Values by the Corresponding 18-kip Legal Axle Load Costs, High Traffic Cases (1 - kip = 454 kg)	121
29. Mean Values of Costs Versus Legal Axle Load Normalized by 18-kip Legal Axle Limit Costs (1 - kip = 454 kg)	122
30. Mean Values of Costs (Dollars) for Overlays Versus Legal Axle Load	127
31. Mean Values of Costs for Overlays Normalized by 18-kip Axle Load Costs Versus Legal Axle Load (1 - kip = 454 kg)	128
32. Results of Permanent Deformation Tests on a Typical Asphalt Concrete Mix	137

	<u>Page</u>
33. Results of Permanent Deformation Tests on a Typical Silty Clay	160
34. Summary of Cracking Index Values and Other Related data	176
35. Summary of Cracking Index Values Using Corrected KAJEK-HAAS EQUATION AND COMPARISON TO ACTUAL VALUE	180
36. Summary Analysis of Residuals (Actual Less Predicted Carcking Index I) for Corrected KAJEK-HAAS EQUATION	182
37. Summary Analysis of Cracking Index Ratios Actual/ Predicted for Corrected HAJEK-HAAS EQUATION	183
38. Summary Analysis to Combine "ACCURACY LEVELS" for Residuals and Cracking Index Ratios for the Corrected HAJEK-HAAS EQUATION	184

CHAPTER I

INTRODUCTION

Background

Recent Federal Legislation (Title 23, Sec. 127 as amended 1975) has permitted States to raise allowable axle loads on Interstate highways from 18,000/32,000 lb (8,160/14,510 kg) to 20,000/34,000 lb (9,070/15,420 kg) on single/dual axles, respectively. There is considerable concern for pavement damage in those States where this option has been exercised; many States already had legal loads of 20,000 lb (9,080 kg) or more under the "grandfather" clause.

A considerable effort has been expended already to predict service life reductions as a function of increases in axle load limits based on data from the AASHO Road Test, Loadometer studies and traffic count surveys. This methodology has developed a predicted 64 percent increase in the equivalent effect on a pavement for a fully loaded truck with an axle weighing 2,000 lbs. (908 kg) more than the present limits. However, these predictions are extrapolated past the range in numbers of axle loads for which the data were developed and are possibly suspect as a result.

There are at present several FHWA research projects underway aimed at producing the needed information using a range of techniques. FHWA Research Project "Effects on Highways of Increased Legal Vehicle Weights Using VESYS IIM" is one of these and has as its objectives: (1) modification and improvement of Computer Program VESYS IIM so that it can be used in a realistic manner to establish relationships between increased legal axle loadings and flexible pavement life cycle costs, and (2) application of VESYS IIM to produce these relationships.

VESYS IIM as modified (modified program will subsequently be called VESYS A for simplicity) is a sophisticated computer code that accepts some 23 control variables and 44 independent variables describing a flexible pavement structure, the traffic loadings it endures and indirectly (through input of pavement temperatures and seasonal materials characterizations) the environment in which it exists. Using this input, it then predicts fatigue cracking, rut depth, slope variance, Present Serviceability Index and expected life as functions of time in terms of truck traffic and axle load distribution. VESYS IIM in the format extant prior to this project is described in varying degrees of detail in a number of references including

References 1¹ and 2². The modifications and improvements in VESYS resulting from this project will be described subsequently.

Program Modifications to VESYS IIM

The modifications to improve VESYS IIM toward more accurate simulation of real pavement structures included (1) discretized representation of axle load distribution, (2) seasonal characterizations of stiffness and permanent deformation properties of materials, and (3) low-temperature cracking predictions.

VESYS IIM introduced the entire spectrum of axle loads experienced by the pavement as a mean axle load and a variance. This was considered to be inadequate for discriminating among the differences due to variations in the small percent of higher axle loads, so a capability was introduced for considering the effects due to discrete segments of the axle load distribution separately and combining them. This allows the theoretical model to more accurately assess the responses of the pavement structure to the various magnitudes of axle loading.

All analytical procedures based on elastic layer theory require definition of the stiffnesses of the various layers as input data. Most operate only with single values for each layer, but VESYS IIM has the additional capability of considering the effects of temperature variations on surface layer stiffness and of including these variations in stiffness in the analysis as damage is accumulated in time. As the stiffnesses of base and subgrade materials also undergo seasonal changes in moisture content and density due to variations in rainfall, frost penetration, spring breakup and other such causes, a more accurate simulation results if they also change rationally on a seasonal basis.

VESYS IIM included a capability for rationally predicting rut depths in time, partially based on permanent deformation characterizations of the three layer materials in the form of two new parameters ALPHA (N) and GNU (N) for N = 1, 2, and 3 (See Reference 1 for

¹Rauhut, J. B., J. C. O'Quin and W. R. Hudson, "Sensitivity Analysis of FHWA Structural Model VESYS IIM, Vol. 1, Preparatory and Related Studies," Report No. FHWA-RD-76-23, March 1976.

²Kenis, W. J., "Predictive Design Procedures - A Design Method for Flexible Pavements Using the VESYS Structural Subsystem," Proceedings, Fourth International Conference, Structural Design of Asphalt Pavements, Volume I, August 1977.

detailed discussion). As the magnitudes of these parameters are heavily dependent on such seasonal variables as moisture content and temperature and are themselves very important to the predictions of rut depth, slope variance, present serviceability index and expected life, arrays of values instead of single values are required to rationally characterize these materials across the seasons of the year. VESYS IIM was modified in this project to allow this capability.

Cracking of the asphalt concrete surface layer due to traffic-induced fatigue is a major form of flexible pavement distress and this phenomena is modeled in VESYS IIM. However, low-temperature transverse cracking is another important form of cracking distress that sometimes predominates over fatigue cracking in northern states. It was desirable to broaden VESYS IIM to predict low-temperature cracking and a statistical model was selected and added to VESYS IIM during this project.

These three additions in VESYS IIM capabilities are believed to have considerably improved its ability to simulate the performance of real flexible pavements.

Development of Input Data for Modified VESYS IIM Analyses

The improvements to Program VESYS IIM resulting in Program VESYS A discussed above may not be employed effectively unless the magnitudes of the input parameters are known. There is a very considerable body of information available for changes in base and subgrade material stiffness with changes in moisture content and dry density, but there is little available information on the permanent deformation parameters ALPHA (N) and GNU (N) due to their recent definition and application to rutting predictions.

Review of available information on permanent deformations in well compacted base materials indicated that a reasonable level of information was available in the literature (References 1, 3¹, and 4²).

¹Proceedings from a Conference on Utilization of Graded Aggregate Base Materials in Flexible Pavements, held March 25-26, 1974 in Oakbrook, Illinois, published by the National Crushed Stone Association, National Sand and Gravel Association and the National Slag Association.

²Kalcheff, I. V. and R. G. Hicks, "A Test Procedure for Determining the Resilient Properties of Granular Materials," Journal of Testing and Evaluation, Vol. I, No. 6, ASTM, 1973.

Consequently, it was decided that additional testing of base materials to establish seasonal trend information could be omitted in favor of testing of typical subgrade and asphalt concrete specimens.

Testing was conducted on a typical silty clay soil in a small factorial of varying moisture content and dry density to provide some insight as to variation of ALPHA (3) and GNU (3) with these parameters. Similarly, asphalt concrete specimens were tested with variations in temperature and stress level to gain insight as to variation of ALPHA (1) and GNU (1) with those parameters. The results of this testing, research of the literature and previous experience were used to assign rational values of ALPHA (N) and GNU (N) for the materials in the three layers and for the four seasons.

The testing performed, its results and results of the literature research are discussed in detail in the Appendices. The resulting values selected appear and are also discussed in Chapters IV and V.

Much of the input data resulted from selection of the four interstate highways to represent the four environments wet-freeze, dry-freeze, wet-no freeze and dry-no freeze and was furnished by personnel of the various State Departments of Transportation and other sources. Other data such as pavement temperatures and axle load distributions for various legal axle limits required some research to develop and their development is discussed in more detail subsequently.

Input data was developed for four test sections each from the AASHO Road Test and the Brampton Test Road as well as the four interstate highways. As previous comparisons had been made between VESYS IIM predictions and measured performance for the same AASHO Road Test and Brampton Test Road sections (Reference 1), it was possible to observe the effects of using the improved program. It was also possible and necessary to compare solutions for the four interstate highway sections to performance observations made available by state personnel. Where predictions appeared errant, the input values were studied to isolate inadequacies and to correct the input values where more rational values could be developed by further study. This iterative approach of comparing predictions and observed performance, studying the input parameters apparently causing differences to see if the input values were adequate or could be rationally improved, new predictions and comparisons, etc., was used to effect a "calibration" of the procedure so that rational predictions could be expected for the test sections to be studied.

Relating Increased Legal Axle Loads to Flexible Pavement Life Cycle Costs

As previously stated, the goals of this research project were to effect certain improvements to VESYS IIM so that it could be used to relate increased legal axle loads to flexible pavement life cycle costs and to apply these capabilities to that task. The application of the improved program was made in a factorial of 64 solutions including the four interstate highways, two levels of pavement section thickness, two levels of traffic and the four levels of legal axle limits. Where either predicted cracking or rutting caused failure before the twenty-year design life was reached, overlays were added and new solutions obtained. This effort is discussed in Chapter VI.

Results in the form of performance and cost data to provide satisfactory service across the design life of the pavement have been accumulated and are presented in Chapter VII.

CHAPTER II

PROGRAM MODIFICATIONS TO VESYS IIM

A complete description of the VESYS IIM program can be found in Reference 1; this should be read prior to reading the following description of changes.

The modifications performed on the program under this project fall into three major categories: (1) the seasonal modification of materials properties; (2) the breakdown of the load distribution by tire radius and corresponding tire pressure; and (3) the addition of low temperature cracking as a distress mechanism. The first two involved additional static solutions and thus required many changes in dimensions and indexing, whereas the third was a relatively simple addition to the repeated load portion of the program. These three changes will be discussed separately below.

Seasonal Characterization of Pavement Materials

VESYS A considers a three layer pavement system: an asphalt layer, a base, and a subgrade. For each layer the permanent deformation parameters are input for each season, instead of remaining constant throughout the year; in addition, the creep compliance functions for the base and subgrade layers are modified by separate seasonal multipliers for each layer and season. These seasonal multipliers permit modeling of the effects of environmental variables on the stiffness of the layers (e.g., spring breakup of frozen soil).

The implementation of these additional parameters requires that a static solution be performed for each season, whereas before only one static solution was required for the entire simulation. A Type I "static solution" for the VESYS system means the solution for the set of desired responses to a loading of 1 psi (6.9 kN/m²) over a circle of specified radius (permanent deformation at the surface and radial strain at the bottom of the surface layer) as a function of load duration, these responses expressed as sets of coefficients of a Dirichlet series. Because of this increase in the number of static solutions, many changes in indexing and in array dimensions were required; these changes will be detailed later.

Since there was already provision for up to 24 seasons, i.e., periods in the year for which a temperature could be input, the number of possible seasons, or static solutions, was maintained at 24 for future flexibility. This many seasons would be too expensive to run in a large factorial for a limited research effort and is not necessary. Use of input values averaged over three-month periods representing the four seasons of the year may be expected to provide characterizations whose accuracy is consistent with the "state-of-the-

art" in materials characterization and model simulations. The decision was also made at this time based on previous experience with the program to replace the capability of executing a Type 3 run (repeated load solution only) based on card input of results from a previous Type 1 run by a similar capability to obtain these results from a computer file. It was decided that too many chances for error existed in the selection of input values; and also, with the addition of multiple static solutions, that the volume of input required was too great to be done conveniently with cards. This decision made possible the removal of some of the input variables and keywords, and thus the program has now after modification approximately the same number of input variables (physical and control) as before.

A list of those key words added and those removed will appear at the end of this chapter, as well as a list of variables added and those whose dimensions were changed.

Changes to the main program involved additions to the input guide, removal of the read statements corresponding to the key words removed, modifications to the read statements which now read data for each season (ALPH, GGU, and SMLT) and corresponding changes to the printout and data validity checks, and insertion in this routine of the call to the master repeated load subroutine for the second part of a TYPE 1 run (this had been in subroutine STATIC, although the call to the same routine in the case of a TYPE 3 run was in the main program).

Subroutine STATIC is the main subroutine for the static load portion of the program. Changes to this routine involve, beyond the changes in dimension and common blocks, the addition of a new loop around most of the routine, the index on which serves to identify the season for which a solution is being made. All references to the values of input permanent deformation parameters ALPHA and GNU must be made by season as well as by layer, and the results of the solutions (the coefficients for the series representing the variation of response with load duration, and coefficients of variation of these series) are also stored by season; the two quantities α_{sys} and μ_{sys} , curve fitting parameters representing the permanent deformation performance of the entire pavement system, also are stored by season. In performing the solutions for each season, the coefficients of the series representing creep compliance for the base and subgrade are multiplied by a seasonal multiplier for the given layer (multiplying each coefficient by a constant has the effect of multiplying the value of the evaluated series by the same constant). This modified creep compliance function is used then in the calculations for the desired responses for that season (radial strain at the bottom and deformation at the top of the asphalt surface layer); the coefficients are then returned to their original values.

Another change, not related to seasonal variation of input parameters, is the revision of the limits on the loop performed to evaluate the system permanent deformation parameters; this is the "unload" portion of the static solution for vertical deformation, in which the layer moduli or creep compliances are modified according to (1) the permanent deformation parameters for the particular layer and season and (2) the number of loads for which the simulation is desired. It is felt that since the actual number of loadings considered is large, the values of repeated axle loads used to obtain α_{sys} and μ_{sys} as a straight line fit to the logarithms of predicted surface deformation as a function of the logarithms of the number of axle loads should be correspondingly large. Consequently, the values for LY1 and LY2 used throughout this project were 6 and 8, corresponding to values for numbers of axle loadings of 10^5 , 10^6 , and 10^7 , respectively. These values were suggested by ARE in a previous study (Ref. 1) but were replaced at FHWA by values for LY1 and LY2 of 1 and 5, corresponding to a range in loadings from 1 to 10^4 , due to numerical difficulties encountered on the computer in use there.

In the repeated (or random) load portion of VESYS A, subroutine RANDOM serves as a calling routine for the rest of the section, as well as performing certain calculations needed for both the rut depth and the fatigue cracking calculations. In this routine, unnecessary common blocks were removed, the variable BYPASS was added to the calling sequence, and an error printout previously in subroutine ERROR was added here instead so that in case an error occurs, the user can tell for which season (which static solution) the problem exists. (The errors considered are: (1) a negative sum of Dirichlet series coefficients for a given response and season; and (2) a negative value in the array DELTA, which contains values used in evaluating these series.) Calls to subroutines CRACKS and ROUGH were removed from subroutine SERVC and added to RANDOM to clarify the sequence of operations.

Subroutines ROUGH and CRACKS have several features in common; a short discussion here will save duplication later. ROUGH deals with surface deformation; CRACKS deals with radial strain at the bottom of the asphalt; they each evaluate the physical result (deformation or strain) at each season using the appropriate Dirichlet series, the value of input load duration, and the time-temperature shift calculated in RANDOM for the temperature corresponding to that season. The desired result and its variance are calculated in subroutine GRESP (Generalized RESPONSE) and are printed. In CRACKS this result (axial strain) is used to calculate the damage per cycle of loading, while in ROUGH the surface deflection is used more directly in the next portion of the routine.

In each routine a loop is then performed over the number of seasons required to attain the last time input in the TRANDOM array. After the accumulated damage is calculated and stored for each of these seasons, a second loop is performed over the number of TRANDOM values for which output is desired. At each value, the damage is linearly interpolated between the two closest "season" times, where the time associated with each season is the end of that season.

Subroutine ROUGH, which calculates the accumulated permanent deformation (rutting) and associated statistical quantities leading to slope variance, was not greatly changed. The common blocks were modified as previously discussed; the variables ALPHA and GNU (previously the single system permanent deformation parameters) were set successively to values for the current season from the arrays ALF and GMU in the process of generating the rutting.

The rutting calculation was not changed except for the indexing of variables which previously had only one value. The interpolation routine was changed so that it was no longer possible to reference the rutting for a season beyond those for which it had been calculated. Under certain conditions (not unusual), this could and did happen previously; the results were not affected but the reference made debugging elsewhere more difficult (a common debugging tool is to preset the computer memory to a value which will cause an error exit if the value is used; this helps to isolate undefined variables and the use of undefined locations in arrays).

The only remaining change in ROUGH was to define GVNRM, a multiplier of the variance of rut depth in the calculation of slope variance, to be the RMS average for all seasons of the values of GCVAR (K,4), the coefficients of variation of the system's vertical deformation. This choice was made rather than a straight mean because it is the square of GVNRM that is actually used in the calculation of slope variance.

Changes to subroutine CRACKS were very similar to those applied to ROUGH. There is no reference to seasonally indexed quantities except for the strain and its variance, however, so the changes are fewer in number. The interpolation for the damage and its variance at time TRANDOM is performed in the same way as for subroutine ROUGH.

Subroutine GRESP was modified to include the seasonal index K on the Dirichlet series G, viz. $G(K, I)$; G is either GNORM (in the call from ROUGH) or GRAD (in the call from CRACKS). GRESP already returned results for each season due to the inclusion of the time-temperature shift. The internal dimension statement for G was changed from G(1), simply indicating that G is a vector, to

G(25, 20). Another formal parameter, S, previously undimensioned, was changed to S(25), and all references to S were changed to S(K). (S corresponds to the variables GCVAR (K,4) or GCVAR (K,7), representing the coefficient of variation of the Dirichlet series coefficients.)

The only other change was the removal of calls to subroutines ROUGH and CRACKS from SERVC, corresponding to their insertion in subroutine RANDOM.

Discretized Representation of Axle Load Distributions

VESYS IIM uses just three parameters to describe distribution of wheel load (taken as one half of axle load) in the flow of traffic: RADIUS, the radius of a circle of area equal to that of the tire footprint; AMPLITUD, strictly the multiplier of the value of LOADING used in the static solutions, the product then representing tire pressure (in practice, since a value of 1.0 is normally used for LOADING, and is the default value, AMPLITUD may be more simply thought of as the actual tire pressure); and VCAMP, the variance of AMPLITUD. AMPLITUD (for LOADING = 1.0, as will be assumed throughout the remainder of this report) and RADIUS together define a specific wheel load, given by

$$\text{wheel load} = \pi(\text{RADIUS})^2 \cdot \text{AMPLITUD}$$

VCAMP then must represent the entire variation of wheel (or axle) load, whereas in fact the loaded area also varies with wheel load. Because the histogram of wheel load is often both skew and double humped, the representation of this histogram simply by a mean and a variance is poor.

Initially it was planned simply to input a series of AMPLITUD values and to represent the variation in wheel load this way, but these values become unrealistic when tied to a single radius, so it was decided to allow static solutions to be made for more than one radius value. An axle load distribution can be broken into several parts and the mean load determined for each part, which, with the assumption of a reasonable tire pressure, leads to a value of RADIUS for that portion of the load distribution. This procedure not only permits a better, more reasonable representation of load distribution, but it also permits isolation of the effect of different portions of that load distribution on the several distress manifestations. Of course, there is considerable extra computational cost involved in performing multi-radius solutions over those for a single radius since the cost of a simulation run is roughly proportional to the total number of static solutions (number of seasons times number of radii).

As might be expected, the implementation of multiple-radius simulations involved changes similar to those previously mentioned concerning the seasonal variation of materials properties: changes/additions to input variables, common blocks, indexing, and output. In both cases, the major change is the increase in the number of static solutions and associated storage and indexing (bookkeeping). The changes required in each major routine or group of routines are outlined below.

In VESYS, the additions consisted of several new input parameters, new variables in common blocks, and removal or changes in the printed output. The variables added are listed in Table 1 and include: (1) NRADIUS (RADIUS and AMPLITUD are now vectors if $NRADIUS > 1$); (2) LOADDIST, which gives the fraction (not percent) of the total axles per day to be associated with a particular wheel load given by RADIUS and AMPLITUD and (3) TRAFMULT, which permits a seasonal variation in the traffic. A new common block, /DIST/, was added to hold these new vectors and the value of NRADIUS, which is limited to $1 \leq NRADIUS \leq 12$ (default is 1). Changes in the lists of default and limiting values as well as in the list of acceptable key words were made in BLOCKDATA. The new arrays were also preset to appropriate values.

In subroutine STATIC, changes beyond dimensions and common blocks involved primarily indexing and access to some of the new variables. Since in the previous set of modifications a loop had been added around the static solution calculation, the variation of radius was handled in the following manner: The total number (variable name NTXNR) of static solutions required (equal to NRADIUS radii times NTEMPS seasons, using keywords rather than actual variable names) was calculated and used as the limit of the loop on static solutions in place of the number of seasons alone. For each season, NRADIUS static solutions were performed; the variable AAA, previously used for the single input radius, was set in turn equal to each value in the array RADIUS.

The indexing was done as follows: ITM is the sequential index on static solutions and now runs from 1 to NTXNR. ITEMP and IRAD, the indices for season and radius corresponding to a given static solution, are calculated by

$$ITEMP = (ITM-1)/NRAD + 1$$

and

$$IRAD = MOD((ITM-1), NRAD) + 1$$

where NRAD is the variable containing the number of radii, MOD is the modulo arithmetic function, and use is made of the fact that results in integer arithmetic in FORTRAN are always truncated. Assuming, for example, a simple case, NRAD = 3, NTEMP (the variable containing the number of seasons) = 4, we derive the following table of indices:

TABLE 1. INDEXING EXAMPLE

<u>STATIC SOLUTION INDEX (ITM)</u>	<u>SEASON INDEX (ITEMP)</u>	<u>RADIUS INDEX (IRAD)</u>
1	1	1
2	1	2
3	1	3
4	2	1
5	2	2
6	2	3
7	3	1
8	3	2
9	3	3
10	4	1
11	4	2
12	4	3

The second equation above is read as: IRAD is equal to the quantity (ITM-1) modulo NRAD plus 1, and can also be expressed, using the truncation of integer arithmetic, as (letting IM represent (ITM-1))

$$IRAD = IM - (IM/NRAD)*NRAD + 1$$

All the output for the static solutions was already stored by index ITM so the only remaining change was to the indices on seasonally varying input parameters (SMLT, GGU, and ALPH) from the index ITM to the new season index ITEMP.

In the repeated load portion of the program, changes in subroutine RANDOM were minor; several unused common blocks were deleted (/SPACE/,/DERV/, AND /NERV/), common block /DIST/ was added, and in the check portion mentioned earlier (in the first modification set) the season and radius indices are derived from the index on static solutions and printed if any solution coefficient set fails the tests.

To discuss changes in CRACKS and ROUGH, it is necessary first to describe the modifications to subroutine GRESP. GRESP as originally written performed the following calculations for each season: (1) evaluate the time-temperature shift to derive an effective load duration from the input duration; (2) evaluate the Dirichlet series for the required normalized response at that effective load duration; (3) evaluate several related stochastic quantities; (4) evaluate the true (unnormalized) response and its variance using AMPLITUD (tire pressure) and its variance, the variance of load duration, and the coefficient of variation of the normalized response. Another term in the variance of the true response involves the covariance of load duration and amplitude, but this covariance had been forced equal to 0 within the program as received, and has not been changed. With the addition of variable radii and corresponding static solutions, and of variable amplitude, it appeared that the two portions of GRESP could be split into two routines; one (GRESPl) would evaluate the normalized strain and its variance for all the static solutions; the other (GRESPl2) would be called in a loop in the calling program which isolates the correct static solution, season, and radius by separate indices, and provides GRESPl2 the proper value of amplitude and of static solution coefficient of variation. By splitting the calculations in this fashion, certain economies of calculation and of bookkeeping can be made, e.g., it is easier to avoid redundant or repetitive calculation of the same quantities. The rewrite of GRESP also permitted a change in the interests of computation efficiency from many divisions by the same quantity to many multiplications by the inverse of that quantity. (The variable Y in GRESP was replaced by the variable Q = 1./Y in GRESPl).

Another lesser change was made in the code which was incorporated in GRESPl2. A number of variables used in the calculation of the response and its variance were then normalized by the final values of response and variance and returned to the calling program; however, they were never used, and only served needlessly to lengthen the calling sequence. They were therefore removed from the calling sequence of GRESPl2 and left unnormalized.

Changes in subroutine ROUGH included: (1) an expansion of the variable list in the common block/RESP1/, which previously had had most of its contents contained in one dummy variable name (this permitted access to the variable AMP, which was set to values of amplitude AMPL corresponding to the current value of the radius index); (2) the addition of block/DIST/; (3) the call to GRESPl; (4) the loops around the call to GRESPl2 and (5) the definition of season radius, and static solution indices where appropriate. Following these calculations a table is printed listing for each static solution, the temperature, radius, total deflection (elastic plus

permanent), variance of deflection, and α_{sys} and μ_{sys} . The total number of seasons over which damage is accumulated is determined by the last value of TRANDOM input (program variable name TIME); this is limited by the dimensions on variables to 480. A loop for the damage estimation at each of these seasons is then initiated, and within this is a loop over the number of radii; thus the static solution for each radius is exercised in order during each season.

The traffic appropriate at each season is determined from the array ADT(I), the average daily traffic over the period TIME(I-1) to TIME(I) (input under the LAMBDA key word). This is done by determining which is the first value of TIME greater than the mid-time of the current season, and using the corresponding value of ADT. For each season, the season index (for position within the year, as opposed to position with the entire simulation period) is defined by the modulo function, and the traffic is expressed in total axles per second by multiplying the ADT value by the inverse of number of seconds per day and by the seasonal traffic multiplier.

Within each season in the simulation period, a loop over the number of radii is executed. The season index has been calculated and the radius index is equal to the inner loop index, hence the static solution index can be immediately obtained and used to retrieve the appropriate values of ALPHA, GNU, response (vertical deformation) and variance of response. The number of loads per second calculated previously is now multiplied by the fraction of traffic assigned to this radius-amplitude (or wheel load) combination.

The damage (rut depth) to date is converted to the time, in seconds, required to generate this damage under the current conditions of environment and traffic; this time is added to the number of seconds per season and the sum is then used, in conjunction with the current traffic, to generate the equivalent total number of axles under current conditions of traffic, environment and wheel load to the end of the season. This number of vehicles is then entered in the equation for permanent deformation along with the current ALPHA and GNU to obtain, after all the solutions for different radius have been exercised, the rut depth and its variance at the end of the current season. The process is repeated to the end of the simulation; the result is a table of rut depth and variance of rut depth for the end of each season in the simulation period. Values of rut depth and its variance are then interpolated for the specific time values in array TIME.

As before, GVNRM, a multiplicative factor in the conversion of variance of rut depth to slope variance, is defined to be the unweighted rms average of the values of the coefficients of

variation of the Dirichlet series for vertical deformation for all of the static solutions. Some thought might be given towards weighting the values for a given radius by the traffic fraction corresponding to that radius, or perhaps by the average (over season) of the effect (vertical deformation) for that wheel load. This was not done here; it was observed that the values did not vary much with radius.

Subroutine CRACKS was modified in ways similar to those used for ROUGH. However, there exist some features unique to each routine, and these will be identified and discussed. CRACKS provides an algorithm for estimation of the two parameters K_1 , K_2 of the usual failure equation

$$N_{fail} = K_1 \epsilon^{K_2}$$

as functions of temperature and of the values for K_1 and K_2 at 70 °F (21 °C) in the case that values are not available for each of the seasonal temperatures. This algorithm and related statements were moved to the beginning of the routine, out of the original loop over the season index. When values either input or calculated for K_1 and K_2 are available for each season, GRESPl is called; then a loop over season index and an inner loop over radius index are initiated, the appropriate amplitude is recalled from the array of amplitude values, and GRESPl is called, returning the radial strain under the asphalt layer and its variance. These values, along with K_1 and K_2 and related stochastic parameters for the current season, are entered into a series of rather long and complex expressions to obtain N_{fail} and its variance for each season and wheel load (indexed by the static solution index).

The values of strain, variance of strain, K_1 , K_2 , N_{fail} and its variance are printed for each static solution, along with its identifying temperature and radius. Then, as in ROUGH, a loop is initiated over the total number of seasons required to reach the last value input under the TRANDOM keyword, the season index is generated for each season, and within that season a loop over radius is performed with its accompanying calculation of the static solution index. The appropriate average daily traffic is selected just as before, but then is converted to total axle (loadings) in the season, rather than to axles per second. This is converted to axles per season for each radius, ($N_{i,k}$) and Miner's Law is then invoked to obtain the damage index for each season.

$$DI(\text{season}_k) = DI(\text{season}_{k-1}) + \sum_{i=1}^{N_{\text{radius}}} \frac{N_{i,k}}{N_{\text{fail } i,k}}$$

The variance of damage index is calculated similarly.

Since cracking damage is a strictly accumulative process (at least as modeled here) it is possible to separately accumulate the damage and its variance attributable to each radius (wheel load). This has been done, and the variables DSUM and VSUM, indexed by the radius index, contain this information at the end of the simulation. These are passed to a new routine, CRPRNT, where they are normalized by the total damage and total variance for all radii and are printed in a table with radius, amplitude, resulting wheel load (the only place wheel load is printed) and fraction of traffic at that wheel load. This allows the effect of higher axle loadings on the pavement performance in to be quickly ascertained in terms of the ratio of fractional damage to fractional number of axle loads.

Low Temperature Cracking Predictions

The available models for prediction of low-temperature cracking include Program COLD (Ref. 5¹), the Shahin-McCullough Model (Refs. 6² and 7³), and the Hajek-Haas Model (Refs. 8⁴ and 9⁵). Study of these models indicated the following:

1. Program COLD is aimed at predicting if cracking will occur, not when it will occur and at what crack frequency.
2. The Shahin-McCullough Model does offer cracking frequencies and output on a probabilistic basis, but requires quite a bit of sophisticated input and does not appear to offer much more reliable predictions than the much simpler Hajek-Haas Model.

¹Finn, F. N., C. Saraf and R. Kulkarni, "Development of Pavement Structural Subsystems," Final Report NCHRP 1-10B, July 1976.

²Shahin, M. Y., "Prediction of Low-Temperature and Thermal-Fatigue Cracking of Bituminous Pavements," University of Texas, PhD Dissertation, August 1972.

³Shahin, M. Y., "Design System for Minimizing Asphalt Concrete Thermal Cracking," Proceedings, Fourth International Conference on Structural Design of Asphalt Pavements, August 1977.

⁴Hajek, J. J., "A Comprehensive System for Estimation of Low-Temperature Cracking Frequency of Flexible Pavements," The Transport Group, Department of Civil Engineering, University of Waterloo, Waterloo, Canada, July 1971.

⁵Haas, R. C. G., "A Method for Designing Asphalt Pavements to Minimize Low-Temperature Shrinkage Cracking," Research Report 73-1, The Asphalt Institute, January 1973.

3. The Hajek-Haas Model is a statistical development based on measured data that is only strictly applicable to the areas of Canada in which the crack observations were taken. However, the parameters it considers are those known to be important to the formation of transverse cracks and it should have reasonable applicability to areas of the northern United States where transverse cracking is most prevalent.

Mr. E. C. Novak reported on a detailed study in Michigan (Ref. 10¹) and found the Hajek-Haas equation to be unreliable for Michigan pavements. Unfortunately, the equation published in Reference 9 was incorrect, so his study was duplicated during this project using the correct equation and the results appear in Appendix D.

It appears that the Hajek-Haas Model offers almost the reliability of the more rational Shahin-McCullough Model and has the important added advantage of relative simplicity in providing input values for its use. Both procedures are limited by the high sensitivity of low-temperature cracking (and indeed any fracture problem involving tensile stresses) to many more parameters than can be reasonably or accurately defined in the analysis, and neither will consistently give reliable predictions. It may be noted from field data such as that in Table 34 of Appendix D that there are wide variations in actual cracking observed for apparently similar pavement sections, so it is not surprising that predictive models should be unable to attain a high confidence level when so much variability exists in nature.

In view of the results noted in Appendix D, the considerations discussed above and the results of a factorial study of computed results for a broad range of input values, the Hajek-Haas Model was selected for use and has been incorporated into VESYS A.

The Hajek-Haas Model consists of a single rather complex regression equation which yields Cracking index I, the number of full plus half the number of half transverse cracks per 500 feet (152 m) of roadway, from the values of: m , the winter design temperature, °C; s , the stiffness of the asphalt cement at temperature m , kg/cm², as defined by McLeod's method; a , the age of the pavement, years; t , the thickness of the asphalt, inches; and d , a dimensionless code for the type of subgrade (5-sand, 3-loam, 2-clay). The correct equation is:

¹Novak, E. C., Jr., "Evaluation of a Model for Predicting Transverse Cracking for Flexible Pavements," Research Division Michigan Highway Commission, February 1976.

$$10^I = 2.497 \times 10^{30} \times (0.1s)^{(6.7966 - .8740t + 1.3388a)} \\ \times (7.054 \times 10^{-3})^d \times (3.193 \times 10^{-13})^{-0.1m} \times d^{(.06026s)}$$

or, in a more usable form (taking the logarithms of both sides),

$$I = 30.3974 + (6.7966 - .8740t + 1.3388a) (\log_{10} s - 1) \\ - 2.1516d + 1.24958m + (.06026s) (\log_{10} d)$$

Subroutine LOTMPC was written to evaluate this equation from the asphalt thickness THICK1, the times TRANDOM, and the values of stiffness, winter design temperature, and subgrade code input under the new keywords STIFF, WINTTEMP, and SUBTYPE. These keywords were added to the appropriate data statement and suitable default, maximum and minimum values were provided (See Table 3 at the end of this chapter). These new parameters are made available to LOTMPCR and the new common block /LOTGR/, which also contains the computed values of cracking index for all the time values input under TRANDOM. These time values are converted to seconds for use in the cracking and roughness calculations, but a loop in CRACKS converts them to years before LOTMPC is called; they are then converted to seconds on return from LOTMPC.

(A note of warning: The variable YEAR which is used for the conversion is perhaps incorrectly named; it actually contains the constant required to convert TRANDOM time values to seconds from whatever units they are input in, specified by the TUNITS keyword. If low temperature cracking is to be calculated, and/or if the column headings YEARS in several of the repeated load subroutines are to be accurate, the times input under the TRANDOM keyword must be in years, and TUNITS must be 6.)

Cracking index values returned from LOTMPC are converted to units of yd^2 cracked per 1000 yd^2 (0.8 m^2 per 800 m^2) as follows:

Let w be the width of the roadway (ft),
and n be the number of full cracks + half the number of
half cracks in a 500 foot (152 m) length of roadway
(cracks assumed to be transverse)

then $\frac{500w}{9}$ is the area in square yards of 500 feet (152 m) of
 nw is the total crack length in feet.

$$\text{thus } \frac{nw}{500w/9} = \frac{9nw}{500w} = \frac{9n}{500} = \frac{18n}{1000}$$

is the total crack length (ft) per square yard of pavement, and we have then

$$\frac{18 n \text{ ft}}{1000 \text{ sq. yd.}} \times (1000 \text{ sq. yds.}) \times \frac{(1 \text{ yd})}{(3 \text{ ft})} = 6n$$

yards of crack length per 1000 square yards of pavement.

If we now assume a single transverse crack $6n$ yards long, it will pass over $6n$ different "square yards"; we can also imagine transverse cracks, well spaced, whose total length is $6n$ yards, and the total number of square yards transverse will remain $6n$. This will remain true until the average crack spacing becomes small enough that the random placement of cracks leaves more than one crack in a "square yard." The smallest average crack spacing observed in this investigation was about 5 yards (4.5 m); therefore the derivation and result are assumed valid here, to the required degree of accuracy.

Finally, the values of cracking index, average crack spacing, and square yards cracked per 1000 square yards for low temperature cracking are printed with the results for fatigue cracking; an additional column contains the total square yards cracked per 1000 square yards, approximated here by the simple sum of the results from the two distress mechanisms. This tends to maximize the effect of low temperature cracking, since the two mechanisms yield cracks in perpendicular directions, and a single square yard could easily have both types of cracks. This total is limited to a maximum value of 1000 before being printed.

It should be noted that in the derivation of the regression equation the winter design temperature was defined as lowest temperature at or below which only 1 percent of the hourly air temperatures in January occur for the severest winter during a 10 year period. Hajek and Haas have provided a relation between the design temperature defined this way and freezing index, and also provide freezing index maps for the United States and Canada. These aids, which will be discussed further in Chapter IV make this method useful even where (as is probably true in most places) such detailed weather records are not available.

Subroutine to Save Static Solutions

In the discussion of program modifications above, reference was made to an alternative capability to that for isolated Type 3 runs (those not following Type 1 runs). This was done for reasons mentioned there, but in addition the isolated Type 3 runs (involving use of punched computer files) are not practical at a remote job entry

site with no card punch facility. However, it is useful and convenient to be able to rerun simulations in which only parameters affecting repeated load solutions are changed; therefore, a new means of saving the results of the relatively more time-consuming static solution was designed and implemented in VESYS A.

The keywords SAVETAPE, READTAPE and NOTAPE control the generation and use of a file (TAPE 1; or on logical unit 1) holding the static solution data. If SAVETAPE is read at the beginning of a type 1 run, then at the end of the computations for static solutions the relevant data (detailed in Appendix E) are written to logical unit 1, followed by an end of file. If this is the first such set of solutions in a job, unit 1 is rewound before the file is written. Physically unit 1 can be either a tape file or a disk file, but one must be careful in the latter case to declare that file to be a permanent file (in CDC terminology) or otherwise to ensure that it will remain accessible at a later time. In the case of magnetic tape files, the initial rewind may be undesirable, as positioning after other files already on the tape might be wanted. In such a situation the statements

```
IF(IENT.EQ.0) REWIND 1
IENT = 1
```

should be removed from subroutine DOTAPE. After writing to logical unit 1, the program then writes the same data on the output file on a special page.

The keyword READTAPE, when read for a Type 3 run, instructs the program to read data from logical unit 1 into special arrays in subroutine DOTAPE, after all other card input data for the run has been read. Validity checks are then made between the card input data and the data read from the external file as follows:

1. Is the number of seasons (keyword NTEMPS) the same?
2. Is the number of radii (NRADIUS) the same?
3. Is the number of Dirichlet coefficients (NDELTA) the same?
4. Is the thickness of asphalt (THICK1) the same, to ± 0.2 inches (0.5 cm)?
5. Is the thickness of the base (THICK2) the same, to ± 0.2 inches (0.5 cm)?

If all these questions are answered affirmatively, the data is then stored in the normal manner for use in the repeated load solution just as if it had been calculated on the same computer run. If one or more of these tests are failed, then the parameters tested, both those input from cards and those input from the data

file, are printed and the program terminates its execution. In all cases, the contents of the title array from the data file are printed along with the above parameters and the values of temperature and radius.

The keyword NOTAPE is used in the second and following data decks (ended by ENDOFRUN, not by ENDOFJOB, which terminates execution) of a multiple Type 3 computer run, where all of the decks are for runs making use of the same set of static solutions. This causes the program to bypass the reading of the file, since the data are already in the memory. It is required, not optional, in such cases. Where more than one file of data exists on logical unit 1, which is never rewound in the read (Type 3) mode, such data could be read and used either by omitting the NOTAPE directive (in the case of one simulation run per set of static solutions) or by entering the READTAPE key word again in the first deck making use of the new set of static solutions.

Appendix E describes the structure of these static-solution files.

Verification of Program Changes

The many changes to VESYS IIM to produce VESYS A required that a program verification analysis be performed: the changes of indexing, dimensions, common blocks and input, even more than those involved in direct computation, were so numerous that small errors could easily creep in. This verification was performed after each major set of program changes, and consisted of tests against previous runs and comparisons with what might reasonably be expected (in the testing of new features).

The first set of verification runs was made after the modification for seasonal variation of materials properties. They were made with a basic data deck corresponding to runs made at ARE in 1975 to test the expected life/service life routines; the deck was modified as necessary for the new features. The term OLD program will refer to VESYS IIM as received from FHWA in June 1976, with the variables LY1 and LY2, used in the UNLOAD portion of the static solutions, returned to their previous (ARE) values of 6 and 8, respectively.

The sequence of runs was as follows (runs are identified by the last two characters of the CDC job name):

<u>RUN</u>	<u>DATE</u>	<u>PROGRAM</u>	<u>COMMENTS</u>
DM	8/30	OLD	Output identical to service life examples, FH-1, 1975.
4E	9/23	OLD	T = 60°F (15.6°C), 1 season.
N3	9/30	NEW	T = 60°F (15.6°C), 1 season. Output identical to 4E.
H7	10/6	NEW	T = 60°F (15.6°C), 4 season. Output identical to 4E and N3 except for variance of cracking.

Jobs DM, 4E, N3, and H7 demonstrate that for NTEMP = 1 the program options selected therein (TYPE 1 and TYPE 3 runs) were not affected by the changes, and further, that, with the exception of the variance of cracking (a separate problem in formulation discussed in Appendix F), the results from the use of four identical "seasons" (involving four static load solutions and the corresponding complex indexing of data and results) are the same as those from a run using only one "season." The exception mentioned is not a result of the program changes, as the particular algorithm involved was not modified; in fact, a later demonstration run on the version as received from FHWA showed the same changes in variance of cracking with number of seasons. The source of the changes was later demonstrated mathematically to be inherent in the algorithm.

The second verification sequence followed the addition of multiple-radius solutions; here there were even more changes of indexing and dimensions (commonly lumped under the term "book-keeping"); in addition a major conceptual change was made in the manner in which a distribution of axle (or wheel) loads was handled. Again, an extensive comparison was performed with the aim of exercising all the new options and all of the new indexing and associated loops.

The following computer runs were made with the data input as indicated (the basic data deck was the same as that used for the previous verification runs; comparison is with job N3 in that verification sequence, and hence to the results from the original program with which job N3 agreed in every detail):

<u>Name</u>	<u>NTEMP</u>	<u>NRADIUS</u>	<u>Comments</u>
B4	1	1	Same as N3 except for the variance of the normal deflection and the

<u>Name</u>	<u>NTEMP</u>	<u>NRADIUS</u>	<u>Comments</u>
			resulting roughness parameters (very slight difference). All cracking output and the rut depth itself agree. (VCAMP = 2644.)
DJ	2	2	4 static solutions, all for T = 60°F (15.6°C), R = 4.24 inches (10.8 cm). Results-4 solutions are all identical, and agree with single solution in B4. Repeated load gives same rut depth as B4. VCAMP = 0 so variances are different (traffic distribution was 75%-25% on the two (equal) radii, each using 75 psi (518 kN/m ²) tire pressure).
UB	1	1	VCAMP = 0. <u>Everything</u> in repeated load solution is identical to that in DJ except the variance of cracking; the value obtained can be mathematically predicted from that for DJ, and the predicted and observed values agree.
60	1	1	VCAMP = 2644. Same input as B4; run after locating and correcting an error in subroutine ROUGH. Now gives answers identical to N3 in all respects (used static solutions generated by B4).
J4	1	4	All radii identical-test of indexing changes. This job and the one following (NB) used a different data set from the others in this sequence. Lambda = 5000 (constant with time).
NB	1	4	Same as J4 (used same static solutions) except LAMBDA = 8000. Test of concept of saving and reusing static solutions, and of changes in repeated load subroutines. The ratio of "value" (J4) to "value" (NB), where "value" is a predicted behavior, was in all cases what one expected from the equations.

In addition to this series of comparisons, computer runs have been made modeling several AASHO test sections and are discussed in Chapter V. Suffice it here to say that using 4 seasons and 4 radii for a total of 16 static solutions in each case, the program generally behaved well and gave answers encouragingly close to those observed.

One point, however, deserves specific notice relative to verification of program changes. In the assumption of a traffic distribution (modeling the graph of number of axles vs. axle load by a 4 bar histogram) the actual random time distribution of loads is replaced by a strict sequence: within each season all the loads of the first weight are applied, then all the loads of the second weight, etc. It was felt that this was indeed more accurate than representing all the loads by a single radius, a single amplitude, and a large value of the variance VCAMP; however, if the order in which the loads were applied made a significant change in the results, there would be a problem in interpreting the results.

For fatigue cracking, the cumulative damage (as modeled in VESYS A) is a completely additive process (Miner's law). and hence the order of the load is immaterial. For rut depth, the process involved is quite different: at the beginning of a new season/load combination, the damage (rut depth) to date is converted in effect to a number of load applications which under the new conditions (load, temperature, etc.) would yield that rut depth. This is added to the number of load applications for the new season/load combination, and a new rut depth calculated. It is not obvious from the structure of the equations involved that the order in which the loads are applied will have little effect on the final rut depth, although after several years (many seasons) the order within seasons might be expected to have less effect.

In fact, however, hand calculations using the same equations and static solutions, but reversing the order of the loads, resulted in very small changes in the final rut depth. Specifically, for AASHO section 266, the program predicted ".092009 rut depth after one year. A hand calculation in the same order differed by .03%; a hand calculation in which the order of loads was reversed (to heaviest first) differed by 0.5%, and a hand calculation (rather extreme) in which the order of seasons was reversed (to Fall, Summer, Spring, Winter) and the loads were applied as in the program (lightest to heaviest) differed by 2.2% after one year. The first year is the one in which the rut depth increases most rapidly. In addition, hand calculations for the second year, for lightest loads first and for heaviest loads first, yielded rut depths differing only by 0.2%; apparently the error becomes less as time goes on, as was expected.

The last step in verification involved the input, calculation and printout of the low temperature cracking; the values printed were compared with values obtained earlier by hand and from a large factorial study using only the low-temperature cracking routine and a simple driver program. The results were the same, indicating again that the new input parameters were being properly indexed, stored and used.

Later extensive use of the program has increased our confidence in the new version; we have encountered nothing in six months of nearly continuous use to suggest the presence of errors in the modification.

Summary of Keywords Added, Deleted and Changed

In the process of modifying the VESYS IIM program to provide the new capabilities described above, new forms of data were required, and the need for some old forms was removed. These changes are reflected in the modifications to the key word "dictionary," all of which are described in the internal user's guide; they will be listed and briefly discussed here also.

Table 2 lists the keywords which were removed. They were associated with card input for isolated Type 3 runs, providing the data summarizing an earlier, single, static solution. The associated variables, with the exception of those associated with GNURAD and ALFRAD (not used previously) are still used in the same manner as before; only the capability of card input for these variables has been removed.

TABLE 2 . LIST OF KEYWORDS REMOVED FROM VESYS-A

Keyword	Associated Variable (original program)
CREEP1	E (I,1), I = 1, NDEL
CREEP2	E (I,2), I = 1, NDEL
CREEP3	E (I,3), I = 1, NDEL
GRADIAL	GRAD(I), I = 1, NDEL
GNORMAL	GNORM(I), I = 1, NDEL
ALFRAD	ALF(7)
ALFNORM	ALF(4)
GNURAD	GMU(7)
GNUNORM	GMU(4)
COEFGRAD	GCVAR(7)
COEFGNRM	GCVAR(4)

Table 3 lists the new keywords, the associated internal variable names and dimensions, the default values, and the upper and lower limits if a single variable and not an array. Some of the limits have not been changed to appropriate values for keywords which replaced others in the keyword data statement; in general these are cases where true limits could be applied where previously the limits were very nearly $\pm \infty$.

It should be noted (as it is in the internal input guide) that the keywords SEASMULT, GNU, and ALPHA are accompanied by an integral value expressed as a decimal digit that indicates the layer to which the data read from the following card apply; hence one will normally have several occurrences of each of these keywords in a data deck.

Another point to note is that if NRADIUS is either set equal to 1 or not specified (defaulting to 1) then the RADIUS and AMPLITUD keywords are interpreted as they were in VESYS IIM: the value in the numeric field immediately following the keyword contains the single value of radius or amplitude required, and no additional data-only card is read. Thus, if NRADIUS = 1, using the default value for TRDIST(1) = 1., the program behaves exactly (with respect to radius and tire pressure specification) as VESYS IIM did.

TABLE 3 . NEW OR CHANGED KEYWORDS

<u>Key Keyword</u>	<u>Associated Variable</u>	<u>Dimensions</u>	<u>Default</u>	<u>Lower Limit</u>	<u>Upper Limit</u>	<u>Comments</u>
SEASMULT	SMLT	(25,2)	1.			Was GGU(3)
GNU	GGU	(25,3)	none			Was ALPH(3)
ALPHA	ALPH	(25,3)	none			Negates the effect of the PUNCH keyword
NOPUNCH	PUNCH	-	No cards punched			To save static solu- tions data, IFSAVE = 1
SAVETAPE	IFSAVE		0			To read static solution data, IFREAD = 1
READTAPE	IFREAD		0			Sets both IFREAD and IFSAVE to 0
NOTAPE						Not used now; intended to be available to control some debug- ging print as needed.
DETAIL	DETAIL		.FALSE.			The limits should be changed to 1 and 12.
NRADIUS	NRAD		1	-10 ¹¹	+10 ¹¹	
RADIUS	RADIUS	(12)	RADIUS(1) = 6.			
AMPLITUD	AMPL	(12)	RADIUS (2-12) = 0. AMPLI(1) = 75.			
LOADDIST	TRDIST	(12)	AMPL(2-12) = 0. TRDIST(1) = 1.			
TRAFMULT	TRMULT	(24)	TRDIST(2-12) = 0. TRMULT(1-24) = 1.			
WINTTEMP	TDW		0.	-100.	+100.	
STIFF	STF		0.	0.	10,000.	
SUBCTYPE	SBCT		2.	2.	5.	

CHAPTER III
SELECTION OF INTERSTATE HIGHWAYS FOR
FOUR ENVIRONMENTAL ZONES

The environment in which a pavement system exists has a significant effect upon that pavement's response to the traffic loads imposed upon it. In order to consider this important parameter in this study, FHWA asked that four interstate highway sections be selected for the study, one from a cold climate and generally high humidity and rainfall to be called "wet-freeze", one from a cold climate with little rainfall and humidity to be called "dry-freeze", one from a relatively warm climate with high humidity and rainfall to be called "wet-no freeze", and one from a relatively warm climate with little rainfall and humidity to be called "dry-no freeze".

As there are numerous highway sections that would meet the environmental requirements, the opportunity existed for making selections based on a number of practical considerations including: 1) Availability of data to describe the pavement structure, the traffic and axle load distribution and the environment from the pavement viewpoint for the VESYS A computer program, 2) The interest level of State Department of Transportation personnel in VESYS and this project as this would impact upon the cooperation received in accumulating the required data, 3) Traffic levels for commercial vehicles so that two levels of traffic may be established, one low and one high and 4) Pavement structure so that two levels could be used, one quite substantial and one relatively thin section.

The Departments of Transportation at both Utah and Florida were engaged in the implementation of the VESYS IIM system and had active programs of their own to accumulate data and test materials in order to service the input requirements. This involvement offered an opportunity to obtain rather directly information significant to the successful idealization of pavement systems from personnel with a vested interest in the VESYS analytical system, so it was decided to utilize a pavement from Utah as dry-freeze and one from Florida as wet-no freeze.

Reference 11¹ also classified pavements studied according to the same environmental designations and gave valuable information on a range of flexible pavements that could be considered for this study. Review of this reference led to the selection of a section of IH-80 from the rehabilitated AASHO Test Road as the wet-freeze section. Other considerations

¹Darter, M. I., E. J. Barenberg and J. S. Sarvan, "Maintenance-Free Life of Heavily Trafficked Flexible Pavements, a paper presented at the 55th Annual Meeting of the Transportation Research Board, January 1976.

leading to this selection were that all aspects of the AASHO Road Test were so thoroughly documented and that permanent deformation and creep compliance test results were already available for soils in this area from previous projects. Data was available for this section of IH-80 in References 12¹ and 13².

This left the selection of an area to represent the dry-no freeze condition, which was reasonably represented by sections of California, Arizona, New Mexico or Texas. On the basis of availability of data, a section of IH-20 between Midland, Texas and Odessa, Texas was selected as it had been thoroughly studied in other projects and considerable data was available about its materials, its traffic and its environment.

Selections of specific sections of Utah and Florida were made in coordination with Department of Transportation personnel in those states. This led to the selection of a section of IH-80N near the border between Utah and Idaho as dry-freeze and a section of IH-10 located approximately 5 miles (8 km) west of Madison, Florida to represent wet-no freeze.

The interstate highway selections were the result of research study, discussion with State Department of Transportation personnel, coordination with the Federal Highway Administration and discussions with other knowledgeable persons. The final selections were as follows:

1. Wet-Freeze - a section of the rehabilitated AASHO Test Road just west of Ottawa, Illinois, that appears as "Flex 7" in Reference 5 and Section 038 in Reference 6. This section is an outside lane 12 ft. (3.6m) wide with a 12 ft. (3.6m) shoulder. The pavement structure consists of 4.5 inches (11.4 cm) of asphalt concrete, 8.5 inches (21.6 cm) of crushed stone, 23.0 inches (58.4 cm) of gravel and a silty clay subgrade.
2. Dry-Freeze - a section of IH-80N just south of the Utah-Idaho border. This is a relatively thin section consisting of 4.25 inches (10.8 cm) of asphalt concrete, 5.0 inches (12.7 cm) of gravel base and a subgrade of non-plastic sandy silt.
3. Wet-No Freeze - a section of IH-10 located approximately 5 miles (8.05 km) west of Madison, Florida. The pavement structure for this section consists of three inches of asphalt concrete, 10.5 inches (26.7 cm) of lime rock base, 12 inches (30.5 cm) of stabilized sand subgrade (natural sand mixed with 25 percent lime rock base) and a natural sand embankment.

¹Little, R. J., L. J. McKenzie and P.G. Dierstein, "The Rehabilitated AASHO Test Road, Part I - Materials and Construction", Interim Report IHR-28, Illinois Department of Transportation, July 1973.

²"The AASHO Road Test - Report 5 - Pavement Research", Highway Research Board Special Report 61E, 1962.

4. Dry-No Freeze - a section of IH-20 in Ecotr County between Midland, Texas and Odessa, Texas. The pavement structure for this section includes 3.3 inches (8.4 cm) of asphalt concrete, 0.6 inches (1.5 cm) of double bituminous surface treatment 19.0 inches (48.3 cm) of flexible base and sand subgrade.

CHAPTER IV

DEVELOPMENT OF INPUT DATA FOR VESYS A ANALYSIS

The data requirements for VESYS A include those input parameters used in VESYS IIM and the new input parameters required for the program improvements described in Chapter II. It was necessary to draw on a number of sources in order to arrive at realistic input values for the solutions required by this study. The previous work reported in Reference 1 provided realistic data for a number of the variables of general nature, but the more specific information required to define the pavement structure, the traffic loads imposed and environment had to be obtained from other publications and from State Department of Transportation personnel.

The pavement sections for which realistic data were required included:

1. Sections 266, 272, 308 and 470 in the AASHO Road Test.
2. Sections 3, 4, 11 and 17 from the Brampton Test Roads.
3. The four interstate highway sections described in the previous section.
4. The factorial of 8 real and hypothetical sections used in the factorial study of cost versus legal axle limits.

The sections identified in Items 1, 2 and 3 above were used for "calibration" of the model while those described in Section 4 were utilized for the study.

The input requirements introduced by the improvements to VESYS IIM embodied in VESYS A necessitated the establishment of seasonal pavement temperatures, seasonal permanent deformation characterizations, seasonal layer stiffness characterizations, low temperature cracking input values and axle load distributions for the four legal axle limits. The development of the input data for these five general parameters are discussed individually below.

Seasonal Pavement Temperatures

It is very important to establish the average pavement temperatures to be expected for the particular environment in which the pavement exists, in terms of environmental data readily available. Pavement temperature has been found to be a strong function of air temperature and of solar radiation as well as other variables, but only the air temperatures are generally readily available. In order to estimate pavement temperatures for the diversity of environmental zones of

interest, relationships between air temperature and pavement temperatures available in the literature were studied to develop a means of predicting pavement temperature from air temperature data for each environmental zone. The data considered included a test pavement at College Park, Maryland (Ref. 14)¹, a pavement near Potsdam, New York (Ref. 15)², a pavement in Michigan (Ref.16)³, a Texas sandstone mix (Ref. 17)⁴, a pavement in Florida (Ref.18)⁵, and the AASHO Road Test pavements (Ref. 13). The approach taken was to study whatever data was available to ascertain how the pavement temperature related to air temperatures on a daily cycle, monthly cycle and seasonal cycle to the extent that the data was available. Study results were accumulated in the form of ratios of pavement temperatures to air temperatures and, in the case of the AASHO Road Test pavements, the difference between pavement temperature and air temperature. The results of this work were compared to similar more general data developed by Witczak (Ref. 19)⁶. Comparisons of the Witczak plotted curves and the data derived from the study indicated that Witczak's curves approximate the College Park, Maryland data, predicted 2 or 3°F (1.1 or 1.7°C) high for Texas, predicted 4 or 5°F (2.2 or 2.8°C) low for Michigan, and predicted as much as 8°F (4.4°C) low for New York. The general conclusion, based on this data would then be that the Witczak plots underestimate pavement temperatures for the north, estimate very closely pavement temperatures for College Park, Maryland, and slightly overestimate pavement temperatures in the south.

The VESYS analytical system can consider temperatures for whatever increments of time are assigned. In previous work, temperatures

¹Kallas, B.F., "Asphalt Pavement Temperatures, College Park, Maryland", Highway Research Record 150, 1968.

²Straub, A.L., H.B. Schenk Jr., and F. E. Przybycien, "Bituminous Pavement Temperature Related to Climate", Highway Research Record 256, 1968.

³Manz, G. P., "A Study of Temperature Variation in Hot-Mix Asphalt Base, Surface Course and Subgrade", Highway Research Record 150, 1968.

⁴Long, R.E., "Relationships Between Control Tests for Asphalt Stabilized Materials", Texas A & M University, PhD Dissertation, May 1971.

⁵Ruth, B.E., "Evaluation of Flexible Pavement Systems to Determine Low Temperature Cracking Potential", Report to Florida Department of Transportation from Engineering and Industrial Experiment Station, College of Engineering, University of Florida, August 1975.

⁶Witczak, M.W., "Design of Full-Depth Airfield Pavement", Proceedings, Third International Conference on the Structural Design of Asphalt Pavements, 1972.

were assigned monthly, utilizing the mean temperatures for that month. For VESYS A, the use of 12 "seasons" was not feasible because VESYS A generates a static solution for each combination of season and radius in the discretized axle load distribution. This means that a combination of 4 seasons and 4 radii in VESYS A will require approximately 16 times as much computational effort as a similar problem for VESYS IIM because the very large majority of the computational effort is required for the static solutions. For the reasons previously discussed on pages 6 and 7, a season for the VESYS A solutions is usually taken to represent a quarter of a year and the corresponding temperature is arrived at by averaging the mean temperatures for those three months comprising the season. It is felt that the use of these average air temperatures modified to pavement temperatures by appropriate ratios representing the same seasons will provide reasonably accurate pavement temperatures. The ratios of pavement temperature to air temperature derived from this limited study appear in Table 4 on a seasonal basis. It was found that these ratios (or multipliers) tend to grow excessively in magnitude as the air temperature approaches zero, so differences in temperature were used for these lower temperatures to arrive at the best estimates for pavement temperatures. For instance, based on the limited data available, it was decided that the pavement temperature was best arrived at for the AASHO Road Test sections by adding 27°F (15°C) to the air temperature if the pavement temperature was less than 40°F (4.4°C). If the pavement temperature was more than 40°F (4.4°C) only 24°F (13.3°C) was added.

The data derived from this study of pavement versus air temperatures plus the curves appearing in Ref 19 were used to convert air temperatures to pavement temperatures for this project. The resulting pavement temperatures appear in Table 5. It should be remembered that these are mean pavement temperatures and that they may be much greater around mid-day and much less at night.

Seasonal Permanent Deformation Characterizations

The ability of VESYS A to consider seasonal permanent deformation characterizations for each of the layers probably represents the most important improvement to its ability to simulate a real flexible pavement system. It is necessary, however, in order to accrue any benefit from this improvement, to define how the permanent deformation potential of the various layer materials vary seasonally. As the permanent deformation parameters ALPHA and GNU are quite new to our profession, very little data exists as to either the correct values that should be used in general or how these values change on a seasonal basis. Consequently, it was necessary to conduct a detailed study for the material types in each layer in order to establish realistic input value for the parameters.

Table 4. Ratios of Seasonal Average Pavement Temperature to Air Temperature at 2 to 4 Inches (5.1 to 10.2 cm) Below the Surface, Various Locations.

<u>Location</u>	Ratio of Pavement Temperature to Air Temperature			
	<u>Winter</u>	<u>Spring</u>	<u>Summer</u>	<u>Fall</u>
Maryland	1.11	1.21	1.23	1.16
Michigan			1.20	
New York	1.46*	1.30	1.24	1.13
Florida	1.17			
AASHO Road Test			1.42*	

* Ratios of pavement temperature to air temperature increase as air temperatures decrease toward zero.

Table 5. Pavement Temperatures by Season

Pavement Identification	Pavement Temperature, °F*			
	Winter	Spring	Summer	Fall
AASHO Sections 266, 272, 308 and 470 and Illinois IH-80 Section 38 (Flex 7)	51	69	96	73
Brampton Test Road Sections 1, 4, 11 and 17	-2	42	75	51
Utah IH-80N	56	71	95	65
Florida IH-10 and Wet-No Freeze, Factorial Study	78	95	106	94
Texas IH-20 and Dry-No Freeze, Factorial Study	54	76	94	75
Wet-Freeze, Factorial Study	35	66	92	60
Dry-Freeze, Factorial Study	38	62	89	49

* °C = 0.5554 (°F-32)

These studies and their results are described in detail in Appendices A, B, and C for asphalt concrete, typical base materials and typical clay subgrade materials, respectively. As discussed in these Appendices, the trends for seasonal variation in these input parameters were established through study of papers available that reported the results of long-term repetitive load tests on various materials in such format that ALPHA and GNU could be determined, from previous testing reported in Reference 1 and other testing conducted for this project. The resulting conclusions appear at the end of each of these Appendices and are given below:

1. Asphalt concrete:

- a. Permanent strain is extremely temperature dependent as indicated by project testing and by all other test results in the literature. As an example, the permanent strain at 100°F (37.8°C) was around 30 times that for 70°F (21.1°C) at a stress of 30 psi (207 kN/m²) and 100,000 load cycles.
- b. GNU(1) and ALPHA(1) both decreased with increasing stress. Decrease in ALPHA(1) dominates to cause an important increase in permanent strain with increasing stress.
- c. It appears that the mechanisms affecting permanent strain differ above and below some temperature in the order of 60°F (15.6°C) to 70°F (21.1°C). Below 15.6°C, GNU(1) increases with temperature and ALPHA(1) increases slightly with temperature for the higher stress levels, but decreases at the lower stress levels. Above 15.6°C, both ALPHA(1) and GNU(1) decrease with increasing temperature. The rate of increase in permanent strain with increasing temperature is much higher after 15.6°C than it is at the lower temperatures.
- d. The dynamic modulus is clearly somewhat stress dependent. Above the 15.6°C to 21.1°C zone, the dynamic modulus increased with stress level. Below 15.6°C, it decreased markedly with increased stress level.
- e. The dynamic modulus has a well defined negative correlation with temperature. It decreases from over 1 million psi (6,900,000 kN/m²) at low temperatures to less than 100,000 psi (690,000 kN/m²) at higher temperatures. This is not new information, but has been noted in all papers in recent years that report the results of repetitive-load tests on asphalt concrete.

2. Base layer materials:

- a. ALPHA(2) for granular base materials appear to be little effected by varying stress levels.

- b. Crushed limestone will generally have less permanent strains than gravel under the same compactive energy and stress conditions.
- c. Permanent strains are greatly increased by increasing moisture content. For example, an increase from 4.7 to 5.5 percent moisture content resulted in an increase in permanent strain for one soil from 0.0015 inches per inch to 0.0071 inches per inch.
- d. The resilient modulus for dry crushed stone may be expected to be much higher than that for the same crushed stone with capillary saturation or inundation.
- e. ALPHA(2) appears to be essentially independent of both deviator stress and lateral stress, but GNU(2) increases with deviator stress, thus causing an increase in permanent strain. GNU(2) decreases with increasing lateral pressure, thus causing decreased permanent strain.

3. Silty clay subgrades:

- a. GNU(3) generally increases as moisture content increases and decreases as density increases. An apparent sharp decrease in GNU(3) may occur if sufficient moisture exists to accept pore pressure.
- b. ALPHA(3) may increase or decrease somewhat with increasing moisture content, depending on the nature of the soil and the amount of moisture present. The variation due to moisture appears to depend on clay content. ALPHA(3) for the silty clays seemed to be almost independent of moisture while ALPHA(3) for the "heavier" clay appears to vary much more with moisture content.
- c. Both ALPHA(3) and GNU(3) increase together as moisture increases until ALPHA(3) reaches some level (higher maxima for higher density), and then ALPHA(3) continues to increase while GNU(3) sharply decreases. This implies that at some point of moisture increase the fraction of total strain that is permanent decreases (fraction of resilient strain increases) although the magnitude of permanent strain is increasing. This probably is due to limitations of a constant triaxial pressure to simulate resistance to large strains (consistent with higher moisture content) imposed by subgrade soils in the field. Stated differently, the passive case for coefficient of lateral earth pressure likely applies after many wheel loadings in the field so that cell pressure needs to increase as the test progresses in order to simulate these conditions accurately.

- d. ALPHA(3) appears to be relatively independent of deviator stress if the clay content is low, but may vary considerably as clay content increases.
- e. GNU(3) appears to be relatively independent of deviator stress at lower moisture contents, but decreases sharply at higher moisture contents as deviator stress increases (possibly due to pore water accepting some of the stress increase).
- f. Typical values of ALPHA(3) appear to range from 0.65 to 0.95.
- g. Typical values of GNU(3) appear to range from 0.01 to 0.40, but can range much higher for unusual cases or materials.

The information on variations of ALPHA and GNU for the three layers were combined with data furnished by State Departments of Transportation in Utah and Florida, data available from Reference 1 for the AASHO Road Test and typical data for sandy soils for the Texas sections were used to arrive at suitable initial values for ALPHA and GNU. These values were later modified in some cases as a result of iterative study of cause and effect engaged in during the calibration phase of this project. This iterative study and these modifications will be discussed in more detail in subsequent chapters. The final values used for ALPHA and GNU appear in Table 6.

Table 6. Seasonal Permanent Deformation Parameters,

ALPHA and GNU

Pavement Identification	Layer Identification	ALPHA				GNU			
		Winter	Spring	Summer	Fall	Winter	Spring	Summer	Fall
AASHO Section 266	Surface	0.93	0.90	0.75	0.87	1.39	0.91	0.21	0.88
	Base	0.94	0.94	0.94	0.94	1.63	5.51	1.63	1.63
	Subgrade	0.97	0.97	0.97	0.97	0.10	0.10	0.10	0.10
AASHO Section 272	Surface	0.94	0.92	0.77	0.88	14.01	10.01	2.70	9.71
	Base	0.94	0.94	0.94	0.94	1.89	6.39	1.89	1.89
	Subgrade	1.00	1.00	1.00	1.00	0.00	0.00	0.00	0.00
AASHO Section 308	Surface	0.93	0.91	0.76	0.88	0.88	0.63	0.15	0.61
	Base	0.93	0.93	0.93	0.93	1.59	5.37	1.59	1.59
	Subgrade	0.97	0.97	0.97	0.97	0.09	0.09	0.09	0.09
AASHO Section 470	Surface	0.93	0.91	0.76	0.88	2.41	1.72	0.40	1.67
	Base	0.94	0.94	0.94	0.94	1.73	5.87	1.73	1.73
	Subgrade	0.79	0.79	0.79	0.79	0.12	0.12	0.12	0.12
Brampton Section 3	Surface	0.70	0.76	0.72	0.81	0.24	0.36	1.00	0.70
	Base	0.93	0.93	0.93	0.93	0.25	0.25	0.25	0.25
	Subgrade	0.88	0.88	0.88	0.88	0.03	0.03	0.03	0.03
Brampton Section 4	Surface	0.77	0.80	0.72	0.87	0.24	0.36	1.50	0.90
	Base	0.88	0.88	0.88	0.88	0.05	0.05	0.05	0.05
	Subgrade	0.84	0.84	0.84	0.84	0.03	0.03	0.03	0.03
Brampton Section 11	Surface	0.64	0.72	0.67	0.72	0.07	0.13	0.70	0.40
	Base	0.89	0.89	0.89	0.89	0.13	0.13	0.13	0.13
	Subgrade	0.84	0.84	0.84	0.84	0.03	0.03	0.03	0.03
Brampton Section 17	Surface	0.64	0.72	0.67	0.72	0.07	0.13	0.70	0.40
	Base	0.88	0.88	0.88	0.88	0.19	0.19	0.19	0.19
	Subgrade	0.84	0.84	0.84	0.84	0.03	0.03	0.03	0.03
Illinois IH-80 Section 38 (Flex 7)	Surface	0.65	0.89	0.80	0.90	0.05	0.10	0.15	0.10
	Base	0.93	0.93	0.93	0.93	2.00	3.00	2.00	2.00
	Subgrade	0.86	0.86	0.86	0.86	0.12	0.12	0.12	0.12
Utah IH-80N	Surface	0.79	0.72	0.45	0.75	0.12	0.18	0.05	0.20
	Base	0.90	0.90	0.90	0.90	0.50	0.50	0.50	0.50
	Subgrade	0.92	0.92	0.92	0.92	0.15	0.15	0.15	0.15
Florida IH-10	Surface	0.59	0.40	0.30	0.40	0.21	0.07	0.03	0.07
	Base	0.89	0.89	0.89	0.89	0.20	0.20	0.20	0.20
	Subgrade	0.90	0.90	0.90	0.90	0.25	0.25	0.25	0.25
Texas IH-20	Surface	0.67	0.65	0.48	0.65	0.40	0.30	0.15	0.30
	Base	0.91	0.91	0.91	0.91	0.20	0.20	0.20	0.20
	Subgrade	0.90	0.90	0.90	0.90	0.30	0.30	0.30	0.30

Table 6. Seasonal Permanent Deformation Parameters,
ALPHA and GNU (continued).

Pavement Identification	Layer Identification	ALPHA						GNU			
		Winter	Spring	Summer	Fall	Winter	Spring	Summer	Fall		
Wet-Freeze, Thin Pavement, Factorial Study	Surface	0.81	0.86	0.68	0.85	0.09	0.15	0.04	0.14		
	Base	0.92	0.92	0.92	0.92	0.35	0.46	0.35	0.35		
	Subgrade	0.90	0.90	0.90	0.90	0.25	0.25	0.25	0.25		
Wet-Freeze, Thick Pavement, Factorial Study	Surface	0.81	0.86	0.68	0.85	0.09	0.15	0.04	0.14		
	Base	0.92	0.92	0.92	0.92	0.25	0.32	0.25	0.25		
	Subgrade	0.90	0.90	0.90	0.90	0.15	0.15	0.15	0.15		
Dry-Freeze, Thin Pavement, Factorial Study	Surface	0.83	0.85	0.70	0.86	0.11	0.15	0.04	0.16		
	Base	0.92	0.92	0.92	0.92	0.35	0.46	0.35	0.35		
	Subgrade	0.90	0.90	0.90	0.90	0.25	0.25	0.25	0.25		
Dry-Freeze, Thick Pavement, Factorial Study	Surface	0.83	0.85	0.70	0.86	0.11	0.15	0.04	0.16		
	Base	0.92	0.92	0.92	0.92	0.25	0.33	0.25	0.25		
	Subgrade	0.90	0.90	0.90	0.90	0.15	0.15	0.15	0.15		
Wet-No Freeze, Thin Pavement, Factorial Study	Surface	0.82	0.70	0.55	0.71	0.11	0.04	0.02	0.05		
	Base	0.92	0.92	0.92	0.92	0.35	0.35	0.35	0.35		
	Subgrade	0.90	0.90	0.90	0.90	0.25	0.25	0.25	0.25		
Wet-No Freeze, Thick Pavement, Factorial Study	Surface	0.82	0.70	0.55	0.71	0.11	0.04	0.02	0.05		
	Base	0.92	0.92	0.92	0.92	0.25	0.25	0.25	0.25		
	Subgrade	0.90	0.90	0.90	0.90	0.15	0.15	0.15	0.15		
Dry-No Freeze, Thin Pavement, Factorial Study	Surface	0.82	0.83	0.72	0.84	0.10	0.14	0.05	0.14		
	Base	0.92	0.92	0.92	0.92	0.35	0.35	0.35	0.35		
	Subgrade	0.90	0.90	0.90	0.90	0.25	0.25	0.25	0.25		
Dry-No Freeze, Thick Pavement, Factorial Study	Surface	0.82	0.83	0.72	0.84	0.10	0.14	0.05	0.14		
	Base	0.92	0.92	0.92	0.92	0.25	0.25	0.25	0.25		
	Subgrade	0.90	0.90	0.90	0.90	0.15	0.15	0.15	0.15		

Seasonal Layer Stiffness Characterizations

The use of seasonal multipliers to modify creep compliance curves on a seasonal basis was discussed briefly in the introduction and in a little more detail in Chapter II. The use of multipliers to modify the creep compliance curve has the effect of maintaining the shape of the creep compliance curve, but increasing or decreasing the magnitudes of the creep compliance array. While there is undoubtedly some variation in the shape of the curve with seasonal changes and moisture content or if the base material is frozen, the creep compliance for base and subgrade materials is not heavily dependent on load duration, so maintaining a constant shape should have little effect on the values of creep compliance used.

There is not appreciable information in the literature as to the variation of creep compliance for subgrades and base material with moisture change or other variables. However, there is considerable body of information available for the variation in resilient modulus with various changes in moisture content, density and freeze-thaw cycles. If one arrives at a set of appropriate multipliers in terms of resilient modulus, the inverse of the multiplier will be the appropriate multiplier for the creep compliance array. Consequently, it is possible to utilize the data available for variation in resilient modulus directly to arrive at multipliers for creep compliance and this was done on this project.

As the seasonal variation in creep compliance (or layer stiffness) may only be arrived at reasonably in terms of the variation in the nature of the material due to some environmental process, it is necessary to define the variation in the material prior to arriving at rational values of the multipliers. The most important single variation in the material to be considered is change in moisture content. A study of the literature was conducted to arrive at the incidence of moisture change at subgrade materials from as wide a base of data as possible. Some of the references included in the study were References 20¹, 21², 22³ and 23⁴. Reference 21 was especially

¹Haliburton, T.A., "Subgrade Moisture Variations", Final Report, Oklahoma Research Program, Project 64-01-3, School of Civil Engineering, Oklahoma State University, August 1970.

²Dempsey, B.J., "Climatic Effects on Airport Pavement Systems State of the Art", Final Report FAA-RD-75-196, U.S. Army Engineer Waterways Experiment Station, June 1976.

³Bergan, A.T. and C.L. Monismith, "Characterization of Subgrade Soils in Cold Regions for Pavement Design Purposes", Highway Research Record 431, 1973.

⁴Cumberledge, G., Cominsky, R. J. and Bhajandas, A.C., "Moisture Variation Beneath Highway Pavements and the Associated Changes in Subgrade Support", Commonwealth of Pennsylvania, Department of Transportation, 1973.

useful as it was itself a detailed summary of the majority of the information available on the subject. The following was concluded from this study and includes only those study results of specific interest to this project:

1. There are few clear trends of a general nature that may be applied to predict moisture content on a seasonal basis at a high confidence level for any pavement subgrade or base other than those upon which the data was based. The moisture content in terms of seasonal trends not only varies from site to site, but may vary from one year to the next at the same site. Consequently, a prediction of moisture content has to be based on the particular environmental conditions at the site of interest, the nature of the subgrade material, the location of the water table and other parameters.
2. Several researchers have found relationships between the equilibrium moisture content under the pavement and the plastic limit of the subgrade soil. Conversely, no good relationship has been developed between precipitation and moisture content in the subgrade.
3. In-situ moisture content for clay subgrades will generally exceed the optimum moisture content. The opposite is true for sands.
4. Several researchers have found that the maximum moisture contents occur during the winter or spring months; however, this may not be true in locations such as Florida where sandy subgrades prevail and periods of high rainfall occur generally in different seasons from most of the United States.
5. Magnitudes of seasonal moisture changes are generally in the order of two or three percent, but such small changes in magnitude of moisture content can result in very considerable changes in layer stiffness.
6. There is a general trend toward increase in moisture content with time.
7. Moisture content correlates better with rainfall after the pavement surface becomes cracked so that moisture may enter the base and subgrade from above.
8. It is important to know the depth of frost penetration as the stiffness is greatly increased for a layer when it is frozen. Also, the moisture content will generally be quite high during the spring thaw, thus greatly decreasing the stiffness (i.e., increasing the magnitudes of creep compliance) for this season.

As there were no truly general trends that could be used to develop seasonal multipliers, it became necessary for specific pavements to draw on regional data wherever possible. For example, Ref.13 provides data on frost penetration depths, seasonal moisture contents of subgrade

and base and measured values of elastic modulus for several sections during the spring and summer of 1960. There were also seasonal measurements of elastic modulus using plate bearing tests on the base, subbase and embankment over a period of nearly two years. This latter gave a rather direct variation in stiffness on a seasonal basis and was used as a basis for defining the seasonal multipliers. For the other locations, regional information on changes in moisture content on a seasonal basis were obtained to the extent possible and seasonal multipliers developed on the basis of anticipated variation in resilient modulus as a function of variation in moisture content.

There are also some variations in dry density that occur seasonally, especially where deep frost penetration and a serious spring breakup occurs. While these variations may only be in the order of one pcf, the effect on the layer stiffness can be worthy of consideration.

The values of seasonal multipliers resulting from this study are listed in Table 7. These seasonal multipliers were applied by VESYS A to modify seasonally the constant arrays of creep compliance values appearing in Table 8. (The development of values of creep compliance in the next chapter).

Low Temperature Cracking

Input values for low temperature cracking were required for all pavement sections analyzed, except for Texas IH-20, Florida IH-10, wet-no freeze and dry-no freeze cases where serious frost penetration was not expected. As the age of pavement and thickness of the bituminous layer are otherwise input to the computer program, the only additional information required is a numerical code representing subgrade soil type (2 for clay, 3 for loam and 5 for sand), the winter design temperature in °C and the original asphalt cement stiffness.

The subgrade soil type may be readily identified from knowledge of the site, but the other values are somewhat more complex and are arrived at as described in Appendix G. The values used for these studies appear in Table 9.

Table 7. Seasonal Multipliers for Creep Compliance Arrays, Base and Subgrade

Pavement Identification	Layer Identification	Seasonal Multipliers			
		Winter	Spring	Summer	Fall
AASHO Sections 266, 272, 308 and 470	Base	0.88	1.23	1.00	0.90
	Subgrade	0.86	1.23	1.00	0.88
Brampton Sections 3,4,11 and 17	Base	0.80	1.25	1.00	0.90
	Subgrade	0.80	1.25	1.00	0.90
Illinois IH-80, Section 38 (Flex 7)	Base	0.88	1.23	1.00	0.90
	Subgrade	0.86	1.23	1.00	0.88
Utah IH-80N	Base	0.90	1.20	1.00	0.95
	Subgrade	0.95	1.20	1.00	0.95
Florida IH-10	Base	1.00	0.77	1.47	1.23
	Subgrade	1.00	1.00	1.00	1.00
Texas IH-20	Base	1.10	1.05	1.00	1.05
	Subgrade	1.00	1.00	1.00	1.00
Wet-Freeze, Factorial Study	Base	0.88	1.23	1.00	0.90
	Subgrade	0.90	1.15	1.00	0.92
Dry-Freeze, Factorial Study	Base	0.90	1.20	1.00	0.95
	Subgrade	0.95	1.10	1.00	0.95
Wet-No Freeze, Factorial Study	Base	0.68	0.52	1.00	0.84
	Subgrade	1.00	1.00	1.00	1.00
Dry-No Freeze, Factorial Study	Base	1.10	1.05	1.00	1.05
	Subgrade	1.00	1.00	1.00	1.00

TABLE 8. Creep Compliance in Constant Value Arrays for Base and Subgrade Layers

<u>Pavement Identification</u>	Creep Compliance, $\text{PSI}^{-1} \times 10^{-5} *$	
	<u>Base Material (LAYER2)</u>	<u>Subgrade (LAYER3)</u>
AASHO Road Test Section 266	6.24	4.50
AASHO Road Test Section 272	6.04	2.35
AASHO Road Test Section 308	6.22	3.75
AASHO Road Test Section 470	6.13	9.00
Brampton Test Road Section 3	6.00	2.86
Brampton Test Road Section 4	6.67	2.00
Brampton Test Road Section 11	5.72	2.50
Brampton Test Road Section 17	5.78	1.67
Illinois IH-80, Sect. 38	3.00	5.00
Utah IH-80N	2.79	2.00
Florida IH-10	2.25	4.00
Texas IH-20	2.79	4.50
Factorial Study:		
Thin Pavement Section	2.50	12.00
Thick Pavement Section	3.00	7.50

* 1 $\text{kN/m}^2 = 0.145 \text{ psi}$

Table 9. Input data developed for low temperature cracking predictions.

<u>Pavement Identification</u>	<u>Subgrade Type</u>	<u>Winter Design Temp. (°C)</u>	<u>Asphalt Cement Stiffness (kg/Cm²)</u>
Brampton Section 3	3	-26	203
Brampton Section 4	3	-26	193
Brampton Sections 11 and 17	3	-26	95
Utah IH-80N	3	-18	30
AASHO Road Test and Illinois IH-80	2	-20.5	45
Dry Freeze	2	-18	37
Wet Freeze	2	-20	37
Texas IH-20 and Dry-No Freeze	South of zone where frost penetration expected		
Florida IH-10 and Wet-No Freeze	South of zone where frost penetration expected		

Axle Load Distributions for the Four Legal Axle Loads

The improvements incorporated into VESYS A, the detailed development of the input data and the careful construction of the study factorial were all critical to the success of this research project, but meaningful results also depend rather directly on identification of axle load distributions representative of those that would occur for the higher legal limits. This is a complex question that is strongly dependent on such specifics as 1) allowable dimensions of equipment, 2) economics of buying new equipment to take advantage of larger weight limits, 3) density of commodities carried, 4) density mix of commodities carried, 5) applicable bridge formulas, 6) user tax structure and many others. Because of the complexity of the question and its importance, axle load distributions for use in this study were developed after careful consideration of the literature, correspondence with agencies representing the trucking industry and study of W-4 tables from a number of states, including those with relatively higher legal axle limits.

Fortunately, this question had been considered in detail previously by Winfrey and others (References 21¹ and 22²) and methods developed for predicting these axle loads. Typical axle load distributions grouped by single and tandem axles (See Figure 1) appear in Reference 24 and include data from states having 18, 20 and 22-kip (8100, 9000, and 9900 kg) single axle limits and related tandem axle limits of 32, 35 and 38-kips (14440, 15750 and 17100 kg), respectively. Predicted axle load distributions for 24-kip (10,900 kg) single and 41-kip (18,600 kg) tandem axles are also included. Further study appeared to reinforce the validity of these axle load distributions, so the decision was made to combine these single and tandem axle load distributions on a rational basis and to use them for this study.

In order to combine the single and tandem axle load distributions, it was necessary to arrive at the ratio of each to the total number of axle loads in a typical truck traffic stream. Study of W-4 tables from California, New York, Maryland, Pennsylvania, New Jersey, South

¹Winfrey, R., and others, "Economics of the Maximum Limits of Motor Vehicle Dimensions and Weights", Volume 1, Report No. FHWA-RD-73-69, September 1968.

²Whiteside, R. E., T.Y. Chu, J. C. Cosby, R. L. Whitaker, and R. Winfrey, "Changes in Legal Vehicle Weights and Dimensions, Some Economic Effects on Highways", NCHRP Report 141, 1973.

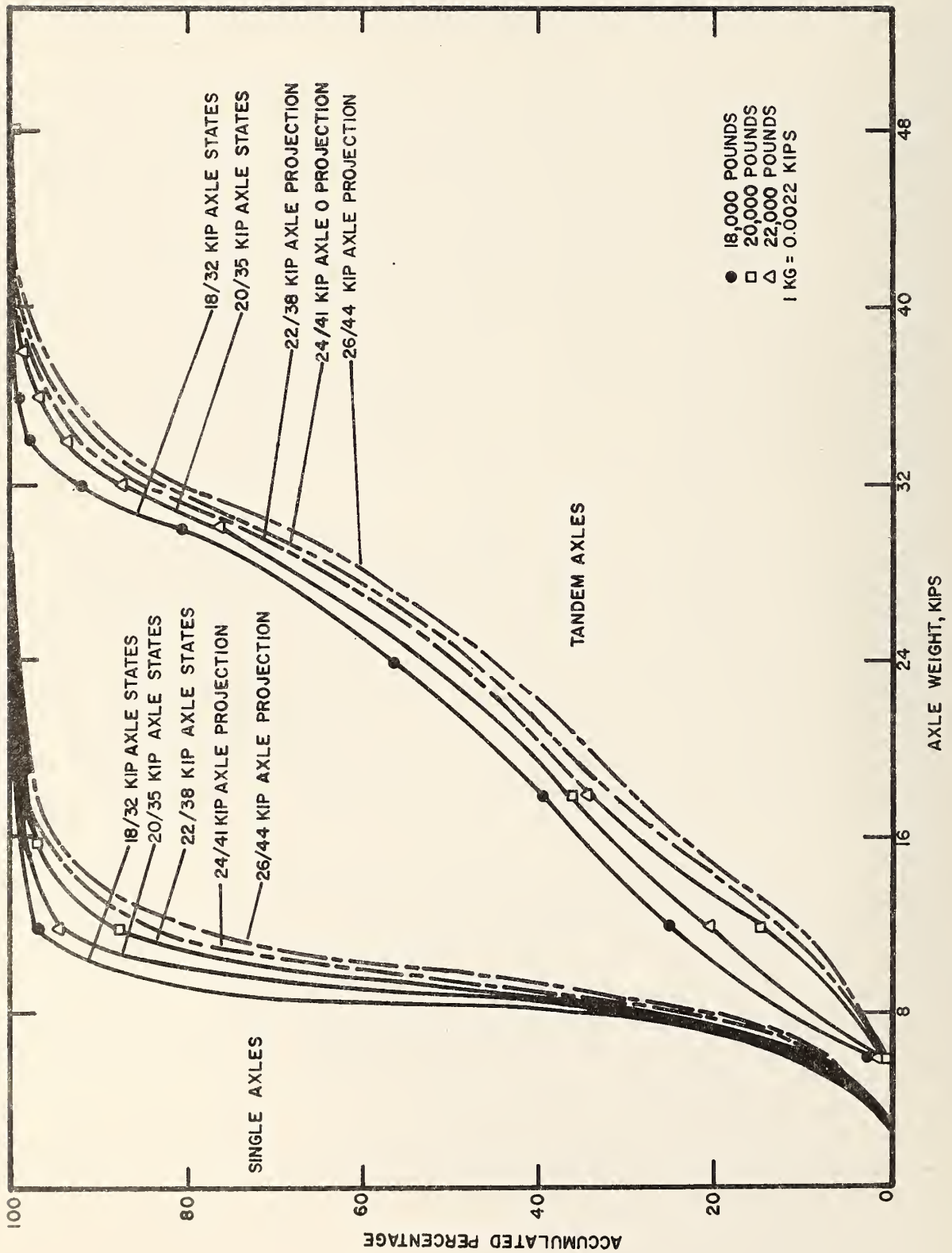


FIGURE 1. Examples of curves showing distribution of axle weight by vehicle class from a truck weight study (solid curves). (From Ref. 24)

Dakota, Kansas and Texas led to a typical axle mix of 52 percent tandem axles to 48 percent single axles. By applying this ratio and multiplying the number of tandem axles by 2.25 (in lieu of 2.0 to consider approximately the superposed effects from the adjacent axle) to convert them to approximate equivalent single axles, the axle load distributions appearing in Table 11 were derived. These values were used for the study.

The axle load distributions shown in Table 11 were each divided into four discrete segments for separate consideration in VESYS A as shown in Table 10.

TABLE 10. Discretized Representations of Legal Axle Load Distributions by Percent of Total

Legal Axle Load Limit (Kips)	1 kg = 0.0022 kips			
	2 to 8 kips	8 to 12 kips	12 to 18 kips	18 to 28 kips
18	34.1	41.9	23.5	0.5
20	30.4	41.6	26.0	2.0
22	27.2	40.7	29.1	3.0
24	23.7	41.0	31.5	3.8

It was assumed that tire pressures for the axle load increments would be 75 psi (5.2 kg/cm²) for the 2 to 8-kip increment, 80 psi (5.5 kg/cm²) for the 8 to 12-kip increment, 85 psi (5.9 kg/cm²) for the 12 to 18-kip increment and 90 psi (6.3 kg/cm²) for the 18 to 28-kip increment. These estimated values were based on general data obtained from queries to agencies representing the trucking industry. Calculations were made for each discrete increment in Table 10, using all included increments in Table 11 to arrive at a weighted mean value of radius of area loaded by a single wheel load (dual wheels considered as a single wheel) for each legal axle load and each discrete increment of the axle load distribution. A mean value of the four mean radii calculated for each axle load increment in Table 11 was then obtained as a common radius for all legal axle load limits. This was done to restrict the number of internal static solutions required without loss of accuracy. The values of AMPLITUD (approximate equivalent of tire pressure) were the modified slightly to insure that the correct weighted wheel load resulted for each legal axle load. The values of radii, AMPLITUD, and resulting values of wheel load used appear in Table 12.

Fatigue Potential Characterizations

Realistic prediction of fatigue cracking damage is necessary as the fatigue cracking mode of distress is the one that most frequently creates the need for overlaying pavements. This means that the materials characterizations used in the classical fatigue equation must be realistic.

TABLE 11. Axle load distributions in percent of total representing different single axle load limits

Legal Axle Load Limits (kips)	Axle Load Increments, Kips *												
	2 to 4	4 to 6	6 to 8	8 to 10	10 to 12	12 to 14	14 to 16	16 to 18	18 to 20	20 to 22	22 to 24	24 to 26	26 to 28
18	7.5	11.2	15.4	30.8	11.1	8.1	11.5	3.9	0.4	0.1			
20	5.8	9.7	14.9	27.7	13.9	9.1	11.6	5.3	1.4	0.4	0.1	0.1	
22	2.5	9.2	15.5	23.8	16.9	10.5	12.5	6.1	1.9	0.6	0.2	0.2	0.1
24	2.0	8.1	13.6	23.2	17.8	11.3	13.1	7.1	2.2	1.0	0.2	0.2	0.2

* 1 kg = 0.0022 kips

NOTE: 52 percent of total number of axles were found to be tandem axles, and one set of two axles in tandem was considered as 2.25 single axles instead of 2.0 to approximate equivalency between tandem and single axles.

TABLE 12. Values of AMPLITUD and resulting wheel loads

Legal Axle Load Limits (kips)	AXLE LOAD INCREMENTS, KIPS							
	2 to 8		8 to 12		12 to 18		18 to 28	
	AMPLITUD (PSI)	Mean Wheel Load, Lbs.	AMPLITUD (PSI)	Mean Wheel Load, Lbs.	AMPLITUD (PSI)	Mean Wheel Load, Lbs.	AMPLITUD (PSI)	Mean Wheel Load, Lbs.
18	71.34	2,730	78.52	4,765	84.71	7,321	87.21	9,700
20	73.15	2,799	79.43	4,820	85.09	7,354	89.01	9,900
22	77.83	2,978	81.19	4,927	85.03	7,349	91.41	10,167
24	78.11	2,989	81.31	4,934	85.24	7,367	92.04	10,237
Radii, Inches	3.49		4.395		5.245		5.95	

1 kN/m² = 0.145 psi 1 inch = 2.54 cm

1 kg = 0.0022 kips

It has been quite common practice to base fatigue cracking predictions on materials characterizations derived from laboratory fatigue testing. The inadequacies of standard laboratory fatigue tests for simulating the stress state in and the fatigue response of a material in a real supported surface layer have been discussed in detail (Refs. 26¹ and 27²). In general, laboratory test such as standard beam tests relate to cracking at the bottom of a pavement whereas the cracking distress of interest is the appearance of cracks the surface. Wheel Tracking Tests reported by Van Dijk (Ref. 27), indicate that it takes around 8 to 10 times as many wheel loads to propagate a crack to the surface as it takes to initiate a crack at the bottom of the surface layer. Consequently, fatigue characterizations generally must be related to studies of real pavements or careful simulations in the laboratory to be meaningful for predictive use.

Kingham (Ref 28)³ and Austin Research Engineers (Ref 29)⁴ have independently conducted multiple regressions on AASHO Road Test data for cracking appearing at the surface. The values for the exponent K_2 were essentially identical, but Kingham's coefficient K_1 , was somewhat larger. Values of $K_1 = 2.6 \times 10^{-13}$ and $K_2 = 5.0$ were used to approximate the fatigue characterizations from the AASHO Road Test at a temperature of 70°F (21.1°C).

The seasonal values of $K_1(T)$ and $K_2(T)$ were arrived at by using the procedures described in References 1 and 21 for converting $K_1(70^\circ\text{F})$ and $K_2(70^\circ\text{F})$ to other temperatures, using the pavement temperatures shown in Table 5. The values of $K_1(T)$ and $K_2(T)$ used appear in Table 13.

Pavement Structure, Truck Traffic and Other Input Values

It was necessary to select typical low and high levels for both pavement structure and truck traffic as these were factorial variables. It was decided to use the Texas IH-20 pavement structure and truck

¹Rauhut, J.B., W. J. Kenis and W. R. Hudson, "Improved Techniques for Prediction of Fatigue Life for Asphalt Concrete Pavements", Transportation Research Record 602, 1976.

²Van Dijk, W., "Practical Fatigue Characterization of Bituminous Mixes", Paper presented at 1975 Annual Meeting of AAPT, Phoenix, February 1975.

³Kingham, R. I., "Failure Criteria Developed From AASHO Road Test Data", Proceedings, Third International Conference on the Structural Design of Asphalt Pavements, London, 1972.

⁴"Development of New Design Criteria for Asphalt Concrete Overlays of Flexible Pavements", Austin Research Engineers, Volume 1, Report No. FHWA-RD-75-75, June, 1975.

TABLE 13. Fatigue life potential characterizations for the four environmental zones and the four seasons

Environmental Zone	Seasons	Pavement Temperature (°F)	$K_1(T)$	$K_2(T)$
Wet-Freeze	Winter	35	2.6×10^{-15}	5.18
	Spring	66	1.7×10^{-13}	5.02
	Summer	92	5.2×10^{-11}	4.89
	Fall	60	4.4×10^{-14}	5.05
Dry-Freeze	Winter	38	3.1×10^{-15}	5.16
	Spring	62	7.3×10^{-14}	5.04
	Summer	89	2.6×10^{-13}	4.91
	Fall	49	1.0×10^{-14}	5.11
Wet-No Freeze	Winter	78	1.0×10^{-12}	4.96
	Spring	95	1.6×10^{-10}	4.88
	Summer	106	2.6×10^{-8}	4.82
	Fall	94	1.2×10^{-10}	4.88
Dry-No Freeze	Winter	54	1.8×10^{-14}	5.08
	Spring	76	5.7×10^{-13}	4.97
	Summer	94	1.2×10^{-10}	4.88
	Fall	75	4.7×10^{-13}	4.98

°C = 0.5554 (°F -32)

traffic as low levels and those for Illinois IH-80 as high values. This resulted in a "thin" pavement section having 3.9 inches (9.91 cm) of surface and 19.0 inches (48.3 cm) of base, and a "thick" pavement section having 4.5 inches (11.4 cm) of surface and 31.5 inches (80.0 cm) of base. The truck traffic values used appear in Table 14. These values are based on real data extrapolated rationally to 20 years. Where overlays were added, the extrapolation was continued past 20 years to allow prediction of expected life.

The same distributions of truck traffic in time were used for all legal axle loads, which implies an increase in tonnage with increasing legal axle loads. An alternative approach could have been decreases in traffic with increases in axle load distributions to maintain constant tonnage, but this was the less severe condition and the relative realism of either extreme is moot.

Creep compliance arrays for the asphalt concrete were developed for each of the pavement sections used in the comparative studies and for the factorial study. The values in these arrays were based on laboratory creep testing in some cases, resilient modulus testing results plus laboratory creep testing or judgment for a few cases based on comparisons of mix characteristics to others for which test data was available. The creep compliance arrays used appear in Table 15.

Other fixed values used as problem input and not discussed separately above appear in Table 16. These values were generally obtained from engineering experience and previous studies aimed at developing realistic input values for VESYS IIM.

TABLE 14. Truck traffic in Axles per Day

Time in Years from Construction (TRANDOM)	Axles per Day (LAMBDA)	
	Low Traffic	High Traffic
1	1770	2340
2	1810	4000
3	1860	5220
4	1910	6470
5	1970	7660
6	2030	8550
7	2100	8750
8	2170	9260
9	2250	9450
10	2330	9700
11	2410	9800
12	2480	10000
13	2590	10150
14	2690	10300
15	2790	10450
16	2890	10600
17	2995	10750
18	3100	10900
19	3210	11050
20	3340	11200

Table 15. Creep compliance arrays for LAYER1, asphalt concrete surface layer.

Permanent Identification	Creep Compliance, PSI-1 x 10 ⁻⁵ *												
	Load Duration, Seconds												
	.001	.003	.01	.03	.10	.30	1.0	3.0	10.0	30.0	1.00		
AASHO Road Test Section 266	.045	.063	.105	.180	.310	.480	.750	1.04	1.04	1.90	2.30		
AASHO Road Test Section 272	.052	.077	.120	.195	.320	.480	.850	1.25	1.75	2.40	3.10		
AASHO Road Test Section 308	.042	.057	.097	.150	.256	.410	.620	.870	1.23	1.56	1.72		
AASHO Road Test Section 470	0.48	.077	.113	.185	.325	.540	.910	1.33	2.00	2.60	3.00		
Brampton Test Road Sections 3&4	.045	.063	.105	.180	.310	.480	.750	1.04	1.45	1.90	2.30		
Brampton Test Road Sects. 11&17	.042	.057	.097	.150	.256	.410	.620	.870	1.23	1.56	1.72		
Illinois IH-80, Section 38	.045	.063	.105	.180	.310	.480	.750	1.04	1.45	1.90	2.30		
Utah IH-80N	.130	.158	.190	.230	.275	.330	.391	.435	.550	.680	.813		
Florida IH-10	.038	.051	.069	.090	.154	.218	.321	.462	.731	1.00	1.48		
Texas IH-20	.037	.049	.066	.085	.146	.207	.305	.440	.695	.950	1.41		
Factorial Study	.041	.056	.087	.133	.228	.343	.527	.740	1.07	1.42	1.85		

* 1 PSI = 0.069 kg/cm²

Table 16. Fixed Input Values

<u>Input Name</u>	<u>Description</u>	<u>Input Value</u>
BETA	Time-temperature shift function	0.054
COEFK1	Coefficient of variation for fatigue coefficient K_1	0.30
COEFK2	Coefficient of variation for fatigue exponent K_2	0.04
CORLCOEF	Materials coefficient B for the spacial auto-correlation function	1.00
CORLEXP	Materials exponent C for the spatial auto-correlation function	0.06
DURATION	Wheel load duration at a point, seconds	0.015
K1K2CORL	Correlation coefficient for K_1 and K_2	-0.867
NTEMPS	Number of points in temperature array	4
NTRADOM	Number of years considered	20
NTSTATIC	Number of points in creep compliance arrays	11
PSIFAIL	Level of serviceability index considered unacceptable	2.5
QUALITY0	Initial serviceability index	4.2
REFTEMP	Reference temperature for master creep compliance curves, °F.	70

TABLE 16. Fixed Input Values (continued).

<u>Input Name</u>	<u>Description</u>	<u>Input Value</u>
STDEVO	Standard deviation of initial serviceability index	0.25
TOLERNCE	Minimum acceptable reliability, percent	50
VARCOEF1	Coefficient of variation for surface layer creep compliance array	0.25
VARCOEF2	Coefficient of variation for base course creep compliance array	0.30
VARCOEF3	Coefficient of variation for subgrade creep compliance array	0.30
VCAMP	Variance of AMPLITUD or tire pressure	0
VCDUR	Variance of DURATION or wheel load duration	5.4×10^{-6}

CHAPTER V

CALIBRATION OF MODEL FOR REALISTIC PREDICTIONS

Several possibilities exist for calibration of a mathematical model such as VESYS A so that it produces calculated responses consistent with the real responses of the engineering system that it models. Three of these considered were: 1) the introduction of multipliers that will cause calculated responses to equal measured responses of the real system, 2) the introduction of functions that will transform the calculated responses to those measured, and 3) development of input data sufficiently consistent with the real conditions modeled and with the nature of the model itself such that the calculated responses are realistic. The introduction of either multipliers or functions is the most direct approach, but the multipliers are too simplistic and cannot be expected to be consistent for a range of conditions and the development of appropriate functions would represent a very considerable research project of its own. Consequently, the procedure employed for this project was an iterative procedure involving exercising the model to arrive at predictions, comparing the predictions to measured performance, analyzing the differences to assess their cause and rationally modifying the problem input where indicated to improve predictions. Only revisions to input values were made that could be justified rationally when short-comings of previous values were identified through analysis.

The initial step in this process was to develop input data for a number of cases for which measured responses were available. This included four sections from the AASHO Road Test, four sections from the Brampton Test Road, one section of IH-80N in Utah, and one section of IH-10 in Florida. The sections of IH-20 in Texas and of IH-80 in Illinois were also included for study although measured responses were not available. Solutions were obtained for these sections and compared to measured data. Studies were then initiated to determine what input variables could have caused differences between calculated and measured responses, whether the input values represented as accurate a characterization as was possible and whether review of the basis for arriving at the input values indicated logical modifications that might be expected to give more accurate calculated responses. Comparisons were also made between the calculated responses and the input data for the entire group of calculations in order to determine if the trends and variations between calculated and measured responses were consistent, if the relative values of inputs were consistent for the various cases considered and if these comparisons identified any obvious anomalies that should be corrected.

As the capability for considering seasonal characterizations of materials was new, it also became necessary, in order to understand

differences in predicted and measured rutting, to run a factorial of separate solutions using an elastic layered program called ELSYM5. Deflections were calculated for the various seasonal conditions and general equations from VESYS A applied to estimate separately the rutting that occurred in each season and in each layer. This gave valuable insight that was used to improve the values of ALPHA and GNU for the four seasons.

The effort conducted to arrive at a "calibrated" test factorial is described in subsequent sections in more detail.

Comparisons to AASHO Road Test Measurements

The four test sections from the AASHO Road Test used for this study were those previously used for similar comparisons in Reference 1. These were Sections 266, 272, 308 and 470. Actual materials from the AASHO Road Test site were tested during the research culminating in Reference 1 to arrive at both the creep compliance arrays in Tables 9 and 15 and the permanent deformation parameters. Therefore, a very considerable data base existed already for these four sections, but this data was in terms of the requirements for VESYS IIM and did not include the sophistication of characterizations in terms of seasonal variations, except for the creep compliance arrays for the asphalt concrete surface materials. Also, the temperatures used for the months of the year in the analyses of Reference 1 were air temperatures in lieu of pavement temperatures.

The pavement temperatures were established as previously described and these temperatures then became the basis for establishing seasonal values of ALPHA(1) and GNU(1) and for the fatigue parameters K_1 and K_2 . These values plus others already available provided the materials characterizations for the surface layer.

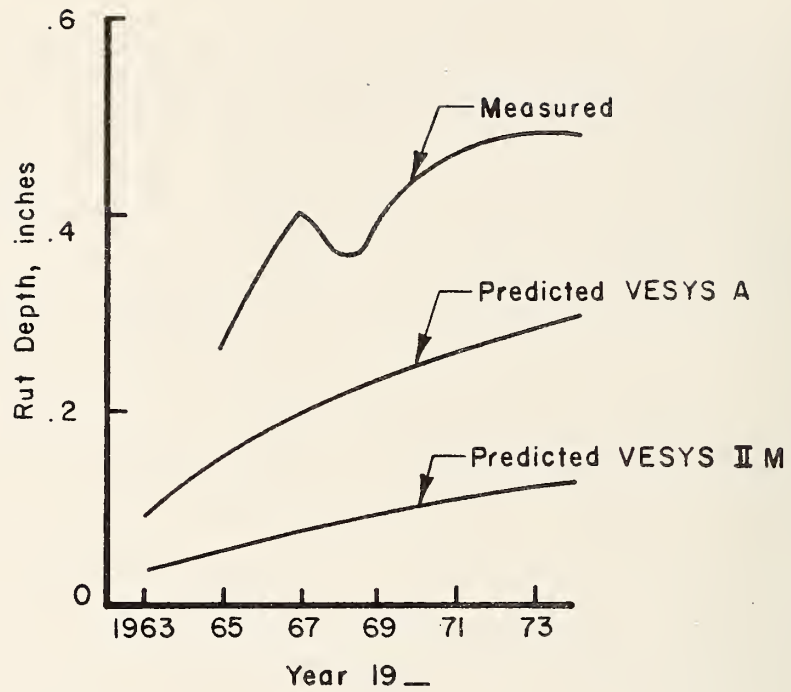
Fortunately, Reference 13 includes very detailed information on all pavement layers over a considerable period of time. Figure 97 in Reference 13 displays the results in terms of elastic moduli of plate bearing tests on the base course, subbase and embankment or subgrade layers. This provides very directly the modifications that should be made seasonally to the creep compliance arrays. By assuming the elastic moduli during summer as the base values (i.e., having seasonal multipliers of 1.00), mean values of elastic moduli for other seasons may be divided by the summer modulus to arrive at multipliers to convert to the appropriate stiffnesses during other seasons. This value can then be inverted to arrive at the appropriate seasonal multipliers for the creep compliance arrays. This was the approach taken to arrive at the seasonal multipliers for the AASHO Road Test sections appearing in Table 7. As VESYS A is a three layer model, it was necessary to combine on a weighted basis the multipliers

for the base and subbase to obtain the seasonal multipliers for the base as shown.

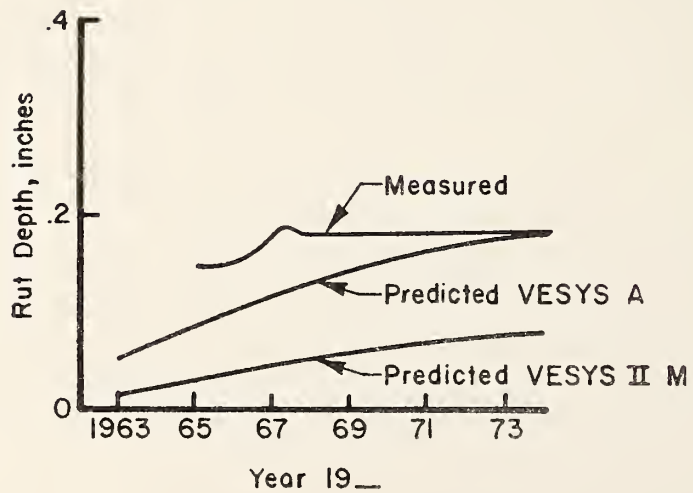
Table 34 of Reference 13 provided variations in moisture and density between Spring and Summer seasons for the base, subbase and subgrade. Depths of frost penetration also appeared on Page 11 as a function of time. Review of this data indicated that the change in moisture content for the subgrade was negligible and that the density variation was only about 0.7 pcf (11.2 kg/m³). A change in moisture content for the subbase from 5.5 percent to 4.8 percent is quite significant, however, as is a change from 4.3 percent to 3.6 percent for the base. These variations in moisture content seasonally and the presence of frost in the winter were considered in arriving at the permanent deformation parameters ALPHA and GNU for the base and subgrade.

The most difficult task, of course, was the establishment of the permanent deformation parameters for the three layers as functions of seasons. Because no precedents existed for doing this, the results of the studies described in detail in Appendices A, B, and C for the surface layer, base and subgrade, respectively, were used for establishing these values. The values of ALPHA and GNU appearing in Reference 1 were used as a starting point and all the information available was applied to arrive at the values of ALPHA and GNU appearing in Table 6.

Figure 2 provides measured rut depths and those predicted by VESYS IIM during the research leading to Reference 1 for AASHO Sections 266 and 308. As can readily be seen, the previous rut depth predictions were very much lower than those measured; the new predictions using VESYS A are also generally lower, but are much closer to those predicted. As air temperatures were used in lieu of pavement temperatures for the AASHO sections previously, this does not represent an entirely fair comparison. Therefore, a new run was made for Section 470 using pavement temperatures for VESYS IIM and these appear for rut depth, slope variance and present serviceability index predictions in Figure 3. Note that the predictions using pavement temperatures in VESYS IIM for rut depth are considerably better than those for air temperatures. A very significant additional improvement was made by including the seasonal materials characterizations in VESYS A, and the addition of the discretized representation of the axle load distribution to finish out the new VESYS A capabilities resulted in almost perfect predictions for the measured rut depth for this section. Looking now at slope variance, the addition of pavement temperature for VESYS IIM made very little difference, but the improvements in VESYS A gave a considerably higher prediction of slope variance. As might be expected, the additional rutting and slope variance predicted by VESYS A resulted in a considerable reduction in serviceability.

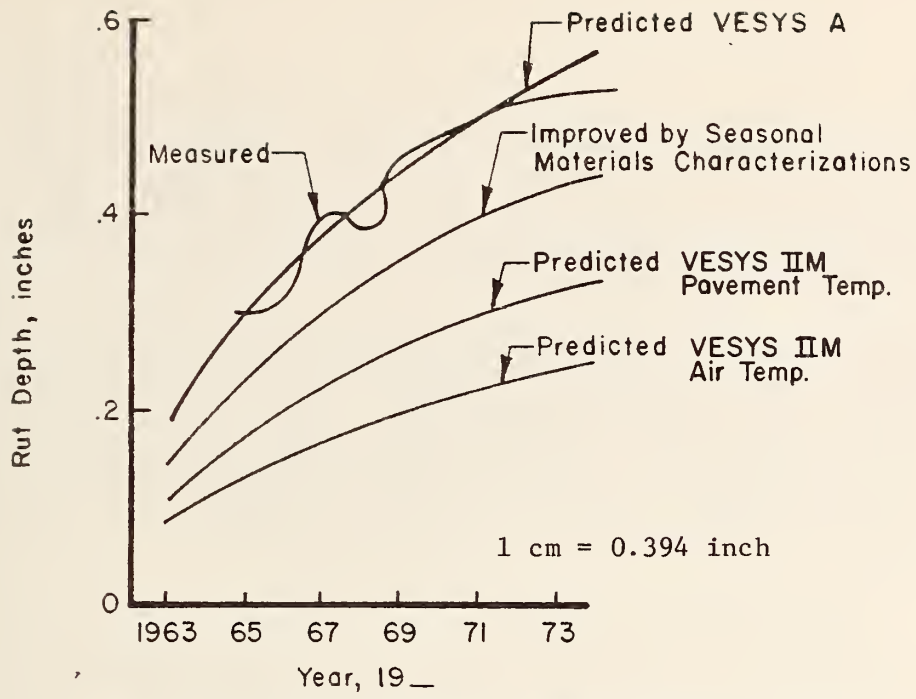


a. AASHO Section 266 1 cm = 0.394 inch

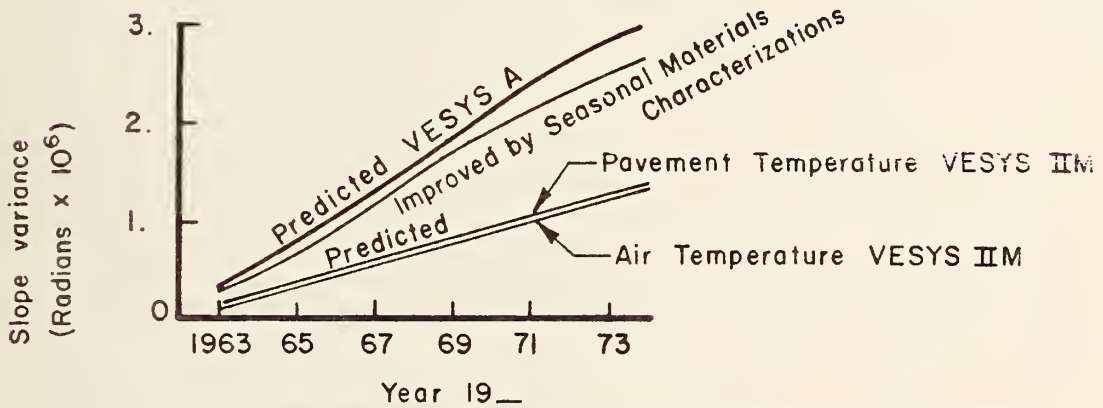


b. AASHO Section 308

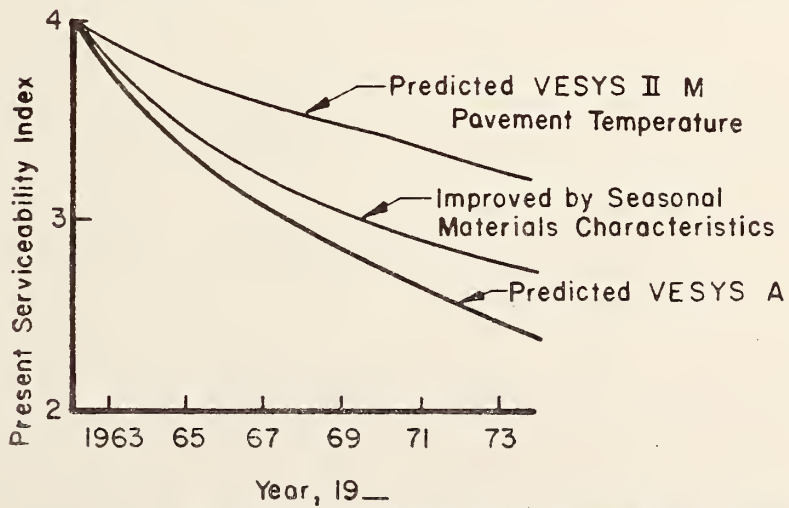
FIGURE 2. Comparisons of measured rut depths and those predicted by VESYS IIM and VESYS A



a. Rut depth predictions versus measured values



b. Slope variance predictions (no measured values available)



c. Serviceability predictions (no measured values available)

Figure 3. Comparisons of measured responses and those predicted by VESYS IIM and VESYS A, AASHO Section 470.

The comparisons are not plotted for AASHO Section 272 because the predictions using air temperature in VESYS IIM reported in Reference 1 exceeded the measured rut depths and those for VESYS A far exceeded the rut depths. This was attributed previously to a very high test value of GNU(1) and this is still believed to be the cause of the overprediction.

These studies for the AASHO Road Test Section provided a base for continued study and development, indicated clearly that the VESYS A model gave improved predictions as expected, showed that the VESYS model had no inherent limitations to predicting reasonable values if appropriate materials and traffic characterizations were provided and provided initial indications as to what changes in input values might be appropriate subject to further study.

Comparisons to Brampton Test Road Measurements

Sections 3, 4, 11 and 17 of the Brampton Test Road were also included in the previous studies and reported in Reference 1. The input used for the current study was a combination of that from the previous study and carefully derived data from References 30¹, 31², 32³, 33⁴, 34⁵, 35⁶, and 36⁷.

¹Schonfeld, R., "Construction of a Full-Scale Road Experiment as Part of a Unit-Price Contract," Department of Highways, Ontario Report No. RR119, December 1966.

²Phang, W. A., "Four Years Experience at the Brampton Test Road," Department of Highways, Ontario Report No. RR153, October 1969.

³Phang, W. A., "The Effects of Seasonal Strength Variation on the Performance of Selected Base Materials," Department of Highways, Ontario Report No. IR 39, April 1971.

⁴Haas, R.C.G., N. I. Kumel and J. Morris, "Brampton Test Road: An Application of Layer Analysis to Pavement Design," University of Waterloo, Ministry of Transportation and Communications Report No. RR182, November 1972.

⁵Kallas, B. F., "The Brampton, Ontario Experimental Base Project," Interim Report, Summary of Asphalt Institute Laboratory Test Results, February 1967.

⁶Kallas, B. F., "The Brampton, Ontario Experimental Base Project," Supplement to February 1967 Interim Report, Summary of Asphalt Institute Test Results, September 1967.

⁷Morris, J., "The Prediction of Permanent Deformation in Asphalt Concrete Pavements," The Transport Group, Department of Civil Engineering, University of Waterloo, Ontario, Canada, September 1973.

The construction of the sections including depths and density of the layers and their moisture content were discussed in Reference 29. Section 3 was basically a "full-depth" asphalt concrete pavement with 11.5 inches (29.2 cm) of asphalt concrete and no base material. Section 4 could be called "deep-strength" with 9.5 inches (24.1 cm) of asphalt concrete and 6 inches (15.2 cm) of select granular base. Sections 11 and 17 were conventional pavements with 3.5 inches (8.9 cm) of asphalt concrete. Section 11 had four inches (10.2 cm) of crushed rock base and 18 inches (45.7 cm) of select granular subbase. Section 17 had 2 inches (5.1 cm) of crushed gravel base and 18 inches (45.7 cm) of select granular base. Traffic information and performance data for the first four years of operation of the Brampton Test Road were provided by Reference 31. Further performance information was provided by Reference 32. Reference 33 provided additional performance data, pavement temperature distribution data, resilient moduli of the granular base, resilient moduli of the sand subbase, resilient moduli of the subgrade material, stiffness modulus of the asphalt concrete material and of the asphalt cements, stress distributions with depth in asphalt/concrete layer predicted by elastic layer theory and other very useful information for characterization of materials for VESYS A. Reference 34 provided information in detail on resilient modulus testing for the asphalt concrete surface material, asphalt concrete base materials, crushed gravel base course, crushed stone base course and sand cushion subbase course. Reference 35 provided resilient modulus data in detail on the subgrade materials. Reference 36 provided information on a substantial test effort to arrive at permanent deformation characteristics for the asphalt base materials used at the Brampton Test Road. The wealth of information available in the references for the Brampton Test Road was considered in detail in developing the seasonal material characteristics.

The first solution obtained was for Section 3 and the results for rut depths are plotted in Figure 4 versus measured depth and the serviceability in Figure 8 versus measured serviceability. The values of ALPHA(1) and GNU(1) for the four seasons are also shown on Figure 4 and this solution is identified as Run 1. As can be seen, rut depth is very considerably overestimated and serviceability underestimated because of the high predictions of rut depths. There appeared to be reason to reduce GNU(1) considerably for the summer and fall seasons and to increase ALPHA(1) for all seasons. The results of this appear as Run 2 in Figures 4 and 8 and amounted to gross underpredictions of rutting and overpredictions of serviceability. For Run 3, ALPHA(1) was decreased and GNU(1) was slightly decreased and the results were very little different from Run 2. Consequently, it appeared that GNU(1) was the variable to be revised and higher values were used for the summer and fall seasons as indicated in Figure 4 for Run 4. These increases in GNU(1) had the effect of producing much improved estimates of rut depth and considerably improved estimates of serviceability.

RUN NO.	WINTER		SPRING		SUMMER		FALL	
	ALPHA(I)	GNU(I)	ALPHA(I)	GNU(I)	ALPHA(I)	GNU(I)	ALPHA(I)	GNU(I)
1	.65	.10	.71	.4	.71	2.01	.77	1.41
2	.75	.26	.80	.40	.80	.39	.88	.59
3	.70	.24	.76	.36	.72	.22	.81	.36
4	.70	.24	.76	.36	.72	1.00	.81	.70

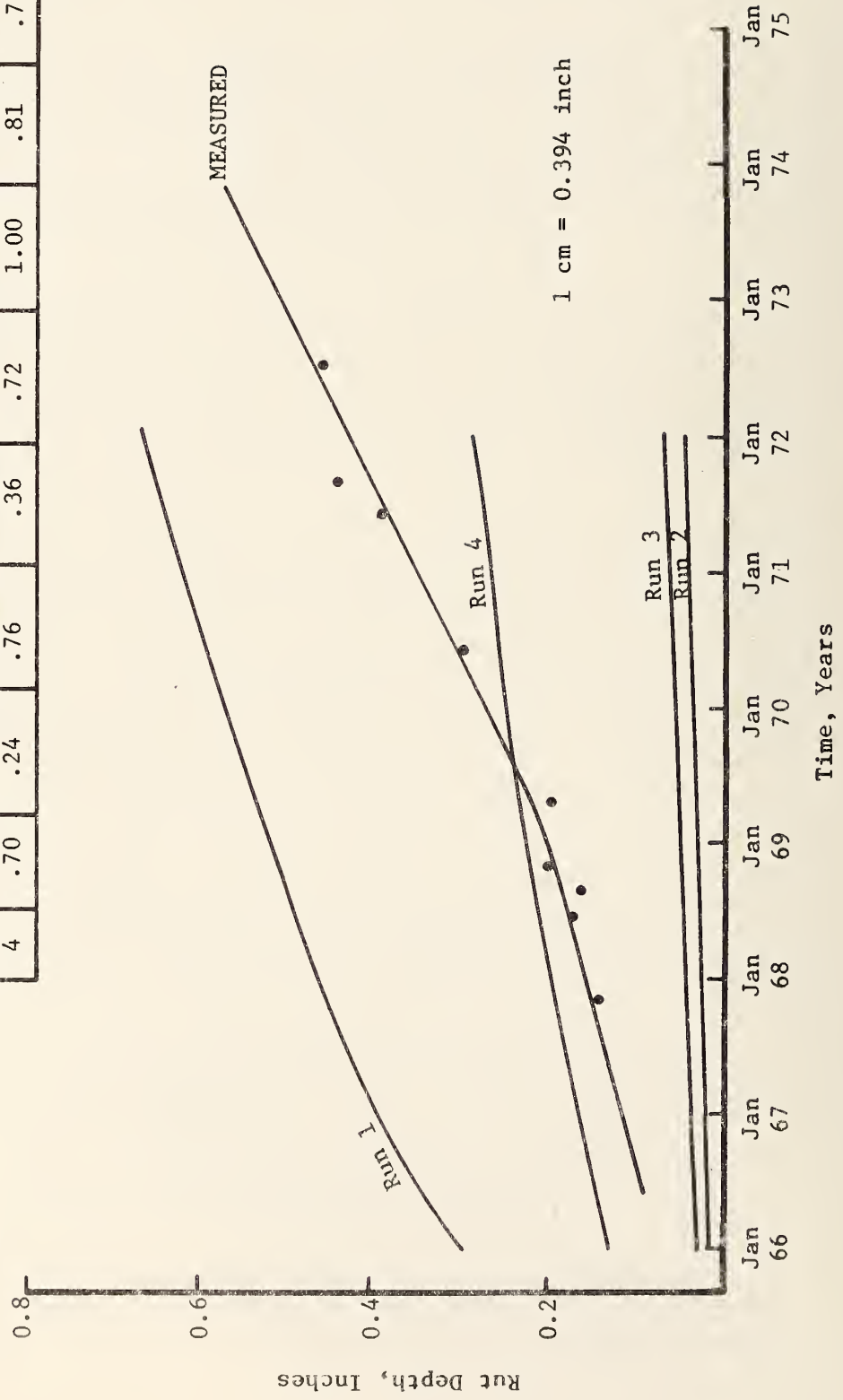


Figure 4. Rut depth versus time, Section 3.

With the information from Section 3, only two runs each were required for Sections 4, 11 and 17 and plots for these solutions appear in Figures 5, 6, 7, 9, 10, and 11. Higher values of ALPHA(1) were generally used for the full-depth and deep-strength sections than for the conventional sections 11 and 17 because of the differences in stress levels in the surface layer and their effects on permanent deformations. For the same reason, generally lower values of GNU(1) were used for the conventional sections. In general, rutting was overpredicted for the first six years of study for the full-depth and deep-strength pavements and underpredicted for the conventional pavements.

The plots of Figure 12 were made after the four runs on Section 3 to gain as much insight as possible as to the effects of varying ALPHA(1) and GNU(1). Figure 12 indicates that relatively small decreases in ALPHA(1) did not greatly increase rut depth, except when accompanied by substantial increases in GNU(1). As the greatest portion of the rutting occurs in the summertime, the values of ALPHA(1) and GNU(1) for the summer season and the four solutions for Section 3 are plotted in Figure 13. Comparison of Figures 12 and 13 indicates that there was very little difference in rutting predictions for Runs 2 and 3, although a substantial reduction was made in ALPHA(1) for Run 3. For essentially the same value of ALPHA(1) but grossly different values of GNU(1), Run 1 gave many times as much rut depth predicted as Run 3. Run 4 at an intermediate value of GNU(1) produced an intermediate value of rut depth. It was concluded that for this particular material, variation in GNU(1) was the most feasible way of improving the permanent deformation characterization.

It should be borne in mind that all of the environmental and mechanistic parameters that control actual rutting in the field are not modeled in VESYS. It should also be noted that the increase in rut depth measured on the Brampton Sections after a certain time is not generally representative of the form of measured rut depth curves. In this case, rutting increased beginning 1969 at a rate higher than it had previously and this is very probably due to some mechanism unmodeled in VESYS A or other mechanistic models.

While the results gained from the study of the Brampton Test Sections were useful, no really strong conclusions could be reached on the basis of this study for direct application to the four environmental zones being considered.

Analysis of Solutions of Four Interstate Highway Pavement Sections

Information was available for development of input data for these four interstate sections from a variety of sources that included direct contact with representatives of the State Departments of

RUN NO.	WINTER		SPRING		SUMMER		FALL	
	ALPHA(I)	GNU (I)	ALPHA (I)	GNU (I)	ALPHA (I)	GNU (I)	ALPHA (I)	GNU (I)
1	.81	.36	.88	.65	.88	.54	.93	.81
2	.77	.24	.80	.36	.72	1.50	.87	.90

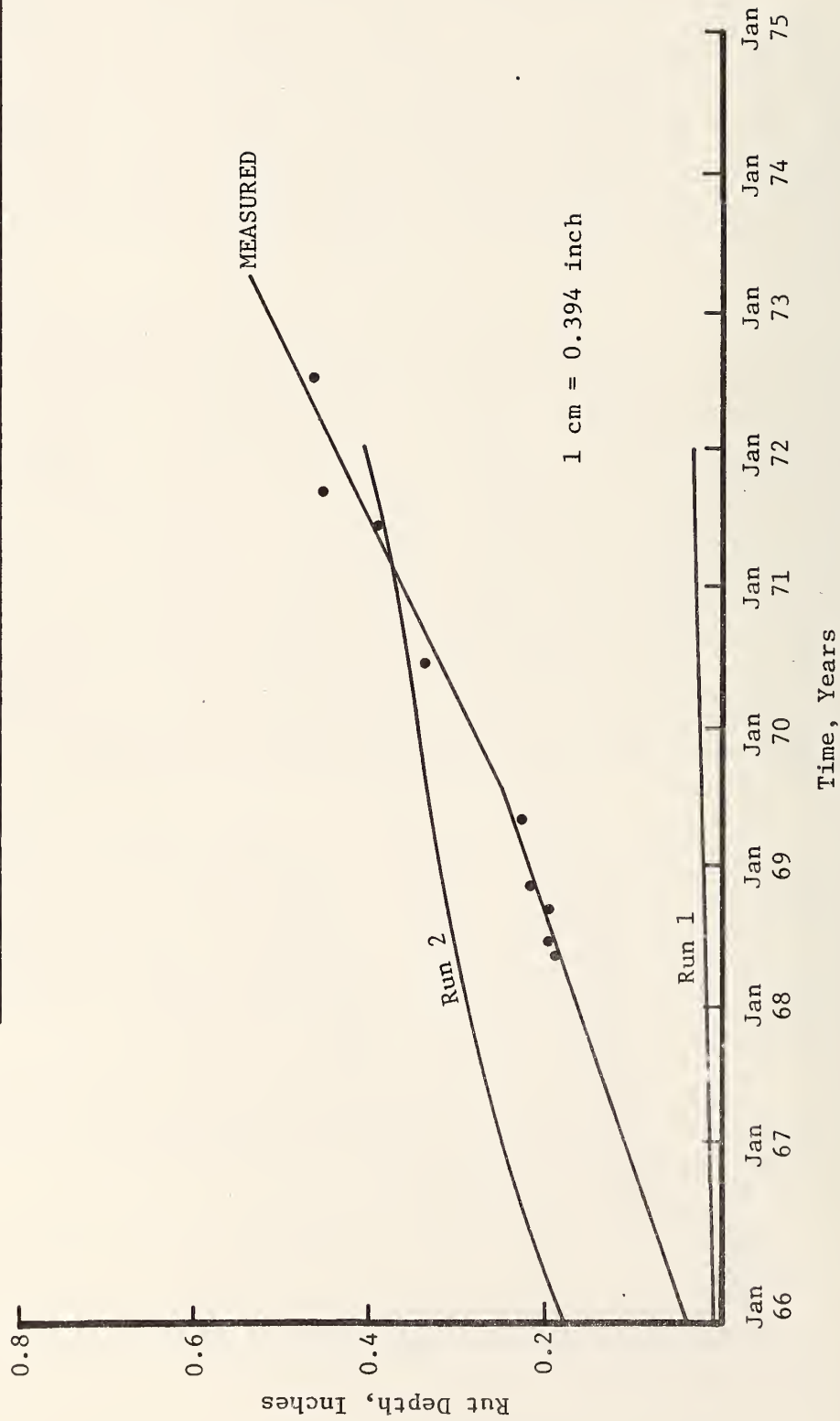


Figure 5. Rut depth versus time, Section 4.

RUN NO.	WINTER		SPRING		SUMMER		FALL	
	ALPHA(1)	GNU(1)	ALPHA(1)	GNU(1)	ALPHA(1)	GNU(1)	ALPHA(1)	GNU(1)
1	.64	.07	.72	.13	.67	.10	.72	.15
2	.64	.07	.72	.13	.67	.70	.72	.40

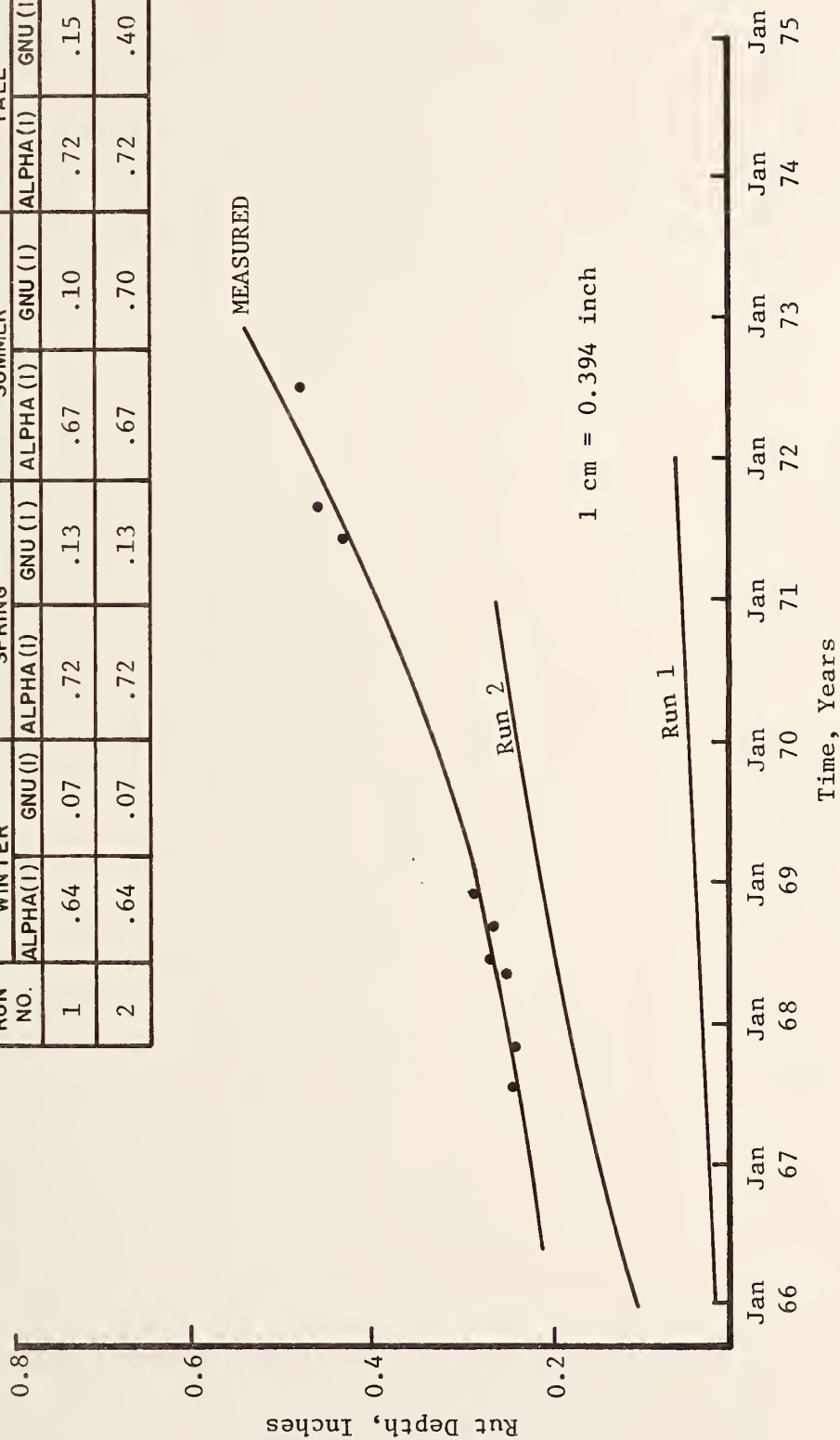


Figure 6. Rut depth versus time, Section 11.

RUN NO.	WINTER		SPRING		SUMMER		FALL	
	ALPHA(I)	GNU(I)	ALPHA(I)	GNU(I)	ALPHA(I)	GNU(I)	ALPHA(I)	GNU(I)
1	.64	.07	.72	.13	.67	.10	.72	.15
2	.64	.07	.72	.13	.67	.70	.72	.40

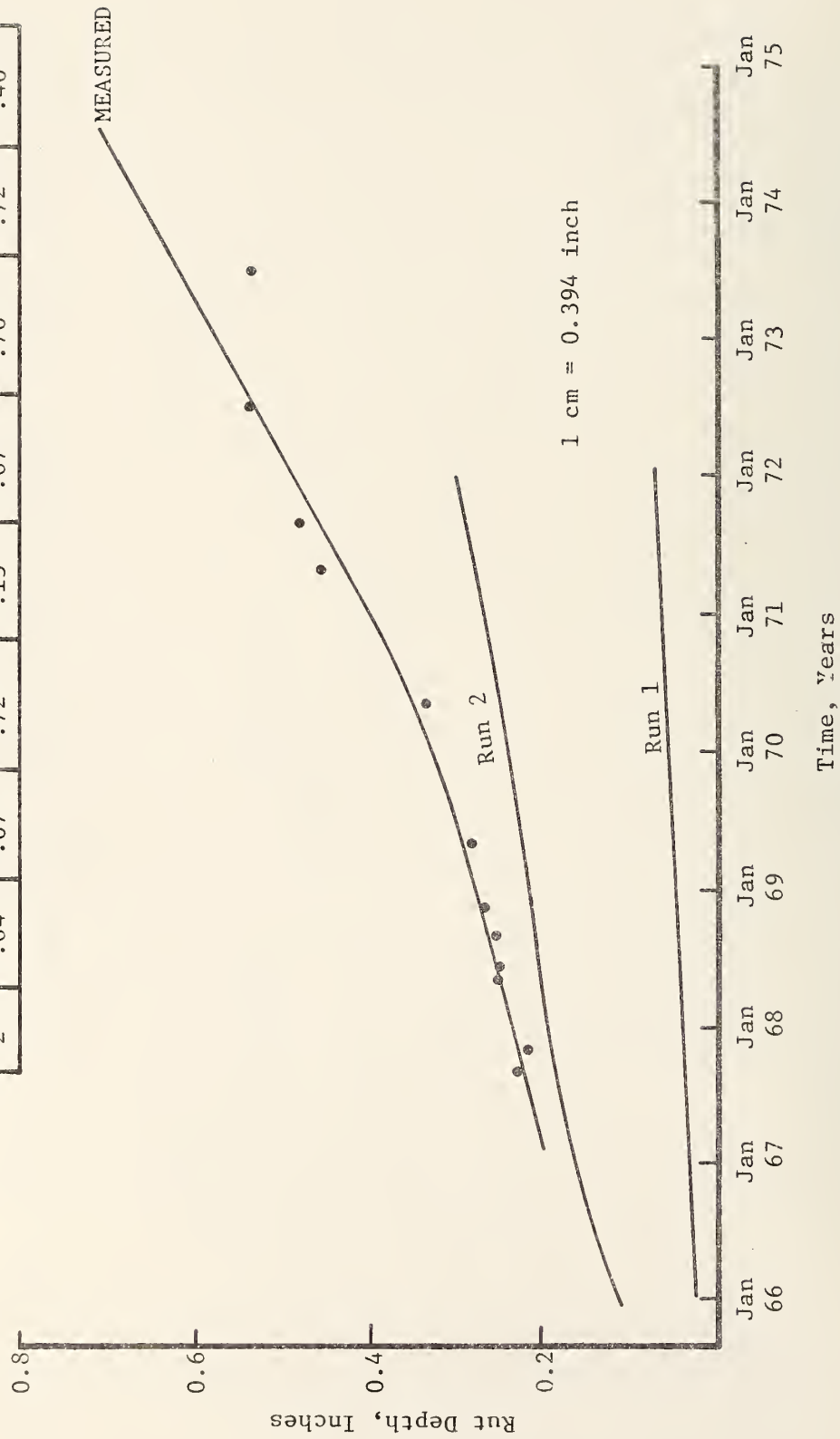


Figure 7. Rut depth versus time, Section 17.

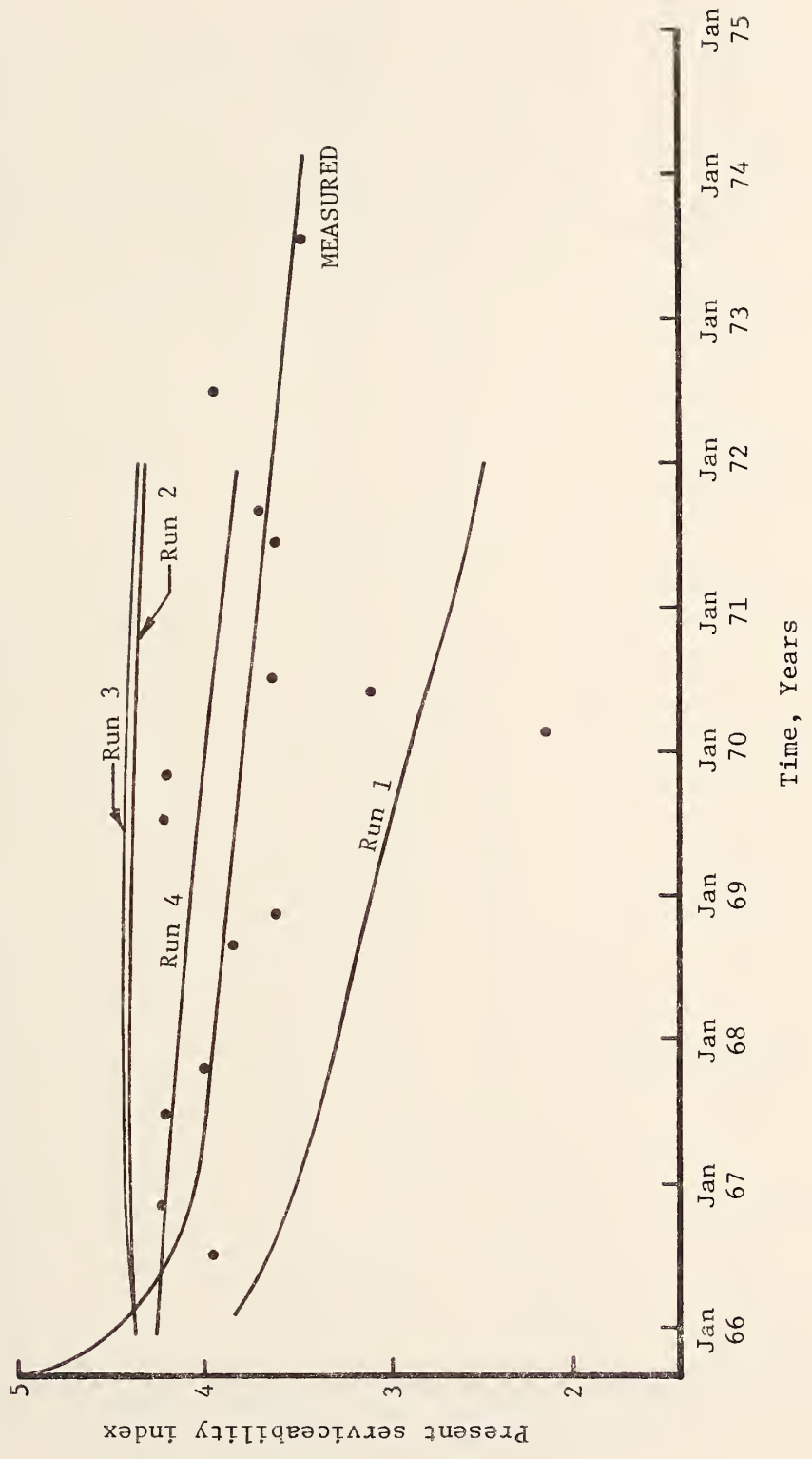


Figure 8. PSI versus time, Section 3.

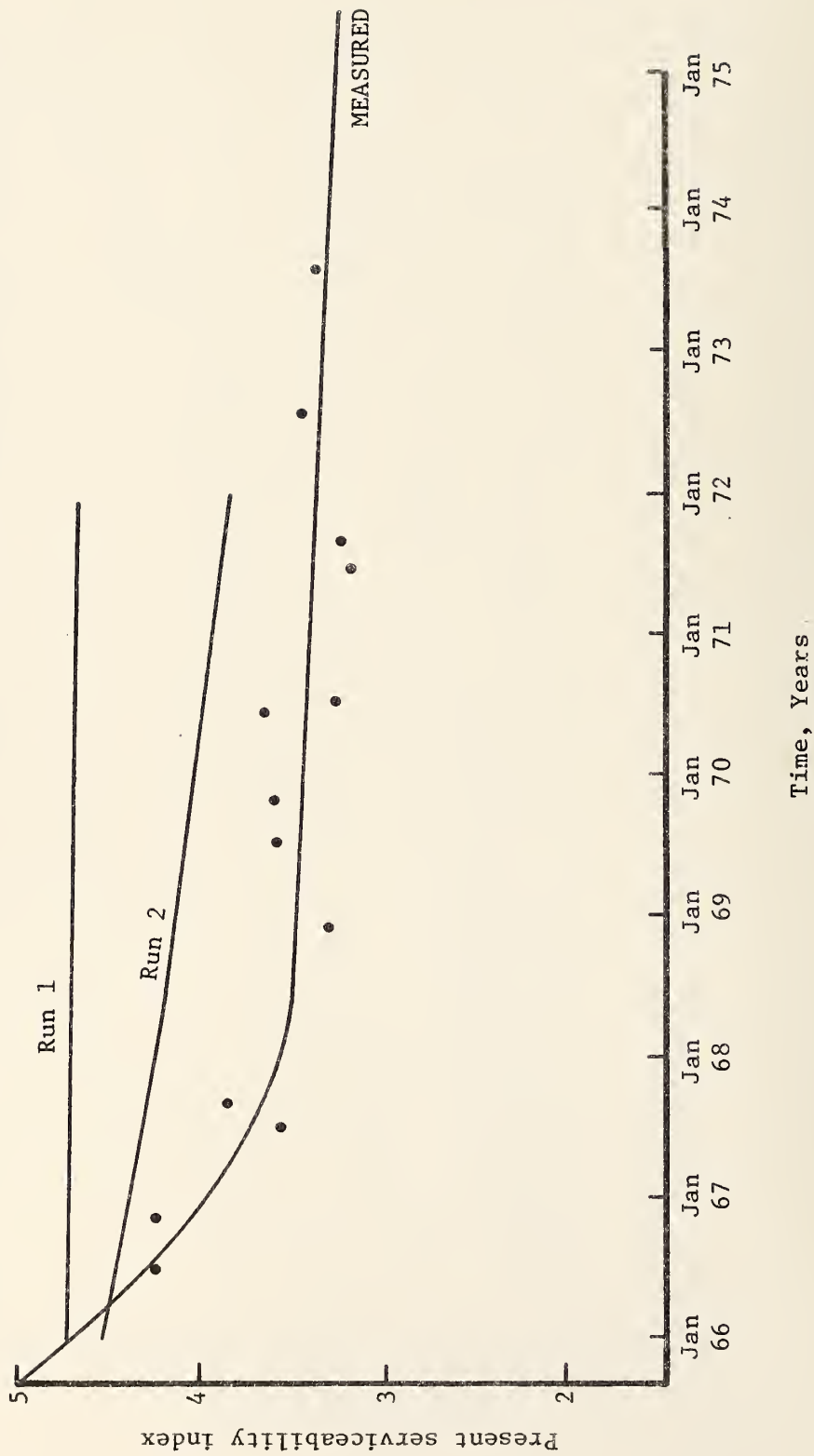


Figure 9. PSI versus time, Section 4.



Figure 10. PSI versus time, Section 11.

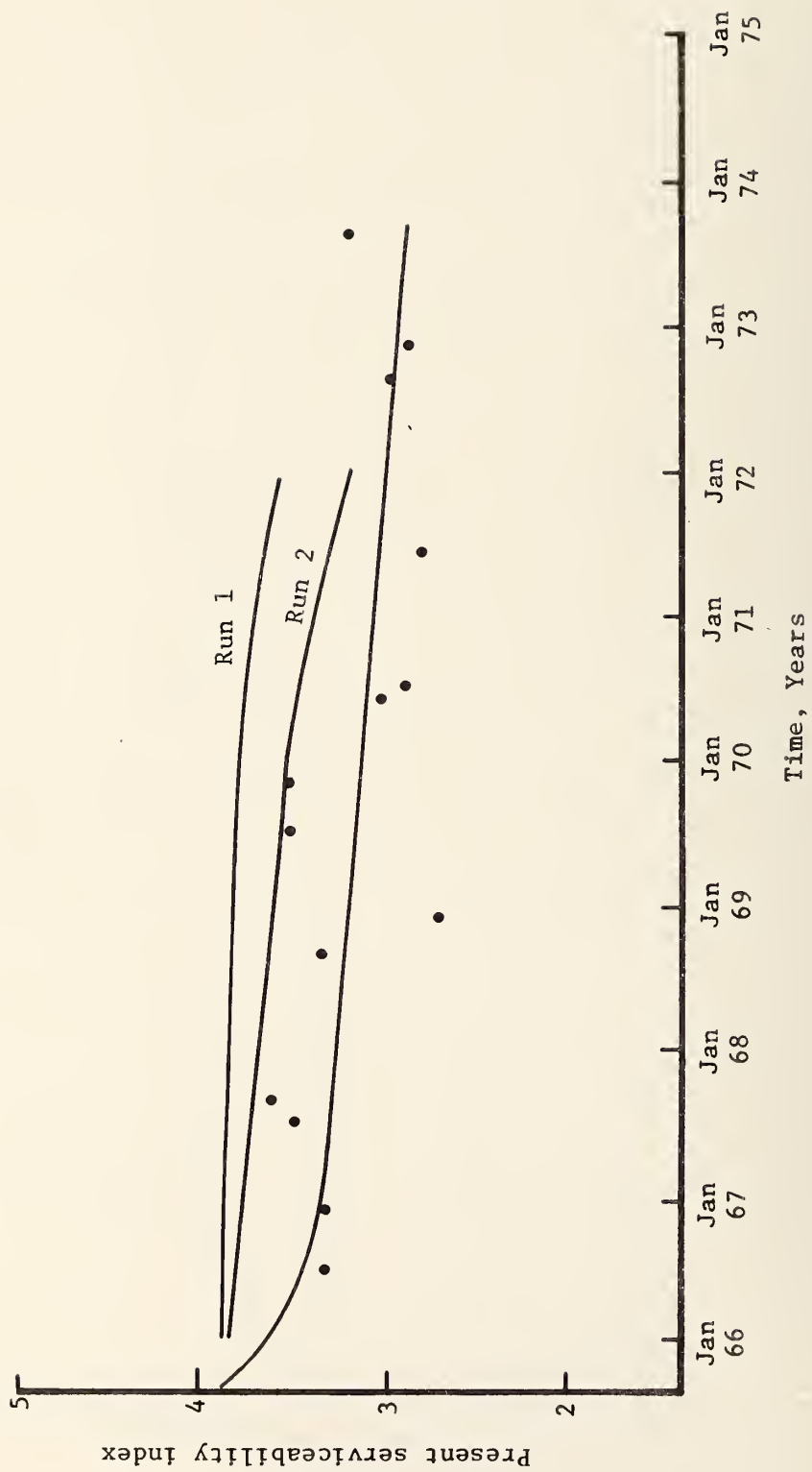
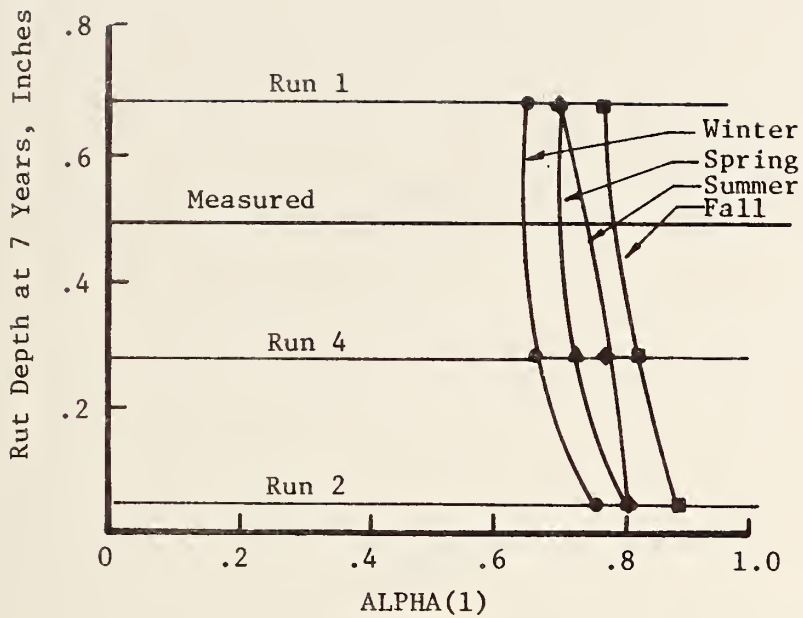
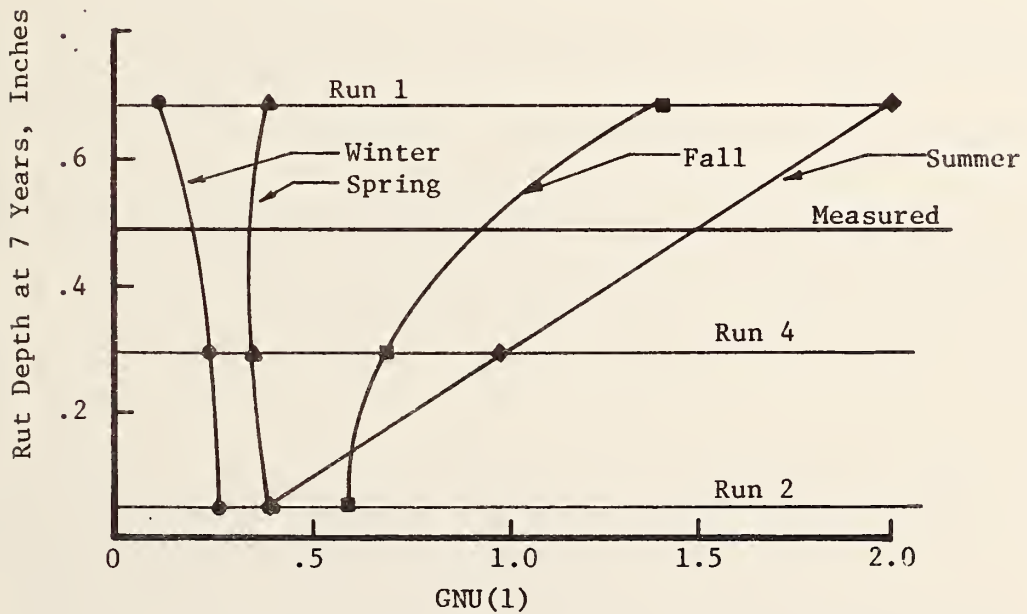


Figure 11. PSI versus Time, Section 17



a. Rut depth versus ALPHA(1) 1 cm = 0.394 inch



b. Rut depth versus GNU(1)

Figure 12. Rut depth predicted after seven years versus the surface layer permanent deformation parameters for Section 3, Brampton Test Road.

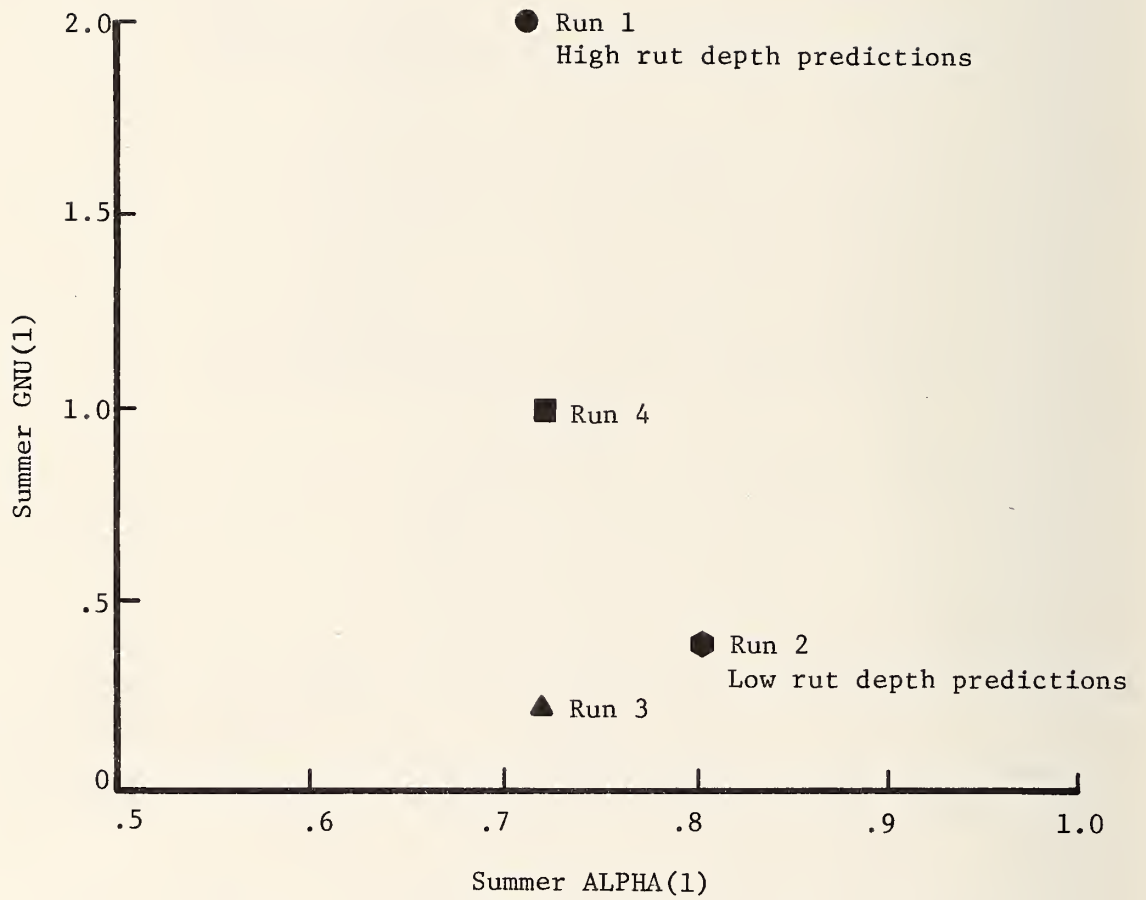


Figure 13. ALPHA(1) versus GNU(1) for summer seasons and four solutions, Brampton Section 3.

Transportation, References 12 and 13 for the section of IH-20 in Illinois, Reference 37¹ for IH-80N in Utah, Reference 38² for IH-10 in Florida and Reference 39³ for IH-20 in Texas. Measured rut depths were available for the Utah and Florida sections and were used on a comparative basis as for previously discussed sections. Although measured responses were not available for the Texas and Illinois sections, solutions were obtained for those sections and they were included in the iterative comparisons and input improvements.

Figures 14, 15, and 16 show measured responses and those predicted with the first solution for a section of IH-80N in Utah between Snowville and the Idaho border. The agreement between predicted and measured responses is considered excellent for rut depth and present serviceability index and is quite good for fatigue cracking. However, there was apparently no low temperature cracking noted whereas the VESYS model predicted a moderate amount. The quality of these predictions indicated that the materials characterizations and other input were probably fairly accurate, so their values were given strong consideration in subsequent studies.

Simultaneous iterative studies were conducted for the pavement sections in Illinois, Florida and Texas. Some of these studies included:

1. Multiple solutions with variations in layer stiffnesses and permanent deformation parameters as indicated by magnitudes of predictions.
2. Separate solutions using program ELSYM5 in order to learn what the strains were in the three layers.
3. Solutions using ELSYM5 and the season values of stiffness for the three layers in order to arrive at deflections at the surface for each of the different seasons. These deflections could then be used with equations from VESYS A to learn what the contributions were to the rutting for each season.

¹Anderson, D. I., J. C. McBride and D. E. Peterson, "Field Verification of the VESYS IIM Structural Subsystem in Utah," Proceedings, Fourth International Conference, Structural Design of Asphalt Pavements, Volume 1, August 1977.

²Sharma, J., L. L. Smith and B. E. Ruth, "Implementation and Verification of Flexible Pavement Design Methodology," Proceedings, Fourth International Conference, Structural Design of Asphalt Pavements, Volume 1, August 1977.

³Written data collected previously by Texas Transportation Institute and furnished ARE for this project.

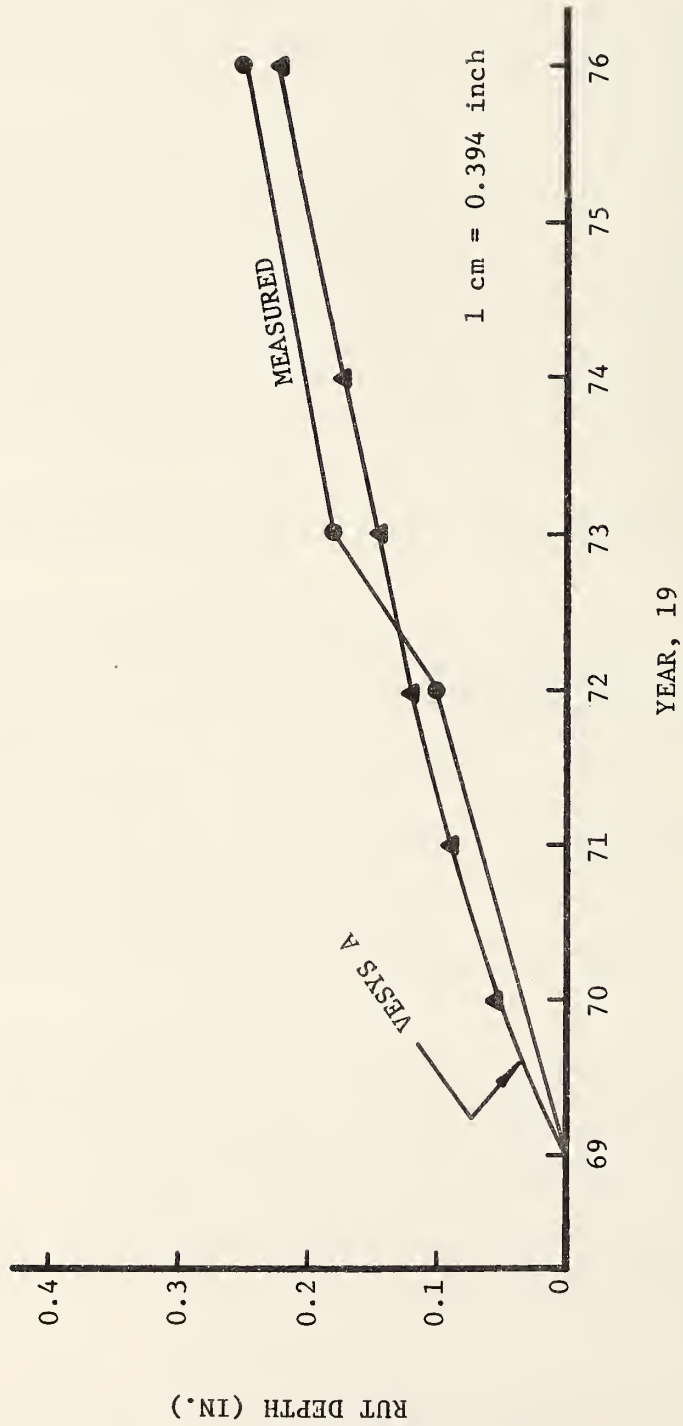


Figure 14. Predicted and measured rut depths for a section of IH-80N in Utah between Snowville and the Idaho Border.

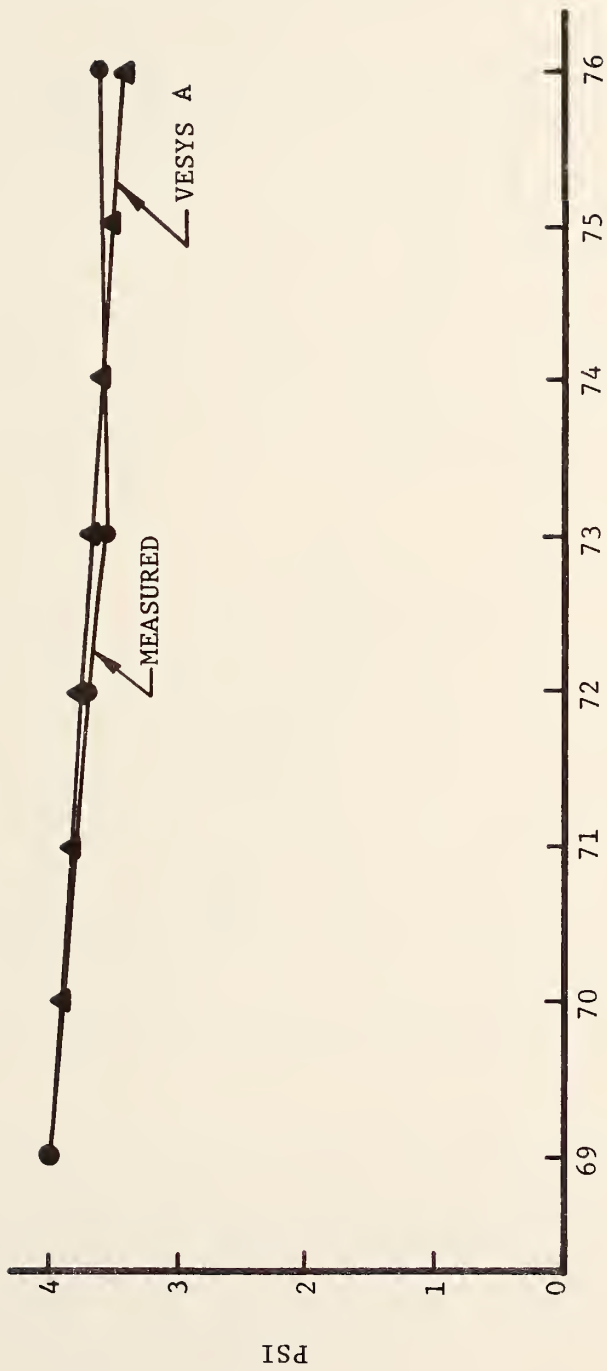


Figure 15. Predicted and measured serviceability for a section of IH-80N in Utah between Snowville and the Idaho Border.

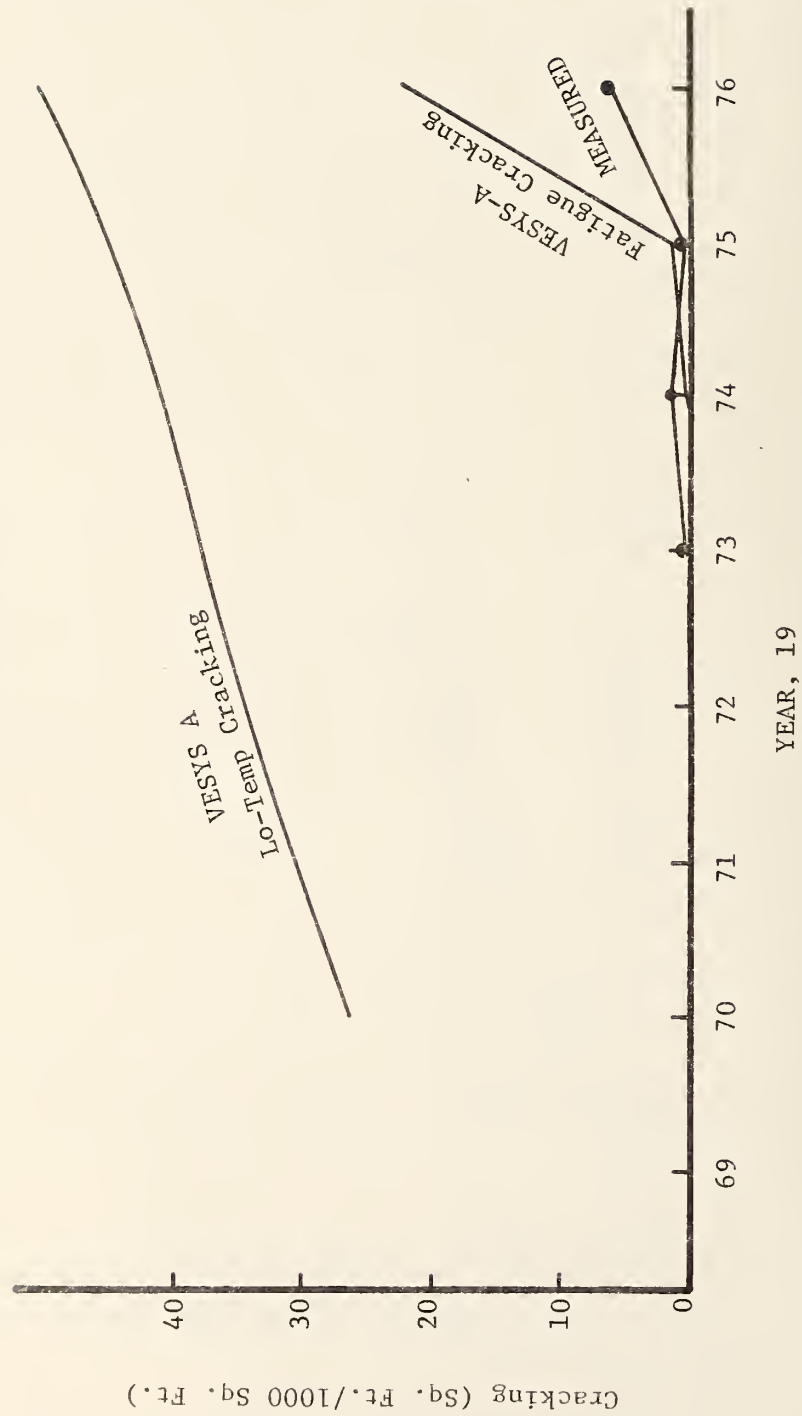


Figure 16. Predicted and measured cracking damage for a section of IH-80N in Utah between Snowville and the Idaho Border.

The initial solutions or predictions for these three sections all yielded predicted rutting that was too high. Analysis indicated that the values for ALPHA(1) were in some cases too low, that ALPHA(3) and GNU(3) were too high for Illinois and that the creep compliance for both the base and subgrade layers were too high for Illinois. It was also determined that too much effect was being assigned to spring break-up in the two northern environments because the spring season was three months in duration and the period for breakup was much shorter than that.

It can be seen from Table 6 that the values of ALPHA(1) for Illinois IH-80 are quite a lot higher than for the other pavements. It is interesting to consider a plot of the various values of ALPHA(1) versus the pavement temperatures for each of the interstate sections considered. Figure 17 shows this data plotted and indicates that most of the values fell on a fairly smooth line, with the exception of all Illinois values and values for the Winter season. The Texas and Illinois Winter values appear to be low so the curve for Illinois was drawn as indicated without consideration of the Winter value (the values for ALPHA for Illinois were extrapolated from testing of AASHO pavement cores that were reported in Reference 1). The higher values of ALPHA(1) for Illinois may be due to the fact that these pavements had undergone years of traffic prior to their being cored and tested.

Figure 18 is indicative of the type of information obtained from separate layer solutions to obtain strain levels in the separate layers and subsequent hand calculations to convert these elastic strains to permanent deformations within each layer. The distribution of permanent deformation between the layers varies considerably between pavement sections considered. For Texas IH-20, the permanent deformation was similar in magnitude for each layer. For Utah, the base material contributed almost nothing to the rutting. For Illinois, only the base material was contributing to the rutting. For Florida also, the base material was contributing most of the rutting with the subgrade and surface layers making some contribution. From this kind of analysis it appears obvious that the input data for certain layers is in error, but it is not at all obvious from comparisons of the input data alone. As a typical result of this analysis, it was obvious immediately that the materials characterizations for the base layer for Illinois IH-80 were in error and should be carefully scrutinized.

Figure 19 provides data in terms of seasonal contributions to rutting much like that in terms of layer contributions in Figure 18. It can be seen that the rutting in Texas was predicted primarily to be in the summer and that the same was true for Florida with more occurring in the spring and fall than for Texas, consistent with Florida's higher pavement temperatures in those seasons. While the results for Texas and Florida appear rational, the occurrence of

- LEGEND
- Florida IH-10
 - ◊ Illinois IH-80
 - Utah IH-80N
 - △ Texas IH-20

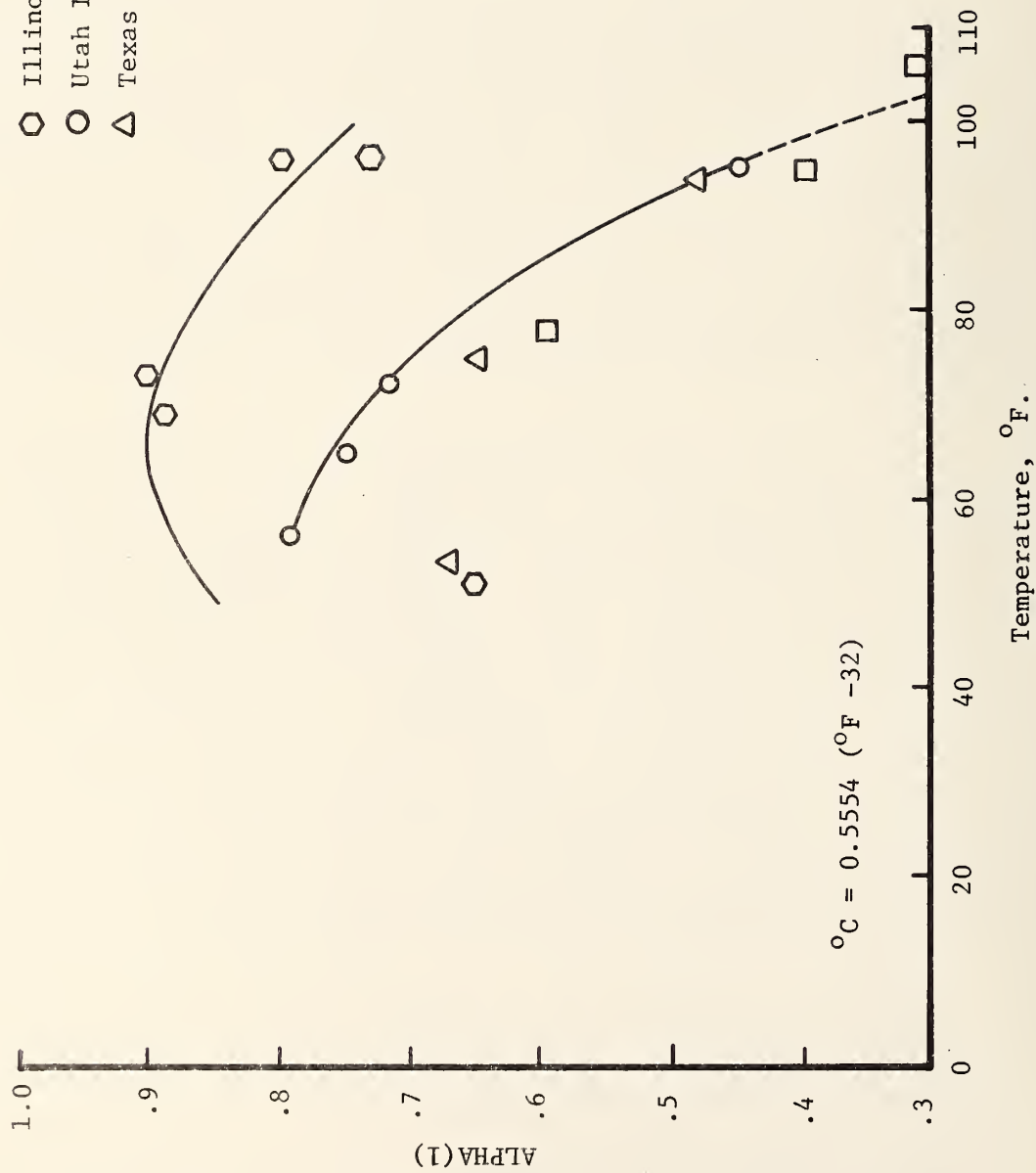


Figure 17. ALPHA(1) versus temperature for the four interstate highway sections considered.

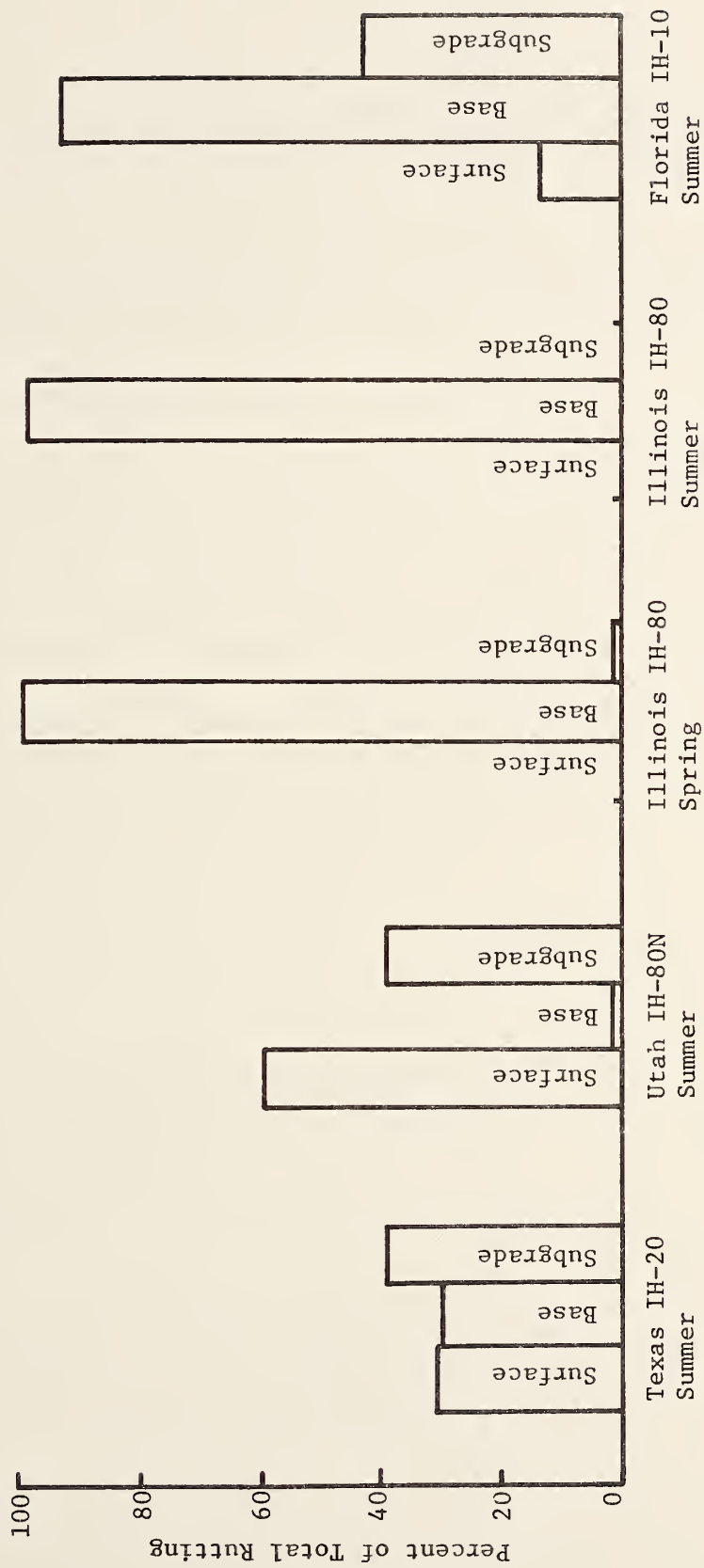


Figure 18. Comparative plots of percent of rutting at the surface contributed by the various layers by pavement section and with seasons identified.

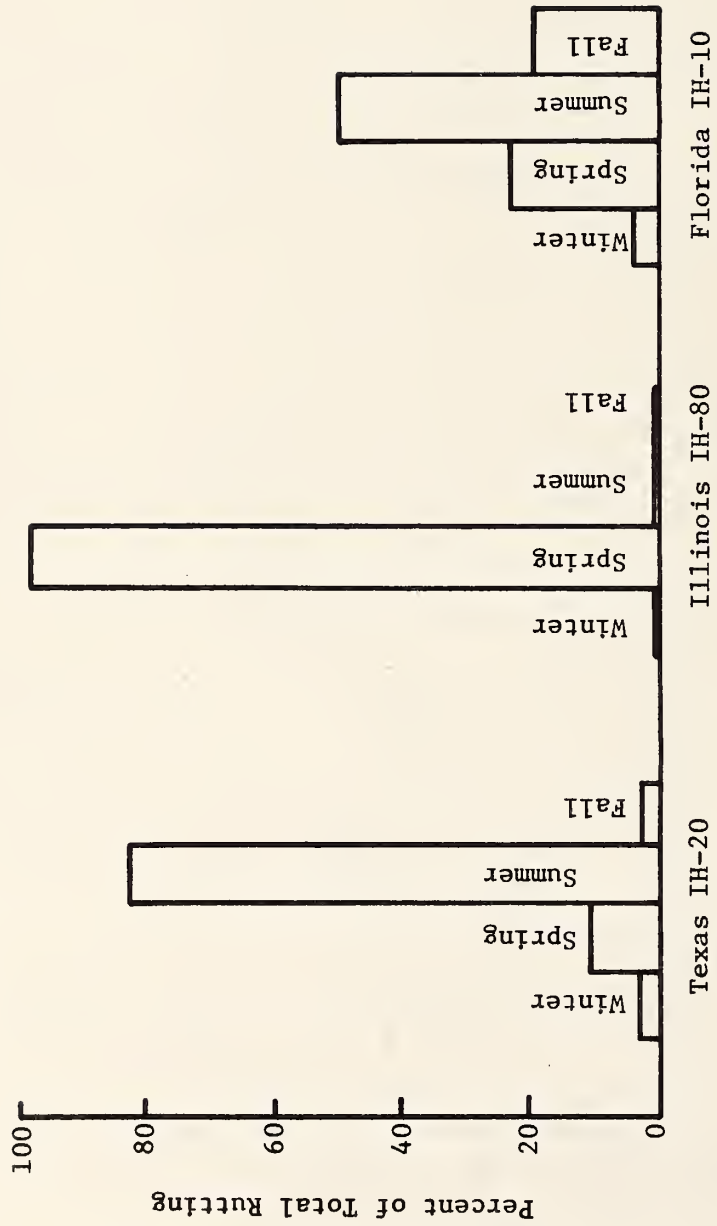


Figure 19. Comparative plots of percent of rutting at the surface by season and pavement section.

virtually all of the rutting in the springtime for Illinois appears to indicate that much too much emphasis was being given to the spring breakup in establishing materials characterizations for the base course and subgrade.

As the study described with typical cases above gave increasingly better results with the iterative trials and comparisons, it became more and more clear what input values would be rational and effective for the factorial study.

Final Input Values for Solution Factorial

The iterative scheme of predictions (comparisons to measured or logical values, analysis of the comparisons to isolate possible causes of differences and analyses of the probable input deficiencies to arrive at rational corrections) applied to input values described above for the AASHO Road Test, Brampton Test Road and interstate highway sections led to the input values for the factorial study defined in the previous chapter. These input values represented the best that could be developed by the authors for producing rational and reasonable predictions of pavement distress and performance. The results of using these input values are discussed in subsequent chapters.

CHAPTER VI

FACTORIAL SOLUTIONS FOR INITIAL CONSTRUCTION AND OVERLAYS

Results From Initial Construction Solutions

A factorial of 64 solutions, using input data developed as described in Chapters III, IV, and V, was run to determine the simulated behavior of initial construction. The solutions were obtained in two parts. First the static solutions required for a given environment and pavement structure were computed and saved and then the eight repeated load solutions for that environment and structure were run. This procedure was made possible by the addition into VESYS A of the capability to write out the results of the static solutions for future use; it proved extremely helpful and economical in both computer and analyst time.

The results of these factorial solutions are presented in Tables 17, 18, 19, and 20 for rut depth, PSI, Fatigue Damage Index, and low temperature cracking index (where applicable), respectively. Values are included for the ends of years 1, 5, 10, 15 and 20. Note that this related only to the distress and performance of the initial construction; no overlays are included in this set of tables. Note also that the predicted low temperature cracking index values are functions only of the pavement structure, age, and environment; there is no dependence on either the quantity or load distribution of traffic.

Overlays to Restore Pavements and Their Simulations in VESYS A

The following overlay strategy, based on common practice, was chosen: For pavements which failed in cracking (prediction of total square yards cracked/1000 sq.yards \geq 999.0), a three-inch (7.6 cm) overlay was added for the low traffic cases and a four-inch (10.2 cm) overlay was added for the high traffic cases. Where a pavement failed in rutting (PSI $<$ 2.5, found only in the wet-no freeze climate), a two-inch (5.1 cm) overlay was added for both high and low traffic.

As we now have a four-layer system and VESYS is only capable of analyzing a three-layer system, it was necessary to combine the two bituminous layers into one layer of some equivalent or "effective" thickness. For the rutting failure cases, the basic structure was felt to be sound (low accumulated fatigue) so the effective thickness adopted was simply the sum of the overlay and original pavement thicknesses. The creep compliance curve used for the new combined layer was the same as for the original asphalt.

Table 17. Predicted Values of Rut Depth for the Solution Factorial in Inches (1 cm = 0.394 inches)

		LOW												HIGH																			
A	G	THIN						THICK						THIN						THICK													
		18	20	22	24	18	20	22	24	18	20	22	24	18	20	22	24	18	20	22	24												
		WET FREEZE		.042	.044	.046	.047	.025	.026	.028	.028	.048	.051	.053	.055	.029	.031	.032	.033	.099	.104	.109	.113	.063	.067	.070	.072	.168	.177	.186	.191	.112	.118
DRY FREEZE		.148	.156	.164	.169	.098	.103	.108	.111	.286	.301	.316	.326	.198	.208	.218	.225	.192	.202	.212	.219	.129	.136	.142	.147	.378	.398	.418	.431	.267	.281	.295	.304
MET-NO FREEZE		.234	.247	.259	.267	.160	.168	.176	.186	.458	.483	.507	.522	.328	.345	.362	.373	.040	.042	.044	.046	.023	.025	.026	.027	.046	.049	.051	.053	.027	.029	.030	.031
DRY-NO FREEZE		.095	.100	.105	.109	.060	.063	.066	.068	.162	.171	.179	.185	.105	.111	.117	.120	.143	.150	.158	.163	.092	.097	.102	.105	.276	.291	.306	.315	.187	.197	.207	.214
		.185	.195	.205	.211	.122	.128	.135	.139	.366	.385	.405	.417	.253	.267	.280	.289	.226	.238	.250	.258	.151	.159	.167	.172	.443	.467	.491	.506	.312	.329	.345	.356
		.057	.059	.062	.064	.042	.044	.046	.047	.066	.069	.072	.074	.049	.051	.053	.054	.202	.211	.220	.226	.206	.215	.225	.230	.514	.537	.561	.576	.418	.437	.456	.468
		.319	.333	.348	.357	.254	.265	.277	.284	.623	.651	.680	.697	.511	.534	.558	.572	.042	.044	.046	.048	.025	.026	.028	.029	.048	.051	.053	.055	.029	.031	.032	.033
		.100	.106	.111	.114	.064	.068	.071	.073	.171	.181	.190	.196	.114	.120	.126	.130	.151	.159	.167	.172	.100	.105	.110	.114	.294	.310	.325	.336	.204	.215	.226	.232
		.196	.207	.217	.224	.132	.139	.146	.151	.391	.412	.432	.446	.277	.291	.306	.315	.240	.253	.266	.274	.164	.173	.182	.187	.475	.500	.525	.541	.341	.359	.377	.389

Table 18. Predicted Values of Present Serviceability Index for the Solution Factorial

A G E	LOW												HIGH											
	THIN						THICK						THIN						THICK					
	18	20	22	24	18	20	22	24	18	20	22	24	18	20	22	24	18	20	22	24	18	20		
WET FREEZE	1	4.12	4.11	4.11	4.11	4.14	4.14	4.14	4.14	4.14	4.14	4.11	4.14	4.11	4.10	4.10	4.10	4.10	4.10	4.14	4.14	4.13	4.13	
	5	3.07	3.96	3.94	3.93	4.07	4.06	4.06	4.05	4.05	4.06	3.61	3.61	3.48	3.42	3.42	3.39	3.39	3.39	3.95	3.95	3.93	3.91	
	10	3.79	3.71	3.54	3.48	3.97	3.95	3.95	3.95	3.95	3.95	3.00	3.00	2.93	2.87	2.83	2.83	2.83	2.83	3.42	3.42	3.35	3.31	
	15	3.39	3.35	3.31	3.28	3.87	3.85	3.82	3.81	3.81	3.82	2.60	2.60	2.52	2.44	2.38	2.38	2.38	2.38	3.11	3.11	3.06	3.00	
	20	3.22	3.16	3.11	3.08	3.75	3.68	3.48	3.46	3.46	3.48	2.27	2.27	2.17	2.07	2.00	2.00	2.00	2.00	2.86	2.86	2.79	2.72	
DRY FREEZE	1	4.11	4.11	4.10	4.10	4.13	4.13	4.13	4.13	4.13	4.13	4.10	4.10	4.10	4.09	4.09	4.09	4.09	4.12	4.12	4.12	4.12	4.12	
	5	3.98	3.96	3.95	3.94	4.07	4.06	4.06	4.05	4.06	4.06	3.53	3.53	3.49	3.45	3.43	3.43	3.43	3.96	3.96	3.95	3.93	3.90	
	10	3.71	3.56	3.53	3.52	3.98	3.97	3.96	3.95	3.95	3.96	3.06	3.06	2.99	2.93	2.89	2.89	2.89	3.45	3.45	3.41	3.37	3.34	
	15	3.43	3.39	3.35	3.33	3.89	3.87	3.78	3.65	3.65	3.78	2.68	2.68	2.59	2.51	2.46	2.46	2.46	3.18	3.18	3.13	3.07	3.04	
	20	3.26	3.21	3.16	3.13	3.72	3.55	3.52	3.50	3.50	3.52	2.35	2.35	2.25	2.16	2.09	2.09	2.09	2.94	2.94	2.87	2.81	2.76	
WET- NO FREEZE	1	4.12	4.12	4.11	4.11	4.16	4.15	4.15	4.15	4.15	4.15	4.10	4.10	4.09	4.08	4.08	4.08	4.08	4.14	4.14	4.14	4.13	4.13	
	5	3.84	3.81	3.78	3.77	3.97	3.95	3.93	3.92	3.93	3.40	3.40	3.35	3.30	3.27	3.27	3.27	3.27	3.63	3.63	3.59	3.55	3.53	
	10	3.53	3.48	3.44	3.41	3.73	3.70	3.67	3.65	3.67	3.67	2.65	2.65	2.57	2.49	2.44	2.44	2.44	2.99	2.99	2.93	2.86	2.82	
	15	3.24	3.19	3.13	3.10	3.50	3.46	3.41	3.38	3.38	3.41	2.10	2.10	2.01	1.90	1.84	1.84	1.84	2.51	2.51	2.43	2.34	2.29	
	20	2.97	2.90	2.84	2.80	3.27	3.22	3.16	3.13	3.13	3.16	1.64	1.64	1.52	1.34	1.17	1.17	1.17	2.01	2.01	1.91	1.85	1.85	
DRY- NO FREEZE	1	4.17	4.17	4.17	4.16	4.19	4.19	4.19	4.19	4.19	4.19	4.16	4.16	4.16	4.15	4.15	4.15	4.15	4.19	4.19	4.18	4.18	4.18	
	5	4.05	4.03	4.02	4.01	4.14	4.13	4.13	4.12	4.13	4.13	3.78	3.78	3.62	3.48	3.42	3.42	3.42	4.02	4.02	4.00	3.99	3.98	
	10	3.89	3.86	3.78	3.66	4.06	4.05	4.03	4.02	4.02	4.03	3.00	3.00	2.94	2.87	2.83	2.83	2.83	3.55	3.55	3.37	3.32	3.29	
	15	3.53	3.36	3.32	3.29	3.97	3.95	3.93	3.91	3.91	3.93	2.60	2.60	2.51	2.43	2.37	2.37	2.37	3.12	3.12	3.06	3.00	2.96	
	20	3.23	3.17	3.12	3.09	3.86	3.83	3.70	3.51	3.51	3.70	2.25	2.25	2.15	2.05	1.98	1.98	1.98	2.86	2.86	2.78	2.71	2.66	

Table 19. Predicted Values of Fatigue Damage Index for the Solution Factorial

A G E	LOW										HIGH					
	THIN					THICK					THIN			THICK		
	18	20	22	24	18	20	22	24	18	20	22	24	18	20	22	24
WET-FREEZE																
1	.064	.078	.093	.104	.027	.033	.040	.044	.085	.104	.123	.137	.036	.044	.052	.058
5	.338	.413	.490	.546	.142	.175	.208	.232	.933	1.14	1.35	1.51	.393	.482	.574	.641
10	.734	.896	1.06	1.18	.309	.379	.451	.504	2.59	3.17	3.76	4.18	1.09	1.34	1.60	1.78
15	1.20	1.47	1.75	1.94	.507	.623	.741	.827	4.43	5.42	6.43	7.15	1.87	2.29	2.73	3.04
20	1.77	2.16	2.56	2.85	.744	.914	1.09	1.21	6.41	7.83	9.29	10.3	2.70	3.32	3.95	4.40
DRY-FREEZE																
1	.083	.101	.120	.134	.034	.042	.050	.056	.109	.134	.159	.177	.045	.056	.066	.074
5	.436	.533	.633	.705	.180	.221	.263	.294	1.20	1.47	1.74	1.94	.496	.610	.726	.810
10	.945	1.16	1.37	1.53	.390	.479	.571	.637	3.34	4.09	4.85	5.40	1.38	1.69	2.02	2.25
15	1.55	1.90	2.25	2.51	.640	.787	.937	1.05	5.71	6.99	8.29	9.24	2.36	2.90	3.45	3.85
20	2.28	2.79	3.31	3.68	.939	1.16	1.38	1.54	8.26	10.1	12.00	13.4	3.41	4.19	4.99	5.57
WET-NO-FREEZE																
1	.006	.007	.009	.010	.004	.005	.005	.006	.008	.010	.012	.013	.005	.006	.007	.008
5	.033	.039	.046	.050	.021	.025	.029	.032	.091	.108	.126	.139	.057	.068	.079	.087
10	.072	.085	.099	.109	.045	.053	.062	.069	.254	.301	.351	.385	.157	.188	.220	.243
15	.118	.140	.163	.179	.073	.087	.102	.113	.434	.515	.600	.658	.269	.322	.377	.415
20	.173	.205	.239	.263	.107	.128	.150	.166	.628	.744	.868	.952	.389	.465	.545	.601
DRY-NO-FREEZE																
1	.052	.063	.074	.082	.023	.029	.034	.038	.068	.083	.098	.109	.031	.038	.045	.050
5	.273	.331	.390	.433	.123	.150	.178	.198	.751	.911	1.08	1.19	.340	.414	.491	.546
10	.591	.716	.846	.939	.267	.326	.386	.429	2.09	2.53	2.99	3.32	.944	1.15	1.36	1.52
15	.970	1.18	1.39	1.54	.438	.535	.634	.705	3.57	4.33	5.12	5.68	1.61	1.97	2.33	2.60
20	1.42	1.73	2.04	2.26	.644	.785	.930	1.04	5.16	6.26	7.40	8.21	2.33	2.85	3.37	3.75

Table 20. Predicted values of low-temperature cracking indices and average crack spacing.

Environmental Zone	Age	Cracking Index		Average Crack Spacing, Feet *	
		Thin Pavement	Thick Pavement	Thin Pavement	Thick Pavement
Wet-Freeze	1	4.46	4.16	112.1	120.1
	5	7.50	7.20	66.6	69.4
	10	11.31	11.01	44.2	45.4
	15	15.11	14.81	33.1	33.8
	20	18.91	18.62	26.4	26.9
Dry-Freeze	1	6.96	6.66	71.9	75.1
	5	10.00	9.70	50.0	51.5
	10	13.81	13.51	36.2	37.0
	15	17.61	17.31	28.4	28.9
	20	21.41	21.11	23.4	23.7

Wet-No Freeze No low temperature cracking predicted

Dry-No Freeze No low temperature cracking predicted

* 1 m = 3.28 feet

For those cases where the original pavement failed in cracking, a separate layered-theory program (LAYER) capable of handling up to five layers was used to calculate strains under the top layer in two different layered systems. The first system consisted of base and subgrade as used in the VESYS solutions (moduli obtained by inverting the constant values of creep compliance used for these layers), the original pavement with a reduced "cracked" modulus of 70,000 psi (483,000 kN/m²) (adopted for Class 2 cracked asphalt in Reference 40¹), and an overlay of either 3 or 4 inches (7.6 to 10.2 cm) of asphalt with a modulus of 752,000 psi (52,061 kg/cm²) derived from the creep compliance curve at a load duration of .03 seconds. The second system had the same base and subgrade, but had a single bituminous layer with the same modulus as that adopted for the overlay and a thickness varying from 2.5 to 6 inches (6.3 to 15.2 cm). For all of these solutions, a Poisson's ratio of 0.5 was used for all layers, as is used in VESYS.

Solutions of both kinds were made for both the thin and the thick original pavement structures and for both 3-inch (7.6 cm) and 4-inch (10.2 cm) overlays. The radial strains calculated for the three-layer system are plotted in Figure 20 versus the four levels of surface layer thickness considered (See solid lines). The radial strains calculated for the four-layer solutions were plotted as horizontal dashed lines and their intersections with the solid lines represent the equivalent single-layer thickness for use in three-layer solutions to produce radial strain levels expected in the four-layer system. The equivalent thicknesses are given in Table 21.

Table 21

Equivalent Thicknesses for Single Layer
Approximation to Overlay + Original Pavement,
Inches (1 cm = 0.394 inches)

Overlay Thickness	Original Pavement Structure	
	Thin	Thick
3	3.9	4.1
4	4.8	4.9

In the factorial runs on the original pavements, there were no cases where an overlay became necessary on a thick pavement under low

¹Austin Research Engineers Inc, "Asphalt Concrete Overlays of Flexible Pavements, Volume 1 - Development of New Design Criteria, FHWA Report No. FHWA-RD-75-75, August 1975.

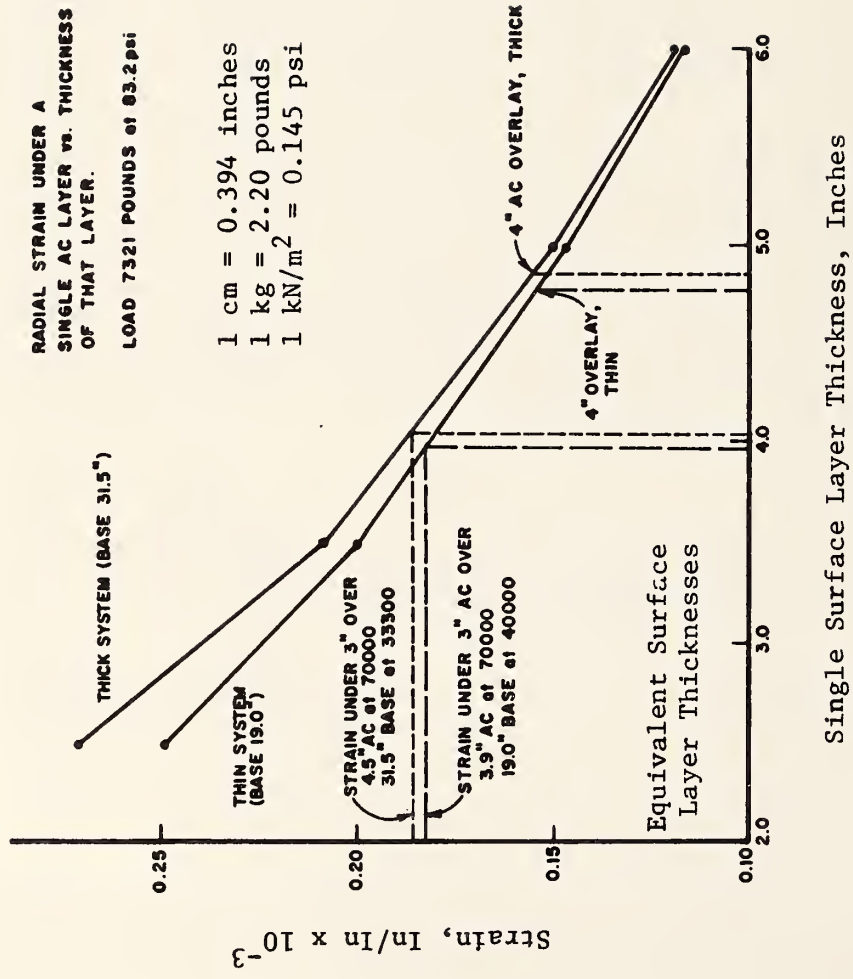


Figure 20. Equivalent surface thickness to represent cracked pavement and overlay.

traffic, corresponding to a 3-inch (7.6 cm) overlay requirement, so solutions with an equivalent thickness of 4.1 inches (10.4 cm) were not required.

New static solutions were performed for the climate/pavement system combinations and top layer thicknesses listed in Table 22. As the equivalent thickness of 3.9 inches (9.9 cm) is identical to one thickness of original pavement, existing static solutions could be used for the thin pavement systems for wet-freeze, dry-freeze and dry-no freeze environments where the low traffic levels were to be simulated.

Table 22. New Static Solutions for Overlays (1 cm = 0.39 inches)

<u>Climate</u>	<u>Pavement System</u>	<u>AC Thickness</u>
Wet-Freeze	Thin	4.8 inches
Wet-Freeze	Thick	4.9 inches
Dry-Freeze	Thin	4.8 inches
Dry-Freeze	Thick	4.9 inches
Wet-No Freeze	Thin	5.9 inches
Wet-No Freeze	Thick	6.5 inches
Dry-No Freeze	Thin	4.8 inches
Dry-No Freeze	Thick	4.9 inches

With this array of static solutions now available, simulations were run using values of average daily traffic (LAMBDA) picking up at the year following the year in which the original pavement failed. All other data remained the same. Where it was necessary to extend the simulations beyond the point (20 years) to which traffic data had been given, a linear extrapolation was used, adding 100 to the value of LAMBDA for each year for the low traffic, and adding 150 each year for high traffic. These extensions were necessary to obtain the estimated lifetime of the original pavement with any overlays when it exceeded 20 years.

In the cases where more than one overlay was required, the cost of the second overlay was simply added at the appropriate year and the lifetime estimated. The equivalent thickness approach was not applied for a second overlay because the extrapolation of this concept to a second overlay did not appear justified, and because the estimated life based on established trend data for the initial pavement and one overlay offered a basis for a reasonably accurate estimate of pavement life for the second overlay.

Results From Overlay Construction Solutions

Repeated load solutions were obtained for the 47 individual sets of conditions requiring at least one overlay. Since these solutions start at many different years with different traffic values over their lifetime, tabulation of rut depth, PSI, and other performance indicators for side-by-side comparison is not appropriate. The performance of the individual overlays is indicated on the graphical displays for each case, Figures 21 through 36.

Table 23 gives for all 64 individual sets of conditions the age at first overlay (if any), the age at second overlay (if any), and the total life of the pavement system as overlaid to achieve at least a 20-year lifetime. All of the total lifetimes in cases where a second overlay was required are marked as estimates since, as mentioned in the foregoing section, no attempt was made to simulate a second overlay with the VESYS program.

It should be noted that, as for the original construction, all the overlay failures were in cracking except for the wet-no freeze environment, where $PSI < 2.5$ occurred usually long before cracking became significant.

Overall Performance Results

The predicted performance for all 16 cases including four levels of environmental zone, two levels of truck traffic volume and two levels of pavement section thickness are plotted separately in Figures 21 through 36. Each figure includes a plot of cracking versus time, a plot of rut depth versus time and a plot of serviceability index versus time. Each plot includes separate graphs for each of the four axle load limits. While there is value in separate study of these plots, the major results and trends noted from such a study follow:

1. The expected increases in cracking and rutting with increased traffic and increased axle loads were predicted.
2. The expected important decreases in cracking and rutting with a thicker pavement section also were predicted. These can be readily seen by comparing the performance plots for the same environment and traffic level, but with differing pavement section thicknesses. For example Figure 21 indicates a need for two overlays to attain 20 years service for low traffic with a legal axle limit of 24-kips (10,900 kg) and a thin pavement, but Figure 25 indicates only one for the thick pavement. Figure 31 shows a need for two overlays to restore ride quality for high traffic with legal limits of 22 and 24 kips (9,980 and 10,900 kg) and a thin pavement section

TABLE 23. Predicted life of pavement and points in time when overlaid in years.

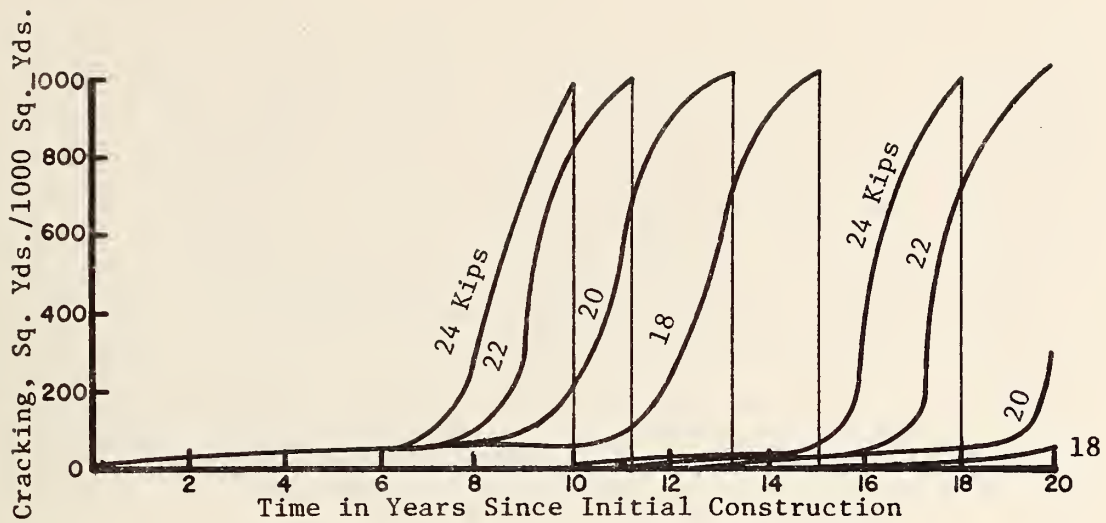
		LOW									HIGH								
		THIN			THICK			THIN			THICK								
* I T E M		18	20	22	24	18	20	22	24	18	20	22	24	18	20	22	24		
	FREEZE WET	15	13	11	10				19	7	6	5	5	11	10	9	8		
					18					18	16	14	13			18	17		
		25	22	20	28E	26	23	21	33	29E	27E	24E	21E	24	21	29E	27E		
	FREEZE DRY	12	10	9	8			17	16	6	5	5	4	9	8	8	7		
			18	16	15					15	13	12	11	19	17	15	14		
		21	28E	24E	22E	23	20	30E	27E	25E	23E	21E	20E	30E	28E	25E	22E		
	NO FREEZE WET									11	11	10	10	15	13	11	11		
												18	18						
		29	28	26	25	37	35	34	33	21	20	25E	24E	28	26	25	24		
	NO FREEZE DRY	19	17	15	14					9	8	7	7	15	13	11	11		
												18	17						
		32	28	25	24	31	27	25	23	23	20	30E	28E	30	26	22	21		

* LEGEND FOR ITEMS

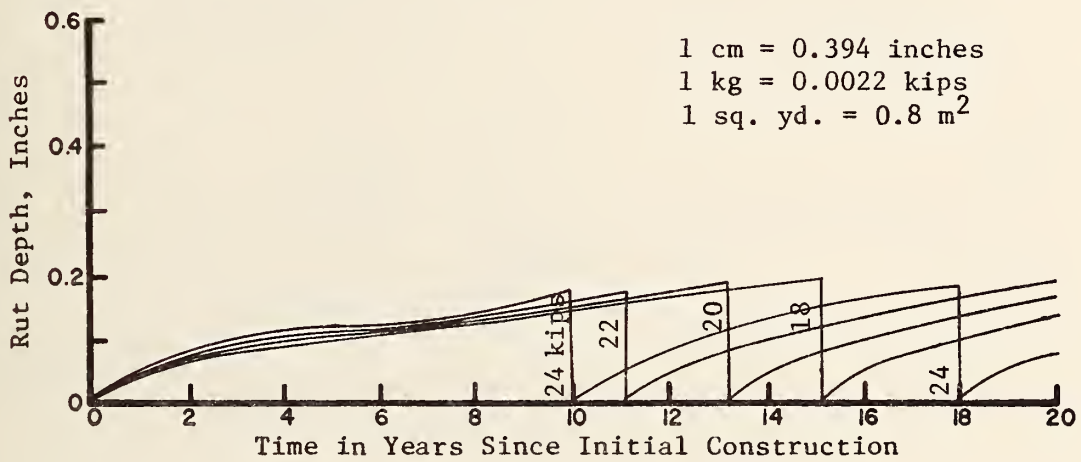
1. Age at first overlay
2. Age at second overlay
3. Life of system (as repaired to serve at least 20 years) (values followed by E are estimates).

in the wet-no freeze zone, while only one overlay is required for the thicker pavement as shown in Figure 35.

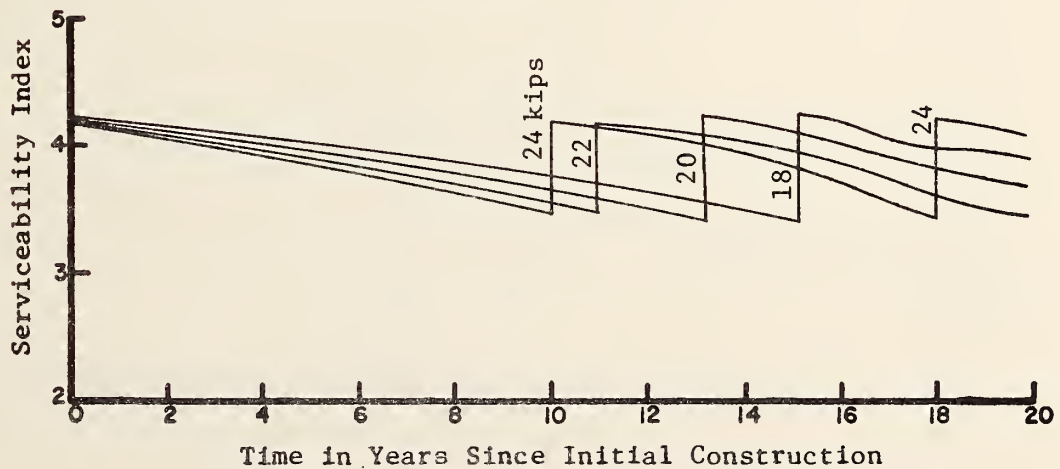
3. Predicted failures were due to cracking in all the environmental zones except the hotter wet-no freeze environment represented by Florida. Overlays for the wet-no freeze environment were necessitated by excessive rutting and consequent loss of serviceability.
4. Predicted cracking failure occurred much more rapidly in the colder wet-freeze and dry-freeze climates than in the dry-no freeze climate represented by Texas. Low temperature cracking also added to the higher levels of the fatigue cracking in the colder climates. The higher temperatures in the wet-no freeze zones reduced the incidence of cracking such that virtually no cracking was predicted, except for a minor amount for the 22 and 24-kip (9,980 and 10,900 kg) axle loads for high traffic on thin pavements.
5. Although the expected increase in incidence of higher axle loads for higher legal axle limits is numerically minor, it can be seen that failures are predicted considerably earlier for the higher legal axle limits than for the more usual 18-kip (8,160 kg) limit. This is, of course, due to the increased rate of damage caused by the higher axle loads.
6. PSI remained higher where cracking was the cause of overlay and overlays were spaced close together in time. More time between the overlays allowed more rut development and loss of serviceability. (Changes in PSI due to cracking as predicted by VESYS A or any other mechanistic model in use today are very small. However, these changes are generally underestimated because moisture entering through the cracks will generally cause loss of stiffness in underlying layers that will result in an increasing rate of rutting.)
7. Twice as many cases (8 cases to 4) with legal limits of 22 and 24 kips (9,980 and 10,900 kg) required two overlays than their corresponding 18-kip (8,160 kg) cases. Also, five cases of 18-kip (8,160 kg) legal limits required no overlays whereas only three at 24 kips (10,900 kg) survived without an overlay.



a. Cracking vs. time

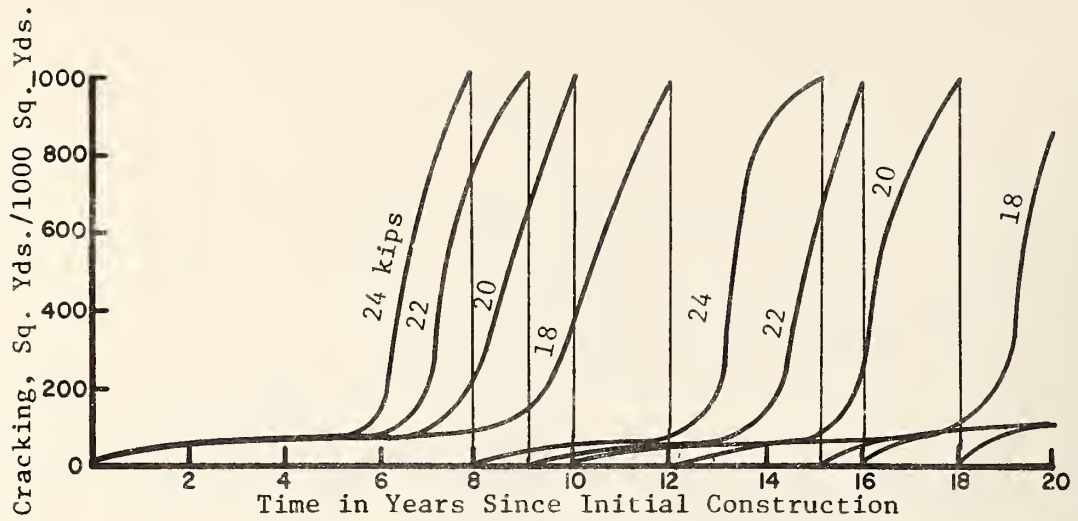


b. Rut depth vs. time

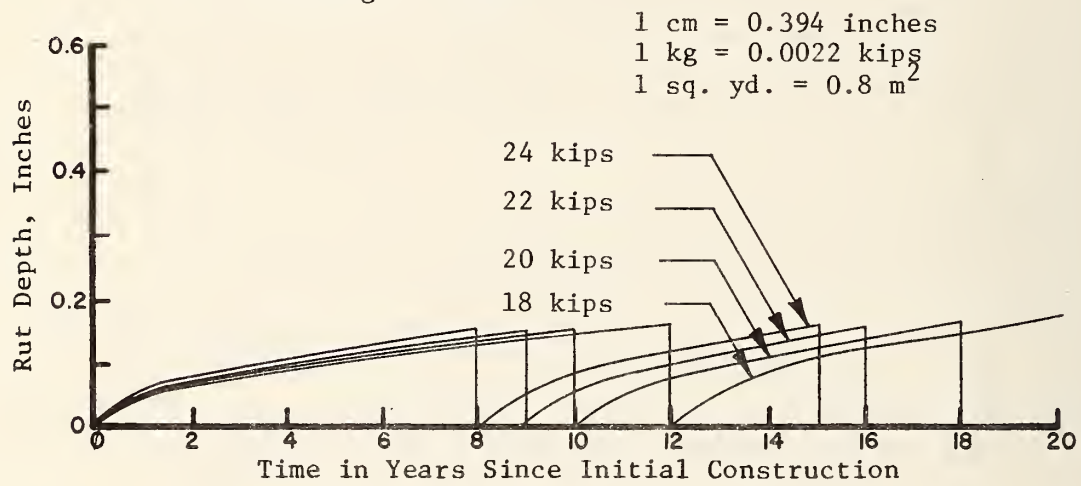


c. Serviceability Index vs. time

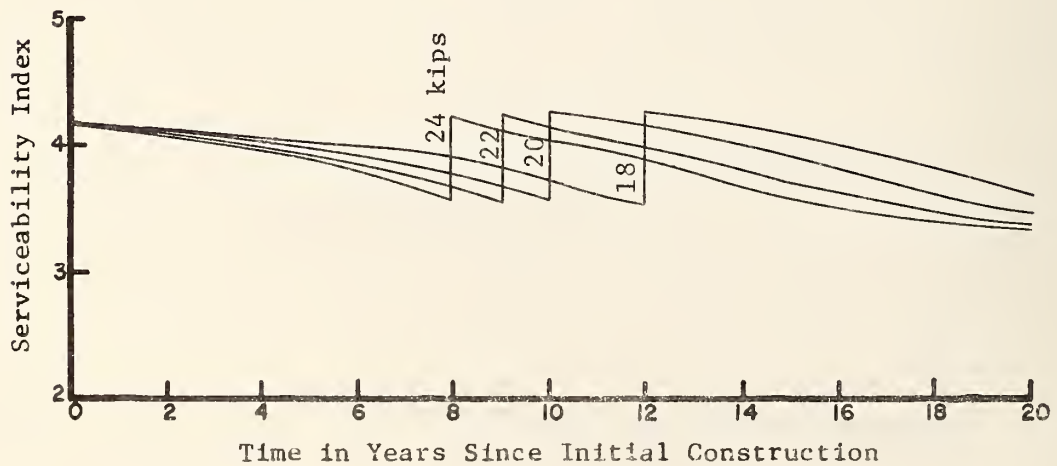
Figure 21. Predicted performance, wet-freeze environment, low traffic and thin pavement sections.



a. Cracking vs. time

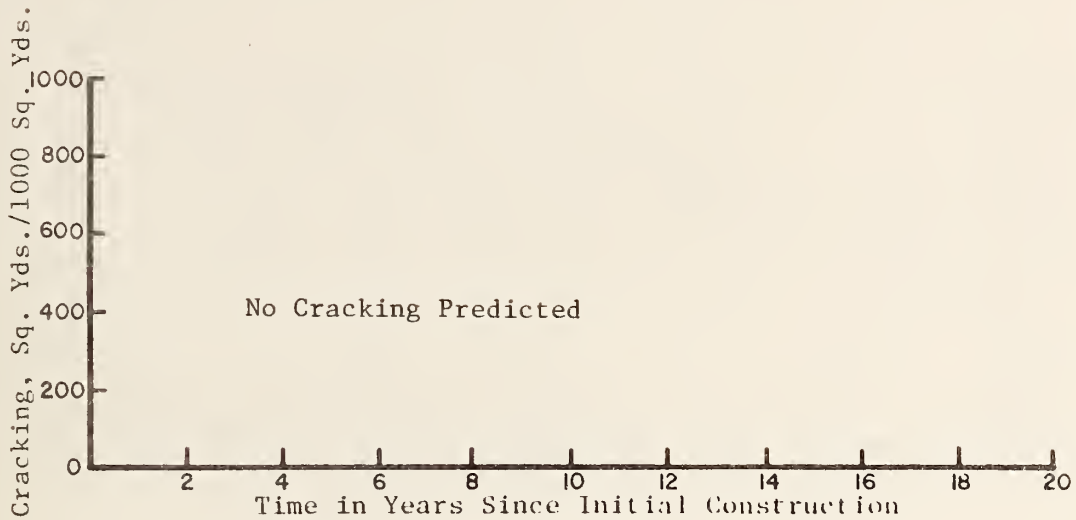


b. Rut depth vs. time

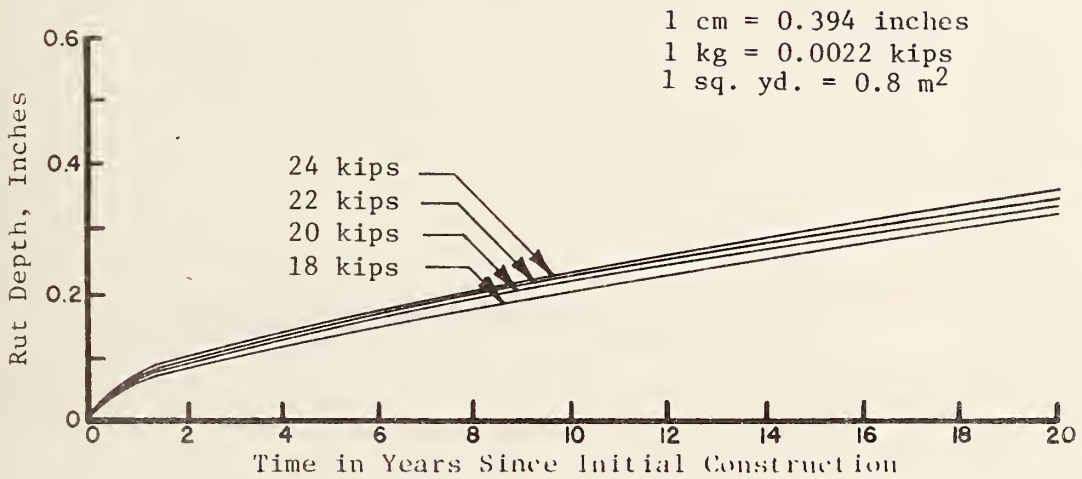


c. Serviceability Index vs. time

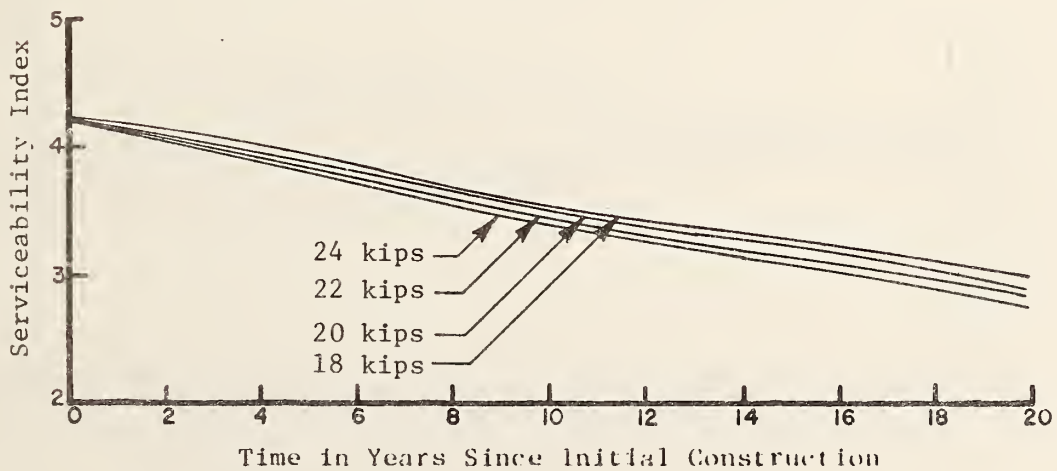
Figure 22. Predicted performance, dry-freeze environment, low traffic and thin pavement section.



a. Cracking vs. time

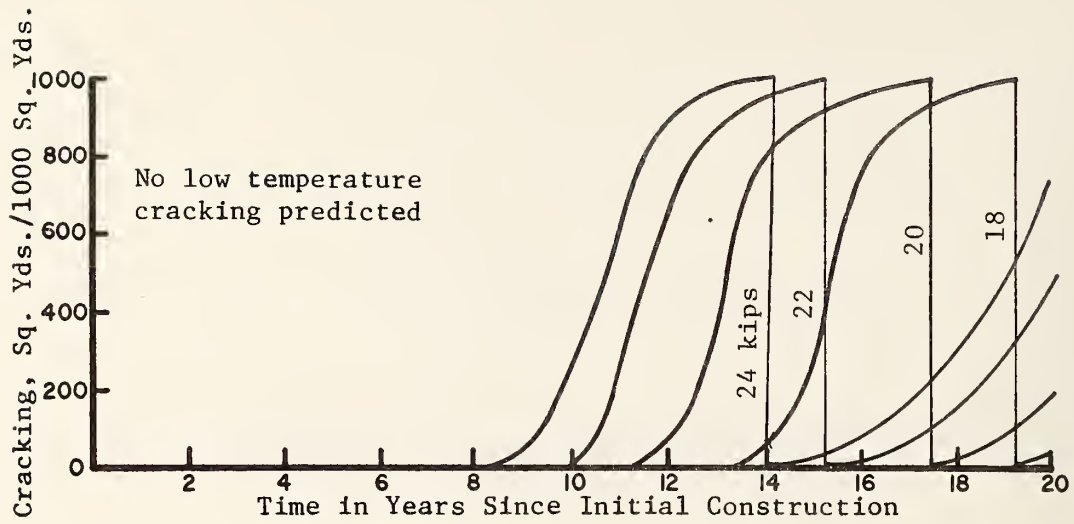


b. Rut depth vs. time

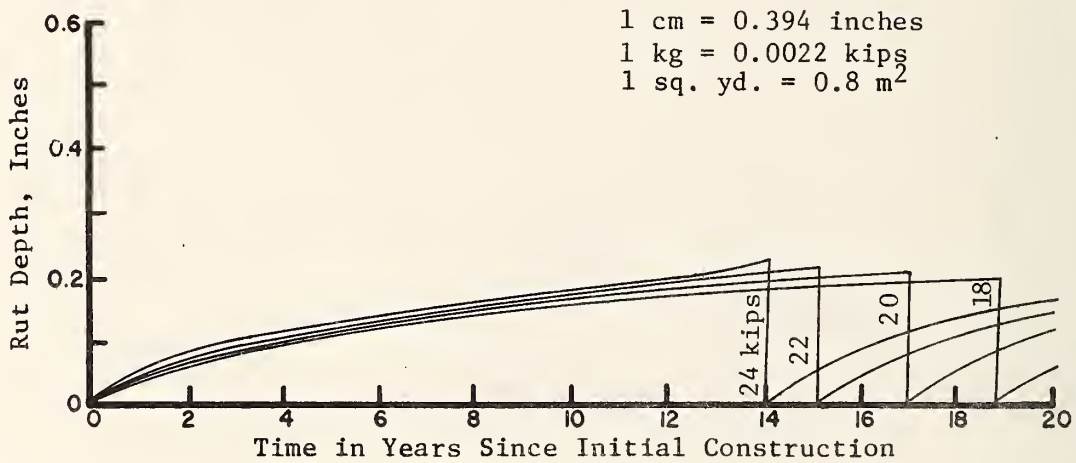


c. Serviceability Index vs. time

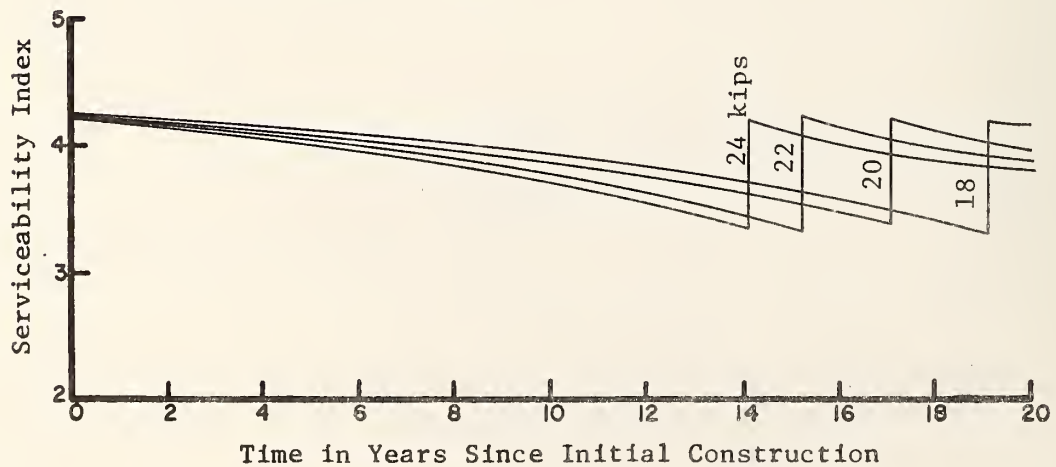
Figure 23. Predicted performance, wet-no freeze environment, low traffic and thin pavement section.



a. Cracking vs. time

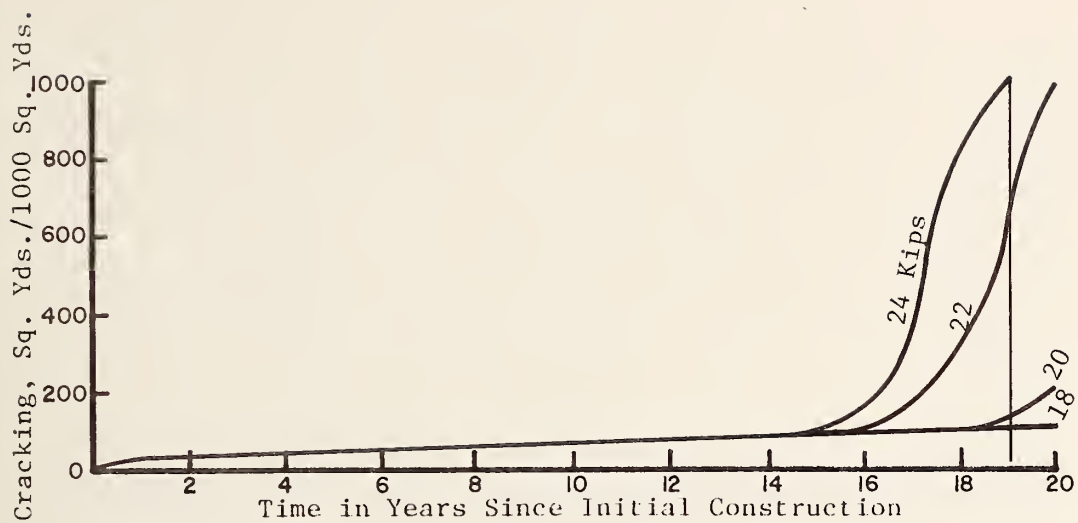


b. Rut depth vs. time

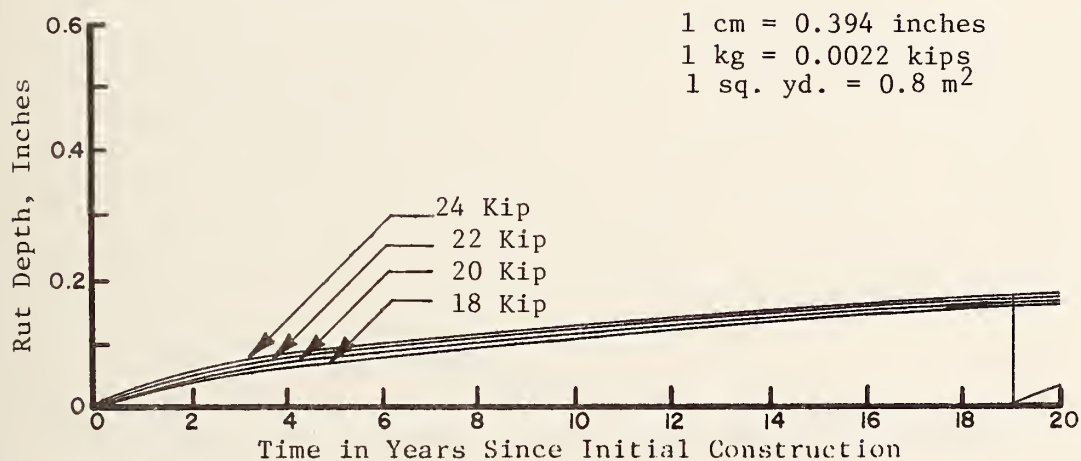


c. Serviceability Index vs. time

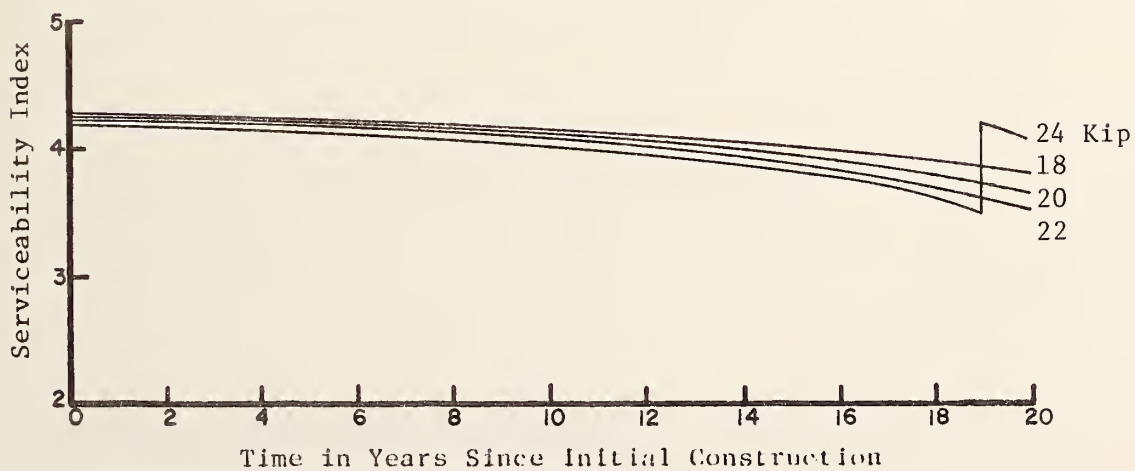
Figure 24. Predicted performance, dry-no freeze environment, low traffic, thin pavement section.



a. Cracking vs. time

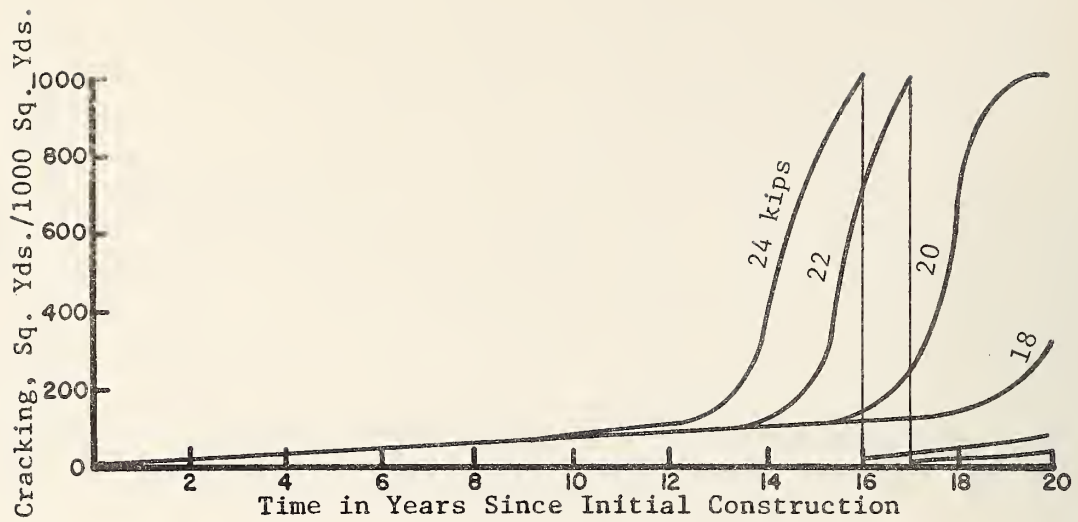


b. Rut depth vs. time

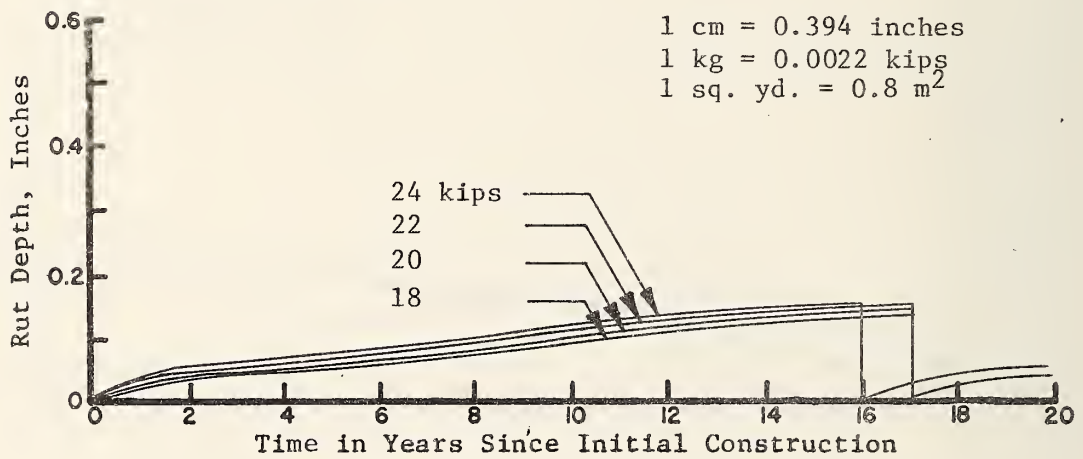


c. Serviceability Index vs. time

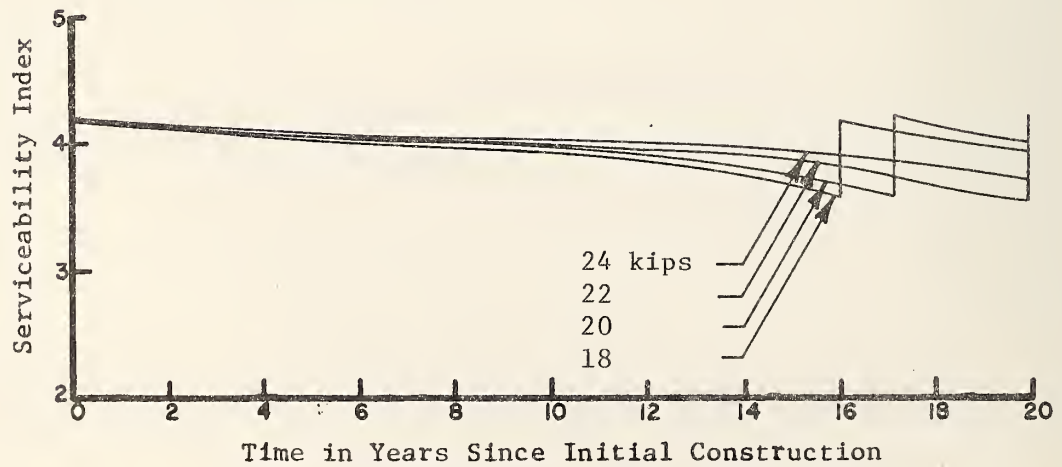
Figure 25. Predicted performance, wet-freeze environment, low traffic and thick pavement section.



a. Cracking vs. time

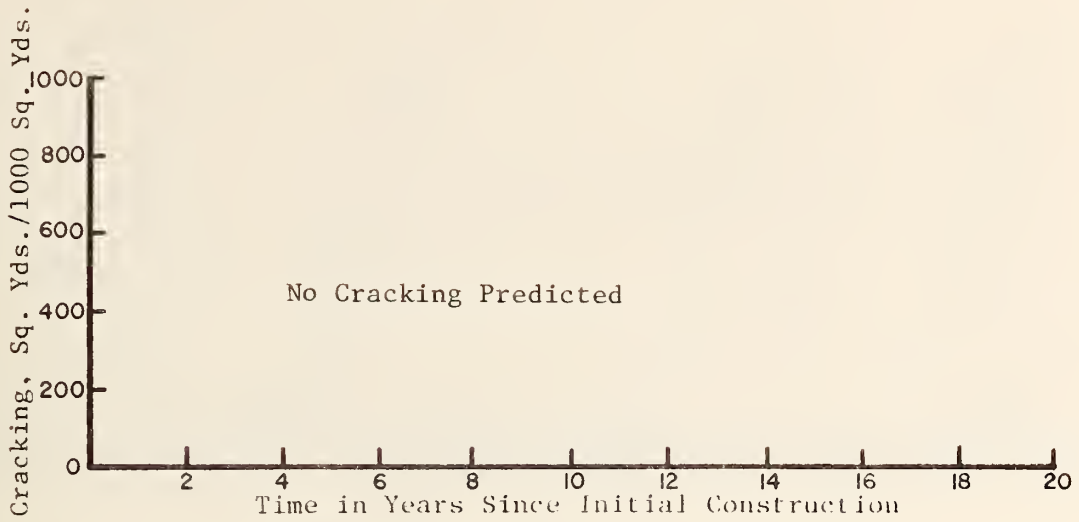


b. Rut depth vs. time

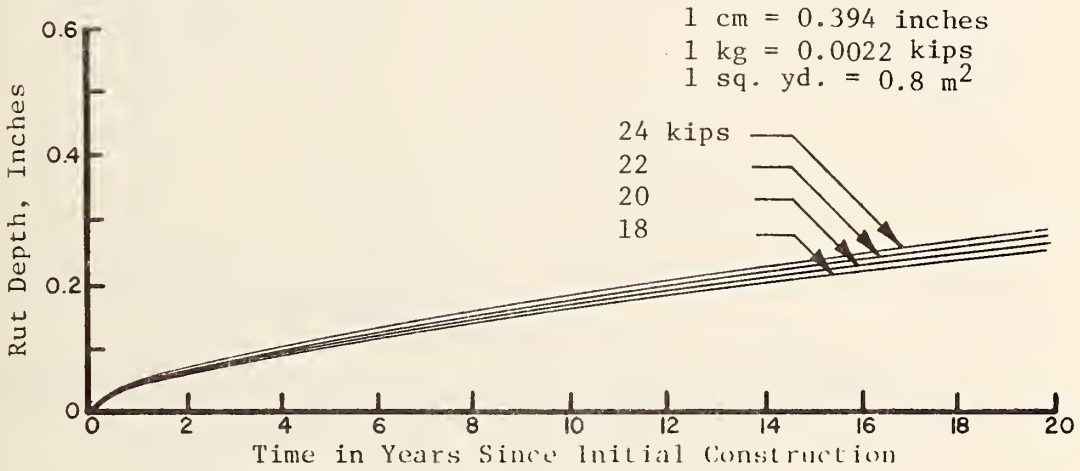


c. Serviceability Index vs. time

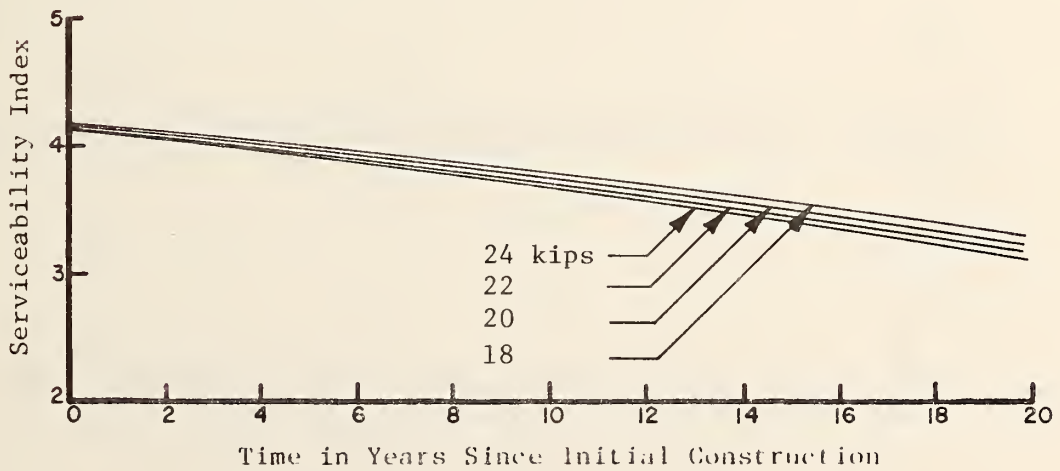
Figure 26. Predicted performance, dry-freeze environment, low traffic and thick pavement section.



a. Cracking vs. time

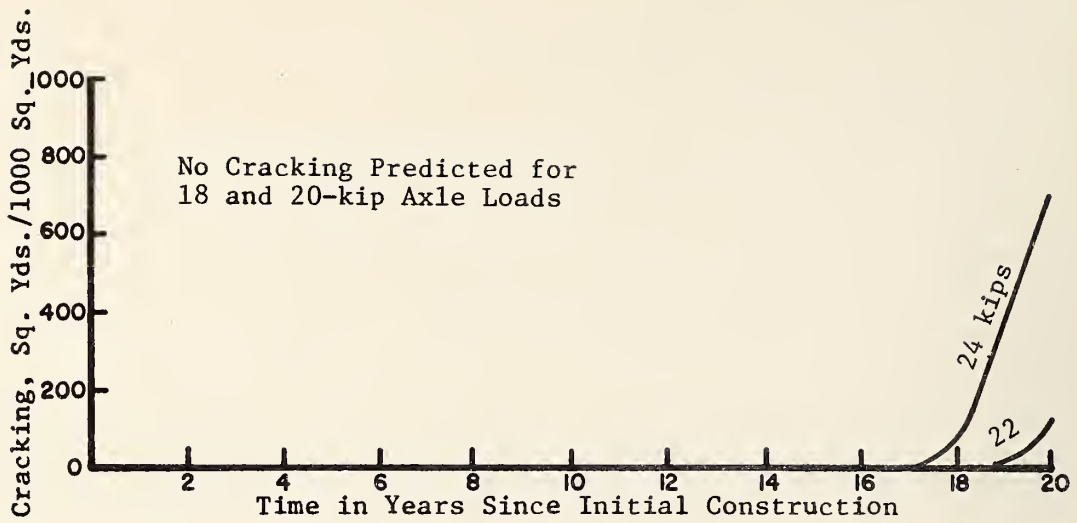


b. Rut depth vs. time

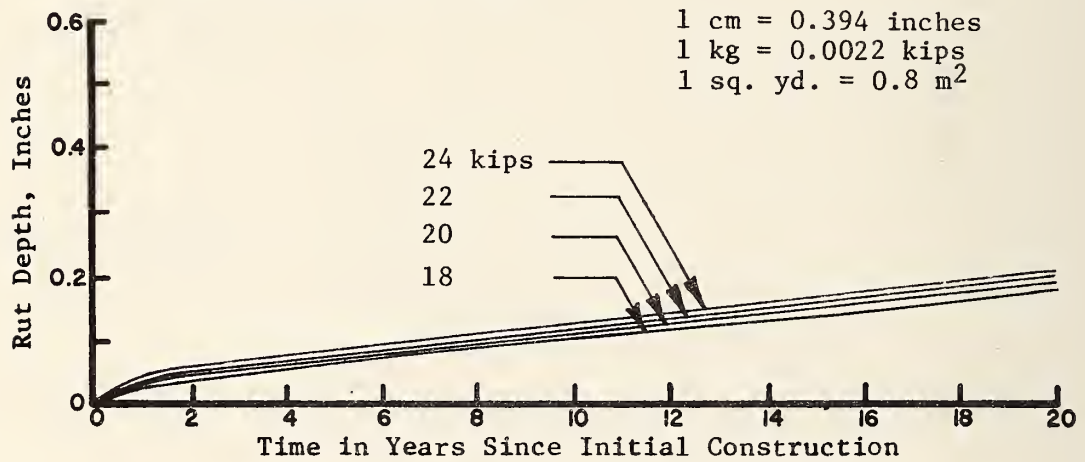


c. Serviceability Index vs. time

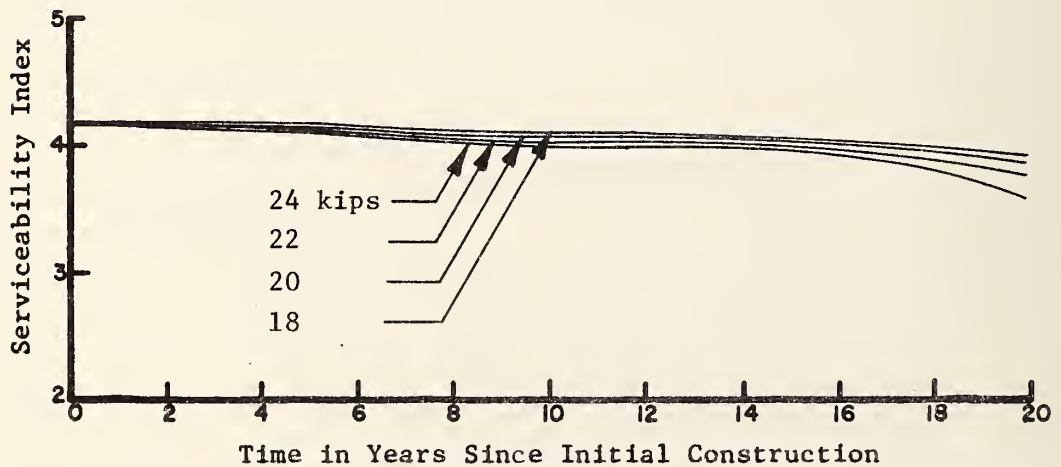
Figure 27. Predicted performance, wet-no freeze environment, low traffic, thick pavement section.



a. Cracking vs. time

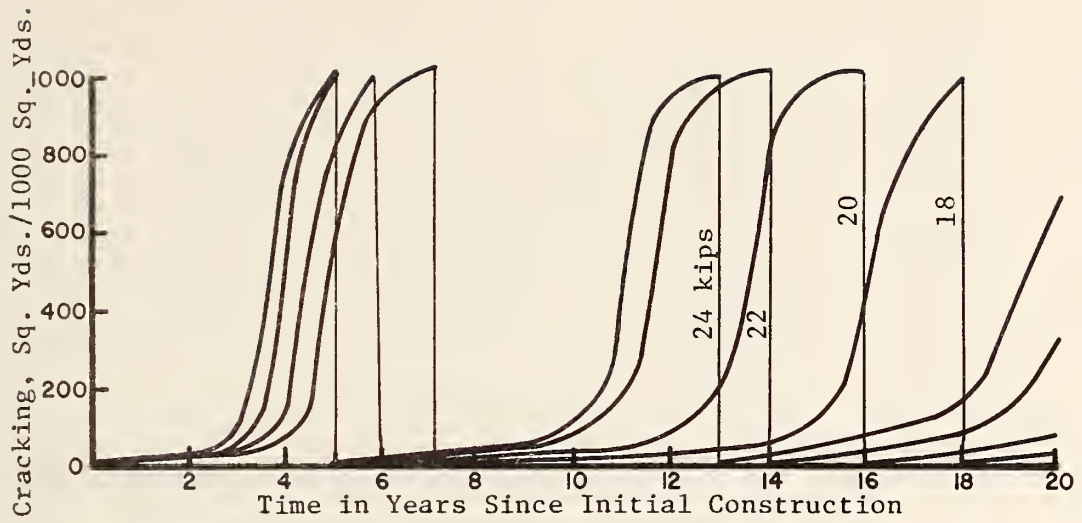


b. Rut depth vs. time

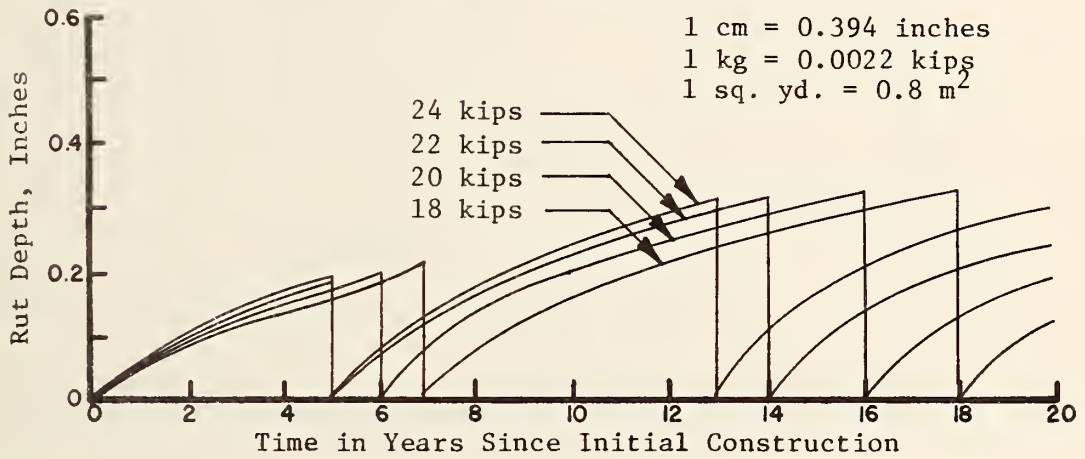


c. Serviceability Index vs. time

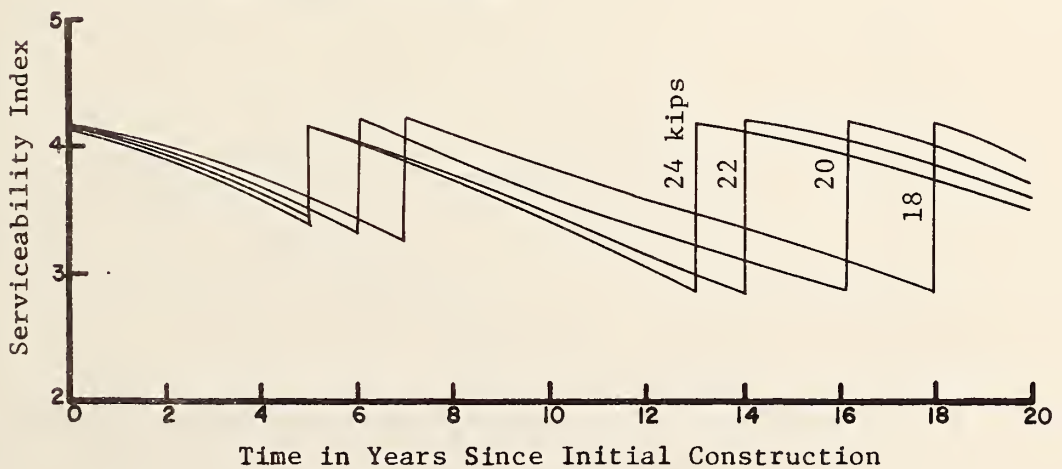
Figure 28. Predicted performance, dry-no freeze environment, low traffic and thick pavement section.



a. Cracking vs. time

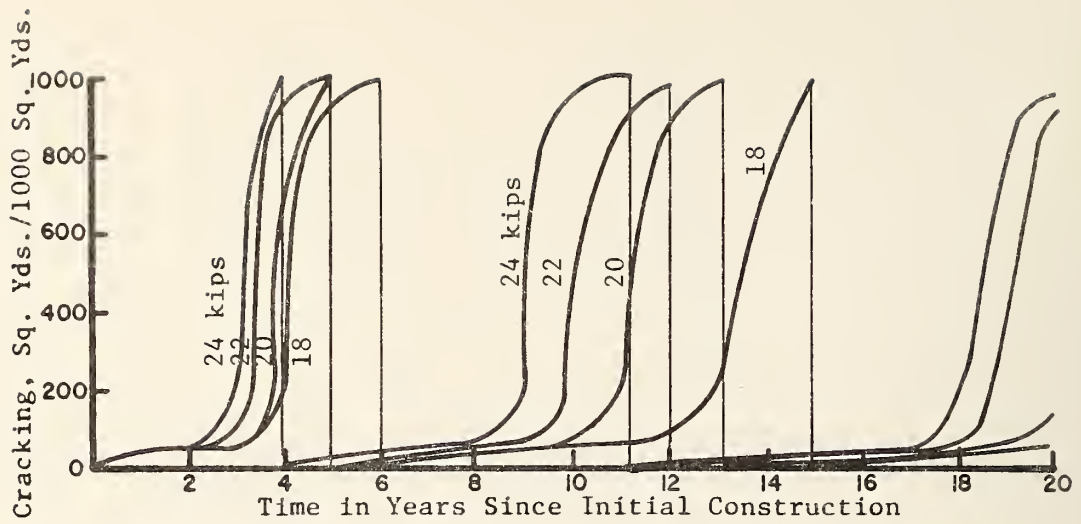


b. Rut depth vs. time

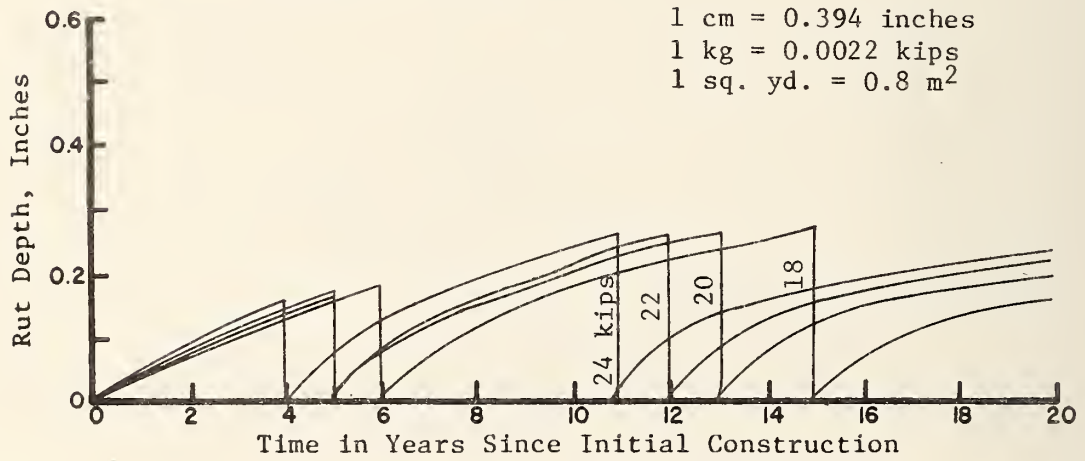


c. Serviceability Index vs. time

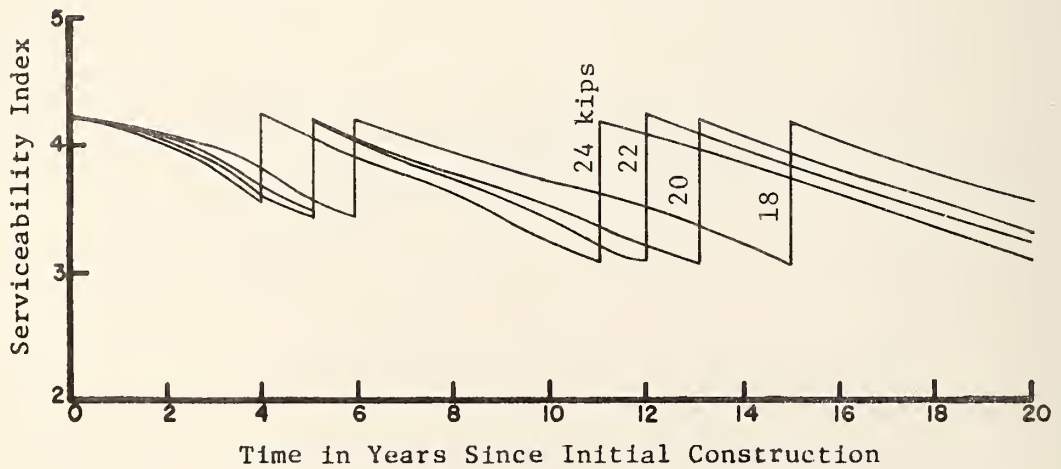
Figure 29. Predicted performance, wet-freeze environment, high traffic and thin pavement section.



a. Cracking vs. time

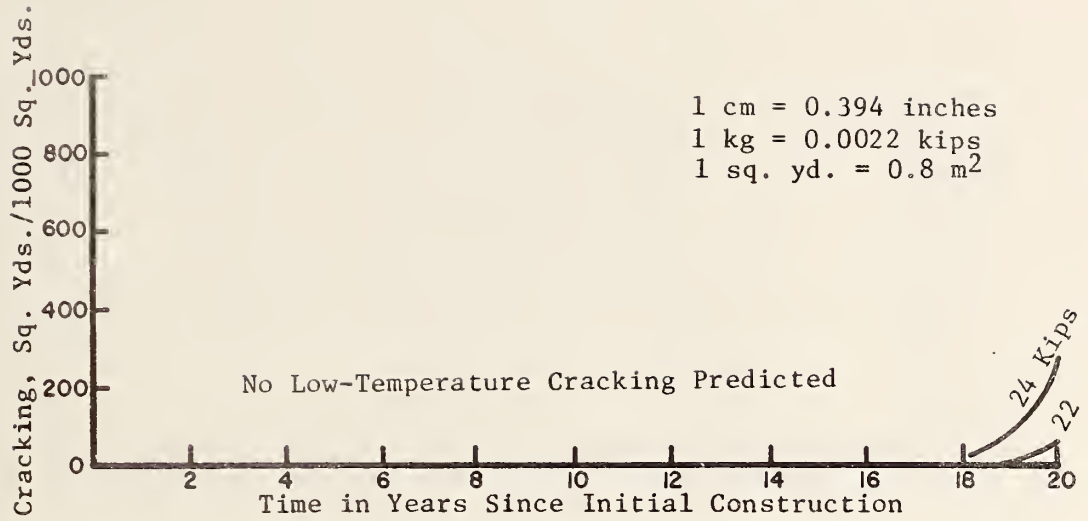


b. Rut depth vs. time

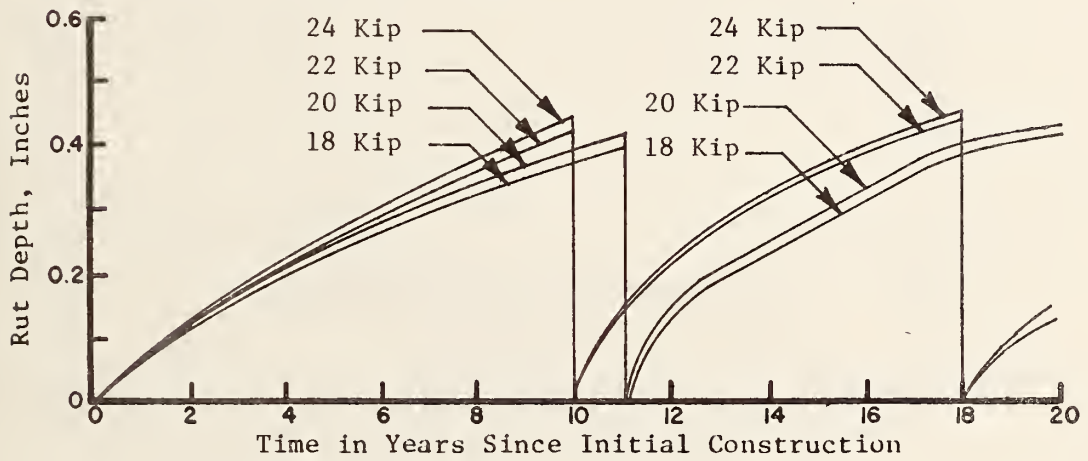


c. Serviceability Index vs. time

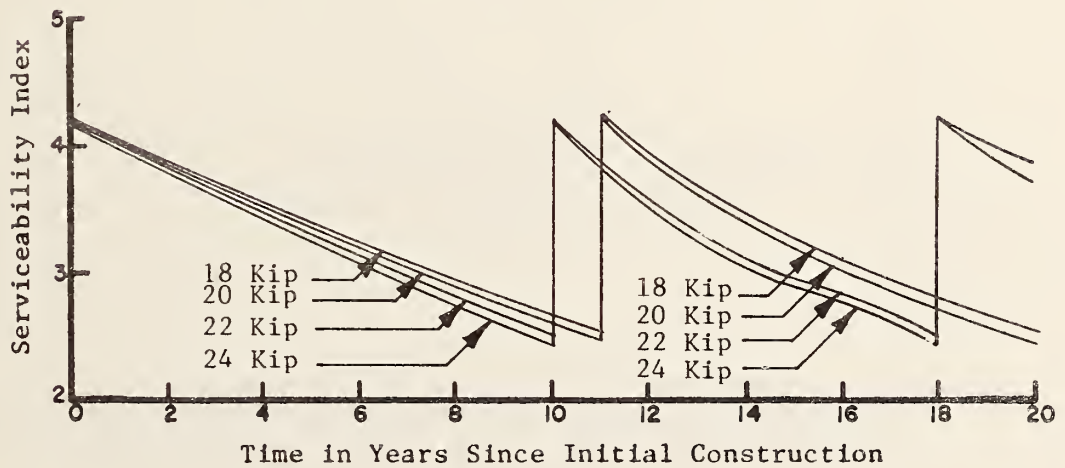
Figure 30. Predicted performance, dry-freeze environment, high traffic and thin pavement section.



a. Cracking vs. time

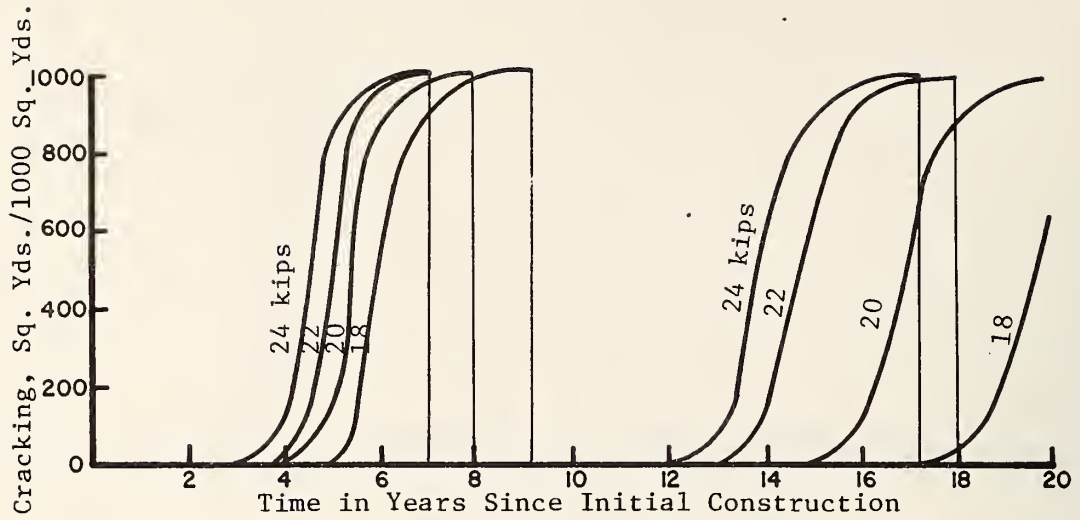


b. Rut depth vs. time

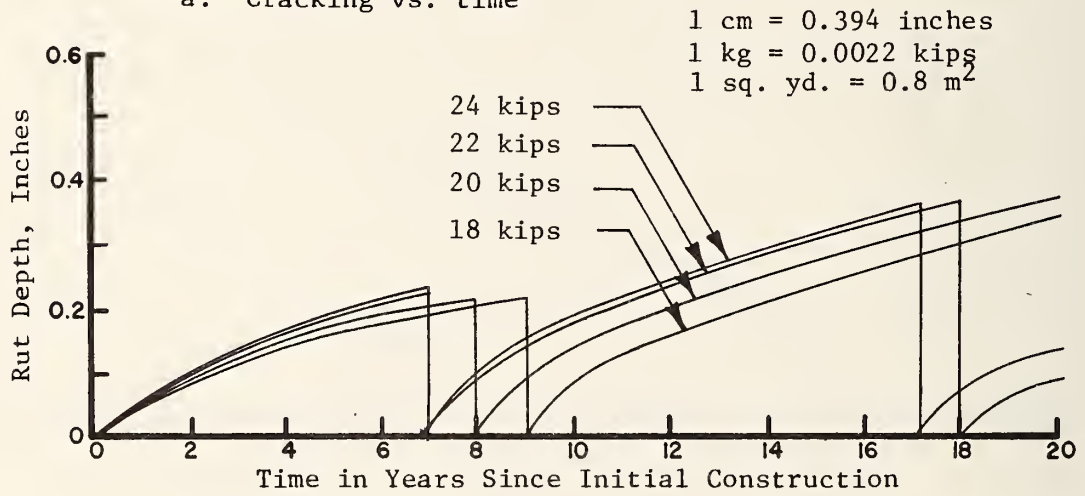


c. Serviceability Index vs. time

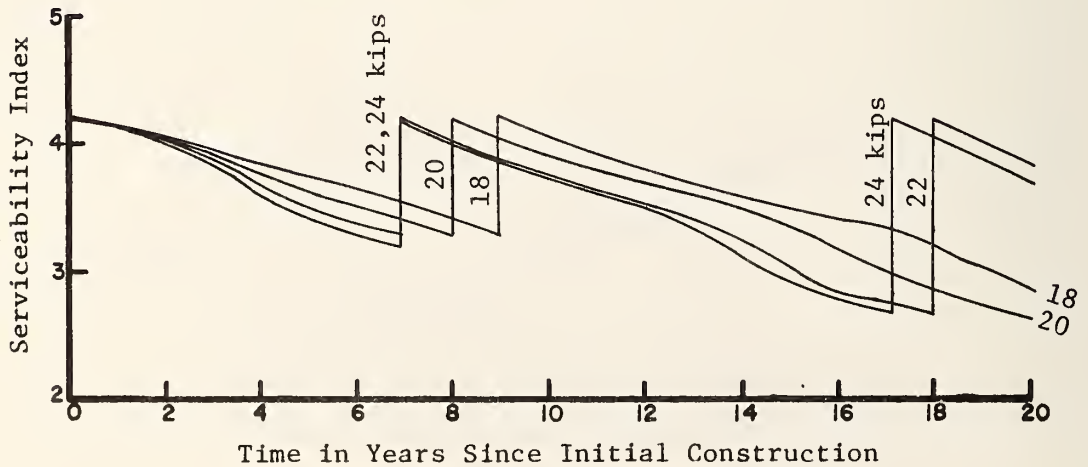
Figure 31. Predicted performance, wet-no freeze environment, high traffic and thin pavement section.



a. Cracking vs. time

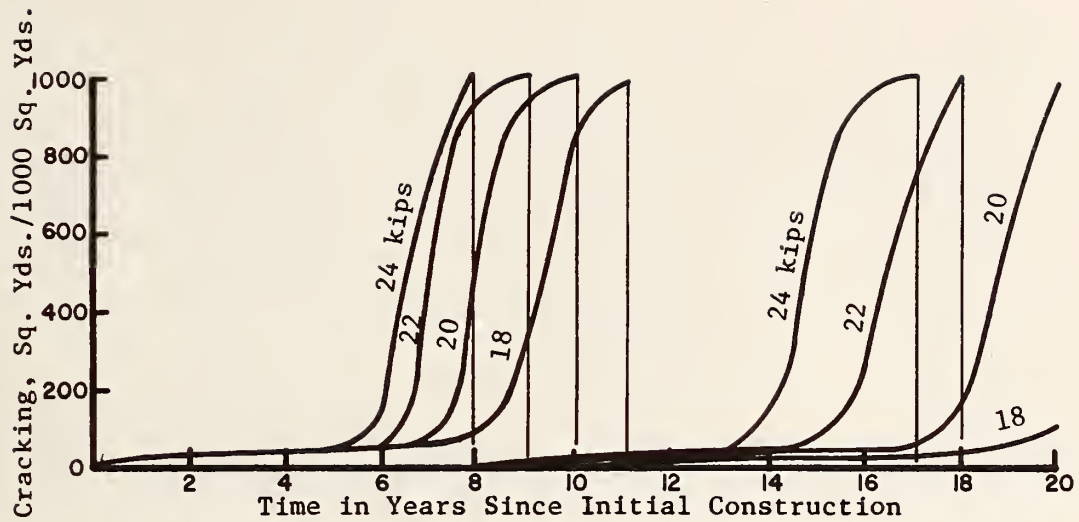


b. Rut depth vs. time

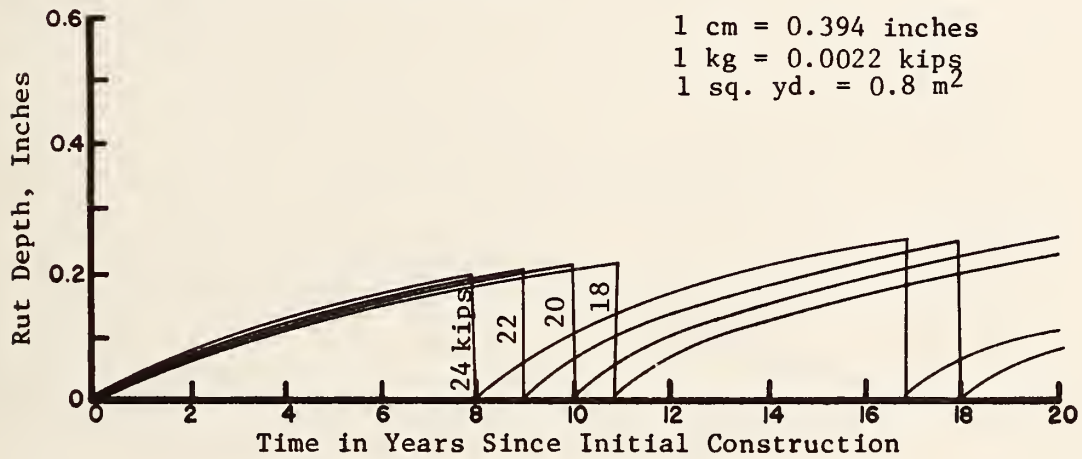


c. Serviceability Index vs. time

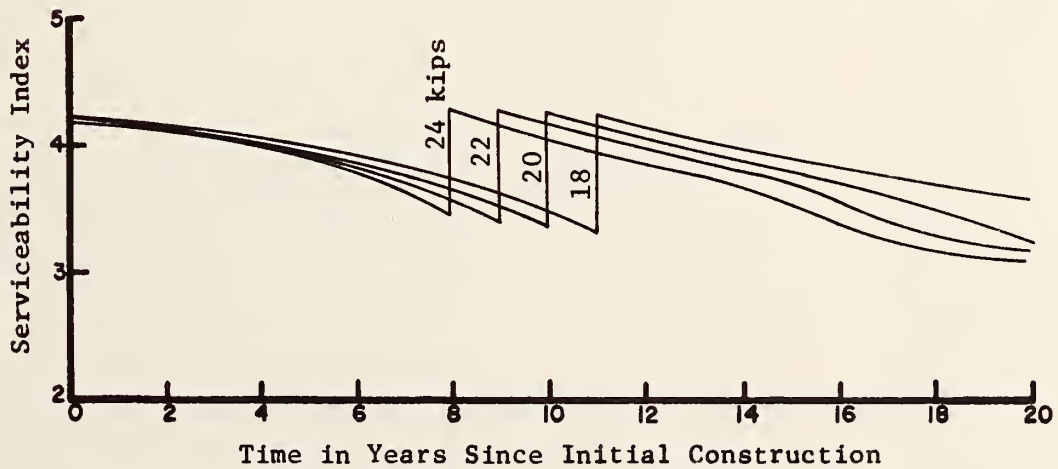
Figure 32. Predicted performance, dry-no freeze environment, high traffic and thin pavement section.



a. Cracking vs. time

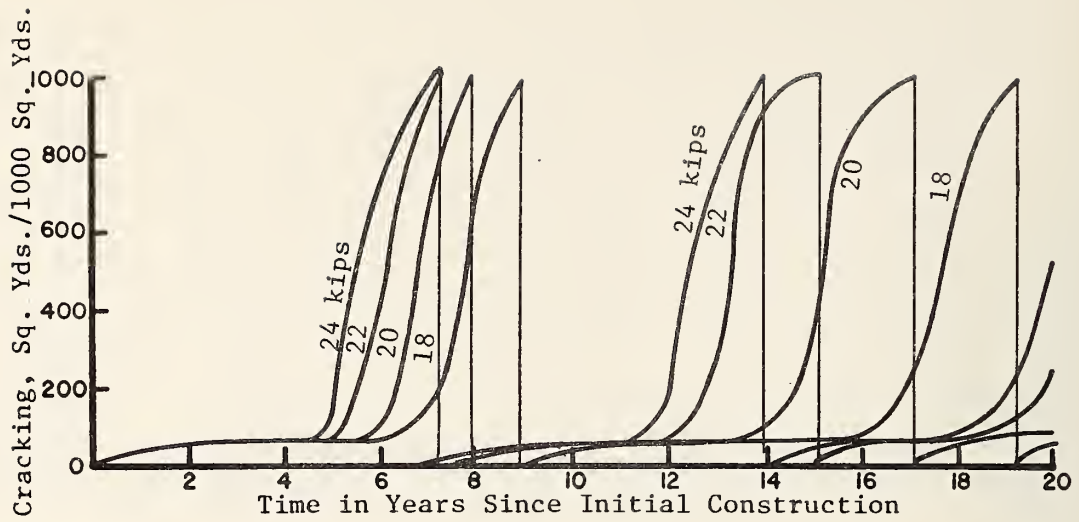


b. Rut depth vs. time

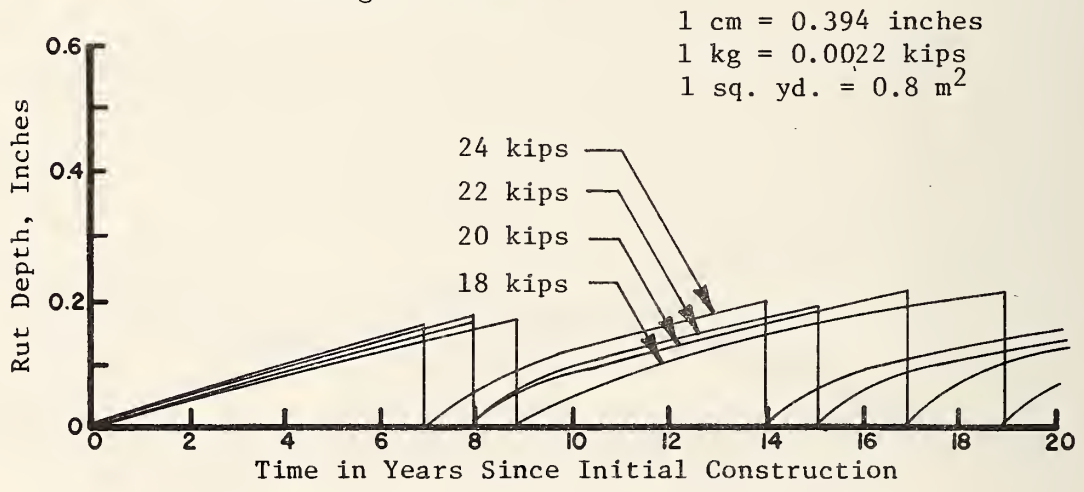


c. Serviceability Index vs. time

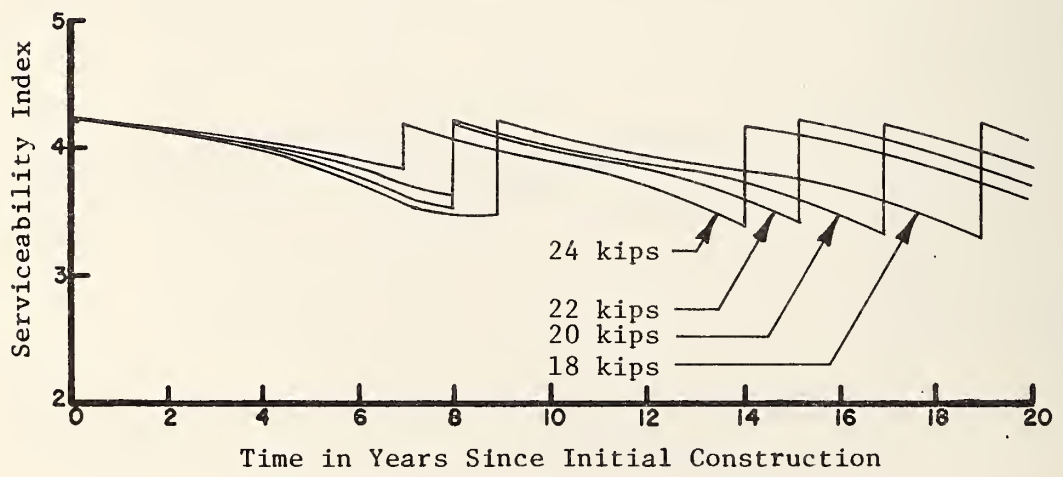
Figure 33. Predicted performance, wet-freeze environment, high traffic and thick pavement section.



a. Cracking vs. time

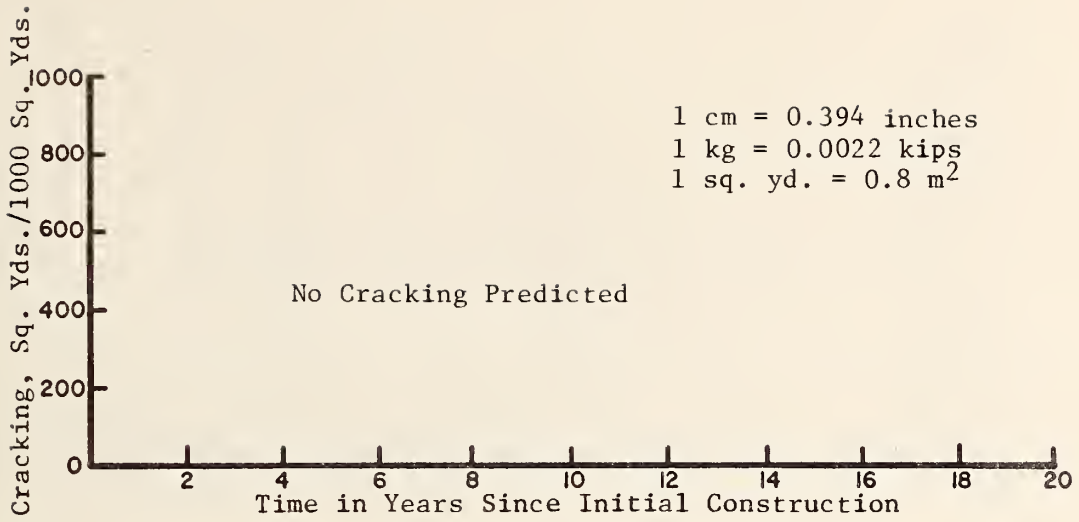


b. Rut depth vs. time

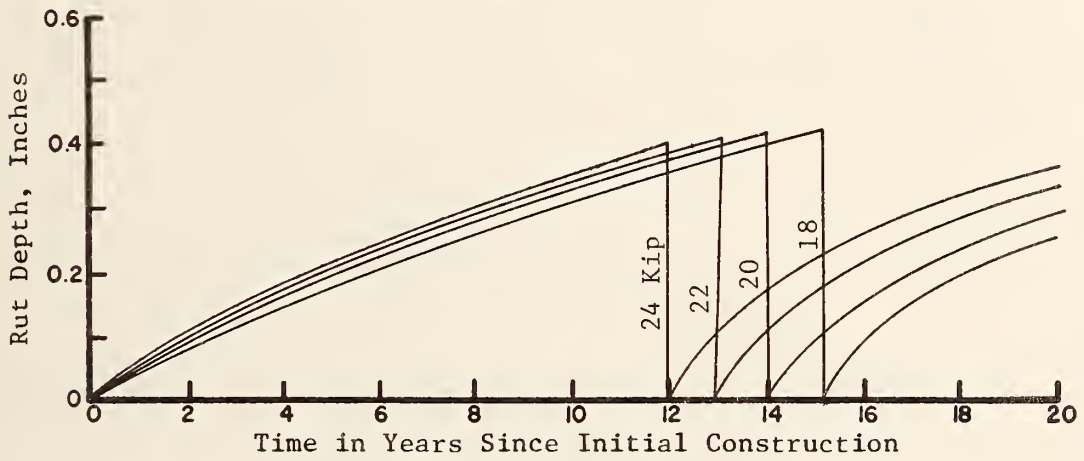


c. Serviceability Index vs. time

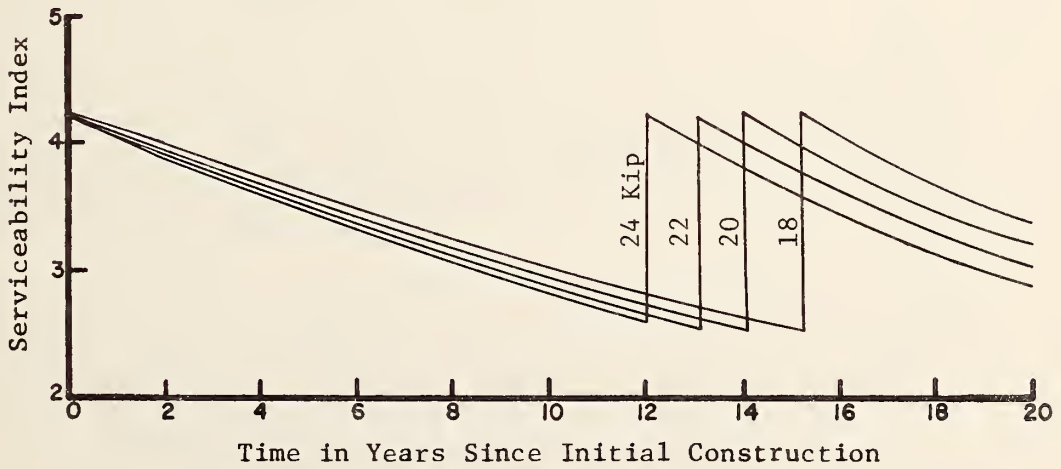
Figure 34. Predicted performance, dry-freeze environment, high traffic and thick pavement section.



a. Cracking vs. time

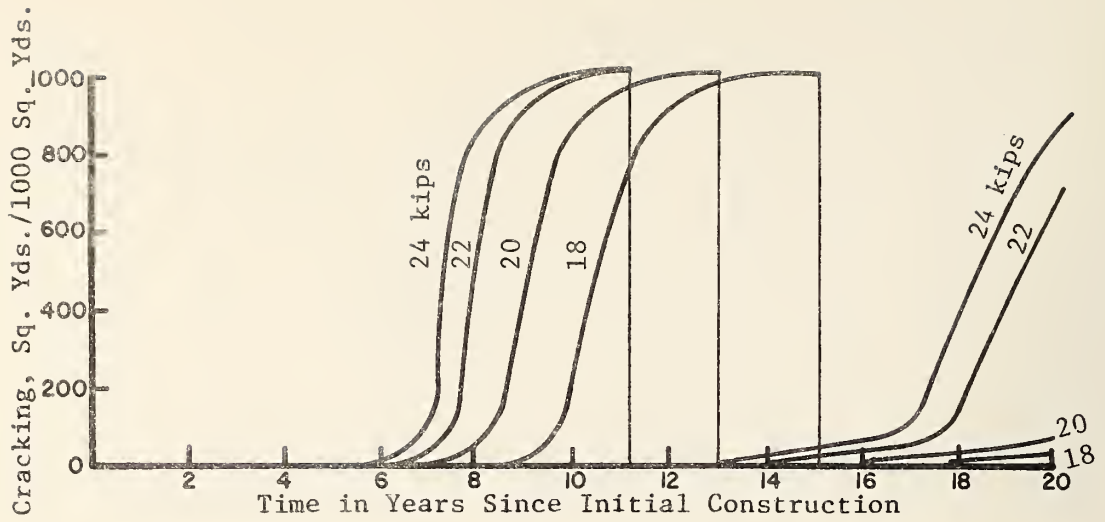


b. Rut depth vs. time

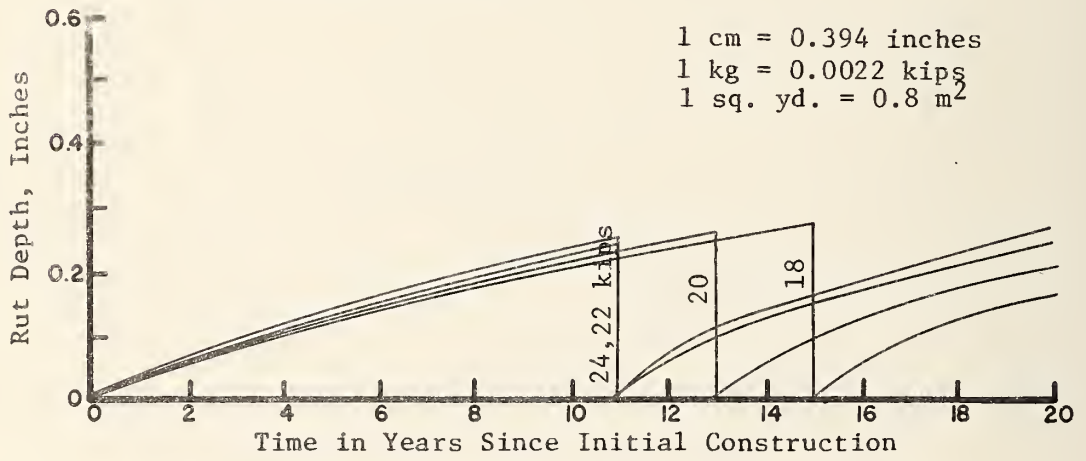


c. Serviceability Index vs. time

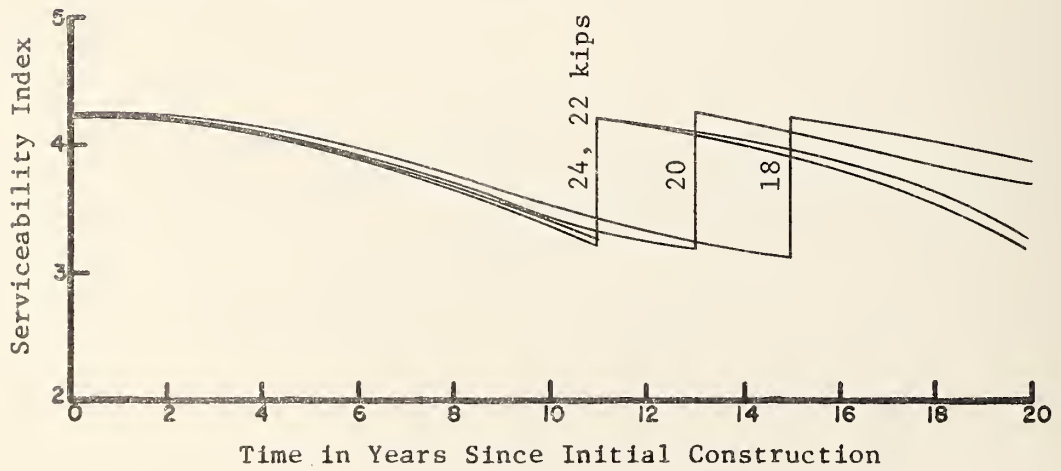
Figure 35. Predicted performance, wet-no freeze environment, high traffic and thick pavement section.



a. Cracking vs. time



b. Rut depth vs. time



c. Serviceability Index vs. time

Figure 36. Predicted performance, dry-no freeze environment, high traffic and thick pavement section.

CHAPTER VII

RELATIONSHIPS BETWEEN LEGAL AXLE LOADS AND LIFE CYCLE COSTS FOR FLEXIBLE PAVEMENTS

The work described in previous chapters provides a realistic data base in terms of pavement sections initially constructed and of major maintenance requirements (considered to be overlays only) to attain the desired 20-year service life. This chapter deals with the final product of this research effort, the relationships between costs to attain a 20-year service life and four levels of legal axle loads.

The data base on which the cost analysis depends consists of a factorial of solutions for original pavement and overlay lives for two pavement thicknesses, two levels of truck traffic, and four load distributions corresponding to four values of legal axle load limit. This data may now be used to develop cost estimates and to relate these estimates in several ways to the legal axle load limits. It is hoped that these cost comparisons will be useful in understanding the study results and that at least one of the four types of costs considered will fit the particular interests or needs of individual pavement engineers.

The unit costs for use in estimating costs of initial construction and of overlays were obtained through studies of Reference 41¹ and correlation with Reference 42². Unit costs per square yard of pavement developed for this study appear in Table 24 for initial construction. The costs for overlays were estimated to be \$2.39 for 2-inch (5.1 cm) overlays, \$3.55 for 3-inch (7.6 cm) overlays and \$4.71 for 4-inch (10.2 cm) overlays. In order to limit the number of variables in the study factorial as much as possible without loss of important detail, the varying features of embankment, shoulders, ditches, other drainage facilities, and other features that might differ between various environmental zones were ignored. Regional cost factors were also ignored. These variables were not included in the study factorial because they would tend to obscure the meanings of the comparative results more than they would improve them through realism.

It was originally intended to carry out the cost estimates in terms of present worth, but the unpredictable variability in time of interest rates and of inflation plus the fact that interest rates and

¹A statistical summary of current bid data for all highway projects in the State of Texas.

²Means Cost Data, 1977.

Table 24. Estimates for initial construction costs for thin and thick pavement sections.

<u>Construction Item</u>	<u>Units</u>	<u>Unit Cost (Dollars)</u>	<u>Unit Cost Per Square Yard, Thin</u>	<u>Unit Cost Per Square Yard, Thick</u>
Preparation of Subgrade	---	---	0.35	0.35
Base Course	dollars per inch of depth per sq. yd.			
Thin - 19 inches		0.157		
Thick - 8.5 inches		0.175	2.98	1.49
Subbase Course	dollars per inch of depth per sq. yd.			
Thin - None		0.135	---	3.11
Thick-23 inches				
Prime Coat	dollars per sq. yd.	0.20	0.20	0.20
Surface Layer				
Thin - 3.9 inches		1.16	4.52	
Thick - 4.5 inches		1.16		5.22
				<u>5.22</u>
			Initial Cost per sq. yd. ---	\$10.37
			\$8.05	

1 cm = 0.394 inches
 1 m² = 1.30 sq. yards

inflation rates have been similar and off-setting in recent years resulted in the decision to base the cost estimates on 1977 costs for both initial construction and subsequent overlays. This represents in effect the present worth based on the assumption of equal interest and inflation rates. Stated differently, the probability of inaccuracy is no higher through assuming equal interest and inflation rates than through attempting to predict their values in time.

Cost Evaluations and Relating Costs to Legal Axle Loads

One of the very difficult decisions made during the research effort was how to meaningfully express the relationships between costs and legal axle loads. One type of cost that must be considered is the total cost to obtain twenty years of acceptable pavement service. While meaningful, this does not discriminate with much sensitivity between the real costs of operating real pavements that are certainly not to be abandoned after twenty years. As can be seen later, the same number of overlays may suffice for several axle load distributions although the relative distresses and performances may differ. Consequently, it was decided that "value of remaining pavement life" or "salvage value" past twenty years should also be included as a part of the analysis and presentation. It also was apparent that costs to retain an existing pavement in service under increased axle load distributions were at least as important as the costs to build and maintain new pavements under various axle load distributions.

From the numerous types of costs that might have been used for this comparative study, four were selected and are identified and defined below:

1. "Total Cost" consisting of the initial construction costs and costs of necessary overlays to maintain satisfactory service for 20 years.
2. "Average Annual Cost" calculated by dividing the "Total Cost" by the total life of the pavement.
3. "Total Cost of Overlays" or the cost for the overlays necessary to attain 20 years of satisfactory service (same as "Total Cost" less initial construction cost).
4. "Average Annual Cost for Overlays" or the "Total Cost of Overlays" divided by the life of the pavement after the first overlay.

"Total Cost" and "Average Annual Cost" include initial construction costs and therefore relate to relative costs for new pavements subjected to truck traffic representative of different legal axle

loads, while the other two cost types relate in an approximate fashion to major maintenance costs for existing pavements subjected to different legal axle loads. Total Cost, Average Annual Cost and Total Cost of Overlays appear to be rather straightforward and their relation to real situations direct. The cost type labelled "Average Annual Cost of Overlays" is not as direct, however, but does give a measure of sorts for relating axle loading to cost of maintaining pavement serviceability. There are other cost terms that can be defined and considered for existing pavements, but none have any more general applicability. Both the "Average Annual Cost" and "Average Annual Cost of Overlays" bring the value of the pavement's remaining life after twenty years of service into consideration.

The "Total Costs" for the sixty-four combinations of conditions studied may be developed by taking the appropriate initial cost (\$8.05 for a thin or \$10.37 for a thick pavement section) and adding to that the cost of the overlays. Table 23 indicates the number of overlays. Their thicknesses and costs as previously described were as follows:

1. Pavements for all environmental zones except wet-no freeze received three-inch (7.6 cm) overlays at \$3.55 per sq. yd. for low traffic and four-inch (10.2 cm) overlays at \$4.71 per sq. yd. for high traffic. (1 sq. yd. = 0.8 m²)
2. Two-inch (5.1 cm) overlays at \$2.39 per sq. yd. were placed on pavements in the wet-no freeze environmental zone.

The estimated costs developed in this manner are tabulated as "Total Cost" in Table 25 for low truck traffic and Table 26 for high truck traffic. The other three cost types are also tabulated in the same tables.

With all the basic data now tabulated, the costs relative to legal axle loads will be considered hereafter in terms of new pavements (initial construction costs considered) and existing pavements (only overlay costs considered).

Cost Relationships for New Pavements

It can be readily seen from review of Tables 25 and 26 that the total cost was not dependent on a legal axle load for nine of the sixteen cases that were considered for each legal axle load. This was because the pavement either did not require an overlay to reach a 20 year design life or an equal number of overlays were required for each of the legal axle loads considered. This does not imply, however, that damage to the pavements and salvage value after 20 years were not affected by the variations in axle loads. Average annual costs always reflect variations in cost due to variations in total service life.

Because of the higher frequency of cracking in colder climates and the lower frequency of overlays required where the failure mode

Table 25. Cost data in dollars as a function of legal axle load, environmental zone, and pavement section for low traffic cases.

ENVIRONMENTAL ZONE	COST TYPE	THIN PAVEMENT SECTION						THICK PAVEMENT SECTION						
		Legal Axle Load, Kips*						Legal Axle Load, Kips						
		18	20	22	24	26	28	18	20	22	24	26	28	
WET-FREEZE	Total Cost	11.60	11.60	11.60	15.15	10.37	10.37	10.37	10.37	10.37	10.37	10.37	10.37	13.92
	Average Annual Cost	.46	.53	.58	.54	.40	.45	.49	.42					
	Total Cost of Overlays	3.55	3.55	3.55	7.10	0	0	0	0	0	0	0	0	3.55
	Average Annual Cost of Overlays	.36	.39	.39	.39	0	0	0	0	0	0	0	0	.25
	Total Cost	11.60	15.15	15.15	15.15	10.37	10.37	10.37	13.92	13.92	13.92	13.92	13.92	13.92
DRY-FREEZE	Average Annual Cost	.55	.54	.63	.69	.45	.52	.46	.52					
	Total Cost of Overlays	3.55	7.10	7.10	7.10	0	0	0	0	0	0	0	0	3.55
	Average Annual Cost of Overlays	.39	.39	.47	.51	0	0	0	0	0	0	0	0	.32
	Total Cost	8.05	8.05	8.05	8.05	10.37	10.37	10.37	10.37	10.37	10.37	10.37	10.37	10.37
	Average Annual Cost	.28	.29	.31	.32	.28	.30	.31	.31	.31	.31	.31	.31	.31
WET - NO FREEZE	Total Cost of Overlays	0	0	0	0	0	0	0	0	0	0	0	0	0
	Average Annual Cost of Overlays	0	0	0	0	0	0	0	0	0	0	0	0	0
	Total Cost	11.60	11.60	11.60	11.60	10.37	10.37	10.37	10.37	10.37	10.37	10.37	10.37	10.37
	Average Annual Cost	.36	.41	.46	.48	.33	.38	.41	.45					
	Total Cost of Overlays	3.55	3.55	3.55	3.55	0	0	0	0	0	0	0	0	0
DRY - NO FREEZE	Average Annual Cost of Overlays	.27	.32	.36	.36	0	0	0	0	0	0	0	0	0

* 1 kg = 0.0022 kips

Table 26. Cost data in dollars as a function of legal axle load, environmental zone, and pavement section for high traffic cases.

ENVIRONMENTAL ZONE	COST TYPE	THIN PAVEMENT SECTION							THICK PAVEMENT SECTION			
		Legal Axle Load, Kips *							Legal Axle Load, Kips			
		18	20	22	24	26	28	30	18	20	22	24
WET-FREEZE	Total Cost	17.47	17.47	17.47	17.47	17.47	17.47	17.47	15.08	15.08	19.79	19.79
	Average Annual Cost	.60	.65	.73	.83			.63	.72	.68	.73	
	Total Cost of Overlays	9.42	9.42	9.42	9.42	9.42	9.42	4.71	4.71	9.42	9.42	
	Average Annual Cost of Overlays	.43	.45	.50	.59			.36	.43	.47	.50	
DRY-FREEZE	Total Cost	17.47	17.47	17.47	17.47	17.47	17.47	19.79	19.79	19.79	19.79	19.79
	Average Annual Cost	.70	.76	.83	.87			.66	.71	.79	.90	
	Total Cost of Overlays	9.42	9.42	9.42	9.42	9.42	9.42	9.42	9.42	9.42	9.42	9.42
	Average Annual Cost of Overlays	.50	.54	.59	.59			.45	.47	.55	.63	
WET - NO FREEZE	Total Cost	10.44	10.44	12.83	12.83	12.83	12.83	12.76	12.76	12.76	12.76	12.76
	Average Annual Cost	.50	.52	.51	.53			.46	.49	.51	.53	
	Total Cost of Overlays	2.39	2.39	4.78	4.78	4.78	4.78	2.39	2.39	2.39	2.39	2.39
	Average Annual Cost of Overlays	.24	.27	.32	.34			.18	.20	.20	.20	.20
DRY - NO FREEZE	Total Cost	12.76	12.76	17.47	17.47	17.47	17.47	15.08	15.08	15.08	15.08	15.08
	Average Annual Cost	.56	.64	.58	.62			.50	.58	.69	.72	
	Total Cost of Overlays	4.71	4.71	9.42	9.42	9.42	9.42	4.71	4.71	4.71	4.71	4.71
	Average Annual Cost of Overlays	.34	.39	.41	.45			.31	.36	.43	.47	

* 1 kg = 0.0022 kips

is rutting rather than cracking, the costs for the northern environmental zones were higher than for the southern environmental zones for thin pavements. For the thick pavements, the differences in costs among environmental zones was minor.

Another useful way to consider the data developed is by normalizing all results presented in Tables 25 and 26 by dividing each value by its corresponding value for the 18-kip (8,180 kg) legal axle load. These normalized values appear in Tables 27 and 28 and indicate rather directly what increases in costs result from increases in legal axle loads. This information has been summarized statistically in Table 29 for new pavements by obtaining mean values for the various groupings of cases and environmental zones as well as for all cases combined.

For ease of observing trends and identifying some unexpected results, the average annual cost (probably more meaningful than total cost because it considers pavement life after twenty years) from Tables 25 and 26 have been plotted in Figures 37 through 40. These figures indicate that the average annual costs generally increase as expected with increasing legal axle loads. However, an unexpected result occurs in some cases (e.g., dry-freeze plot in Figure 38) where cost is shown decreasing with increasing legal axle load. This is not generally consistent with expectations from field experience and is partially due to the fact that accelerating deterioration as moisture percolates through surface cracks into underlying layers and reflection cracking are not modeled by mechanistic models such as VESYS A.

The cause of the decreasing cost (in terms of average annual costs over the total predicted service life of the pavement) with increasing legal axle load is that increasing damage predictions necessitate an overlay, which in turn increases the predicted pavement life sufficiently that its effect in decreasing average annual costs is greater than the increase caused by the added overlay cost.

It should be remembered, however, that the modeling limitations mentioned above apply not only to overlays, but also to initial construction predictions as well. That is to say that pavement life should always be overpredicted if the modeling limitation is serious. As the predictions do not appear unrealistic for either original pavements or overlays, it can be concluded that the model limitations may not be the primary cause of this unexpected result. It may simply mean that an overlay can not only meet an immediate need to maintain service, but may be cost effective. The Florida Department of Transportation has in fact found it cost effective to extend the life of a pavement through a relatively thin overlay when cracking begins at the bottom of the surface layer rather than to apply a thicker overlay after the cracks have propagated to the surface.

Table 27. Cost data from Table 25 normalized by dividing all values by the corresponding 18-kip legal axle limit costs, low traffic cases.

ENVIRONMENTAL ZONE	COST TYPE	THIN PAVEMENT SECTION				THICK PAVEMENT SECTION			
		Legal Axle Load, Kips**				Legal Axle Load, Kips			
		18	20	22	24	18	20	22	24
WET-FREEZE	Total Cost	1.00	1.00	1.00	1.31	1.00	1.00	1.00	1.34
	Average Annual Cost	1.00	1.14	1.25	1.17	1.00	1.13	1.23	1.05
	Total Cost of Overlays	1.00	1.00	1.00	2.00	1.00	1.00	1.00	*
	Average Annual Cost of Overlays	1.00	1.08	1.08	1.08	1.00	1.00	1.00	*
DRY-FREEZE	Total Cost	1.00	1.31	1.31	1.31	1.00	1.00	1.34	1.34
	Average Annual Cost	1.00	0.98	1.14	1.25	1.00	1.15	1.03	1.14
	Total Cost of Overlays	1.00	2.00	2.00	2.00	1.00	1.00	*	*
	Average Annual Cost of Overlays	1.00	1.00	1.21	1.31	1.00	1.00	*	*
WET-NO FREEZE	Total Cost	1.00	1.00	1.00	1.00	1.00	1.00	1.00	1.00
	Average Annual Cost	1.00	1.02	1.10	1.15	1.00	1.06	1.09	1.12
	Total Cost of Overlays	1.00	1.00	1.00	1.00	1.00	1.00	1.00	1.00
	Average Annual Cost of Overlays	1.00	1.00	1.00	1.00	1.00	1.00	1.00	1.00
DRY-NO FREEZE	Total Cost	1.00	1.00	1.00	1.00	1.00	1.00	1.00	1.00
	Average Annual Cost	1.00	1.14	1.28	1.33	1.00	1.15	1.24	1.35
	Total Cost of Overlays	1.00	1.00	1.00	1.00	1.00	1.00	1.00	1.00
	Average Annual Cost of Overlays	1.00	1.19	1.33	1.33	1.00	1.00	1.00	1.00

* Indeterminate as cannot divide by zero.

** 1 kg = 0.0022 kips

Table 29. Mean Values of Costs Versus Legal Axle Load Normalized by 18-Kip Legal Axle Limit Costs.

<u>Data Sample from which mean values are derived</u>	<u>Legal Axle Loads, Kips*</u>			
	<u>18</u>	<u>20</u>	<u>22</u>	<u>24</u>
Total Costs:				
All thin pavements	1.00	1.04	1.12	1.16
All thick pavements	1.00	1.00	1.05	1.12
All low traffic volumes	1.00	1.02	1.09	1.14
All high traffic volumes	1.00	1.04	1.09	1.16
Wet-Freeze Environment	1.00	1.00	1.08	1.12
Dry-Freeze Environment	1.00	1.00	1.00	1.23
Wet-No Freeze Environment	1.00	1.08	1.16	1.16
Dry-No Freeze Environment	1.00	1.00	1.06	1.06
All pavements	1.00	1.00	1.09	1.09
Average Annual Costs:				
All thin pavements	1.00	1.08	1.16	1.22
All thick pavements	1.00	1.12	1.15	1.20
All low traffic volumes	1.00	1.10	1.17	1.20
All high traffic volumes	1.00	1.10	1.14	1.23
Wet-Freeze Environment	1.00	1.12	1.14	1.18
Dry-Freeze Environment	1.00	1.07	1.16	1.23
Wet-No Freeze Environment	1.00	1.01	1.03	1.04
Dry-No Freeze Environment	1.00	1.05	1.09	1.13
All pavements	1.00	1.10	1.15	1.21

* 1 kg = 0.0022 kips

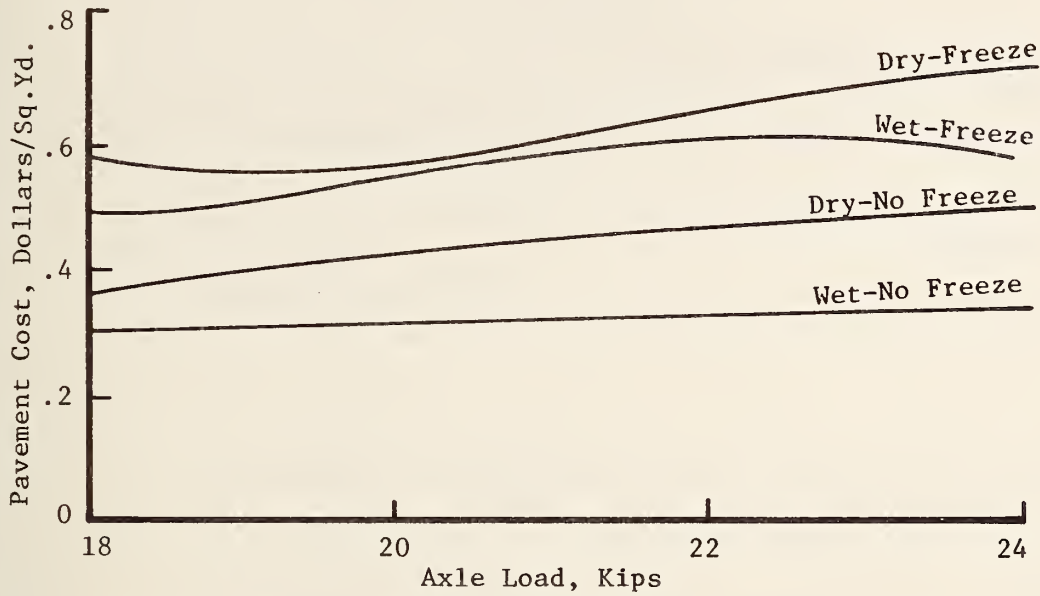


Figure 37. Average annual cost by environmental zone for low traffic and thin pavement section.

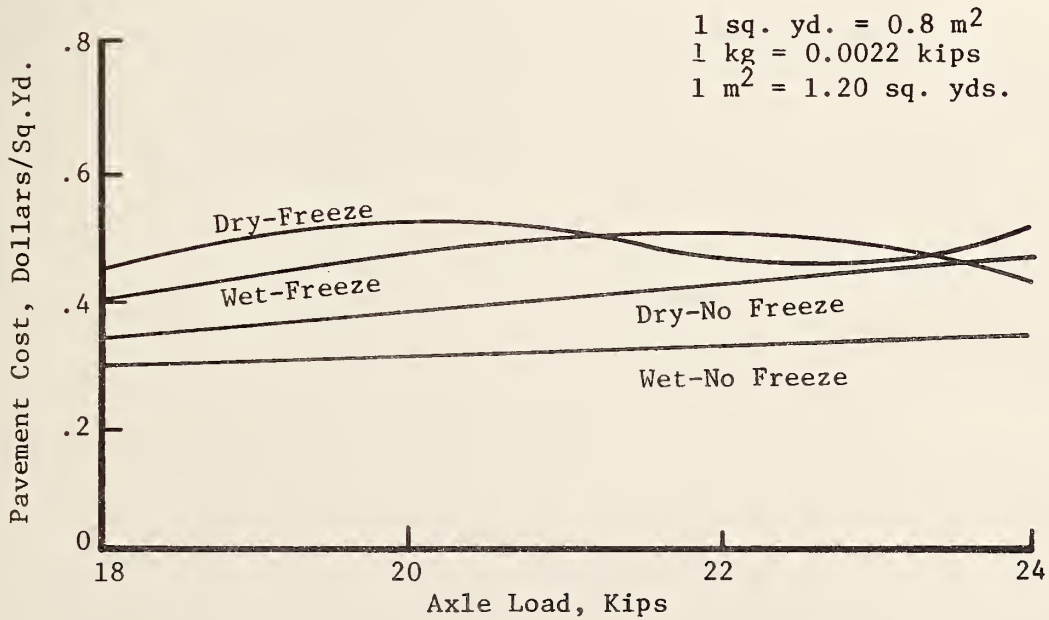


Figure 38. Average annual cost by environmental zone for low traffic and thick pavement section.

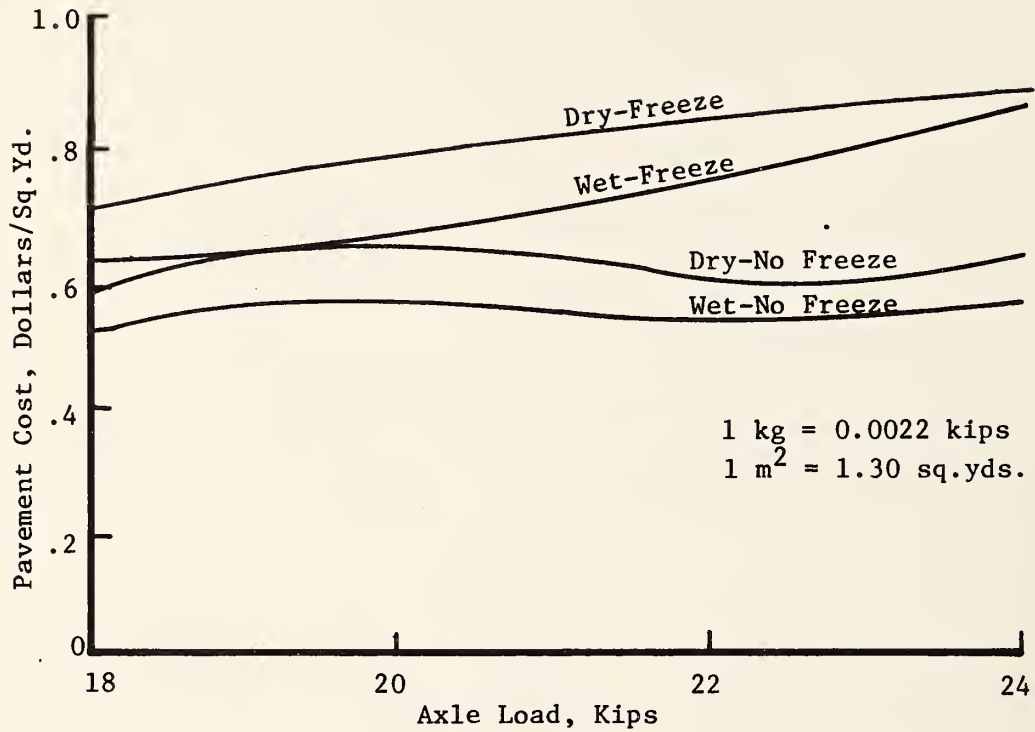


Figure 39. Average annual cost by environmental zone for high traffic and thin pavement.

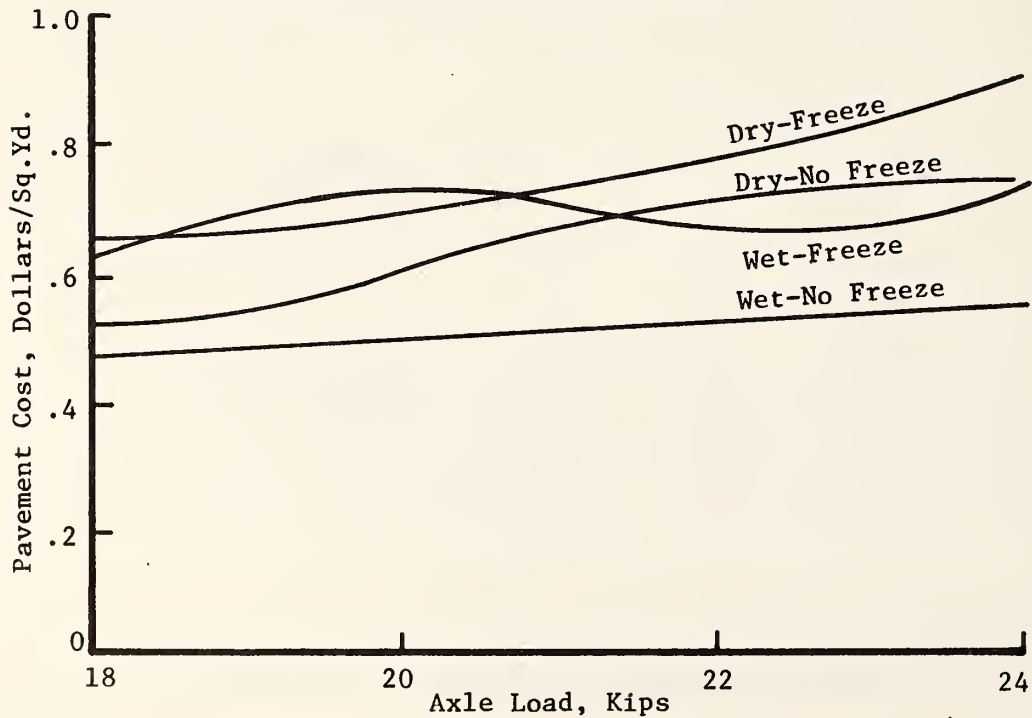


Figure 40. Average annual cost by environmental zone for high traffic and thick pavement.

It should be noted that the increase in costs predicted for the increased axle load distributions (See Table 10) that result from a change in legal axle limit are not very severe. There is no real similarity at all, for instance, to a road test such as the AASHO Road Test where an increase in test axle load means that essentially all subsequent traffic has that axle load.

While it may not be appropriate to claim quantitative accuracy for the predicted costs, it does appear reasonable to expect that all the results will be biased in the same way; the trends would thus be reliable and the costs erring (if at all) toward the low side.

Continuing with analysis of the cost predictions developed, the following general conclusions may be drawn from the summary values of Table 29:

1. The total cost for a 20 year service life may be expected to:
 - a. Increase nominally for an increase from 18 to 20 kips (8,180 to 9,000 kgs) in legal single axle load limits.
 - b. Increase up to 16 percent for an increase in legal axle limit from 18 to 22 kips (8,180 to 10,000 kgs) (dependent primarily on pavement thickness and environment), with a general expected cost increase less than 10 percent.
 - c. Increase from 6 to 23 percent for an increase in legal axle limit from 18 to 24 kips (8,180 to 10,900 kgs), with an average increase of 9 percent for all the pavements.
2. The average annual cost (considering the value of the pavements remaining life after 20 years) may be expected to:
 - a. Increase from one to 12 percent for an increase in legal axle limit from 18 to 20 kips (8,180 to 9,000 kgs), with an average increase of 10 percent.
 - b. Increase from three to seventeen percent for an increase in legal axle limit from 18 to 22 kips (8,180 to 10,000 kgs), with an average increase to 15 percent.
 - c. Increase from 4 to 23 percent for an increase in legal axle limit from 18 to 24 kips (8,180 to 10,900 kgs), with an average increase of 21 percent.
3. The overall effect of increased axle loads is more severe for thin than for thick pavements and for colder than for warmer climates.
4. While the effect on damage due to different levels of truck traffic volume on a pavement section is obvious, the rates of increase in costs for accommodating the traffic at different legal axle limits are not very sensitive to levels of truck traffic.

Cost Relationships for Existing Pavements

The cost types previously described as "Total Costs of Overlays" and "Average Annual Costs for Overlays" relate to an analysis of effects of increased legal axle limits on existing highways because the initial construction costs are not included in the analysis. Table 30 provides mean costs for overlays arrived at as previously described for new highways except that initial construction costs were omitted. These values were normalized by dividing through by the corresponding 18-kip (8,180 kg) axle load costs and the normalized values appear in Table 31.

As would be expected, the percentage increases in overlay costs for increases in legal axle limits are much greater when a relatively large fixed initial construction cost is not included. Analysis of the results in Tables 30 and 31 indicates that:

1. The predicted overlay costs for the higher legal axle limits in the wet-no freeze environmental zone (or warm temperature) represented by Florida IH-10 are nominal.
2. As would be expected, the total cost for maintaining the highway is much less for low than for high traffic volumes, but the percentage increase in total overlay costs with increase in axle loads is much higher for the low traffic case. For instance, a mean predicted total overlay cost for a 24-kip (10,900 kg) legal axle load on all low traffic volumes is 2.34 times as much as for an 18-kip (8,180 kg) legal axle load compared to only 20 percent more for all high traffic volumes.
3. The predicted overlay costs themselves are much higher for northern than for southern environments, but the percentage increase in overlay cost with increasing legal axle load are similar to those for the southern highways.
4. The cost of overlaying pavements was logically predicted to be greater for thin than thick pavements, but the percentage increase in overlay cost with legal increasing axle load was greater for the thick pavements.
5. In general, total overlay costs may be expected to increase about 6 percent for an increase in legal axle limit from 18 to 20 kips (8,180 to 9,000 kg), 33 percent for an increase from 18 to 22 kips (8,180 to 10,000 kg) and 45 percent for an increase from 18 to 24 kips (8,180 to 10,900 kg).
6. An increase in legal axle limit from 18 to 20 kips (8,180 to 9,000 kg) increases the average annual cost of overlays about 10 percent, an increase from 18 to 22 kips (8,180 to 10,000 kg) increases it about 30 percent and an increase from 18 to 24 kips (8,180 to 10,900 kg) increases it about 46 percent.

Table 30. Mean Values of Costs (Dollars)
for Overlays versus Legal Axle
Load.

Data Sample from which mean values are derived	Legal Axle Loads, Kips*			
	18	20	21	22
Total Costs of Overlays:				
All thin pavements	4.57	5.02	5.90	6.35
All thick pavements	2.65	2.65	3.69	4.13
All low traffic volumes	1.33	1.78	2.22	3.11
All high traffic volumes	5.90	5.90	7.07	7.07
Wet-Freeze Environment	4.42	4.42	5.60	7.37
Dry-Freeze Environment	5.60	6.49	7.37	7.37
Wet-No Freeze Environment	1.20	1.20	1.79	1.79
Dry-No Freeze Environment	3.24	3.24	4.42	4.42
All pavements	3.61	3.84	4.80	5.24
Average Annual Costs of Overlays:				
All thin pavements	0.316	0.344	0.380	0.404
All thick pavements	0.163	0.183	0.240	0.296
All low traffic volumes	0.127	0.138	0.186	0.229
All high traffic volumes	0.351	0.389	0.434	0.471
Wet-Freeze Environment	0.288	0.318	0.340	0.433
Dry-Freeze Environment	0.335	0.350	0.470	0.513
Wet-No Freeze Environment	0.105	0.118	0.130	0.135
Dry-No Freeze Environment	0.230	0.268	0.300	0.320
All pavements	0.239	0.263	0.310	0.350

* 1 kg = 0.0022 kips

Table 31. Mean Values of Costs for Overlays Normalized by 18-Kip Axle Load Costs versus Legal Axle Load.

Data Sample from which mean values are derived	Legal Axle Loads, Kips *			
	18	20	22	24
Total Costs of Overlays:				
All thin pavements	1.00	1.10	1.29	1.40
All thick pavements	1.00	1.00	1.39	1.56
All low traffic volumes	1.00	1.34	1.67	2.34
All high traffic volumes	1.00	1.00	1.20	1.20
Wet-Freeze Environment	1.00	1.00	1.27	1.67
Dry-Freeze Environment	1.00	1.16	1.32	1.32
Wet-No Freeze Environment	1.00	1.00	1.49	1.49
Dry-No Freeze Environment	1.00	1.00	1.36	1.36
All pavements	1.00	1.06	1.33	1.45
Average Annual Costs of Overlays:				
All thin pavements	1.00	1.09	1.20	1.28
All thick pavements	1.00	1.12	1.47	1.82
All low traffic volumes	1.00	1.09	1.46	1.80
All high traffic volumes	1.00	1.11	1.24	1.34
Wet-Freeze Environment	1.00	1.10	1.18	1.50
Dry-Freeze Environment	1.00	1.05	1.40	1.53
Wet-No Freeze Environment	1.00	1.12	1.24	1.29
Dry-No Freeze Environment	1.00	1.17	1.30	1.39
All pavements	1.00	1.10	1.30	1.46

* 1 kg = 0.0022 kips

It is hoped that the distress and performance predictions, the predicted costs related to legal axle load and the analysis and interpretation of the data will provide valuable insight into the effects of raising legal axle limits on our highways. The data has been presented in detail so that other more specific analyses may be made to serve special interests as required.

CHAPTER VIII

SUMMARY

The important results of the reasearch effort reported herein are:

- 1) Relationships between costs for twenty years of acceptable pavement service and established legal single axle limits. These relationships are based on distress and performance predicted by Computer Program VESYS A, using the best traffic, environment and materials characterizations possible in a factorial study of sixteen cases with legal single axle loads of 18, 20, 22 and 24-kips (8,180, 9,000, 10,000 and 10,900 kg) for each.
- 2) Improvements to VESYS IIM resulting in an improved computer code called VESYS A. VESYS A includes all the capabilities of VESYS IIM plus capabilities for:
 - a) discretized representation of axle load distribution,
 - b) seasonal characterizations of stiffness and permanent deformation properties of materials, and
 - c) low-temperature cracking predictions.

These improvements allow more accurate modeling of the flexible pavement structure and more accurate predictions of distress and performance.

- 3) Increased understanding of the input parameters for the VESYS system, especially those permanent deformation parameters that are relatively new to the engineering profession. Primary emphasis in this effort was on definition of trends in variation of the permanent deformation parameters ALPHA and GNU for asphalt concrete as functions of stress and temperature and of base and subgrade materials as functions of moisture content and density.

Relationships between costs for twenty years of acceptable pavement service and established legal axle loads are developed and enumerated in detail in the previous chapter for both new and existing pavements. These results are summarized below:

1. New Pavements:
 - a. The total cost for a 20 year service life may be expected to:
 - 1) Increase nominally for an increase from 18 to 20 kips (8,180 to 9,000 kgs) in legal single axle load limit.

- 2) Increase up to 16 percent for an increase in legal axle limit from 18 to 22 kips (8,180 to 10,000 kgs) (dependent primarily on pavement thickness and environment), with an average expected cost increase of 9 percent for all pavements.
 - 3) Increase from 6 to 23 percent for an increase in legal axle limit from 18 to 24 kips (8,180 to 10,900 kgs), with an average increase of 9 percent for all the pavements.
- b. The average annual cost (considering the value of the pavements remaining life after 20 years) may be expected to:
- 1) Increase from 1 to 12 percent for an increase in legal axle limit from 18 to 20 kips (8,180 to 9,000 kgs), with an average increase of 10 percent.
 - 2) Increase from 3 to 17 percent for an increase in legal axle limit from 18 to 22 kips (8,180 to 10,000 kgs), with an average increase to 15 percent.
 - 3) Increase from 4 to 23 percent for an increase in legal axle limit from 18 to 24 kips (8,180 to 10,900 kgs), with an average increase of 21 percent.
- c. The overall effect of increased axle loads is more severe for thin than for thick pavements and for colder than for warmer climates.

2. Existing Pavements:

- a. The predicted overlay costs for the higher legal axle limits in the wet-no freeze environmental zone (or warm temperature) represented by Florida IH-10 are nominal.
- b. As would be expected, the total cost for maintaining the highway is much less for low than for high traffic volume cases, but the percentage increase in total overlay increase in axle loads is much higher for the low traffic case. For instance, a mean predicted total overlay cost for a 24-kip (10,900 kg) legal axle load on all low traffic volumes is 2.34 times as much as for an 18-kip (8,180 kg) legal axle load compared to only 20 percent more for all high traffic volumes.
- c. The predicted overlay costs themselves are much higher for northern than for southern environments, but the percentage increases in overlay costs with increasing legal axle load are similar to those for the southern highways.
- d. The cost of overlaying pavements was logically predicted to be greater for thin than thick pavements, but the percentage increase in overlay cost with legal increasing axle load was greater for the thick pavements.

- e. In general, total overlay costs may be expected to increase about 6 percent for an increase in legal axle limit from 18 to 20 kips (8,180 to 9,000 kgs), 33 percent for an increase from 18 to 22 kips (8,180 to 10,000 kgs) and 45 percent for an increase from 18 to 24 kips (8,180 to 10,900 kgs).
- f. An increase in legal axle limit from 18 to 20 kips (8,180 to 9,000 kgs) increases the average annual cost of overlays about 10 percent, an increase from 18 to 22 kips (8,180 to 10,000 kgs) increases it about 30 percent and an increase from 18 to 24 kips (8,180 to 10,900 kgs) increases it about 46 percent.

It is clear that the accuracy of these cost relationships is dependent on the ability of the flexible pavement structural model VESYS A to simulate real pavements and on the accuracy of the characterization of traffic, axle load distribution, environment and material input to the model. VESYS A is certainly one of the most complete mechanistic models of a flexible pavement, but it shares the limitation of most, if not all, other such models in that it does not model reflection cracking or the accelerating deterioration of its structural components as surface cracking progresses and moisture enters the base and subgrade layers, nor does it consider loss of stiffness in the asphalt concrete surface due to cracking nor changes in stiffness and visco-elastic properties as the asphalt hardens in time. Also, the distress and performance predictions are very sensitive to materials characteristics that are difficult to accurately quantify. Consequently, exceptional quantitative accuracy may not be claimed, but all solutions are subject to the same biases so that the trends established may be expected to be reliable and the quantitative relationships sufficiently accurate to offer valuable insight until the results of other much more comprehensive studies are available.

APPENDIX A

PERMANENT DEFORMATION PARAMETERS ALPHA(1) AND GNU(1) FOR ASPHALT CONCRETE AS FUNCTIONS OF TEMPERATURE AND DEVIATOR STRESS

The new capabilities developed in this project for VESYS A include seasonal variations in the permanent deformation parameters ALPHA(1) and GNU(1) in order to more rationally model the contributions of the surface layer to rutting by season. A limited amount of information existed as to realistic values of ALPHA(1) and GNU(1), most of which was collected and reported in Reference 1. It is commonly known that rutting or permanent deformation in asphalt concrete is heavily dependent on temperature and stress level, but insufficient information existed to define sufficiently the seasonal variation of these input quantities if values were known for one set of conditions. The purpose of this study was to learn how ALPHA(1) and GNU(1) vary with pavement temperature and deviator stress. The resulting information was used as a partial basis for selected input values appearing in Table 6 and applied to the study factorial of VESYS A solutions.

Two major sources of information were utilized in the study. The first was a small factorial of eighteen tests on a typical asphalt concrete mix conducted by Austin Testing Engineers Inc. The second was analysis of data of data appearing in the literature (References 1, 43¹, 44², and 45³).

¹McLean, D. B., and C. L. Monismith, "Estimation of Permanent Deformation in Asphalt Concrete Layers Due to Repeated Traffic Loading," Transportation Research Record 510, 1974.

²Morris, Jack, "The Prediction of Permanent Deformation in Asphalt Concrete Pavements," The Transport Group, Department of Civil Engineering, University of Waterloo, Waterloo, Ontario, Canada, September, 1973.

³Kenis, W. J., and M. G. Sharma, "Prediction of Rutting and Development of Test Procedures for Permanent Deformation in Asphalt Pavements," paper prepared for presentation in the symposium entitled "Deformation Characteristics of Pavement Sections" held during the 55th Annual Meeting of the TRB, January 1976.

Permanent Deformation Testing for a Typical
Asphalt Concrete Mix by Austin Testing Engineers

Asphalt Concrete Mix Description and Sample Preparation

An AC-10 asphalt cement with an original penetration of 92 and a penetration at the time of mixing of 83 was used with crushed limestone aggregate graded as shown in Figure 41. The asphalt cement content was 6 percent and the resulting specimens had a rather high mean density of 151.0 pcf (2416 kg/m³) and varied from 148.7 to 153.9 pcf (2379 to 2468 kg/m³).

Aging was simulated to some extent by mixing longer than usual during preparation of the samples. The mix was heated to 250°F (121°C) and then compacted by a motorized gyratory-shear molding press in molds 6 in. (15.24 cm) in diameter and 8 in. (20.32 cm) in height. The compacted specimens were then cured at room temperature.

As the diameter of specimens desired was 4 inches (10.16 cm), the specimens were cooled to 40°F (4.44°C) to stiffen them and then cored out to produce specimens 4 inches (10.16 cm) in diameter and 8 inches (20.3 cm) in height. A special split tube (firmly secured around the specimen) and base plate were used to strengthen and protect the specimens during coring.

Permanent Deformation Testing

The test factorial included duplicate tests of specimens at three levels of temperature, 40, 70 and 100°F (4.4, 21.1 and 37.8°C), and three levels of deviator stress, 15, 30 and 45 psi (104, 207 and 310 kN/m²). Specimens were both brought to temperature and tested in a special controlled-temperature chamber.

The equipment used and the test setup was essentially that now considered common for dynamic modulus testing of asphalt concretes, except that loads were applied as "square wave" pulses. Each load was applied for 0.1 second duration and with a 0.9 second rest period. Vertical strain was measured periodically with two LVDT's mounted in clamps near the top and bottom of the specimen and recorded by an oscillographic recorder such that both resilient and permanent strain could be read.

All tests were conducted to 100,000 cycles of loading. Loading was in unconfined compression such that the deviator stress was that applied vertically.

Permanent strains were plotted versus number of load cycles on log-log paper in order to determine ALPHA(1) and GNU(1) as described in Reference 1.

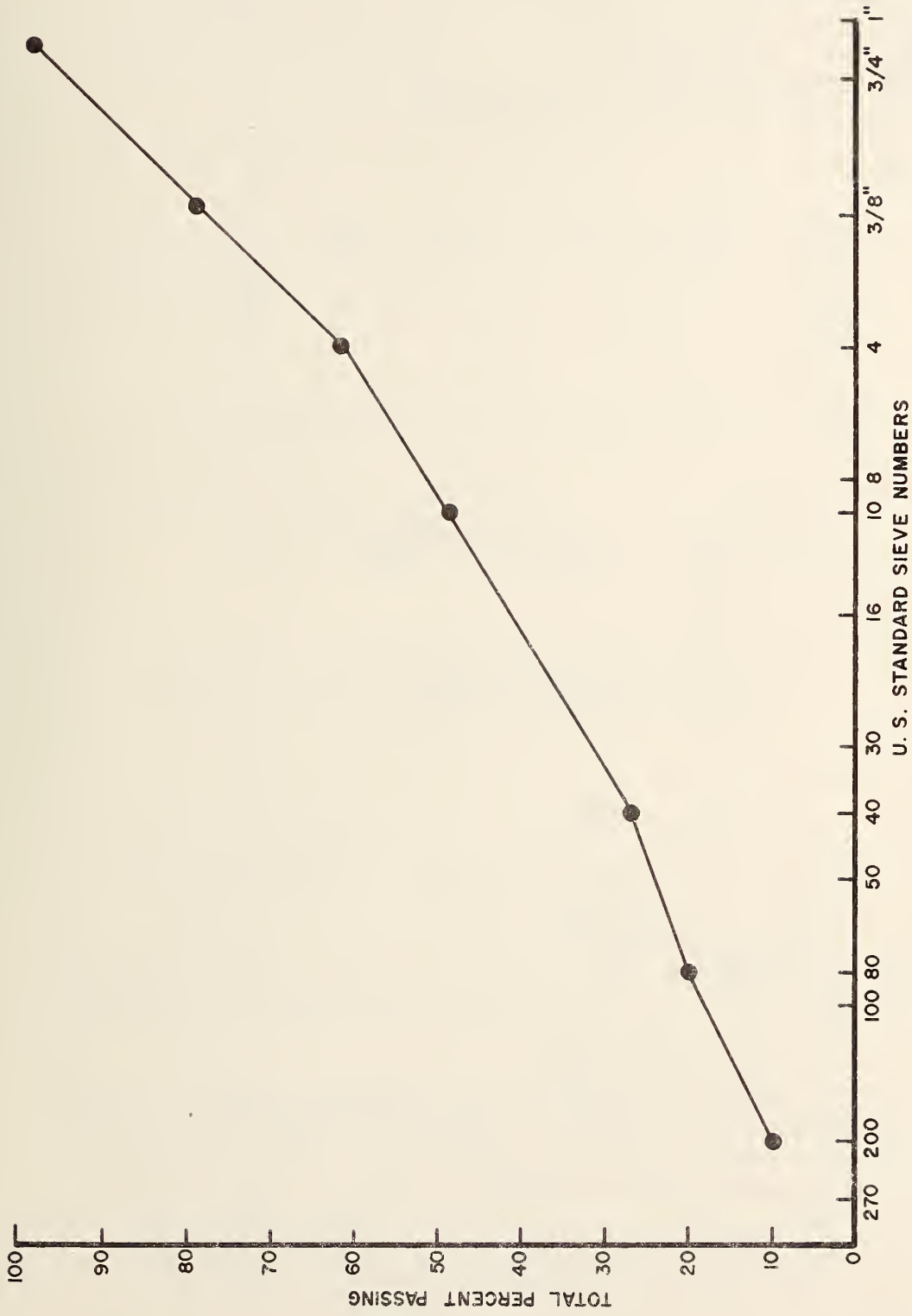


Figure 41. Aggregate grading curve for typical asphalt concrete mix used for permanent deformation testing.

Test Results

The results of this test program appear in Table 32. The sample numbers are coded such that the first digit is the test number for a specific temperature and the digits after the dash mark give the test temperature in °F. These results have also been plotted in various ways in Figures 42 through 47 for ease of studying the data and trends in variability.

The general trend information gained from this test program was:

1. Permanent deformation is extremely temperature dependent as indicated by all other testing in the literature. For example, the permanent strain at 100°F (37.8°C) and 100,000 load cycles was around 30 times that for 70°F (21.1°C) at a stress of 30 psi (207 kN/m²).
2. GNU(1) and ALPHA(1) both decrease with increasing stress. The decrease in ALPHA(1) dominates to cause an important increase in permanent deformation with increasing stress.
3. It appears that the mechanisms affecting permanent deformation differ above and below some temperature in the order of 60 to 70°F (15.6 to 21.1°C):
 - a. Below 60°F (15.6°C):
 - 1) GNU(1) increases with temperature.
 - 2) ALPHA(1) increases slightly with temperature for the higher stress levels, but decreased at the lower stress level.
 - b. Above 60 to 70°F (15.6 to 21.1°C):
 - 1) GNU(1) decreases with increasing temperature.
 - 2) ALPHA(1) decreases with increasing temperature.

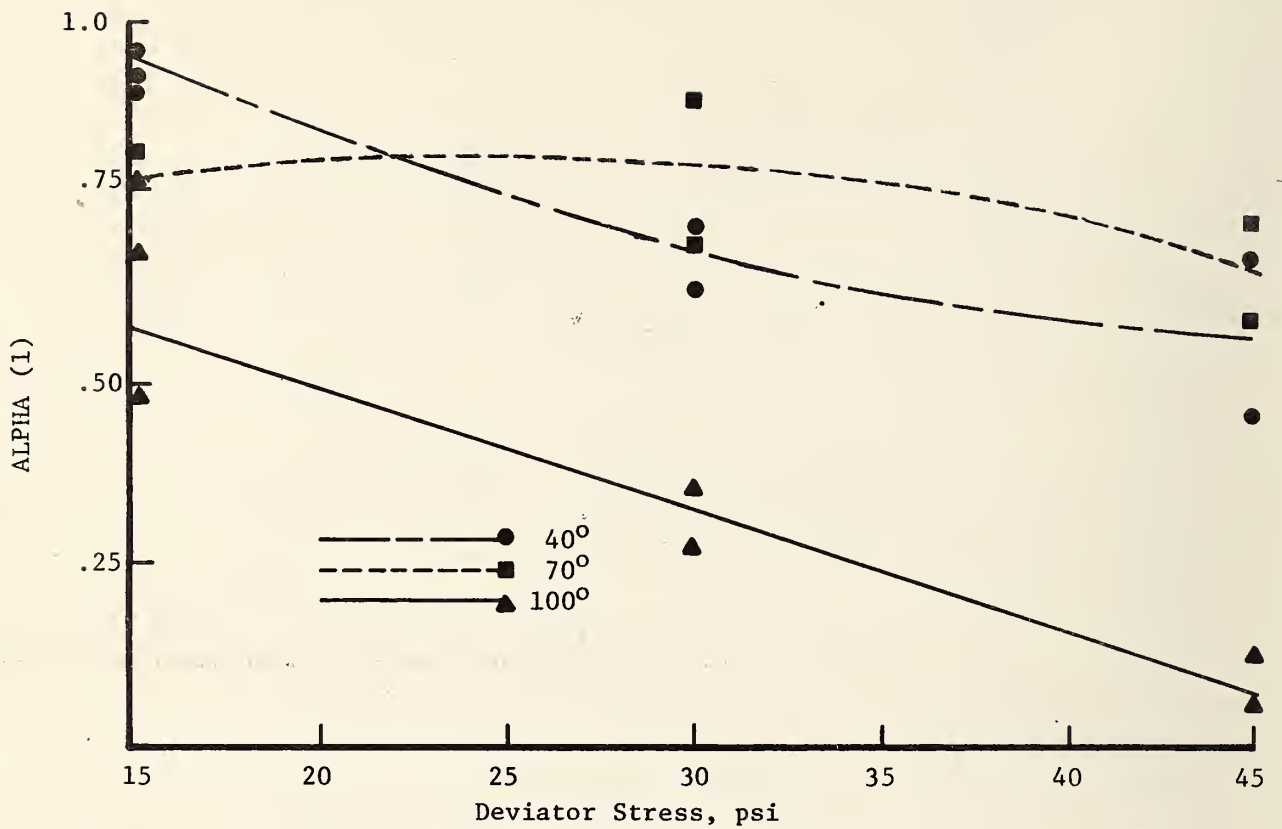
The rate of increase in permanent deformation is much higher after 60 to 70°F (15.6 to 21.1°C) than it is at the lower temperature.

4. The dynamic modulus is clearly somewhat stress dependent. Above the 60 to 70°F (15.6 to 21.1°C) zone, E_R increased with stress level, while below it decreased markedly with increasing stress level.
5. The dynamic modulus has a well-defined negative correlation with temperature. It decreases from greater than 1,000,000 psi (6,900,000 kN/m²) at low temperatures to less than 100,000 psi (690,000 kN/m²) at higher temperatures.

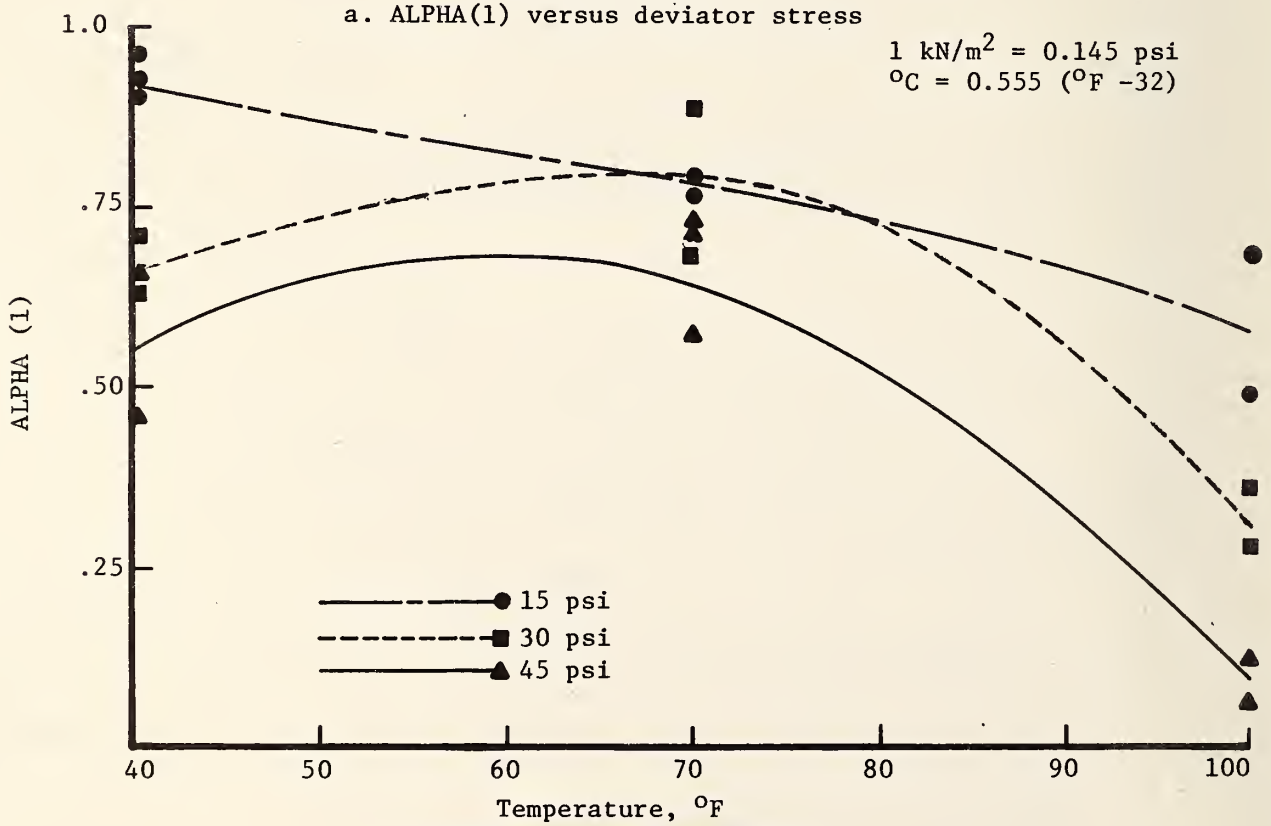
Table 32. Results of Permanent Deformation Tests on a typical asphalt concrete mix.

Sample Number- Temperature (°F)	Deviator Stress (psi)	Resilient Strain (in./in. x 10 ⁻⁶)	Resilient Modulus (psi x 10 ⁶)	Slope (in./in. x 10 ⁻⁵)	Intercept (in./in. x 10 ⁻⁵)	ALPHA(1) GNU(1)	Permanent Strain at 100,000 cycles (in./in. x 10 ⁻⁴)
1-40	15	2.35	6.40	.095	0.23	.905	0.06
2-40	15	2.35	6.40	.078	2.14	.922	0.87
3-40	30	7.62	3.94	.369	1.12	.631	7.44
4-40	30	7.39	4.06	.289	1.60	.711	4.37
5-40	45	12.3	3.65	.538	.183	.462	9.04
6-40	45	8.74	5.15	.345	.180	.655	0.92
1-70	15	17.2	.87	.206	10.0	.794	10.6
2-70	15	14.7	1.02	.231	18.0	.769	25.2
3-70	30	61.7	.486	.112	100.0	.888	35.9
4-70	30	44.6	.446	.303	11.3	.697	35.8
5-70	45	82.6	.545	.422	4.42	.578	56.7
6-70	45	49.5	.909	.274	14.4	.726	34.0
1-100	15	412	.036	.314	47.0	.686	171
2-100	15	334	.045	.502	7.8	.498	240
3-100	30	625	.048	.725	2.00	.275	780
4-100	30	698	.043	.641	13.80	.359	2100
5-100	45	689	.057	.875	1.27	.125	2700
6-100	45	1013	.044	.934	1.38	.066	5700

1 kN/m² = 0.145 psi



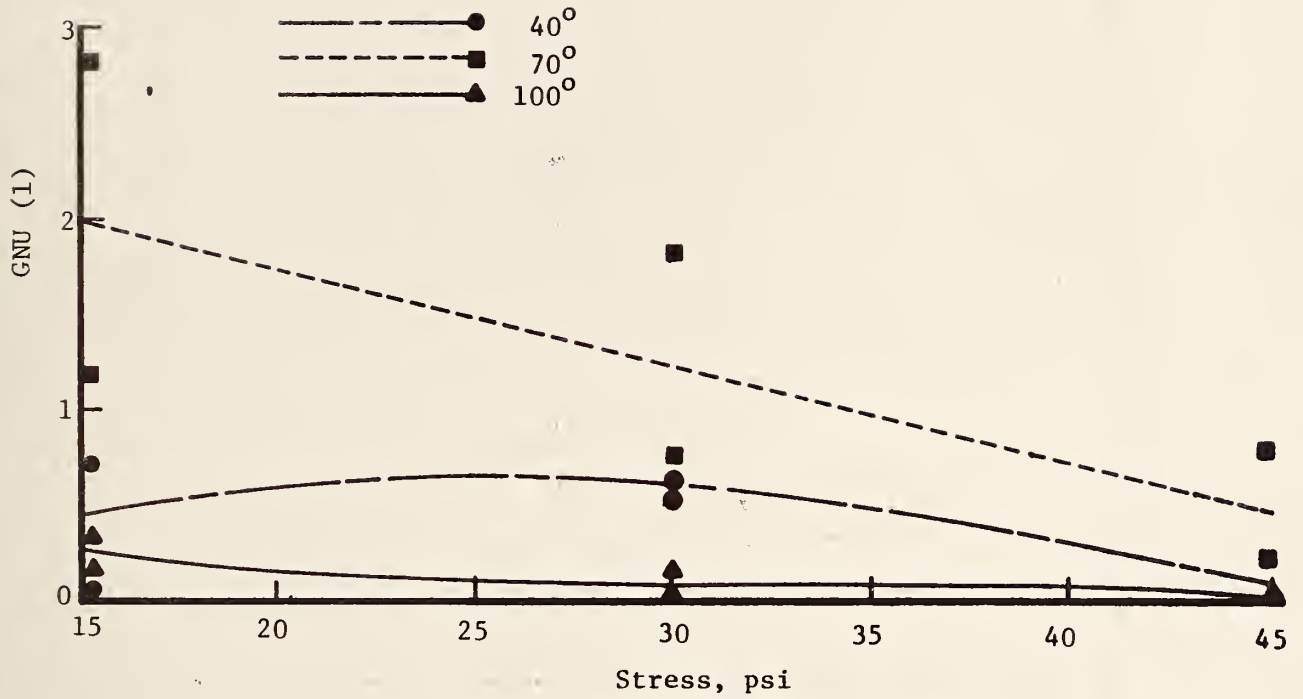
a. ALPHA(1) versus deviator stress



1 kN/m² = 0.145 psi
 °C = 0.555 (°F - 32)

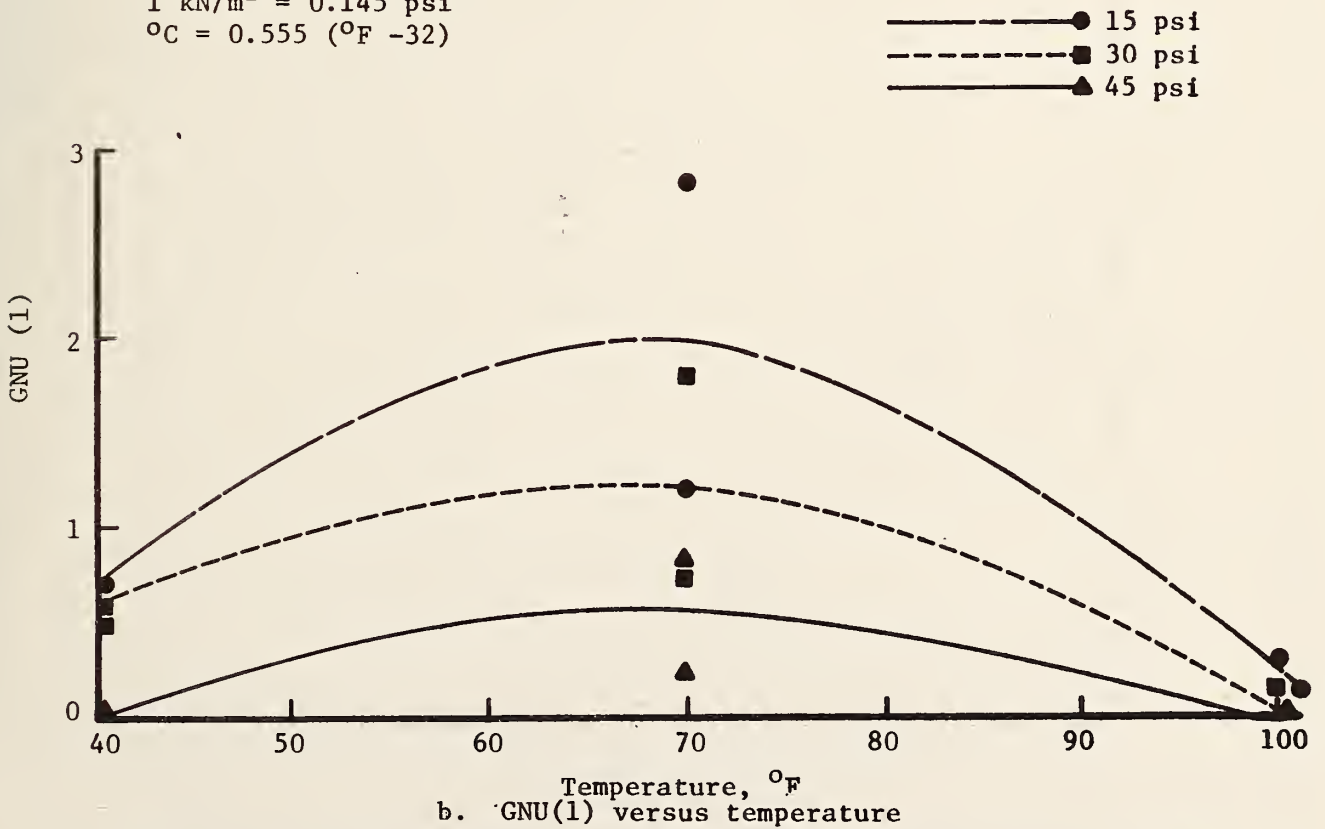
b. ALPHA(1) versus temperature

Figure 42. Effects of deviator stress level and temperature on ALPHA(1).



a. GNU(1) versus deviator stress

1 kN/m² = 0.145 psi
 °C = 0.555 (°F - 32)



b. GNU(1) versus temperature

Figure 43. Effects of temperature and deviator stress level on GNU(1).

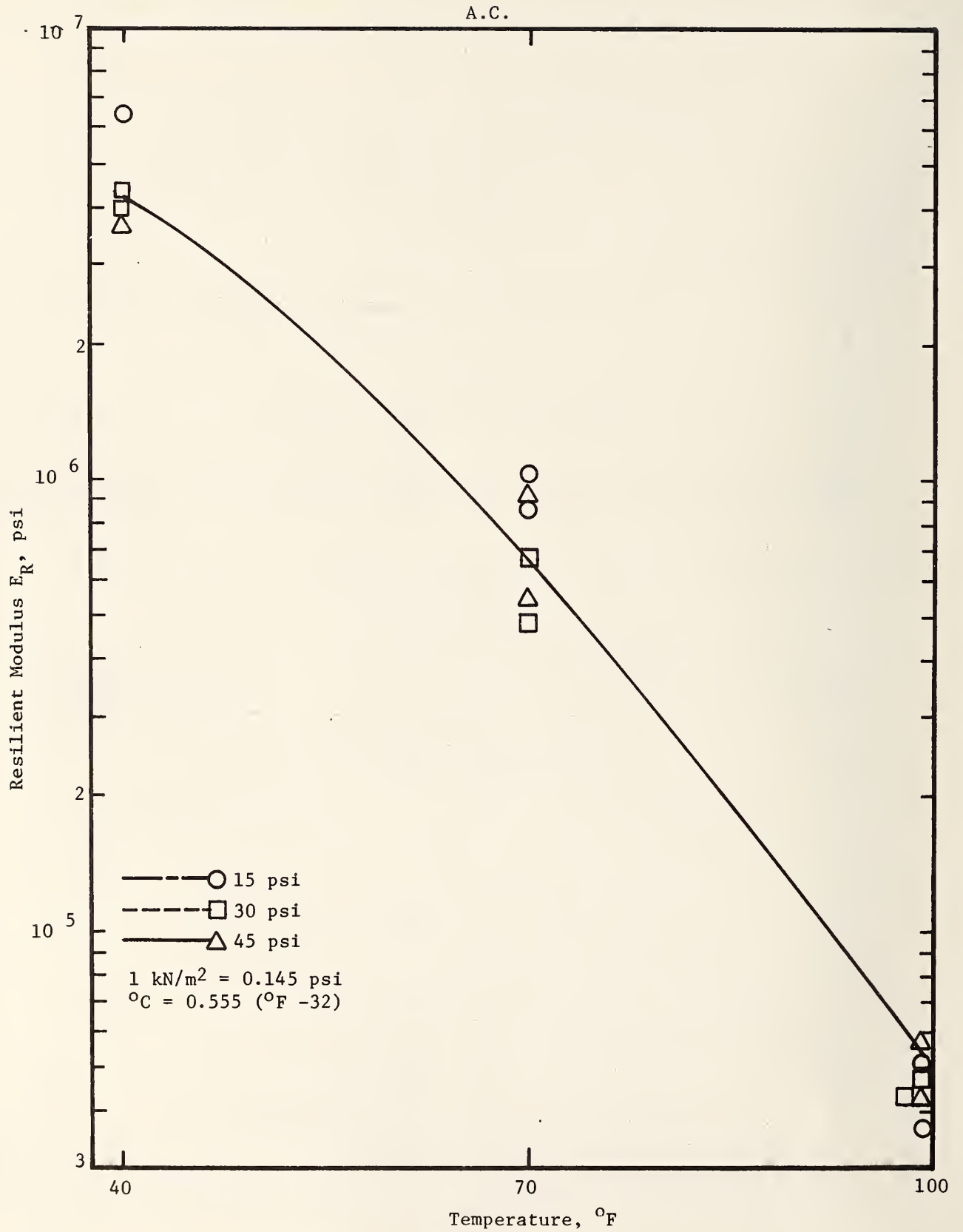


Figure 44. Resilient modulus for the typical asphalt concrete versus temperature.

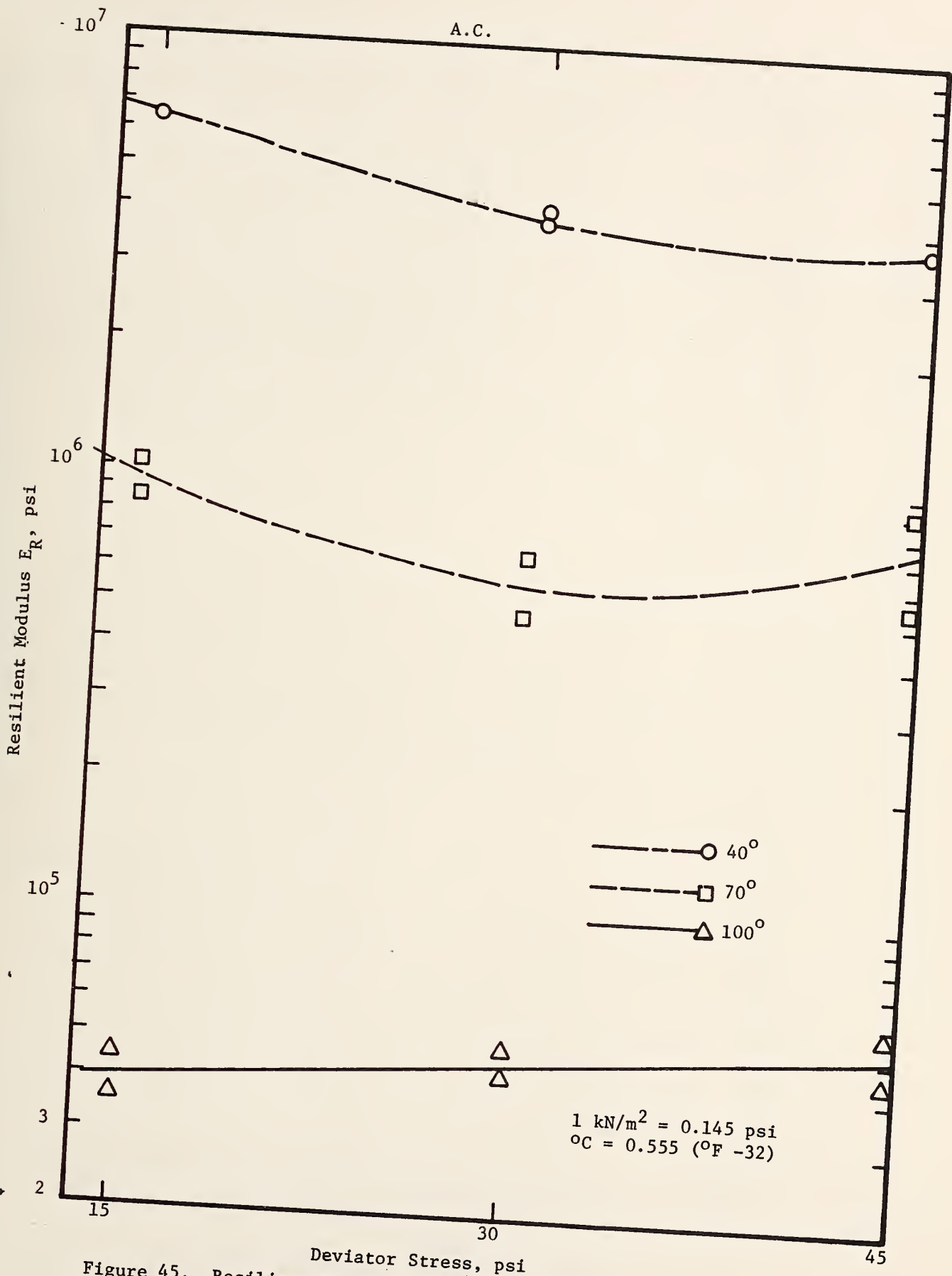


Figure 45. Resilient modulus versus stress for the typical asphalt.

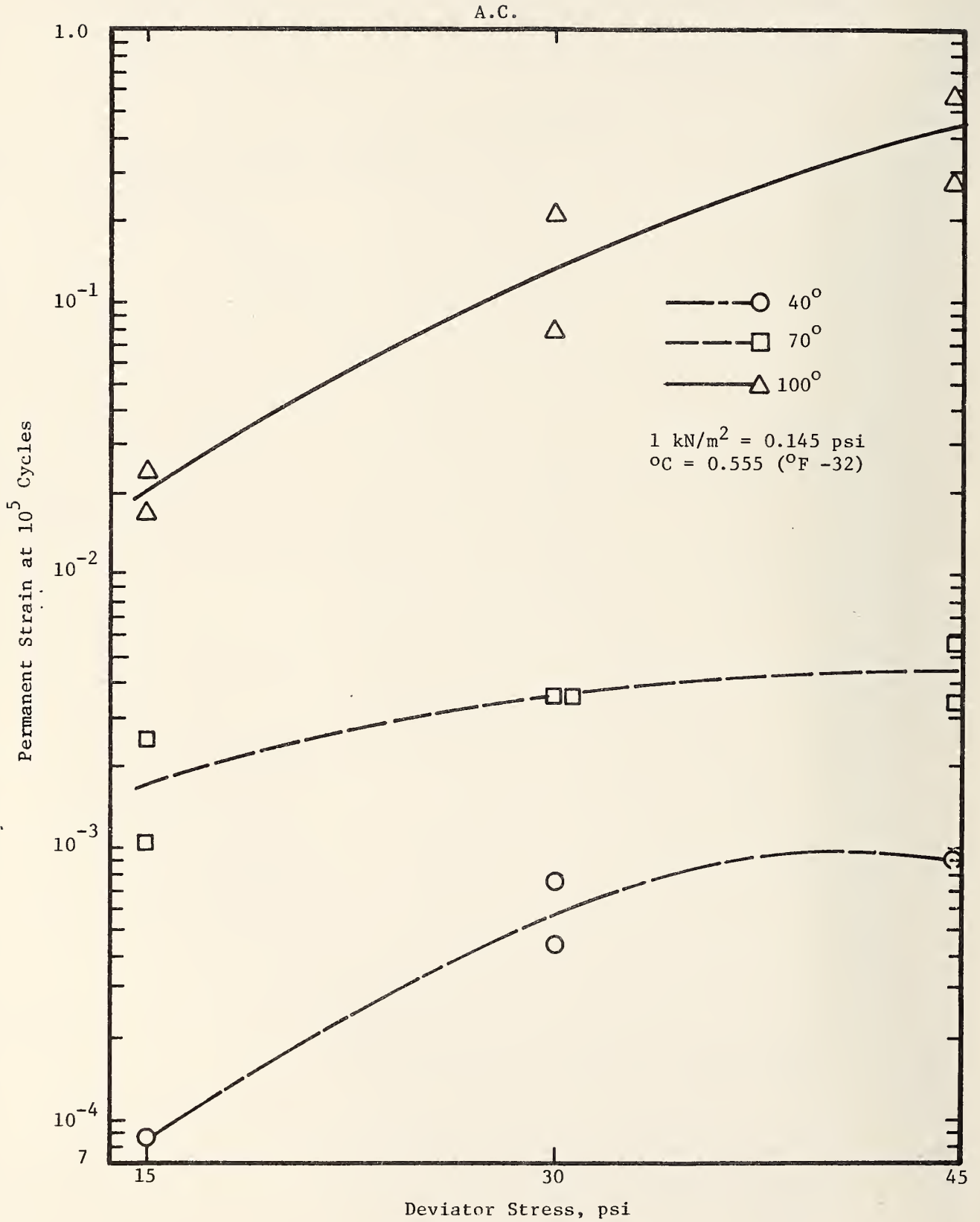


Figure 46. Permanent strain after 100,000 cycles of load as a function of deviator stress.

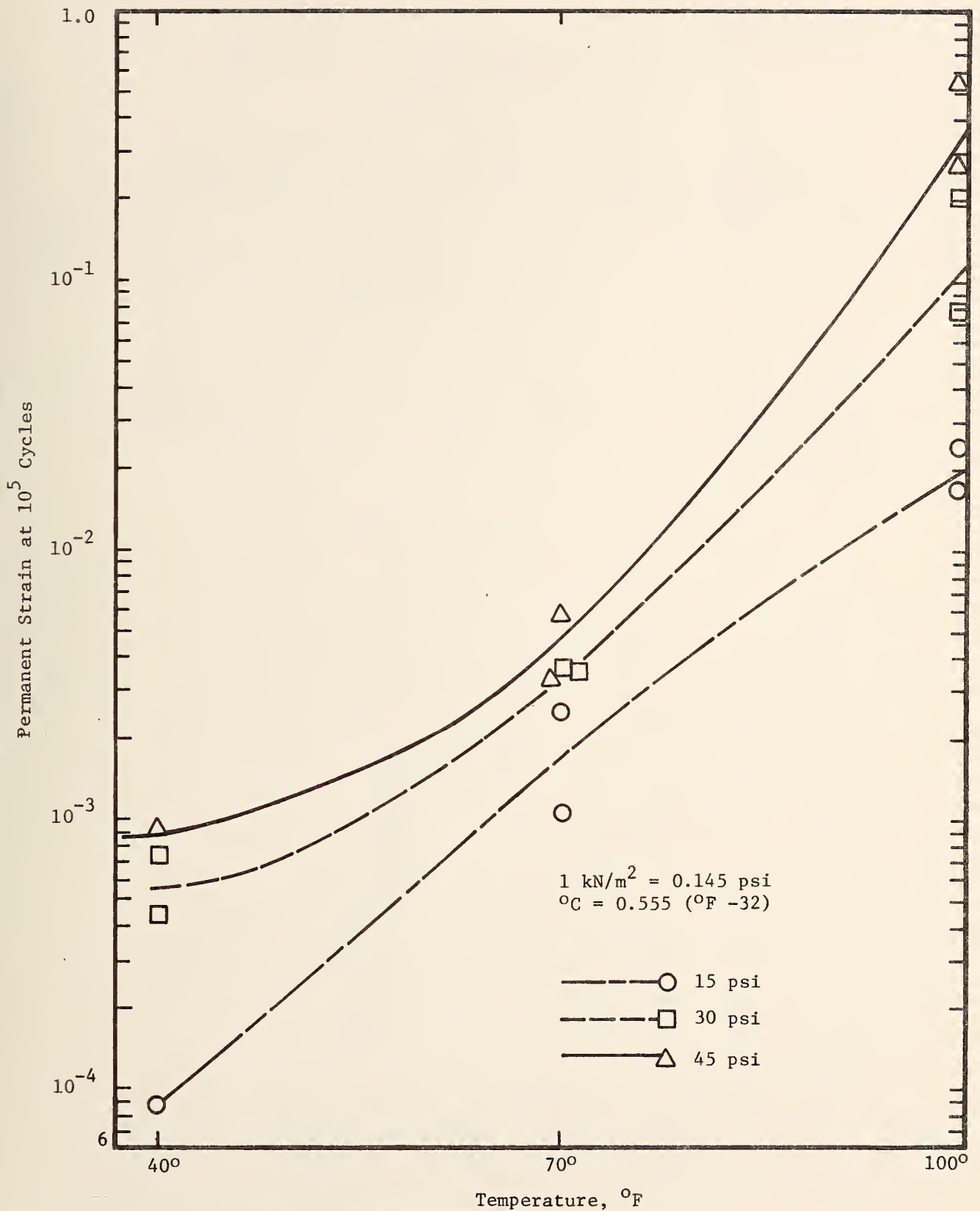


Figure 47. Permanent strain after 100,000 cycles of load as a function of temperature.

Results of Reviewing Other Permanent Deformation Data in the Literature

Review of the permanent deformation test data in References 39, 40 and 41 served to corroborate the trends noted from the ATE test factorial and previously described. No additional or conflicting trends were noted.

Combining the New Test Data With Data Reported in Reference 1

It is useful to add the test data produced by the ATE test factorial to Figures 52, 61 and 62 of Reference 1. These augmented figures appear in this appendix as Figures 48, 49 and 50, respectively. As can be seen, the additional data at lower and higher temperatures add considerable insight to the nature of these parameters ALPHA(1) and GNU(1).

LEGEND

- Brampton Base
- Penn State
- ◇ AASHO Cores
- ▽ McLean and Monismith
- △ Texas Cores - Indirect Tensile tests to failure
- Brown and Snaith
- ATE 40°F (4.4°C).
- ▲ ATE 70°F (21.1°C).
- ▼ ATE 100°F (37.8°C).
- ◆ Utah Indirect Tensile σ_d at 20 psi (138 kN/m²) horizontal

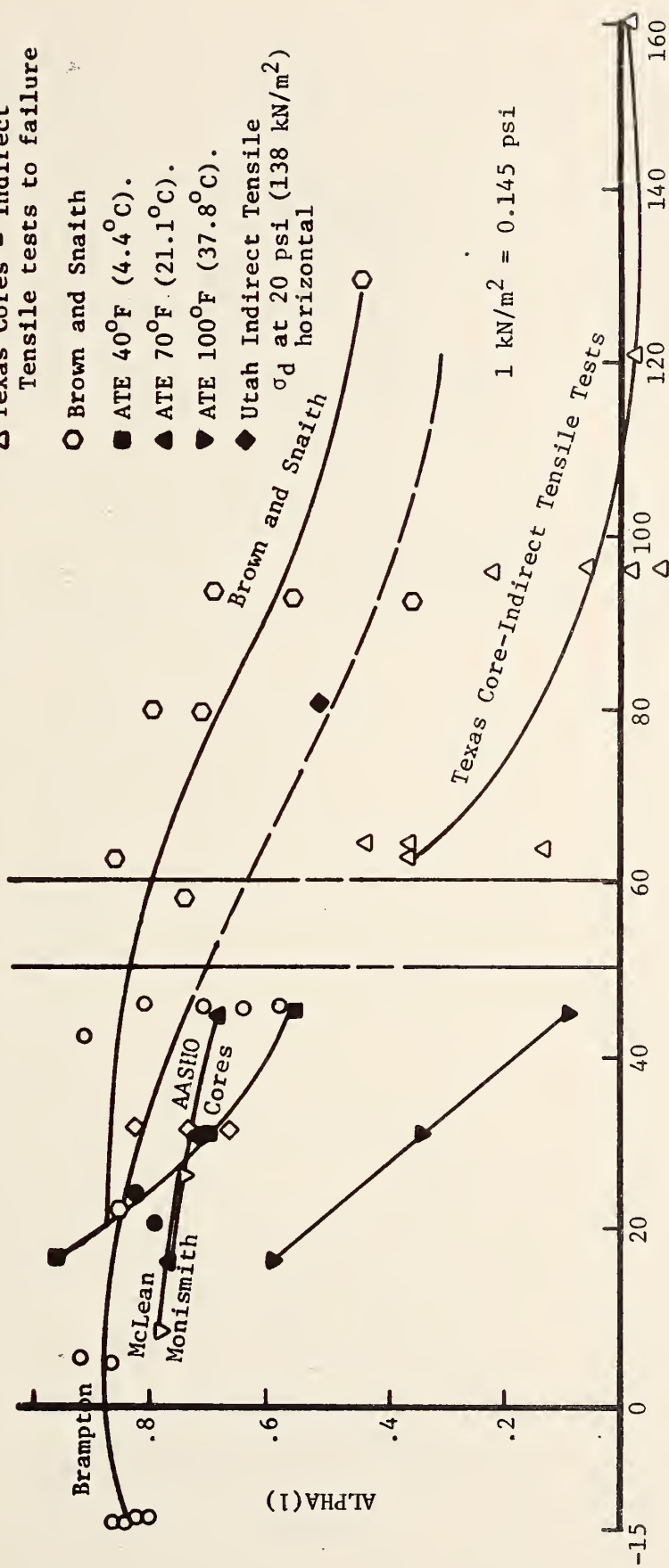


Figure 48. Plot of ALPHA(1) versus deviator stress for asphaltic concrete.

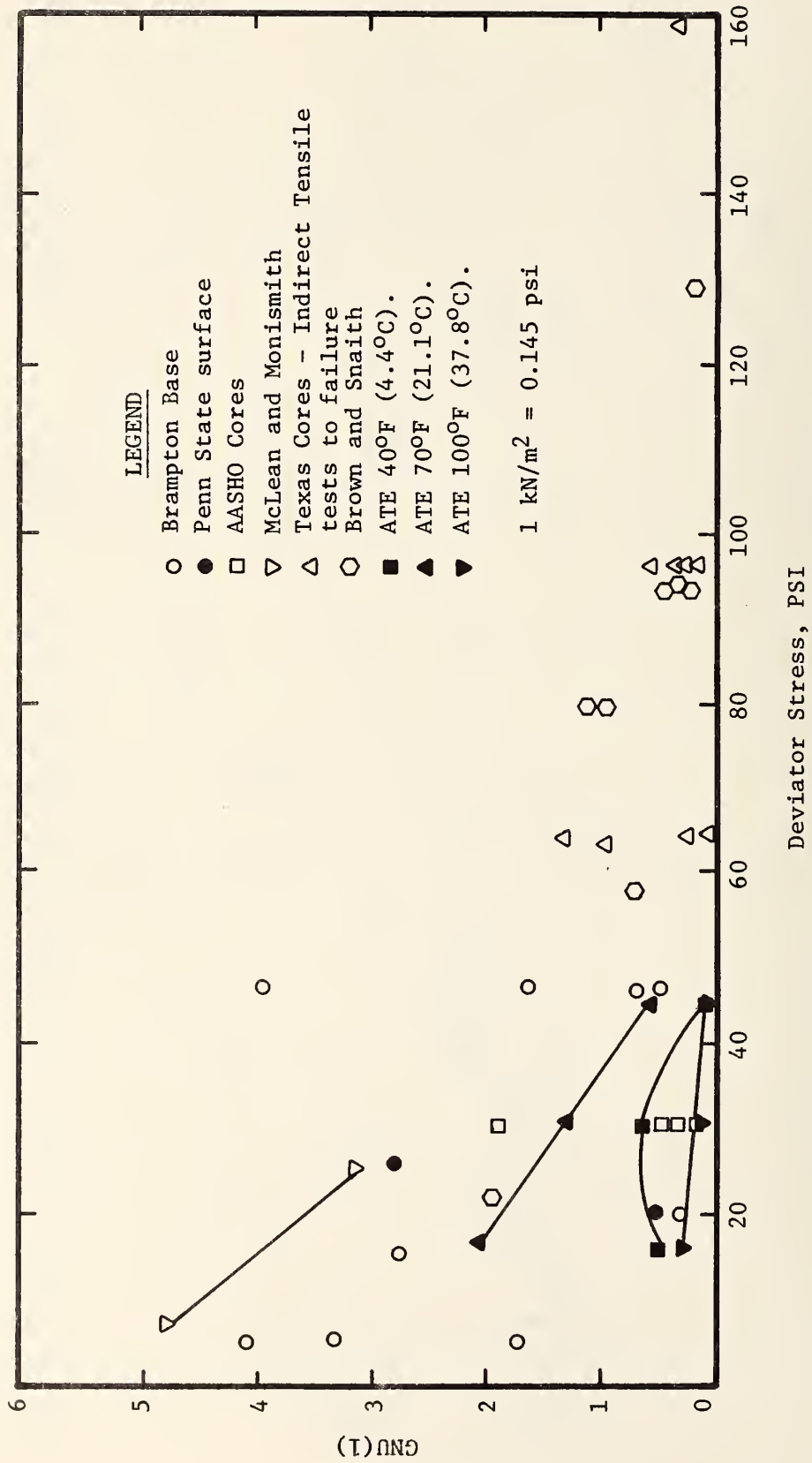
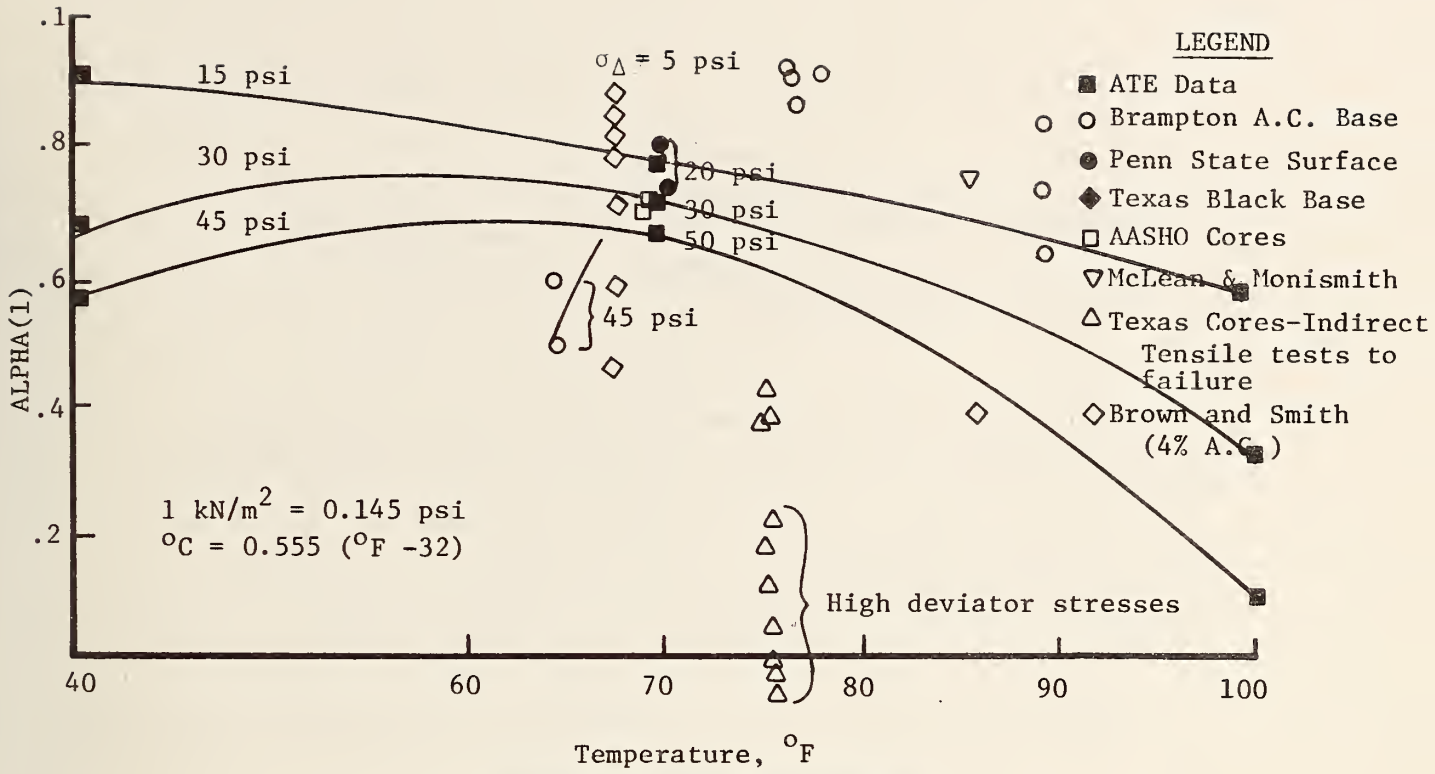
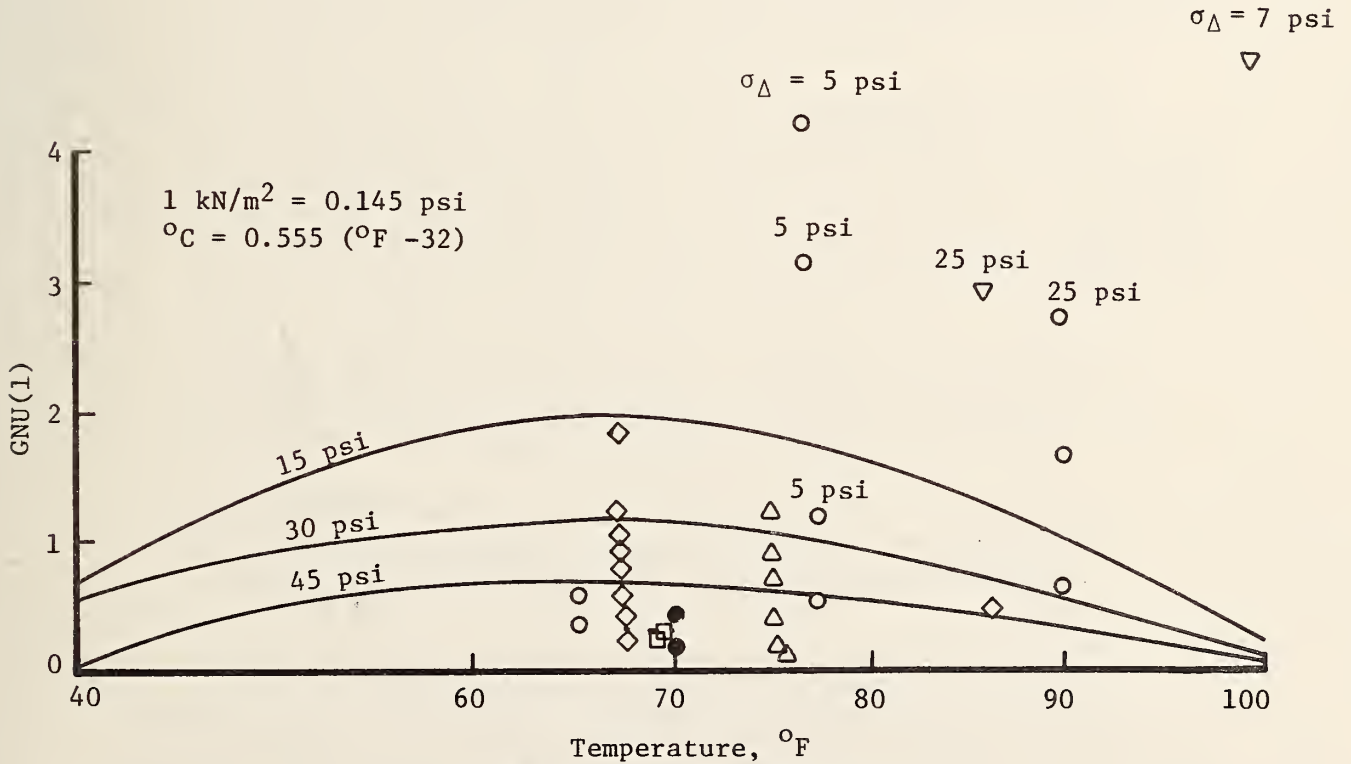


Figure 49. Plot of GNU(1) versus deviator stress for asphaltic concrete.



a. ALPHA(1) versus temperature



b. GNU(1) versus temperature

Figure 50. Plots of ALPHA(1) and GNU(1) versus temperature.

APPENDIX B

PERMANENT DEFORMATION PARAMETERS ALPHA(2) AND GNU(2) FOR GRANULAR BASE MATERIALS AS FUNCTIONS OF DENSITY AND MOISTURE CONTENT

The new capabilities developed in this project for VESYS A include seasonal variations in the permanent deformation parameters ALPHA(2) and GNU(2) in order to take into account seasonal changes in moisture content and possible changes in density (such as might occur during spring breakup). It was decided that the limited testing budget available could best be committed to asphalt concrete and subgrade testing, so the results of literature research and past experience reported in Reference 1 were the basis for this study.

Sources other than Reference 1 used for this study were References 3, 4, 46¹ and 47².

Permanent Deformation Testing Reported by Kalcheff and Hicks

This test regime included gravel with soil and stone dust fines, samples with varying amounts of fines, crushed limestone and a material called "VA21A Diabase" at 95 percent and 100 percent of T180 compaction. The results of this study have been expanded to calculate values of ALPHA(2) and GNU(2) in some cases and general conclusions of interest to this research project drawn and discussed below:

1. There is a considerable difference in permanent strain for different materials. Crushed limestone will generally undergo less permanent strain than gravel when the same compactive energy is applied to prepare specimens and the same stress conditions applied.
2. The amount of permanent strain is greater when the fines are soil as compared to fines of stone dust. It also increases with percent of fines passing the No. 200 mesh sieve.

¹Chisolm, E. E. and F. C. Townsend, "Behavioral Characteristics of Gravelly Sand and Crushed Limestone For Pavement Design," Report No. FAA-RD-75-177, U. S. Army Waterways Experiment Station, September 1976.

²Raymond, G. P., "Research on Rail Support Improvement," Paper presented at Session 73, Transportation Research Board, January 1977.

3. The material called VA21A Diabase underwent much more permanent strain than gravel when compacted to a similar density.
4. The permanent strain for the VA21A diabase compacted to 146 pcf was approximately five times that compacted to 154 pcf.
5. Table 6 of Reference 4 shows nearly 5 times as much permanent strain for a base at 5.5 percent moisture content as for the same base at 4.7 percent moisture content. This is demonstrated by Figure 51.
6. The resilient modulus for dry crushed limestone may be expected to be much higher than the same material after capillary saturation or inundation.

Permanent Deformation Testing Reported

by Chisolm and Townsend

Tests were conducted to 100,000 cycles of loading on a crushed limestone and a gravelly sand. General results of expanding the test data to obtain ALPHA(2) and GNU(2) and further study are:

1. The resilient modulus for the crushed limestone was generally higher than that for the gravelly sand.
2. Gravelly sand results:
 - a. ALPHA(2) is essentially independent of deviator stress, so variations in permanent strain with variations in deviator stress relate to variations in GNU(2). (See Figure 52).
 - b. Permanent deformation increased almost linearly for the test results appearing in Figure 52a, but are probably not typical.
3. Crushed limestone results:
 - a. Figure 53b shows that ALPHA(2) was essentially independent of lateral stress when deviator stresses were held constant.
 - b. Slight variations in GNU(2) accompanied great differences in permanent strain.
 - c. Increasing lateral stress (or confinement) greatly decreased permanent strain.
 - d. The samples tested at the very high deviator stress of 116 psi (800 kN/m²) showed decreases in both ALPHA(2) and GNU(2). This is not considered typical.

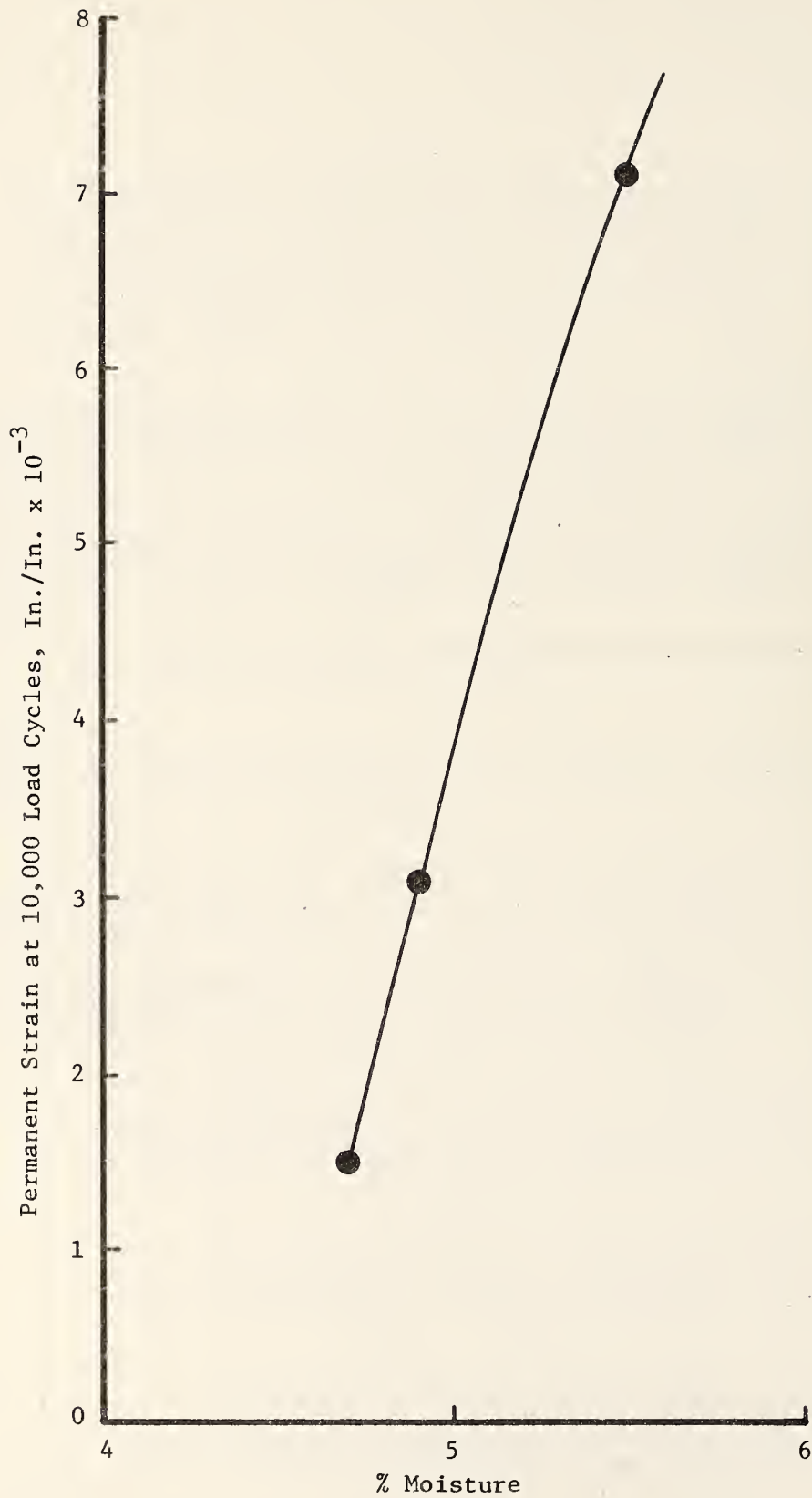
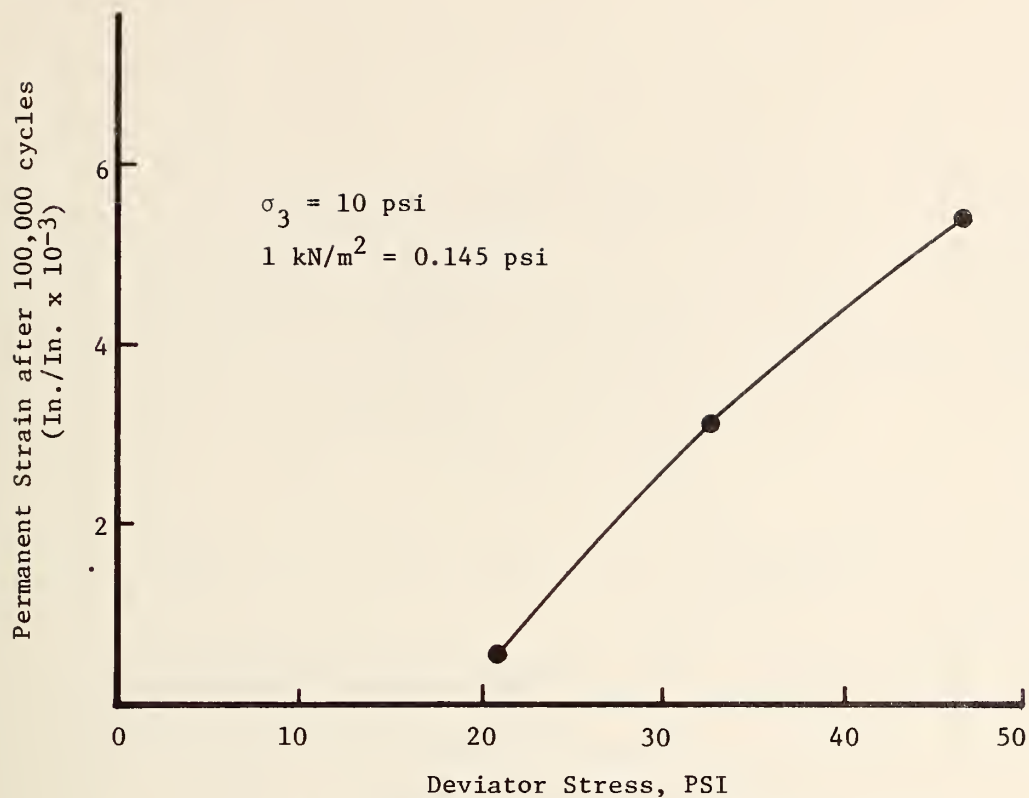
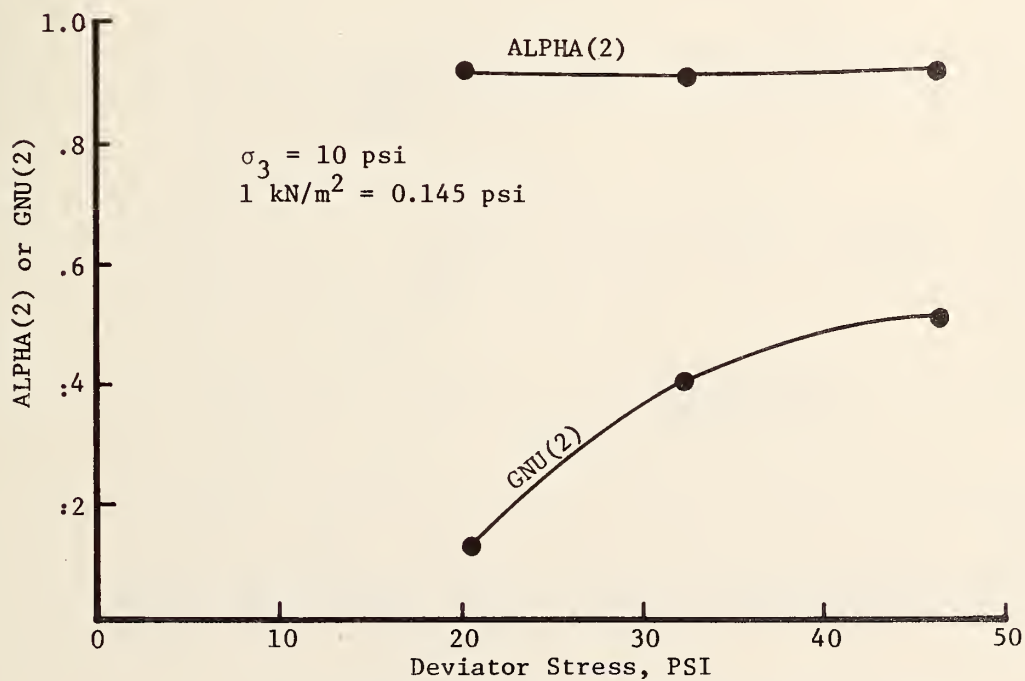


Figure 51. Permanent strain versus percent moisture for a gravel base with plastic fines.

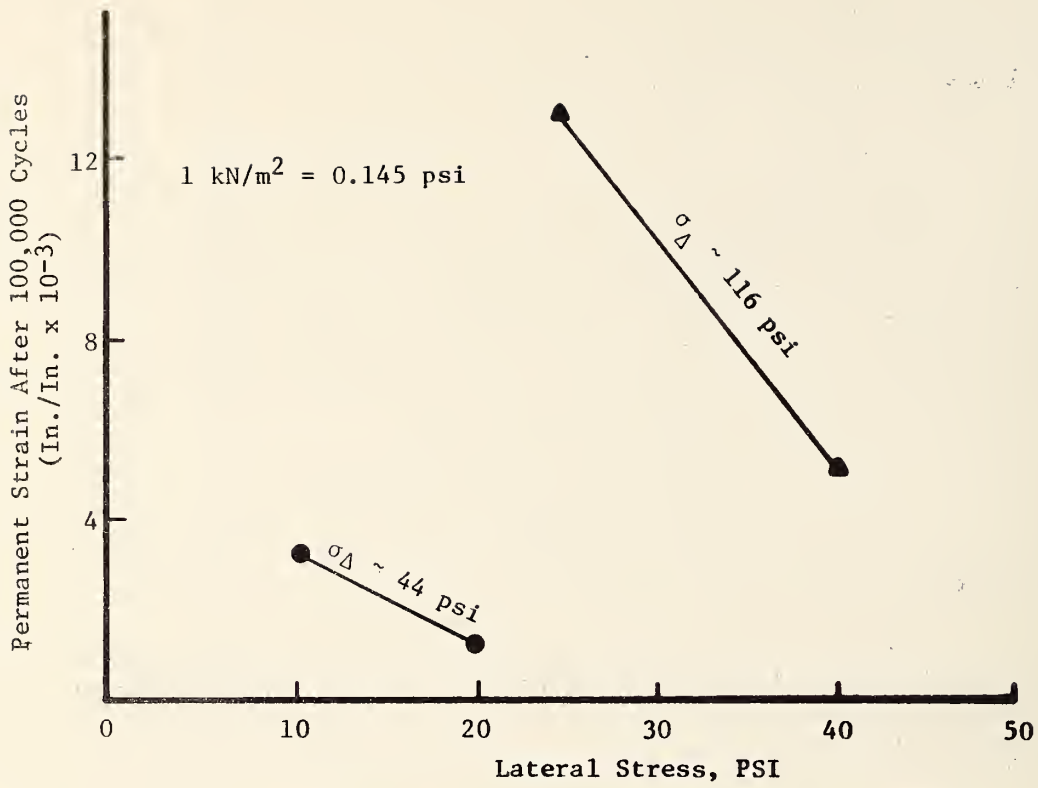


a. Permanent strain versus deviator stress

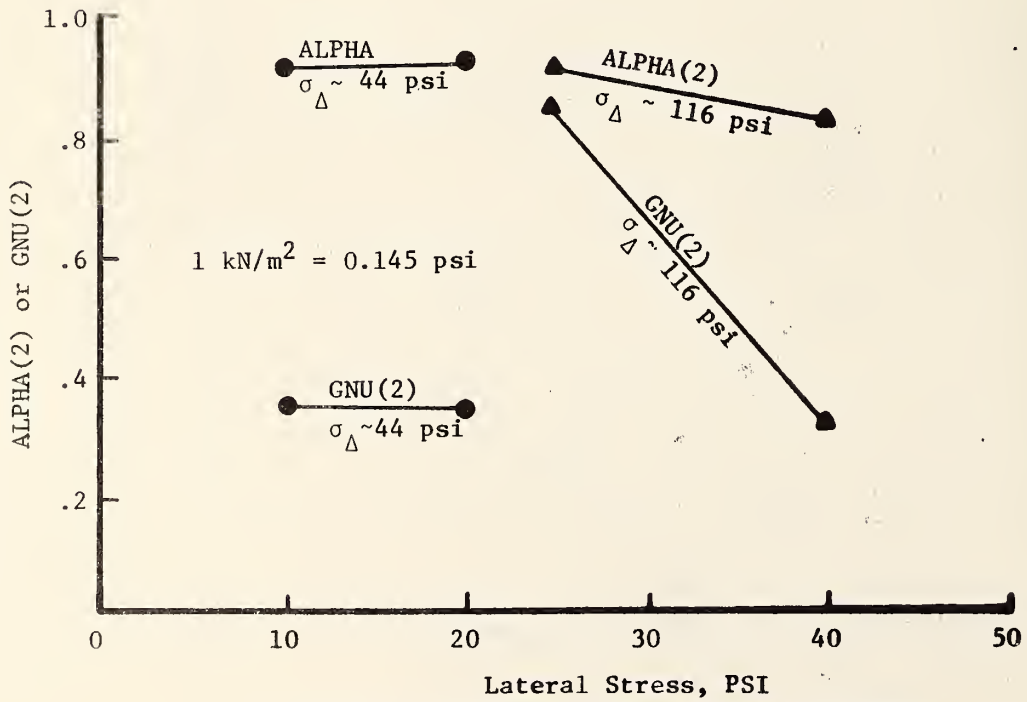


b. ALPHA(2) and GNU(2) versus deviator stress

Figure 52. Relationships between ALPHA(2), GNU(2) and permanent strain for a gravelly sand after 100,000 load cycles versus deviator stress with lateral pressure constant at 10 psi.



a. Permanent Strain versus Lateral Stress



b. ALPHA(2) and GNU(2) Versus Lateral Stress

Figure 53. Relationship between ALPHA(2), GNU(2) and permanent deformation for a crushed limestone after 100,000 load cycles versus lateral pressure at approximate constant deviator stresses σ_{Δ} .

4. ALPHA(2) appears in general to be fairly independent of stress, but GNU(2) varies to account for variations in permanent strain.
5. Permanent strain increases with increasing deviator stress and decreases with increasing lateral stress.

Permanent Deformation Testing

by G. P. Raymond

Rail ballast is by virtue of its usual gradation and degree of compaction a different material from a highway base, but it was felt that some information of value might result from studying the results of Raymond's tests. The primary information gained was that ALPHA(2) was also for this material essentially independent of deviator stress and that GNU(2) values were high for relatively loose, open graded ballast of low density. Also, permanent strain increased with deviator stress. All of these conclusions are consistent with the results of testing of highway bases reported above.

General Trends for Variations in ALPHA(2) and GNU(2)

1. Crushed limestone will generally have less permanent strains than gravel under the same compactive energy and stress conditions.
2. Permanent strains are greatly increased by increasing moisture content. For example, an increase from 4.7 to 5.5 percent moisture content resulted in an increase in permanent strain for one soil from 0.0015 inches per inch to 0.0071 inches per inch.
3. The resilient modulus for dry crushed stone may be expected to be much higher than that for the same crushed stone with capillary saturation or inundation.
4. ALPHA(2) appears to be essentially independent of both deviator stress and lateral stress, but GNU(2) increases with deviator stress, thus causing an increase in permanent strain. GNU(2) decreases with increasing lateral pressure, thus causing decreased permanent strain.

APPENDIX C

PERMANENT DEFORMATION PARAMETERS ALPHA(3) AND GNU(3) FOR SUBGRADE AS FUNCTIONS OF MOISTURE CONTENT, DENSITY AND DEVIATOR STRESS

The new capabilities developed in this project for VESYS IIM include seasonal variations in materials characterizations. While much information exists in the literature as to variations in stiffness of subgrade-type soils with moisture change and density, little exists for permanent deformation parameters. The purpose of this study was to learn how the permanent deformation parameters ALPHA(3) AND GNU(3) vary with moisture content and density. The resulting information was used as the basis for seasonal variation of input values in predictions of pavement responses of axle loads, traffic, pavement designs and environmental conditions.

Two major sources of information were utilized in the study. The first was a small factorial of eighteen tests on a typical silty clay subgrade conducted by Austin Testing Engineers, Inc. The second was analysis of data appearing in the literature during the course of the project References 48¹, 49², 50³ and 51⁴.

¹ Monismith, C. L., N. Ogawa and C. R. Freeme, "Permanent Deformation Characteristics of Subgrade Soils in Repeated Loading," draft of a prepared paper.

² Townsend, F. C., and E. E. Chisolm, "Plastic and Resilient Properties of Heavy Clay Under Repetitive Loadings," Report No. FAA-RD-76-107, U. S. Army*Engineer Waterways Experiment Station, Soils and Pavements Laboratory, November 1976.

³ Sharma, J., L. L. Smith and B. E. Ruth, "Implementation and Verification of Flexible Pavement Design Methodology," paper prepared for presentation at the Fourth International Conference on Structural Design of Asphalt Pavements, October 1976.

⁴ M. G. Sharma, "Prediction of Rutting and the Development of Test Procedures for Permanent Deformation in Asphalt Pavements," paper prepared for presentation at the 55th Annual Transportation Research Board, January 1976.

Permanent Deformation Testing for a Typical Silty
Clay Subgrade Soil by Austin Testing Engineers

Soil Description

The subgrade soil selected for testing is a brown silty clay having a liquid limit of 37% and a Plasticity Index of 19%. Its gradation is as follows:

<u>Sieve No.</u>	<u>Percent Passing</u>
4	99
10	97
40	90
200	76

The classifications for the soil selected are CL for the Unified Soil Classification System and A-6 (11) for the AASHTO Classification System.

Approach to Development of a Test Factorial and Specimen Preparation

It was desired to test over the practical range of density and moisture conditions. The approach used to gather data for consideration was to conduct standard moisture-density compaction testing at three levels of compactive energy. The compactive energies selected approximated a range of standard to modified Proctor and included 7.16, 13.26 and 32.5 ft.-lbs/in³ (0.38, 0.71 and 1.74 m-N/m³). Using a standard 4-inch mold with a volume of 1/30 cu. ft. (.00094 m³) and the 10-lb. (4.54 kg) hammer dropping 18 inches, the number of blows for each of the five layers was 5.5, 10.2 and 25, respectively. Fractions of blows were obtained by one more blow on such layers as necessary to obtain the average. (1 inch = 2.54 cm)

The data from the compaction tests were then plotted in the usual moisture-density curves with one curve for each compactive energy, and subsequently with dry density as a function of compactive energy in blows per layer with a curve for each moisture content. Study of the first set of curves allowed selection of feasible ranges of moisture content and dry density to consider and the second how many blows to obtain the dry densities desired. The number of blows were then converted to compactive energy and this applied to the split mold having 2.8-inch diameter and 5.8-inch height (7.11 cm diameter and 14.73 cm height) used to prepare the triaxial specimens. The relationship developed was that the number of blows per layer in the 2.8-inch (7.11 cm) specimen mold was that for the 4-inch (10.16 cm) compaction mold multiplied by 0.642. Both were compacted in five layers. As might be expected, some adjustment in compactive energy was required to obtain the desired density in the triaxial specimens.

The plots for dry density versus moisture content appear in Figure 54 and those for dry density versus number of blows in Figure 55. As can be seen, the optimum moisture content varies from about 14% to 20%, depending on compactive energy. Similarly, the maximum dry density varied from about 100 to 112 pcf (1600 to 1792 kg/m³).

The objective was to simulate a typical subgrade for an interstate highway. This is believed to imply in most cases the higher range of comparative efforts, so emphasis was placed on the 13.26 to 32.5 (modified AASHTO density) in-lb/in³ (1.92 to 4.71 m-N/m³) plots. The region of densities and moisture contents considered appears in Figure 54 as a hatched rectangle. The eight specific combinations to be considered in the test series are indicated by the squared points on the periphery and the center of the rectangular region. The resulting factorial experiment is shown in Figure 56. The sample at 22% moisture content and a density of 110 pcf (1760 kg/m³) could not be obtained as it fell over the zero air voids curve.

In order to obtain the maximum simulation of field conditions and to minimize variability between specimens, an attempt was made to compact all specimens at 12% moisture and to obtain other moisture contents through capillarity. It was not possible, however, to obtain constant moisture contents throughout the sample and this was abandoned. Instead, the samples were dried and moisture added to approximate as closely as possible the moisture content desired. The number of blows indicated by Figure 55 were applied as a starting point and revised as necessary to arrive at specimens having the desired density and moisture content. Duplicate specimens were prepared for each point in the factorial.

Test Procedures

The equipment used and test setup was essentially that now considered common for resilient modulus testing for soils. In order to obtain maximum uniformity except in the control variables moisture content and dry density, all specimens were tested in a triaxial cell to 100,000 cycles of loading with a deviator stress of 2.0 psi (14 kN/m²) and a lateral pressure of 3.5 psi (24 kN/m²). Each load was applied as a "square wave" of 0.1 second duration and with a 0.9 second rest period. Vertical strain was measured periodically with two LVDT's mounted in clamps in the usual manner and recorded by an oscillographic recorder such that both resilient and permanent strain could be read.

Permanent strains were plotted versus number of load cycles on log-log paper as previously described for the asphalt concrete tests and ALPHA(3) and GNU(3) determined in the same manner.

Test Results

The results of this test program appear in Table 33. The sample

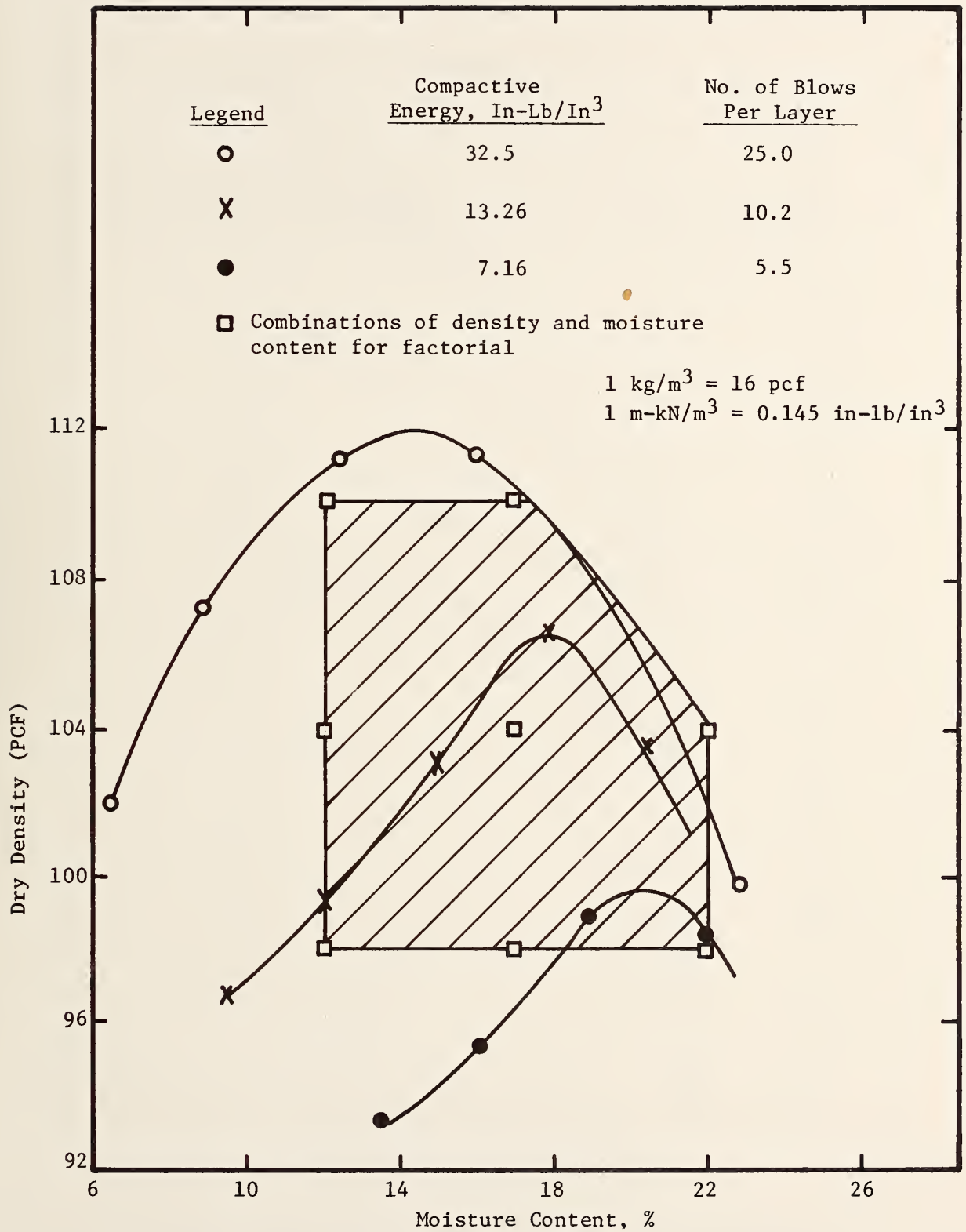


Figure 54. Plots of dry density versus moisture content.

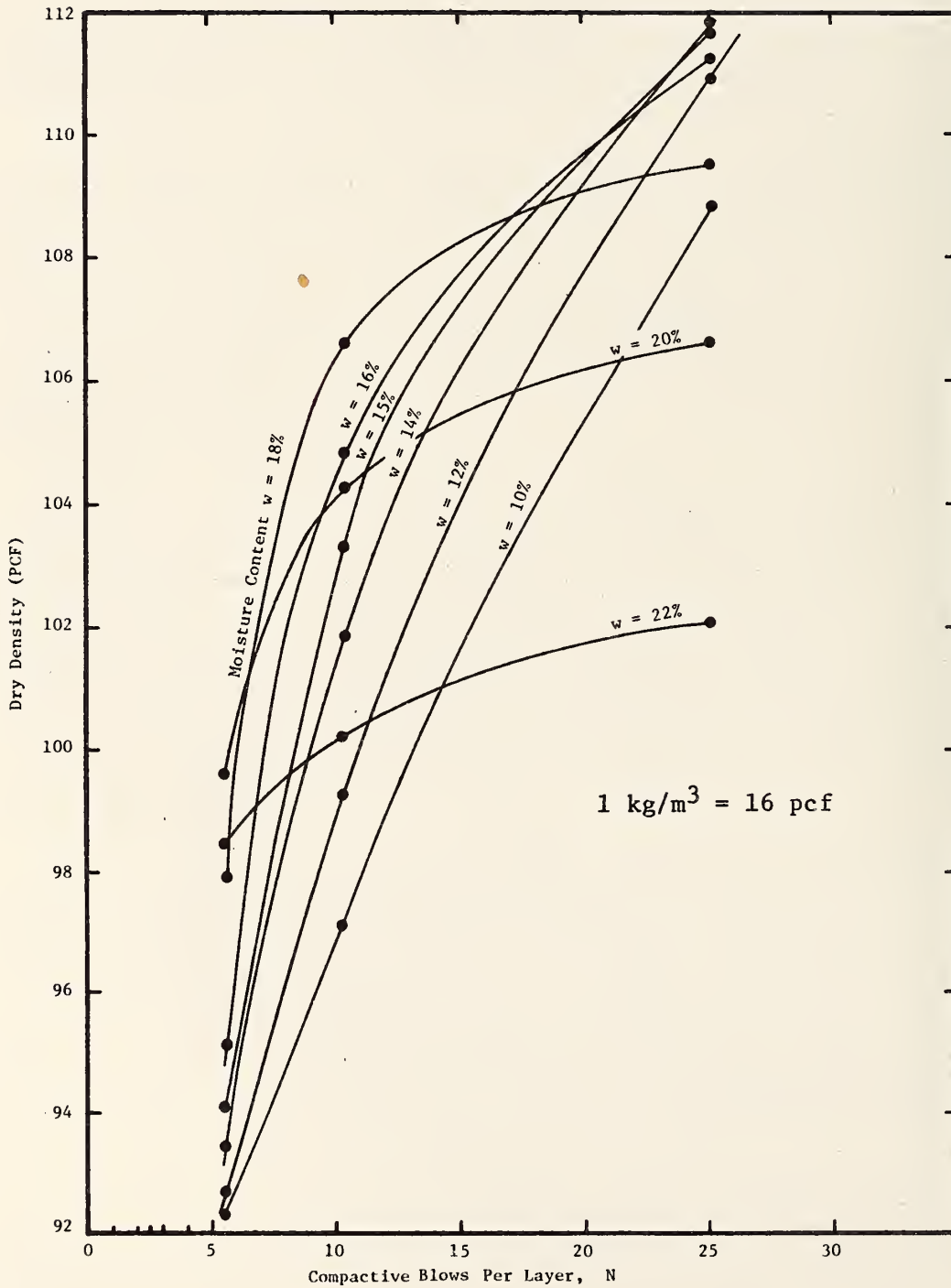


Figure 55. Plots of dry density versus compactive blows per layer in the specimen mold.

$1 \text{ kg/m}^3 = 16 \text{ pcf}$

Moisture Content	12%	17%	22%
Dry Density (pcf)			
98	X	X	X
104	X	X	X
110	X	X	

Figure 56. Factorial experiment for subgrade soil.

Table 33. Results of Permanent Deformation Tests on a Typical Silty Clay

Sample Number	Moisture Content (Percent)	Dry Density (PCF)	Resilient Strain ₅ (in/in x 10 ⁻⁵)	Resilient Modulus ₄ (psi x 10 ⁴)	Slope	Intercept ₅ (in/in x 10 ⁻⁵)	Alpha (3)	GNU (3)	Permanent Strain at 100,000 cycle (in/in x 10 ⁻⁴)
12-98A	11.7	97.7	1.24	16.13	.328	0.20	0.67	0.05	0.8
12-98B	12.7	97.8	4.76	4.20	.181	1.72	0.82	0.07	2.0
12-104A	12.1	104.8	2.46	8.13	.191	1.30	0.81	0.10	1.2
12-104B	12.0	103.6	4.61	4.34	.086	2.18	0.91	0.04	0.6
12-110A	11.7	109.8	1.09	18.35	.030	96.0	0.97	2.64	13.4
12-11B	12.4	109.8	3.40	5.88	.114	5.60	0.89	0.19	2.1
17-98A	17.9	97.7	6.25	3.20	.258	23.0	0.74	0.95	43.0
17-98B	16.9	97.1	1.85	10.81	.279	4.03	0.72	0.61	9.8
17-104A	18.6	103.2	1.89	10.58	.373	8.30	0.89	0.50	2.5
17-104B	18.9	103.6	3.53	5.67	0	420.0	1.00	0	42.0
17-110A	16.5	108.8	3.40	5.88	.020	17.0	0.98	0.10	2.0
17-110B	15.4	108.5	3.51	5.70	.143	10.3	0.86	0.42	5.2
22-98A	22.9	99.0	8.75	2.29	0.250	15.2	0.75	0.43	25.0
22-98B	21.6	99.0	3.83	5.22	0.167	1.30	0.83	0.06	0.9
22-104A	21.0	103.2	5.78	3.46	0.347	2.79	0.65	0.17	14.8
22-104B	21.2	103.9	3.25	6.15	0.057	5.00	0.94	0.09	1.0

1 kg/m³ = 16 pcf

1 kN/m² = 0.145 psi

numbers are coded such that the first two digits represent the desired moisture content, the next two the desired dry density in PCF and the letters A and B discriminate between the duplicate samples.

As can be seen, there is some unavoidable variability in the actual moisture contents and densities obtained in the prepared specimens, but this was taken into account by plotting actual values during analysis. The results appear in the form of plots in Figures 57, 58 and 59. As can be seen, there was considerable variability in results and only very general trend information was obtained.

It is believed that the variability was due primarily to:

1. Changes in length of the measuring rods between clamps for the LVDT's over the approximately 23 hours of test due to inadequate temperature control. The lesson learned here was that invar steel rods should be used due to their insensitivity to temperature change and that close control of temperature is likely required for long-term repetitive-load soil tests as well as for asphalt concrete.

2. It is believed that pore water pressures came into play at some point during the tests at the higher moisture content-density combinations and affected results.

3. Some natural variability between samples (despite care in preparation) that cause important variations in permanent deformation responses to long-term loading.

The general trend information gained was that for a silty clay such as that tested:

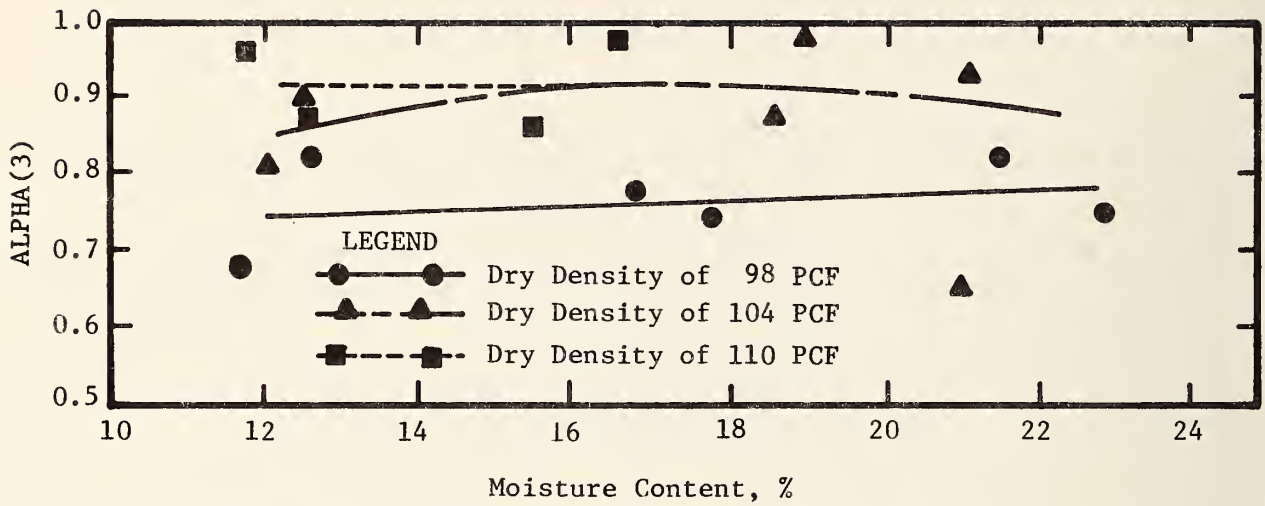
1. ALPHA(3) is fairly constant with moisture content and increases with increasing density. There is also some indication that it increases near optimum moisture content.

2. GNU(3) increases with increasing moisture content and decreases with increasing density.

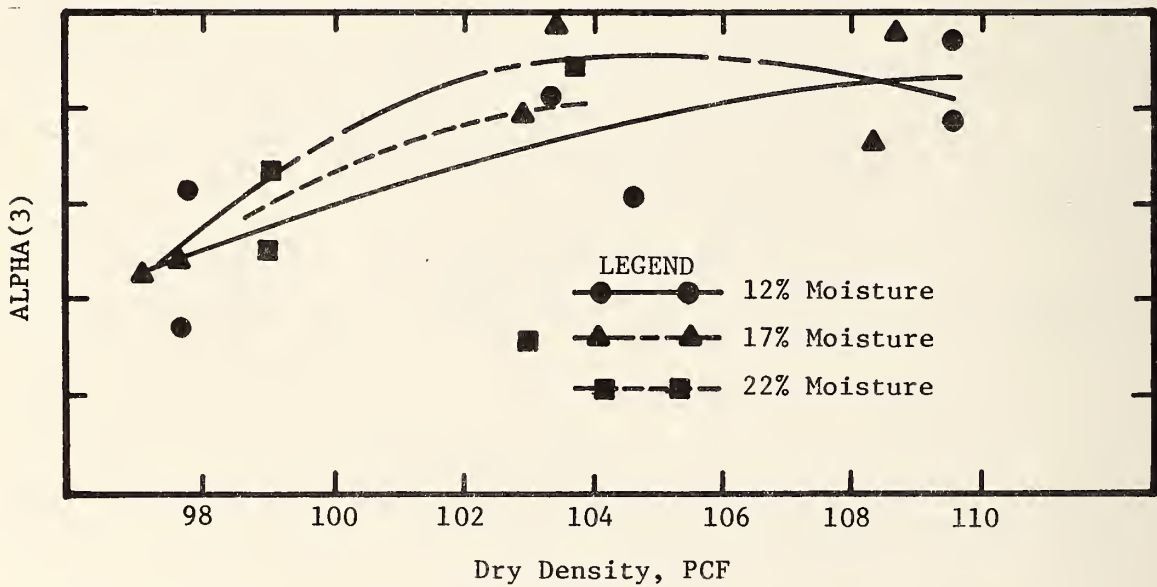
As a general note, GNU (3) is dependent on resilient strain, so the stress level used during testing needs to be simulative of that in the field.

Permanent Deformation Testing for a Silty Clay
Reported by Monismith, Ogawa and Freeme

Monismith et al (Reference 48) reported test results for repetitive



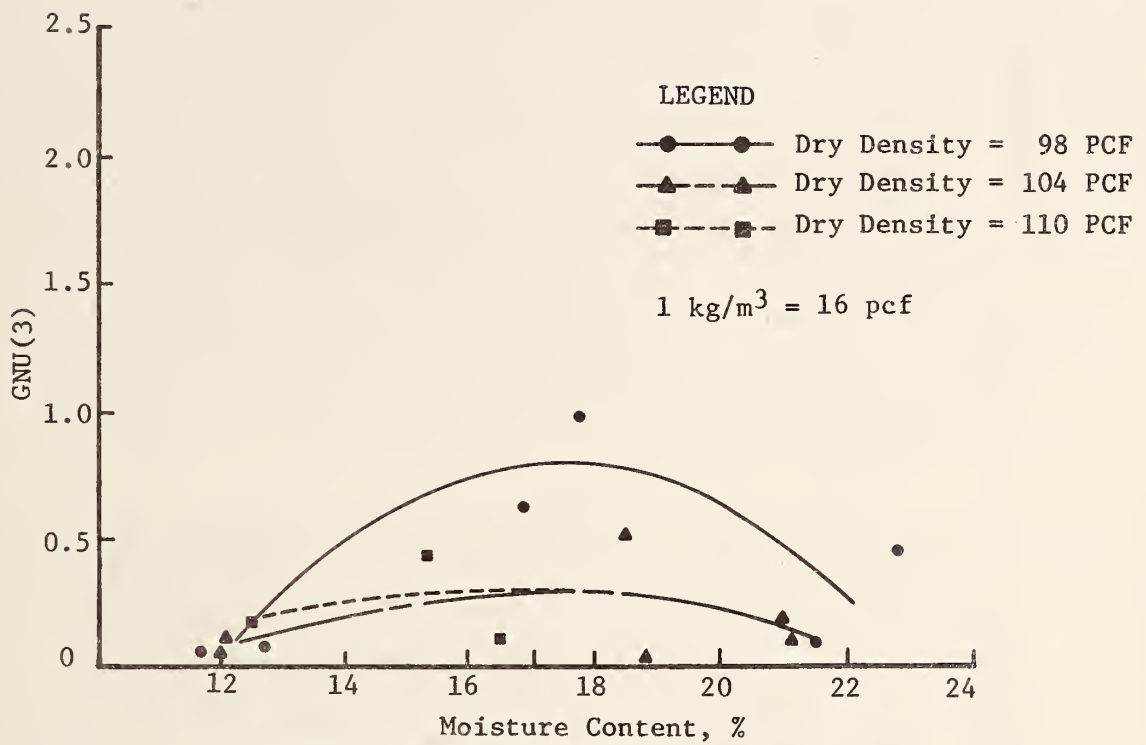
a. ALPHA(3) as a function of moisture content.



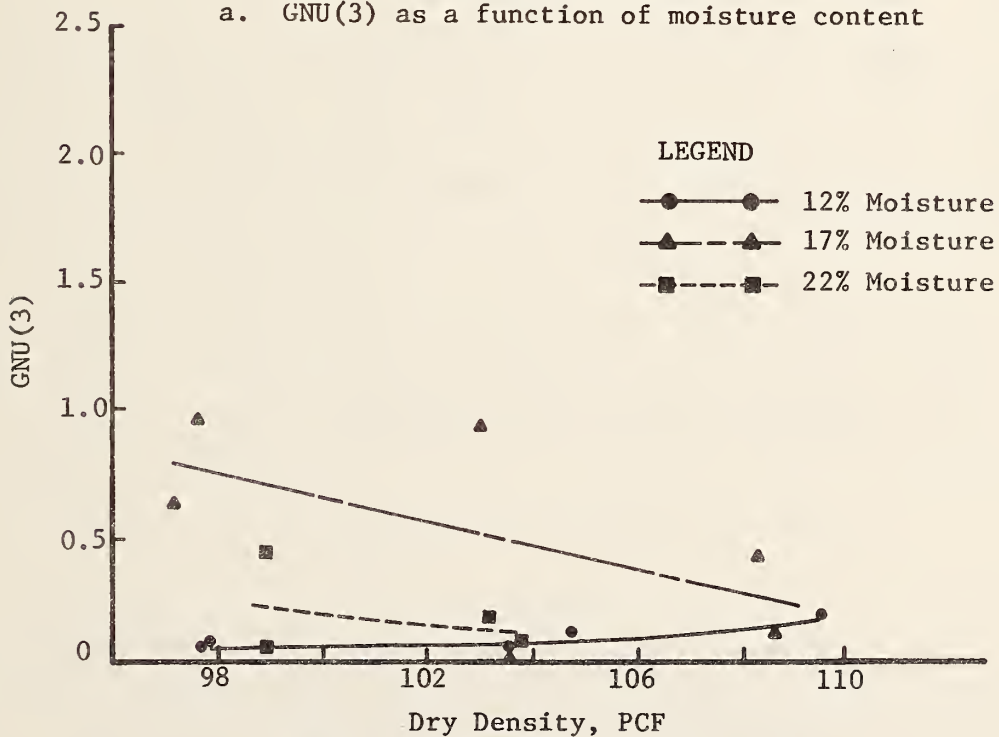
b. ALPHA(3) as a function of dry density.

$$1 \text{ kg/m}^3 = 16 \text{ pcf}$$

Figure 57. Variations in ALPHA(3) with moisture content and dry density.



a. GNU(3) as a function of moisture content



b. GNU(3) as a function of dry density

Figure 58. Variations in GNU(3) with moisture content and dry density.

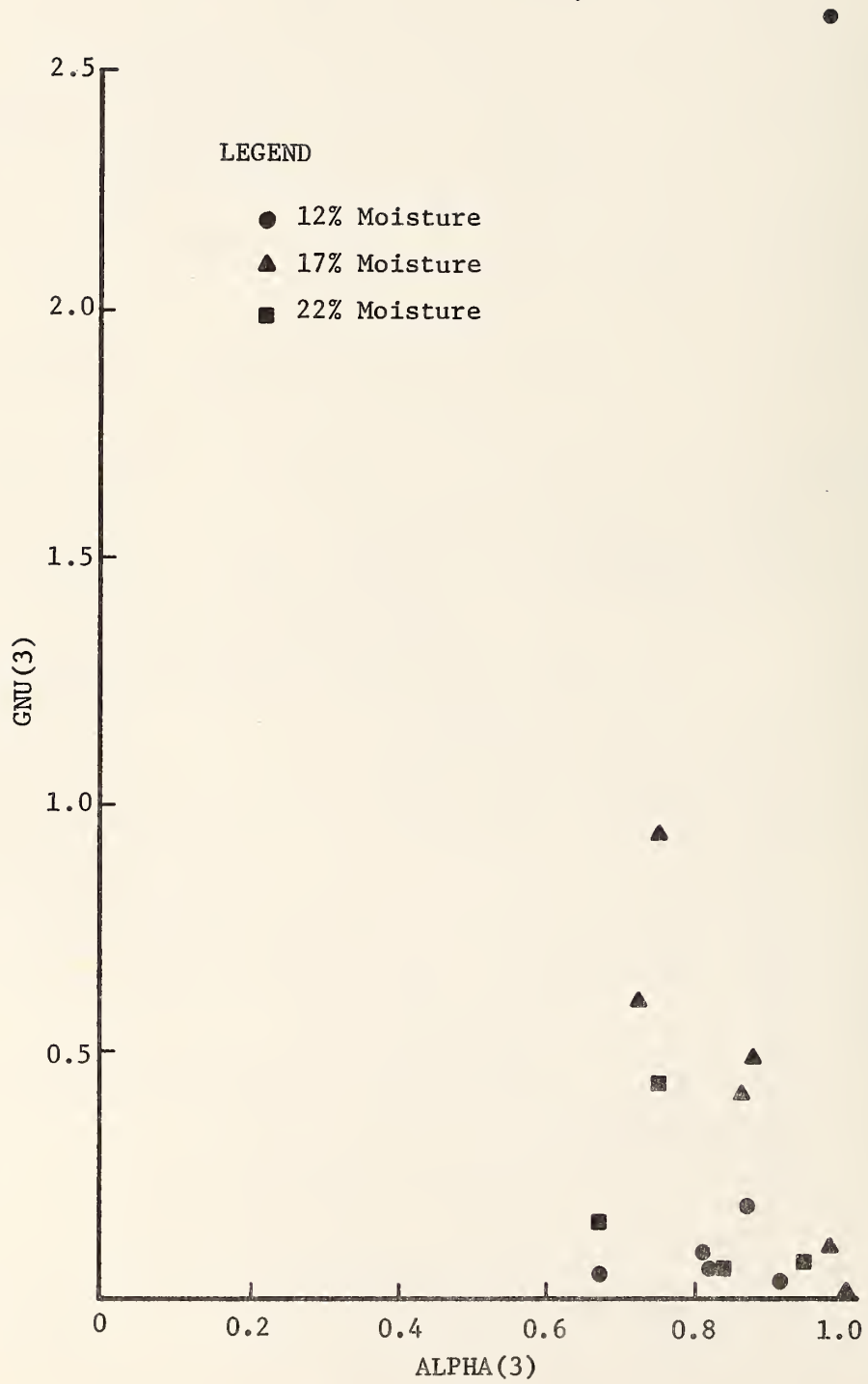


Figure 59. Relation between ALPHA(3) and GNU(3) for variations in moisture content and dry density.

loads on a silty clay subgrade from Contra Costa County, California having a liquid limit of 35 and plasticity index of 15. Plots of these results in the referenced paper were used in this project to obtain values of ALPHA(3) and GNU(3) for three cases and these are replotted in Figures 60 and 61 at the same scales as previous Figures 57 and 58. Study of these test results led to the following conclusions:

1. ALPHA(3) at higher stresses did not appear to be greatly affected by moisture content or density for this limited sampling.
2. While this limited sampling does not provide clear trends, it may be roughly concluded that GNU(3) increases with increasing moisture content and decreases with increasing density.
3. Lower stresses generally gave lower permanent strains and lower values of ALPHA(3) and GNU(3). (Lower values of ALPHA(3) imply more of the total strain is permanent, although total strains are smaller for lower stresses).

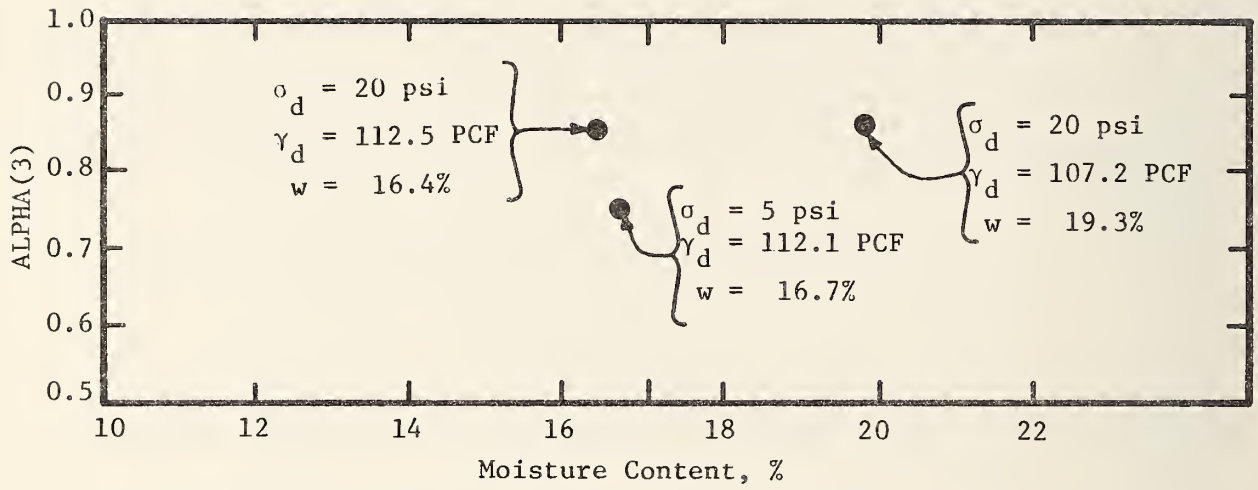
Permanent Deformation Testing for a Heavy Clay Reported by Townsend and Chisolm

Townsend and Chisolm (Reference 49) reported test results for repetitive loads on a heavy clay having a liquid limit of 73 and a plasticity index of 48. Tabulations of these results allowed values of ALPHA(3) and GNU(3) to be obtained for three batches of four specimens each. Moisture contents and densities varied between batches and vertical stress was varied within a batch. All tests were run at a lateral pressure of 2 psi (13.8 kN/m²) within the triaxial cell and were carried to a maximum of 50,000 load cycles.

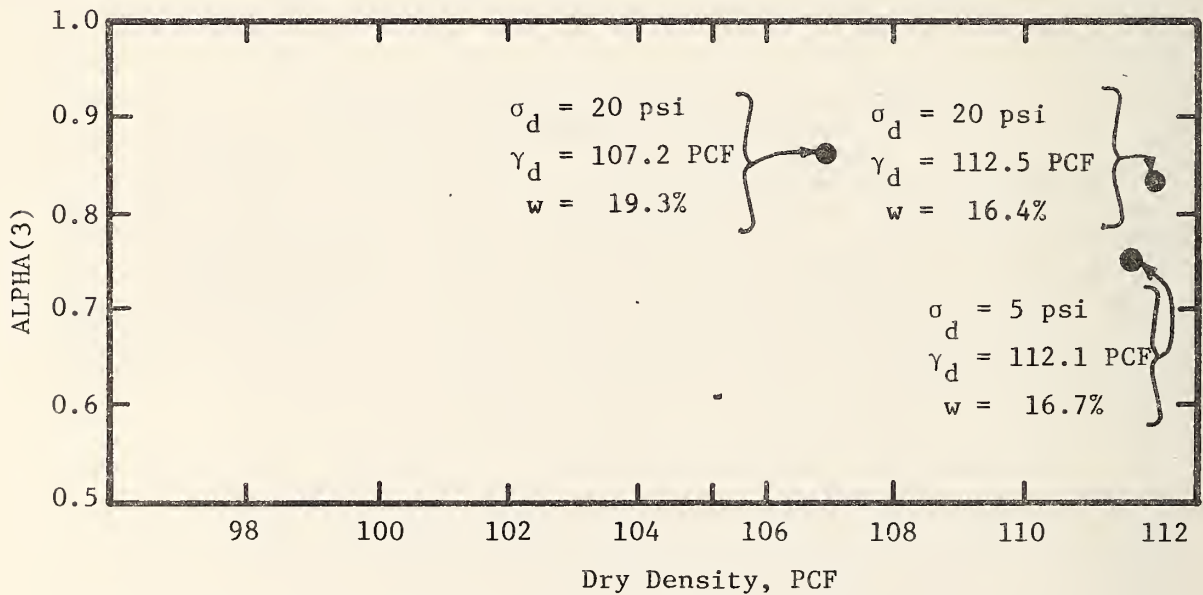
The results of these tests in terms of ALPHA(3), GNU(3) and permanent strain after 50,000 cycles appear in Figures 62, 63, and 64. As the range of deviator stresses are much higher than that usually experienced in a highway subgrade, this data was extrapolated to a deviator stress of 3 psi (20.7 kN/m²) and plots of this extrapolated data appear in Figure 62.

The following was concluded for the heavy clay tested:

1. (ALPHA(3) varies considerably with moisture content (0.7 to 0.9) between 24% and 30% of moisture. The general trend was increasing ALPHA(3) as moisture content increased up to some "optimum" after which it decreased with additional moisture.



a. ALPHA(3) as a function of moisture content.

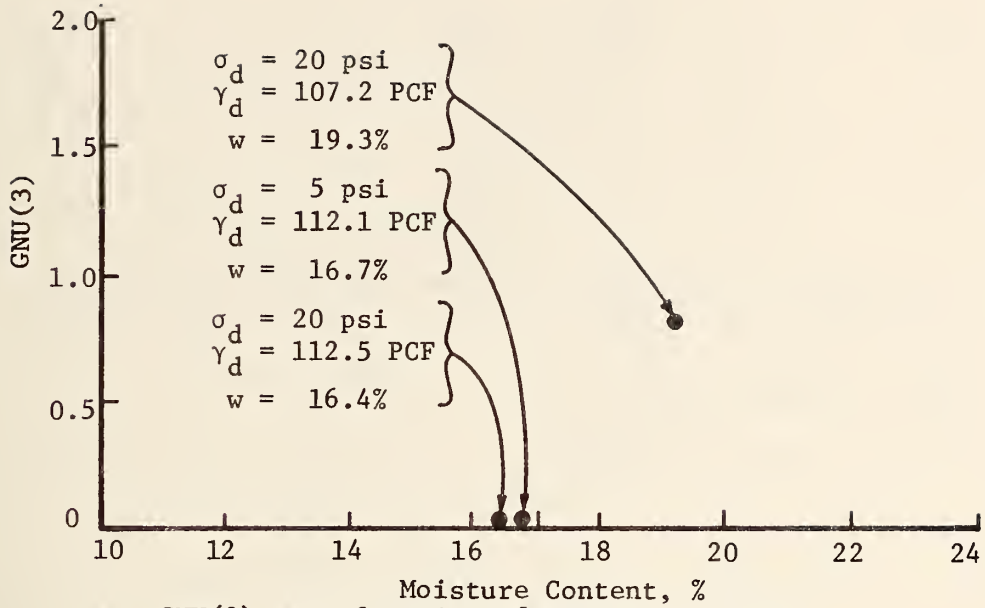


b. ALPHA(3) as a function of dry density.

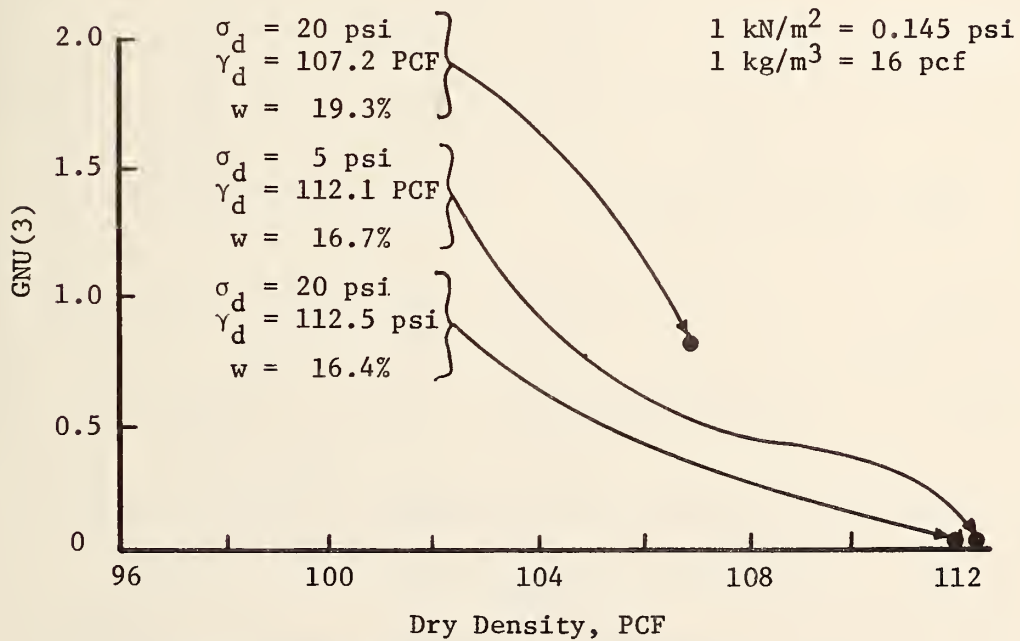
$$1 \text{ kN/m}^2 = 0.145 \text{ psi}$$

$$1 \text{ kg/m}^3 = 16 \text{ pcf}$$

Figure 60. Variations in ALPHA(3) with moisture content and dry density from data in Reference 48.



a. GNU(3) as a function of moisture content.



b. GNU(3) as a function of dry density.

Figure 61. Variations in GNU(3) with moisture content and dry density from data in Reference 48.

1 kg/m³ = 16 pcf

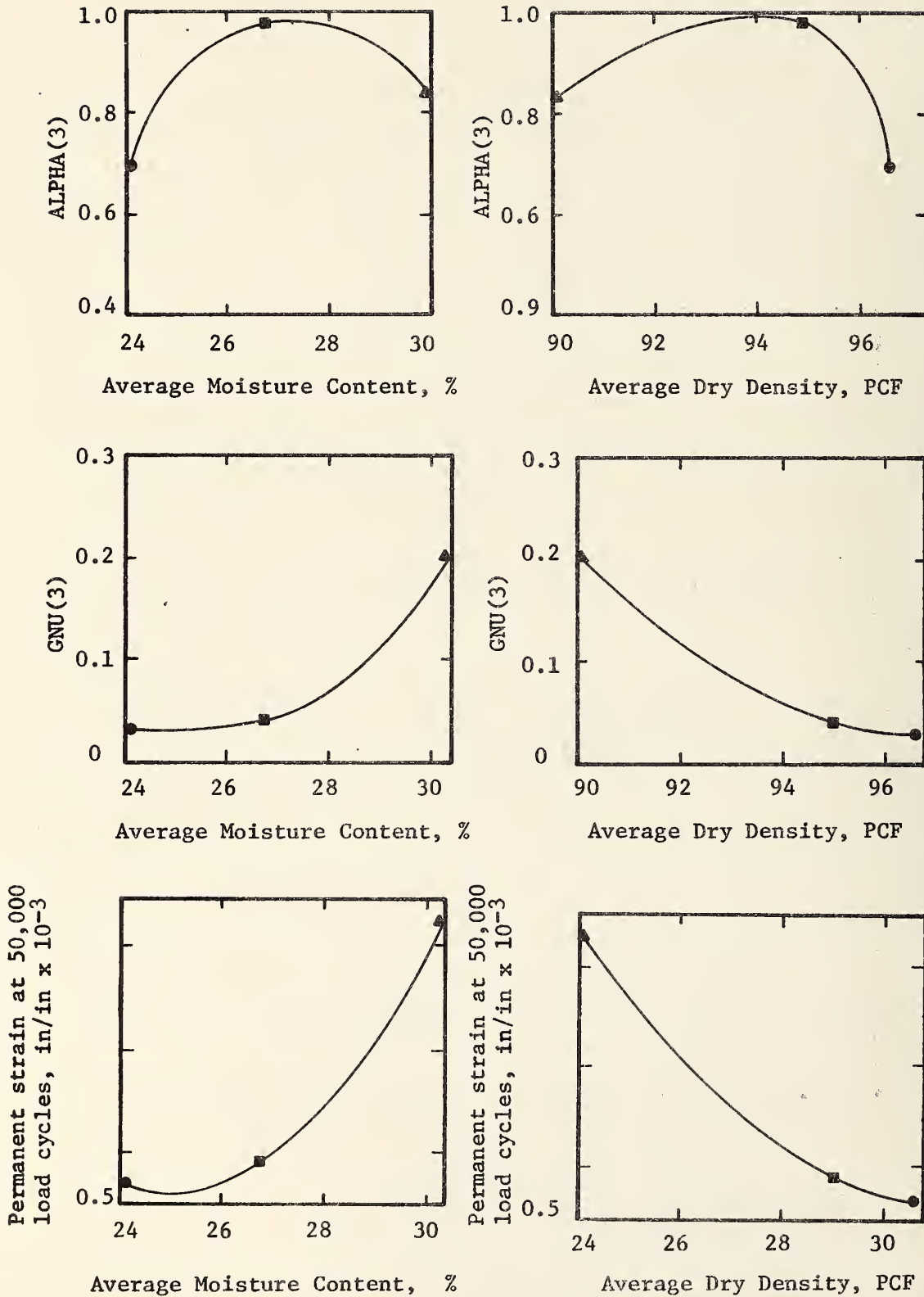
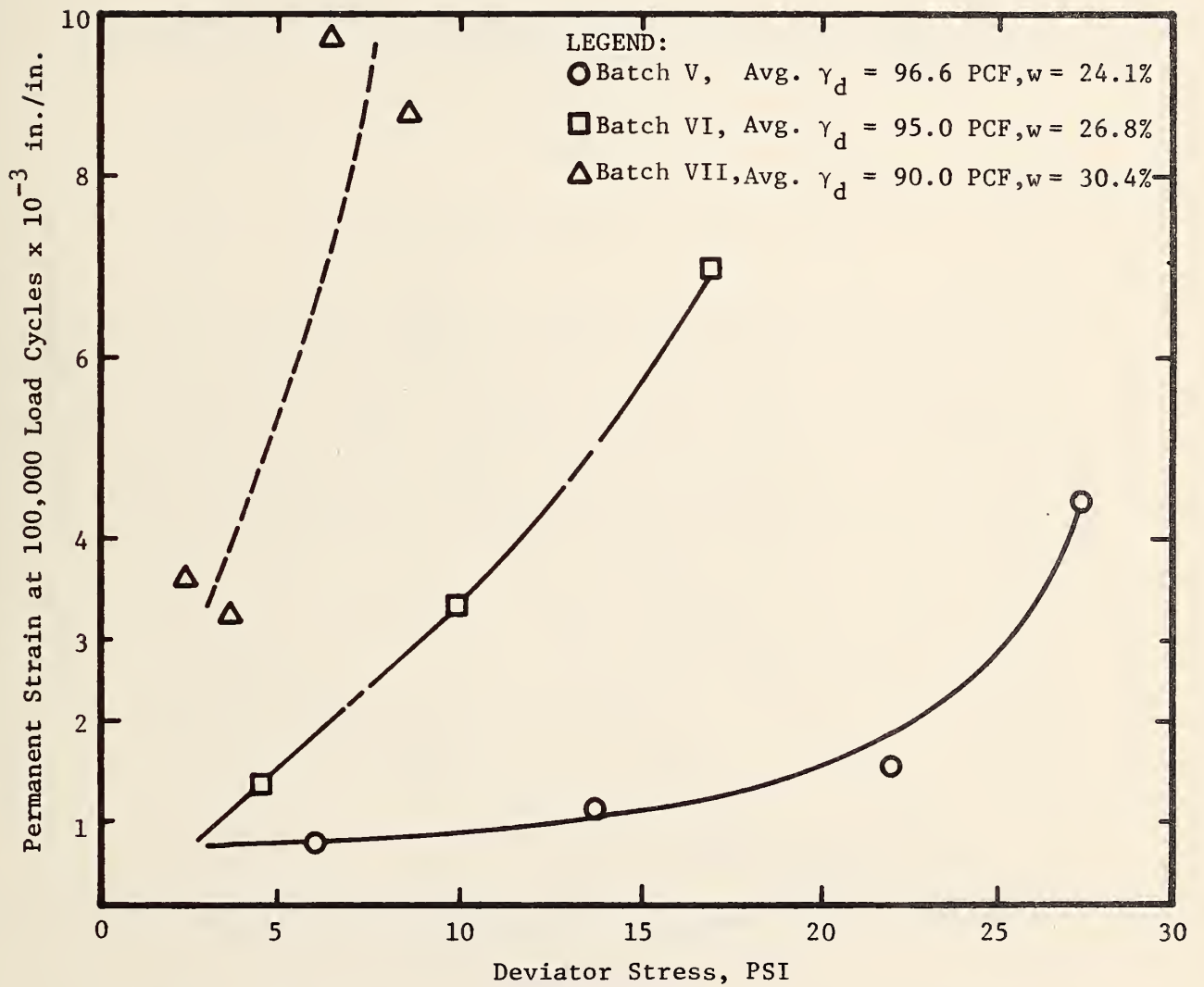


Figure 62. Variations in ALPHA(3), GNU(3) and permanent strain at 50,000 cycles of load as functions of moisture content and dry density from data in Reference 49.



1 kN/m² = 0.145 psi
 1 kg/m³ = 16 pcf

Figure 63. Permanent strain at 10,000 cycles of load versus deviator stress.

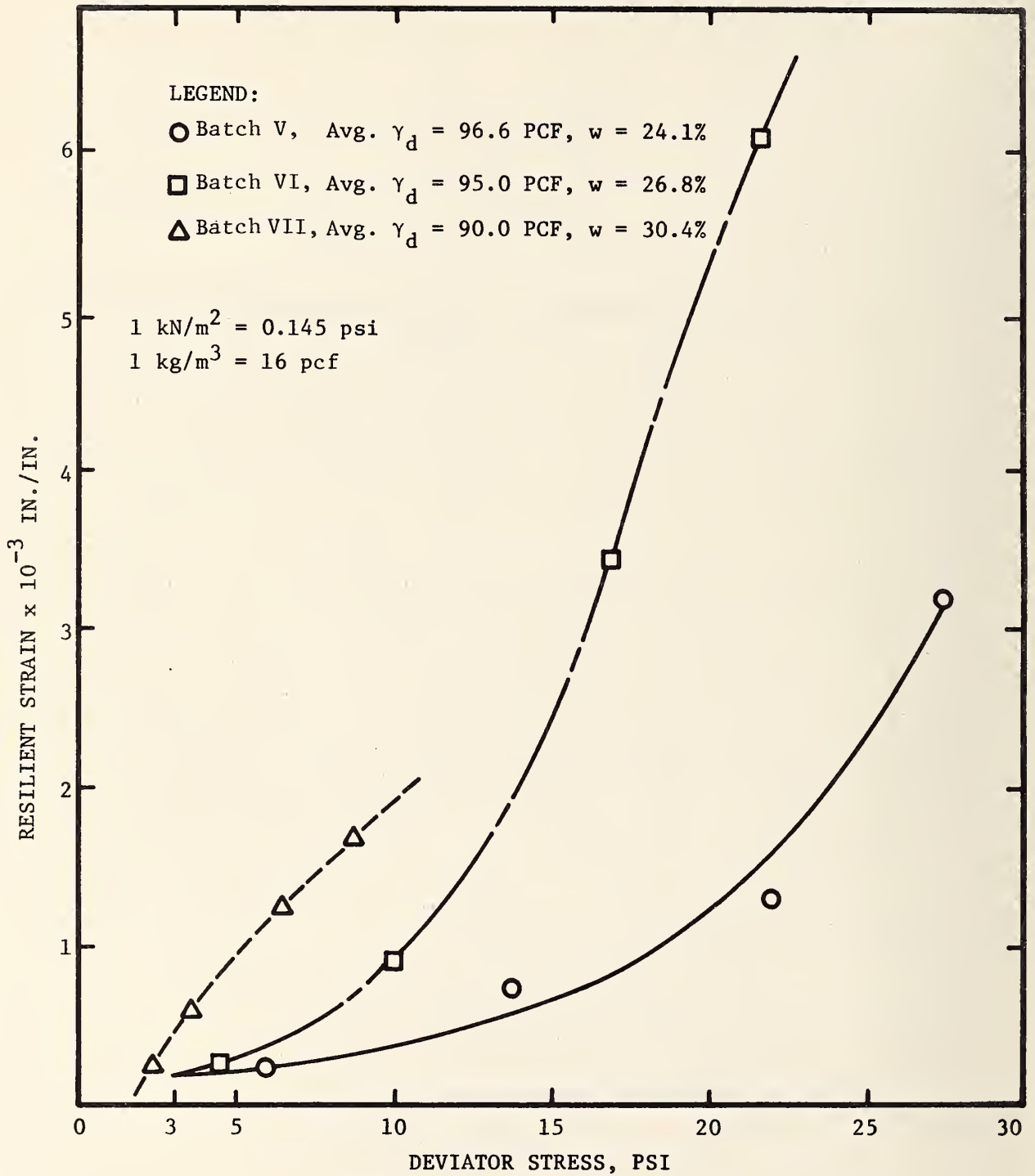


Figure 64. Resilient strain vs. deviator stress.

2. GNU(3) increased with increasing moisture and decreased with increasing density.
3. Permanent deformations increased with moisture content increases and decreased as density increased.
4. ALPHA(3) was erratic with a deviator stress increase at medium or higher optimum moisture content, but generally increased with increasing deviator stress.
5. GNU(3) was rather independent of deviator stress at lower moisture content, but decreased sharply with increasing deviator stress at the higher moisture content.
6. Resilient strain increased with deviator stress and at an increasing rate as deviator stress increased.

Permanent Deformation Testing for Penn State Clay
Subgrade Reported by Sharma, Kenis, Larson and Grambling

Sharma et al (Reference 50) reported test results for repetitive loads on a clay subgrade soil from the Pennsylvania State University Test Track. The data available was for two moisture contents. For a moisture content of 20.5%, the resilient modulus was approximately 83,000 psi (572,410 kN/m²), ALPHA(3) was 0.71, GNU(3) was 0.0199 and the permanent strain after 100,000 cycles of load was 1.44×10^{-4} in./in. For a moisture content of 23.5%, the resilient modulus was approximately 15,300 psi (105,520 kN/m²), ALPHA(3) was 0.64, GNU(3) was 0.036 and permanent strain after 100,000 cycles of load was 8.40×10^{-3} in./in.

Based on this limited data, the following apparent trends were noted:

1. ALPHA(3) decreased with increasing moisture content, but only based on two pieces of data.
2. GNU(3) increased with increasing moisture content.
3. Permanent deformation at 100,000 cycles increased 58-fold for an increase in moisture from 20.5% to 23.0%.

Permanent Deformation Testing for Sand Embankment
Reported by Sharma, Smith and Ruth

Sharma et al (Reference 51) reported test results for 100,000 cycles of repetitive loads on a sand embankment material from the Chiefland Test Road Experiment in Florida. The data available was for samples prepared at four moisture contents and three levels of dry density. One set of values for ALPHA(3) and GNU(3) appeared in the paper and others were calculated from plots of test results. The resulting data are tabulated top of Page 172.

Permanent Deformation Test Results on
Florida Sand Embankment Material

<u>Moisture Content (Percent)</u>	<u>Dry Density (PCF)</u>	<u>ALPHA(3)</u>	<u>GNU(3)</u>	<u>Permanent Strain @ 10⁵ Cycles (In./In.)</u>
3.4	109.1	0.917	0.492	4.02×10^{-3}
3.4	111.5	0.920	0.592	3.84×10^{-3}
5.9	107.8	0.861	0.718	5.22×10^{-3}
12.1	107.5	0.913	1.317	7.70×10^{-3}

1 kg/m³ = 16 pcf

Comparisons may be made between the two specimens at equal moisture content of 3.4% and differing dry densities and between the two specimens having essentially the same density and differing moisture contents. The results of these limited comparisons are:

1. ALPHA(3), GNU(3) and permanent strain all three increased with moisture content.
2. ALPHA(3) was almost independent of dry density, but increased slightly with the moisture content increase.
3. GNU(3) increased with increasing dry density.
4. Permanent strain after 100,000 cycles decreased with increasing dry density.

Possible Effects of Pore Water Pressure on Permanent
Deformation Testing of Clay Subgrade Material

Repeated load testing was conducted by Brown, Lashine and Hyde (Reference 52¹) on a silty clay (liquid limit of 32% and plasticity index of 14%) reduced to slurry and reconsolidated at various overconsolidation ratios to produce different saturated moisture contents and densities. The results of this testing indicated decreasing permanent strains with increasing density as expected and noted previously.

¹ Brown, S. F., A.K.F. Lashine and A.F.L. Hyde, "Repeated Load Triaxial Testing of a Silty Clay," Geotechnique 25, No. 1, 95-114, 1975.

Pore water pressures during the tests were measured and offer some valuable insight as to the effective stresses applicable during the test. Some of these results follow:

1. Pore water pressure increases as loading continues until some level is reached at which it stabilizes.
2. The pore water pressures stabilized at around 30% to 35% of the deviator stresses, so effective stresses were about two-thirds of the deviator stress.
3. Pore pressures stabilized much earlier in the test for denser samples with lower moisture contents than for those of less density and higher moisture content.

These tests were carried out to several million cycles if they did not fail. It is important to note that ALPHA(3) and GNU(3) were still increasing after a million cycles of load if no failure was imminent. For instance, ALPHA(3) for one sample at a moisture content of 19.7% increased from 0.83 at 100,000 cycles to 0.867 at 1,000,000 cycles, while GNU(3) increased from 0.24 to 0.305. The indication is that a set of ALPHA(3) and GNU(3) taken at 100,000 cycles as in current practice may be expected to overpredict long-term permanent deformations (say 100,000 or more cycles).

Brown, et al also concluded that resilient strains were a function of applied stress, while permanent strain was heavily dependent on stress history as well as applied stress.

While most subgrade soils are not fully saturated, it should be expected that pore pressures may develop during repetitive load tests of long duration due to consolidation of the specimen with repeated loads. The effect may be to produce erroneous values of ALPHA(3) and GNU(3).

General Conclusions on ALPHA(3) and GNU(3) as Functions of Moisture Content, Density and Deviator Stress

After studying the available test results individually and collectively, the following general conclusions were reached:

1. GNU(3) generally increases as moisture content increases and decreases as density increases. An apparent sharp decrease in GNU(3) may occur if sufficient moisture exists to accept pore pressure.
2. ALPHA(3) may increase or decrease somewhat with increasing moisture content, depending on the nature of the soil and the amount of moisture present. The variation due to moisture appears to depend on clay content. ALPHA(3) for the silty clays seemed to be almost independent of moisture

while ALPHA(3) for the "heavier" clay appears to vary much more with moisture content.

3. Both ALPHA(3) and GNU(3) increase together as moisture increases until ALPHA(3) reaches some level (higher maxima for higher density), and then ALPHA(3) continues to increase while GNU(3) sharply decreases. This implies that at some point of moisture increase the fraction of total strain that is permanent decreases (fraction of resilient strain increases) although the magnitude of permanent strain is increasing. This is probably due to limitations of a triaxial pressure to simulate resistance to large strains (consistent with higher moisture content) imposed by subgrade soils in the field. Stated differently, the passive case for coefficient of lateral earth pressure likely applies after many wheel loadings in the field so that cell pressure needs to increase as the test progresses in order to simulate these conditions accurately.
4. ALPHA(3) appears to be relatively independent of deviator stress if the clay content is low, but may vary considerably as clay content increases.
5. GNU(3) appeared to be relatively independent of deviator stress at lower moisture contents, but decreased sharply at higher moisture contents as deviator stress increases (possibly due to pore water accepting some of the stress increase).
6. Typical values of ALPHA(3) appear to range from 0.65 to 0.95.
7. Typical values of GNU(3) appear to range from 0.01 to 0.40, but can range much higher for unusual cases or materials.

APPENDIX D

EVALUATION OF CORRECTED HAJEK-HAAS MODEL FOR PREDICTING LOW TEMPERATURE CRACKING FOR FLEXIBLE PAVEMENTS

Mr. E. C. Novak, Jr., Research Laboratory Section, Testing and Research Division, Michigan Highway Commission, published in February 1976, a paper entitled "Evaluation of a Model for Predicting Transverse Cracking of Flexible Pavements." This paper was aimed at comparing the predicted low-temperature cracking derived from the Hajek-Haas model (References 8 and 9) and actual cracking measured on various sections of highways in Michigan. This involved a very significant effort including: (1) A survey of some 32 sections of highway around Michigan including numerous sub-observations within each section to arrive at actual Cracking Indices I as described in Reference 9. These surveys were conducted using the procedures described by Fromm and Phang in Reference 52.* (2) Searching out information on each of the sections to arrive at the data required to estimate the stiffness of the asphalt cement at 20,000 seconds. (3) Assignment of base temperatures and winter design temperatures for the various sections, calculation of the predicted values of cracking index for the 32 observations and the many sub-observations. (4) Statistical analyses to evaluate the applicability of the multiple regression model to observed cracking on Michigan pavements. (5) Extensive laboratory studies of the asphalt properties and the stiffnesses of cores removed from various pavements. These cores included representation of areas of high, medium and low cracking indices. The purpose of this testing was to see how well the estimated asphalt stiffness values correlated with the actual stiffness values of the cracked pavement as determined by laboratory testing. The test method used was a tensile-creep test.

The mean actual cracking indices and those predicted are shown along with the data used in the Hajek-Haas equation in Table 34. The majority of Mr. Novak's summary and conclusions is quoted below to provide the detailed results of this study:

Summary and Conclusions

"In this study the Hajek-Haas model, designed to predict transverse cracking susceptibility of flexible pavements, was statistically evaluated by testing its ability to predict the mean cracking index of selected Michigan pavements. A supplemental study was conducted when it was found that the model was not suitable, in an effort to determine why the model failed and to provide direction for possible future work in this area. These studies have produced the following observations and conclusions:

*52 Fromm, H.J., Phang, W.A., "A Study of Transverse Cracking of Bituminous Pavements," Department of Transportation and Communications, Ontario, Report No. RR176, January 1972.

TABLE 34. SUMMARY OF CRACKING INDEX VALUES AND OTHER RELATED DATA

Observation Number	Cracking Index Standard		Mean Predicted I	Residual I - I	No. of Sub-Observations	Original Asphalt			Penetration at 77 F	Viscosity at 275 F	Penetration Index	Base Temp, C	Winter Design Temp, C	Thickness of Pavement, in.	Age of Pavement, years	Estimated Stiffness of Asphalt Cement at 20,000 S _{cc} , kg/cm ²
	Mean Actual I	Dev. of Mean Actual I				Penetration at 77 F	Viscosity at 275 F	Penetration Index								
1	0.7	0.9	8.8	8.160	27	87	322	-0.64	46	-20	2.1	5	40			
2	3.3	4.5	8.6	5.353	129	94	333	-0.39	45	-20	2.5	6	35			
3	0.0	0.1	2.5	2.447	75	130	257	-0.38	43	-20	2.5	4	13			
4	0.1	0.3	5.9	5.774	106	94	325	-0.44	46	-20	2.5	4	27			
7	0.0	0.0	1.3	1.304	132	123	256	-0.36	38	-25	3.3	3	50			
8	0.1	0.3	4.4	4.352	39	126	288	-0.26	44	-30	2.5	6	120			
9	1.0	1.9	0.0	-1.007	76	228	180	-0.25	38	-30	2.5	4	35			
10	0.3	0.7	0.0	-0.314	156	243	210	+0.09	38	-30	2.5	6	18			
11	0.0	0.0	0.0	0.000	137	211	178	-0.40	38	-35	2.5	2	140			
12	0.0	0.0	0.0	0.000	95	127	290	-0.25	42	-30	2.5	1	115			
13	0.4	1.0	0.0	-0.368	95	223	222	-0.02	38	-35	2.5	6	100			
14	3.4	4.2	2.7	-0.610	94	149	224	-0.56	41	-30	2.8	4	150			
15	1.0	1.6	6.8	5.733	47	92	470	+0.07	48	-30	3.3	9	200			
16	0.0	0.1	0.0	-0.027	75	231	186	-0.18	37	-25	2.5	5	60			
17	0.0	0.3	12.0	11.920	63	91	344	-0.45	47	-25	2.5	8	100			
18	0.0	0.0	4.7	4.741	64	231	191	-0.18	37	-25	2.5	5	60			
19	0.0	0.0	0.0	-0.004	121	133	286	-0.09	43	-25	2.5	2	30			
20	1.9	3.7	10.3	8.373	110	97	330	-0.40	46	-25	2.5	8	95			
21	0.0	0.1	3.3	3.339	115	152	242	-0.32	42	-25	2.5	9	30			
22	0.0	0.1	2.7	2.690	52	155	239	-0.27	41	-25	2.5	9	30			
23	2.6	2.3	25.9	23.225	63	60	442	-0.59	51	-25	4.5	11	250			
24	5.4	3.3	28.3	22.883	32	61	395	-0.73	51	-25	4.5	12	300			
25	1.0	1.4	20.5	19.535	71	62	365	-0.84	49	-20	4.5	11	100			
26	3.1	2.4	20.5	17.365	120	61	438	-0.60	50	-20	4.5	11	100			
27	1.5	1.3	21.8	20.339	76	61	432	-0.61	50	-20	4.5	12	100			
28	10.7	4.3	20.5	9.822	92	61	438	-0.60	50	-20	4.5	12	100			
29	0.2	0.4	15.5	15.301	59	68	426	-0.53	50	-20	4.5	9	75			
30	10.4	6.7	25.9	15.494	81	61	432	-0.61	50	-20	4.5	12	250			
31	21.2	5.4	23.7	2.466	44	66	424	-0.56	50	-25	4.5	12	210			
32	20.3	4.8	23.7	3.380	48	66	424	-0.56	50	-25	4.5	12	210			
33	12.5	3.9	23.7	11.213	102	66	424	-0.56	50	-25	4.5	12	210			
34	0.2	0.9	25.9	25.616	72	61	459	-0.53	50	-25	4.5	11	210			

°C = 0.5554 (°F-32)

1 cm = 0.39 inches

1 kg/cm² = 14.5 psi

1. For Michigan's flexible pavements, the Hajek-Haas model lacks the ability to predict, within reason, transverse cracking performance.

2. Modification of the model, based on data collected in Michigan, failed to improve predictive ability sufficiently to warrant its use.

3. Of the model's five independent variables, only stiffness modulus was significantly related to the cracking frequency of Michigan flexible pavements.

4. Rational studies of transverse cracking indicate that it is the bituminous concrete stiffness modulus, tensile strength, and coefficient of expansion properties acting in combination with climatic conditions, that governs an asphalt's susceptibility to transverse or thermal cracking.

5. The Hajek-Haas model demonstrated poor predictive ability because it included only one of several bituminous concrete properties which affect transverse cracking.

6. No direct correlation could be found between cracking index and the following stiffness modulus characteristics:

a. The modulus of field aged bituminous concrete determined by creep test;

b. The estimated modulus of field aged asphalt cement determined using McLeod's method of estimating modulus from penetration viscosity data;

c. The estimated modulus of field-aged bituminous concrete determined using Heukelom and Klomp's chart for converting estimated cement stiffness to mix stiffness on the basis of the volume concentration of the aggregate, C_v .

7. The stiffness modulus of asphalt cement can be lowered to such an extent that other properties of the bituminous mix which also influence transverse cracking are diminished to a non-effective level.

8. The ability of very soft asphalts to override other mix properties apparently enable criteria to be established that will permit designers to essentially eliminate transverse cracking based on the estimated stiffness of the asphalt cement.

9. Based on the transverse cracking performance of Michigan's flexible pavements, McLeod's method of selecting penetration grades of asphalt that will produce essentially crack-free pavements is conditionally recommended depending on the cost and availability of soft asphalt grades and the ability to develop mix designs of suitable high temperature stability.

10. The data collected for this study indicate that stiff grades of asphalt, 60 to 70 penetration grade, can also perform in a crack-free manner. Because of this and the fact that harder asphalt cements are desirable from a stability standpoint, there is a need to develop a method of more accurately assessing the susceptibility of bituminous mixes to transverse or thermal cracking.

11. Michigan flexible pavements consist of three separately constructed layers of bituminous concrete. For convenience, the total bituminous concrete layer is usually considered homogeneous and isotropic for most design purposes. However, this study indicates this assumption to be incorrect since the rheologic and fracture properties of each layer differ significantly. This increases the difficulty with which the properties of the bituminous layer can be characterized and, of course, increases the difficulty of predicting all types of surface cracking.

12. The tensile strength of bituminous mixes, at low temperature, is dependent on the tensile strength of the aggregate as indicated by the large percentage of tensile failure through the aggregate itself."

Unfortunately, the equation published in Reference 9 was not correct and this is the equation that was used for the Novak study. This equation is shown below:

$$10^I = 2.497 \times 10^{30} \times S^{(6.7966 - 0.8740t + 1.3388a)} \times (7.054 \times 10^{-3})^d \times (3.193 \times 10^{-13})^m \times d^{0.6026s} \dots \dots \dots (1)$$

where

I = the cracking index - number of full plus half of the transverse cracks per 500 ft (152 m)

s = stiffness of the asphalt, kg/sq cm

a = age of the pavement, years

t = thickness of asphalt, in. (1 cm = 0.39 in.)

d = type of subgrade, dimensionless code (Sand-5, Loam-3, Clay-2)

m = winter design temperature, degrees centigrade

As the equation given in Reference 9 did not provide the same results as the nomographs in the reference, Dr. Haas was contacted and questioned in this regard. He advised that there was an error in the equation as it appeared in the reference and that the corrected equation could be obtained by multiplying the winter design temperature m by -0.1 and multiplying the stiffness s by 0.1. The resulting corrected equation is then:

$$10^I = 2.497 \times 10^{30} \times 0.1 s^{(6.7966-0.8740t + 1.3388a)} \cdot x (7.054 \times 10^{-3})^d \times (3.193 \times 10^{-13})^{-0.1m} \times d^{0.06026} s \dots \dots \dots (2)$$

Using the corrected equation (2) with the data appearing in Table 34, new predictions of Cracking Index were developed and compared to the actual mean cracking indices. These values appear in Table 35, along with new residuals and the ratio of actual to predicted cracking indices. As can be readily seen, the corrected equation generally improves the predictive capability of the Hajek-Haas model.

Analysis of the data in Table 35 for the predictions using the corrected equation indicate the following: (1) The model predicted correctly that the 10 sections that did not crack would not crack. It also predicted that four of the nine sections with one crack or less for 500 feet (152 m) would not crack. This appears to indicate that the model does a quite reasonable job of determining whether important cracking will or will not occur. (2) The corrected equation like the published equation generally over predicts the cracking where moderate cracking actually occurs, but it tends to over predict less than the published equation. (3) There were two actual cases of cracking index above 20 for observations 31 and 32. The predicted values for these cases were very close to the actual, however, observations 33 and 34 were virtually identical pavements, ages and winter design temperatures, but they displayed much less actual cracking. This seems to imply that the model is tuned to

TABLE 35. SUMMARY OF CRACKING INDEX VALUES USING CORRECTED HAJEK-HAAS EQUATION AND COMPARISON TO ACTUAL VALUE

Observation Number	Mean Actual	Predicted Published Equation	Predicted Corrected Equation	Cracking Index I		Mean Actual* Predicted	Cracking $C_L = 6I$ (yds./1000 sq. yds)	Average Crack Spacing = 500/I
				Residual Predicted* Actual	Predicted* Actual			
1	0.7	8.8	3.4	2.7	0.21	20	149	
2	3.3	8.6	1.3	-2.0	2.46	8	37	
3	0.0	2.5	0.0	0.0	1.00	0	-	
4	0.1	5.9	0.8	0.7	8.45	.5	591	
7	0.0	1.3	0.0	0.0	1.00	0	-	
8	0.1	4.4	0.0	-0.1	-	0	-	
9	1.0	0.0	0.0	-1.0	-	0	-	
10	0.3	0.0	0.0	-0.3	-	0	-	
11	0.0	0.0	0.0	0.0	1.00	0	-	
12	0.0	0.0	0.0	0.0	1.00	0	-	
13	0.4	0.0	0.0	-0.4	-	0	-	
14	3.4	2.7	0.0	-3.4	-	0	-	
15	1.0	6.8	11.3	10.3	11.34	68	44	
16	0.0	0.0	0.0	0.0	1.00	0	-	
17	0.0	12.0	0.0	0.0	1.00	0	-	
18	0.0	4.7	0.0	0.0	1.00	0	-	
19	0.0	0.0	0.0	0.0	1.00	0	-	
20	1.9	10.3	7.4	5.5	0.26	44	68	
21	0.0	3.3	0.0	0.0	1.00	0	-	
22	0.0	2.7	0.0	0.0	1.00	0	-	
23	2.6	25.9	23.5	20.9	0.11	141	21	
24	5.4	28.3	29.0	23.6	0.19	174	17	
25	1.0	20.5	16.4	15.4	16.45	174	17	
26	3.1	20.5	16.4	13.3	0.19	10	30	
27	1.5	21.8	17.1	15.6	0.09	10	29	
28	10.7	20.5	17.1	6.4	0.62	10	29	
29	0.2	15.5	10.9	10.7	0.02	65	46	
30	10.4	25.9	25.4	15.0	0.41	152	20	
31	21.2	23.7	22.3	1.1	0.95	134	22	
32	20.3	23.7	22.3	2.0	0.91	134	22	
33	12.5	23.7	22.3	9.8	0.56	134	22	
34	0.2	25.9	20.5	20.3	0.01	123	24	

*Predicted values using corrected equation.

1 m = 1.1 yds.

pavements in this category except there are other variables involved that are not considered by the model.

There appears to be two direct approaches for deciding whether the Hajek-Haas equation is suitable for use. One is the accuracy of the predictions in terms of actual number of cracks per 500 feet (152 m) and how many cracks are predicted with relation to actual cracks experienced. A summary analysis of the residuals or difference between actual and predicted cracking indices appears in Table 36. A summary analysis of cracking index ratios, actual divided by predicted, appears in Table 37.

It can be seen from Table 36 that some 47% of the crack predictions were within one crack or less, 56% were within two cracks or less, 63% within 4 cracks or less and that some 31% predicted seven or more cracks in excess of those actually occurring. Similar review of Table 37 indicates that 38% of the predictions were within 10% in number of cracks, 14% were within 50%, and 56% of the predictions differed from the actual predictions by more than 50%. As neither of these analyses is complete within itself, it is necessary to look a little deeper. For instance, a prediction of $I = 0.2$ to an actual cracking index of 1 crack per 500 ft. (150 m) gives a cracking index ratio of 5.0, but really is a quite acceptable prediction. A combined summary analysis appears in Table 38 to more clearly identify the success levels of the predictions. Review of Table 38 shows that some 53% of the predictions missed the number of cracks either by 1 or less or were within 10% of the total number or less. 69% predicted within 5 cracks or within a difference of 50% of the actual number of cracks and 31% predicted in excess of these latter limits.

It is clear that the corrected Hajek-Haas equation does a considerably better job of predicting than the erroneous published one. It is still obvious that it is not an especially accurate model. However, considering the wide variations in actual cracking indicated in Table 34 for apparent similar pavement sections and the limited basis for its development, it does a remarkably good job. After review of several other models that have been developed in recent years and the overall nature of the prediction problem, the writer has concluded that this much more simplistic model will give almost, if not as good, predictions as some more complex models such as that of Shahin and McCullough (References 6 and 7). The real problem is that low temperature cracking (and indeed any fracture problem involving tensile stresses) is subject to many more parameters than can reasonably be included in a practical model. In addition, the relationship of these parameters to the formation of the crack is in general poorly defined. It is concluded that the corrected Hajek-Haas model does a reasonable job of predicting

TABLE 36. SUMMARY ANALYSIS OF RESIDUALS (ACTUAL LESS PREDICTED CRACKING INDEX I)
FOR CORRECTED HAJEK-HAAS EQUATION

Magnitudes of Residuals in <u>Number of Cracks</u>	<u>One</u>	<u>Two</u>	<u>Three</u>	<u>Four</u>	<u>Seven</u>	<u>Greater</u>
	<u>or Less</u>	<u>than Seven</u>				
Number of Observations	15	18	19	20	22	10
Percent of Total of 32 Observa- tions	47	56	59	63	69	31

TABLE 37. SUMMARY ANALYSIS OF CRACKING INDEX RATIOS (ACTUAL/PREDICTED) FOR CORRECTED HAJEK-HAAS EQUATION

Magnitudes of Cracking Index Ratio	0.9 to 1.1 (10% Diff.)	0.8 to 1.20 (20% Diff.)	0.7 to 1.30 (30% Diff.)	0.6 to 1.40 (40% Diff.)	0.5 to 1.50 (50% Diff.)	Greater than 50% Diff.
Number of Observations	12	12	12	13	14	18
Percent of Total of 32 Observations	38	38	38	41	44	56

TABLE 38. SUMMARY ANALYSIS TO COMBINE "ACCURACY LEVELS" FOR RESIDUALS AND CRACKING INDEX RATIOS FOR THE CORRECTED HAJEK-HAAS EQUATION

Magnitudes of Combined Residual & Cracking Index Accuracy Levels	Residual of 1 or Less or 10% or Less Diff.	Residual of 2 or Less or 20% or Less Diff.	Residual of 3 or Less or 30% or Less Diff.	Residual of 4 or Less or 40% or Less Diff.	Residual of 5 or Less or 50% or Less Diff.	Residual Greater than 5 or Diff. Greater than 50%
Number of Observations	17	18	19	21	22	10
Percent of Total of 32 Observations	53	56	59	66	69	31

whether important low temperature cracking will or will not occur and that it does a marginal job of predicting number of cracks or crack spacing if cracking does occur.

APPENDIX E

STRUCTURE OF THE SAVED STATIC SOLUTION FILE

The file created by VESYS A when a SAVETAPE keyword is encountered for a type 1 run is as follows:

```

ITITLE (20 words, alpha numeric)
NTEMP (= the number of seasons)
NDEL (= the number of terms in each Dirichlet series)
NRAD (= the number of tire footprint radii considered)
NTXNR (NTEMP x NRAD)
H1 } thickness of the asphalt and base layers, respectively.
H2 }
(TEMP(I), I = 1, NTEMP) NTEMP values of season temperature
(RADIUS(I), I = 1, NRAD) NRAD values of radius
(GCVAR(I,4), I = 1, NTXNR) a coefficient of variation for the
                          Dirichlet series for vertical
                          deformation for each static solution
(GCVAR(I, 7), I = 1, NTXNR) the same as above, but for radial
                          strain
(ALF(I), I = 1, NTXNR) } permanent deformation parameters for
(GMU(I), I = 1, NTXNR) } each static solution

((GRAD(I,J), I = 1, NTXNR), J = 1, NDEL) { the NDEL Dirichlet co-
((GNORM(I,J), I = 1, NTXNR), J = 1, NDEL) { efficient for the radial
                                          strain and vertical defor-
                                          mation responses for each
                                          static solution.

```

It can be seen that the file will be of variable length, depending on the number of static solutions. This is helpful in reducing the storage charges for desk-resident permanent files, since no unused space is required.

APPENDIX F

VARIANCE OF CRACKING AS A FUNCTION OF EVALUATION FREQUENCY

In the process of verifying changes made for Task A-1, which involved allowing seasonal variation of ALPHA and GNU for the three layers, and of the creep compliance arrays for layers 2 and 3, a comparison was made between: (1) a run on the old version with a particular data set (using NTEMP = 1); (2) a run on the modified program with the same data set; and (3) a run on the modified program with the same data except that NTEMP was set to 4, and four identical values of ALPHA and GNU were entered for each layer (the same as the single value previously used); the four "season" multiplier for creep compliance for layers 2 and 3 were set to 1.0, as had the single values for run (2). The four values of TEMP were likewise equal to the single value used before.

The results of runs (1) and (2) agreed exactly. The results of runs (2) and (3) differed, but only in the predicted variance of cracking; the value from run (3) was almost exactly 1/4 the value from run (2). Examination of the equations used to calculate the variance of cracking soon showed that, at least under some conditions, this was a result to be expected. The relevant equations from subroutine CRACKS can be written as follows:

(We refer to a "season" as the period of time into which the year is divided by NTEMP.)

$TDEL = 7200. * 365.25 * 12 / NTEMP =$ number of seconds per season.

$TDDAY = TDEL / 3600. / 24. = 365.25 / NTEMP =$ number of days per season.

$ADT_j =$ average daily traffic (axles/day) during the j^{th} period of time (j^{th} entry in TRANDOM).

$EN_i = ADT_j * TDDAY =$ number of axles in the i^{th} (cumulative) season (which occurs during the j^{th} entry in TRANDOM).

EMF_k } complicated functions of the results from GRESP and
 $VEMF_k$ } of the fatigue relation for the k^{th} season, where k runs from 1 to NTEMP.

then

$$DMG_{\ell} = \sum_{i=1}^{\ell} \cdot EMF_k \cdot EN_i \text{ where } k = 1 + [(i-1) \text{ modulo } NTEMP]$$

and ℓ is the
(cumulative) season
number at which the
estimate is being
calculated

and

$$VDMG_{\ell} = \sum_{i=1}^{\ell} EN_i \left[(EMF_k)^2 + EN_i \cdot VEMF_k \right]$$

In our problem, assume that ADT is held constant. Then EN (and hence each term in the sum for DMG) will be inversely proportional to NTEMP (see the definition of TDDAY) and at any particular time DMG will be the same for any value of NTEMP because the number of terms in the sum will be directly proportional to NTEMP.

The situation for VDMG depends on which term within the parentheses dominates. If the first, then

$$VDMG_{\ell} \approx \sum_{i=1}^{\ell} EN_i (EMF_k)^2 \quad (k \text{ depends on } i)$$

and, since EMF does not depend on the amount of traffic or the period of time involved, the same argument applies as for DMG.

In our situation, however, the second term dominates:

$$(VEMF \cdot EN) \gg (EMF)^2$$

and hence we have

$$VDMG_{\ell} \approx \sum_{i=1}^{\ell} (EN_i)^2 \cdot VEMF_k \quad (k \text{ depends on } i)$$

Thus the number of terms depends directly on NTEMP but the size of each is inversely proportional to the square of NTEMP; hence the value of the sum is inversely proportional to NTEMP. It is this result which does not seem grounded in physical reality, namely that the variance of cracking at a given time depends on how often it has been evaluated prior to that time.

For our particular case, we used

ADT = 8000 (constant)
AMPLITUD = 75.
DURATION = .0125
TEMP = 60. (for both NTEMP = 1 and NTEMP = 4)

and, with this particular data set,

$$\begin{aligned} \text{EMF} &= .289 \times 10^{-10} \\ \text{VEMF} &= 1.989 \times 10^{-22} \\ \text{EN} &= 2.922 \times 10^6 \end{aligned}$$

so that the two terms in the equation for VDMG are

$$\begin{aligned} \text{EN (EMF)}^2 &= 2.44 \times 10^{-15} \\ (\text{EN})^2 \cdot \text{VEMF} &= 1.698 \times 10^{-9} \end{aligned}$$

and the dominance of the second term is quite complete.

APPENDIX G
GUIDE FOR DEVELOPING INPUT FOR
LOW TEMPERATURE CRACKING PREDICTIONS

The values required to evaluate the regression equation for low temperature cracking (Hajek-Haas model) are:

1. age of the pavement, in years.
2. thickness of the bituminous layer, in inches.
3. subgrade soil type, in a numerical code (5-sand; 3-loam; 2-clay).
4. winter design temperature, °C.
5. stiffness of original asphalt cement, according to McLeod's methods, at the winter design temperature, in Kg/cm².

Items 1 and 2 are provided automatically by input already required by VESYS A. These are the values input under the TRANDOM and THICK1 keywords, respectively. Item 3 is a simple input based on observation of the soil type. Item 4 and 5, however, are very specifically defined, using tables and/or charts which may not be readily available. Therefore, these two parameters are described in more detail, including the specific steps needed to go from readily available data to the desired input.

The winter design temperature is defined to be "the lowest temperature at or below which only 1% of the hourly air temperatures in January occur for the severest winter during a ten year period" (Haas, Ref. 9). Where such detailed records are not available, Haas (ibid) has given a relationship between air freezing index (40 year average) and winter design temperature, covering a range from 500 to more than 3000 degree days in freezing index, as well as a suggested extrapolation to lower value of freezing index. This is shown in Figure 65.

Freezing index contour maps for Canada and for the United States are given in Figures 66 and 67, respectively, and may be used with Figure 65 to obtain approximate values of winter design temperature if other more accurate data are unavailable.

The asphalt stiffness value to be used is to be derived in a very specific manner, and hence considerable detail is given here to that derivation. The required input data to the procedure are the viscosity at 279°F (137°C) and the penetration at 77°F (25°C) derived from laboratory tests. From Figure 68, obtain the penetration index (PI) from the above data by visual interpolation, or by the following interpolation formula

$$PI = \frac{\log L - \log X}{\log L - \log M} \cdot (1.5)$$

where:

X = viscosity in centistokes at 275°F (135°C) for the asphalt cement for which P.I. is to be determined.

L = viscosity in centistokes at 275°F (135°C) for a P.I. of 0.0, determined from Figure 68 for the penetration at 77°F (25°C) for the given asphalt cement.

M = viscosity in centistokes at 275°F (135°C) for a P.I. of -1.5, determined from Figure 68 for the penetration at 77°F (25°C) for the given asphalt cement.

The ring and ball temperature ($T_{R\&B}$) or base temperature is required for the next step and may be measured in the laboratory or determined from P.I. and penetration using the nomograph of Figure 69, which gives a temperature difference ΔT between base temperature and the temperature employed for the penetration test (T_{pen}) in the sense.

$$\text{Base } T = T_{pen} + \Delta T \text{ (nomograph)}$$

Determine the stiffness at a loading time of 20,000 seconds (5.6 hours) from the nomograph of Figure 70, entering the temperature scale with the difference between the base temperature and the winter design temperature ($^{\circ}C$). Note that ΔT from Figure 69, is in $^{\circ}C$, so the value of T_{pen} must be converted to $^{\circ}C$ before the base temperature is obtained.

The regression equation is not meaningful for values of asphalt cement stiffness S equal to or less than 10 kg/cm^2 , so a value of zero would be input and no low-temperature cracking predicted. This is essentially realistic as low-temperature cracking is generally not a serious problem in the southern United States where such low winter stiffness would occur.

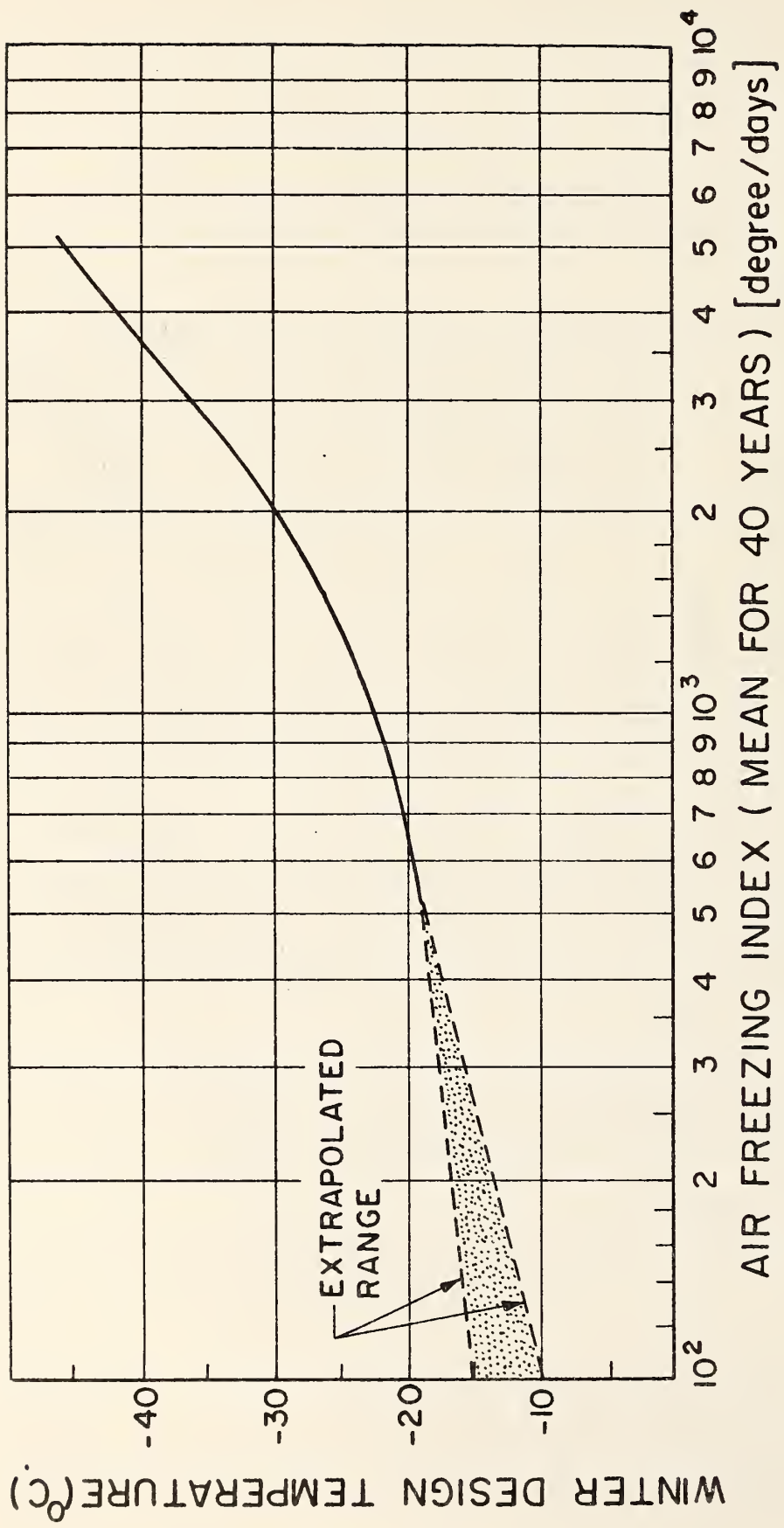


Figure 65. Relationship between freezing index and winter design temperature.

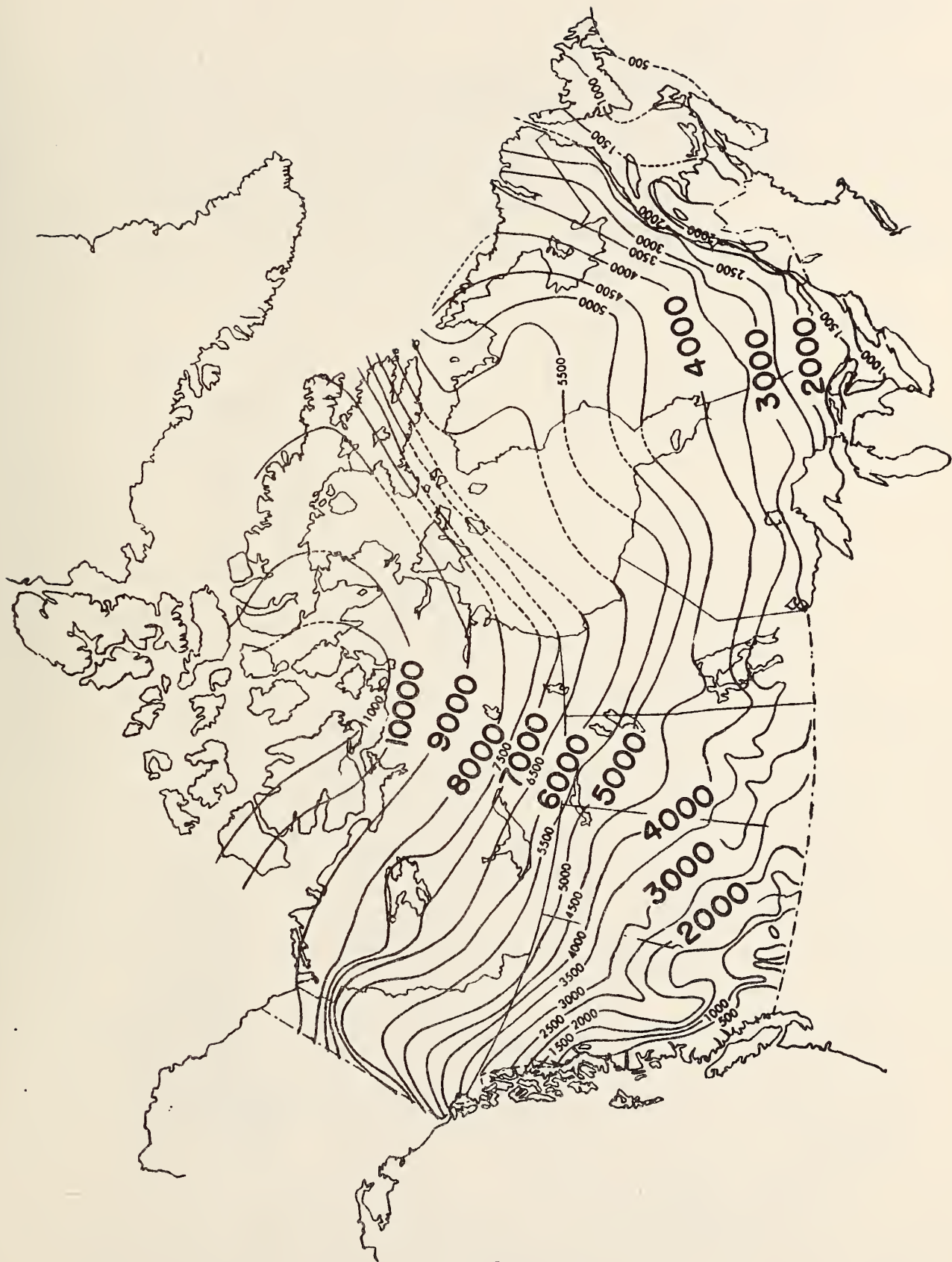


Figure 66. Map of Canada illustrating Freezing Indices.

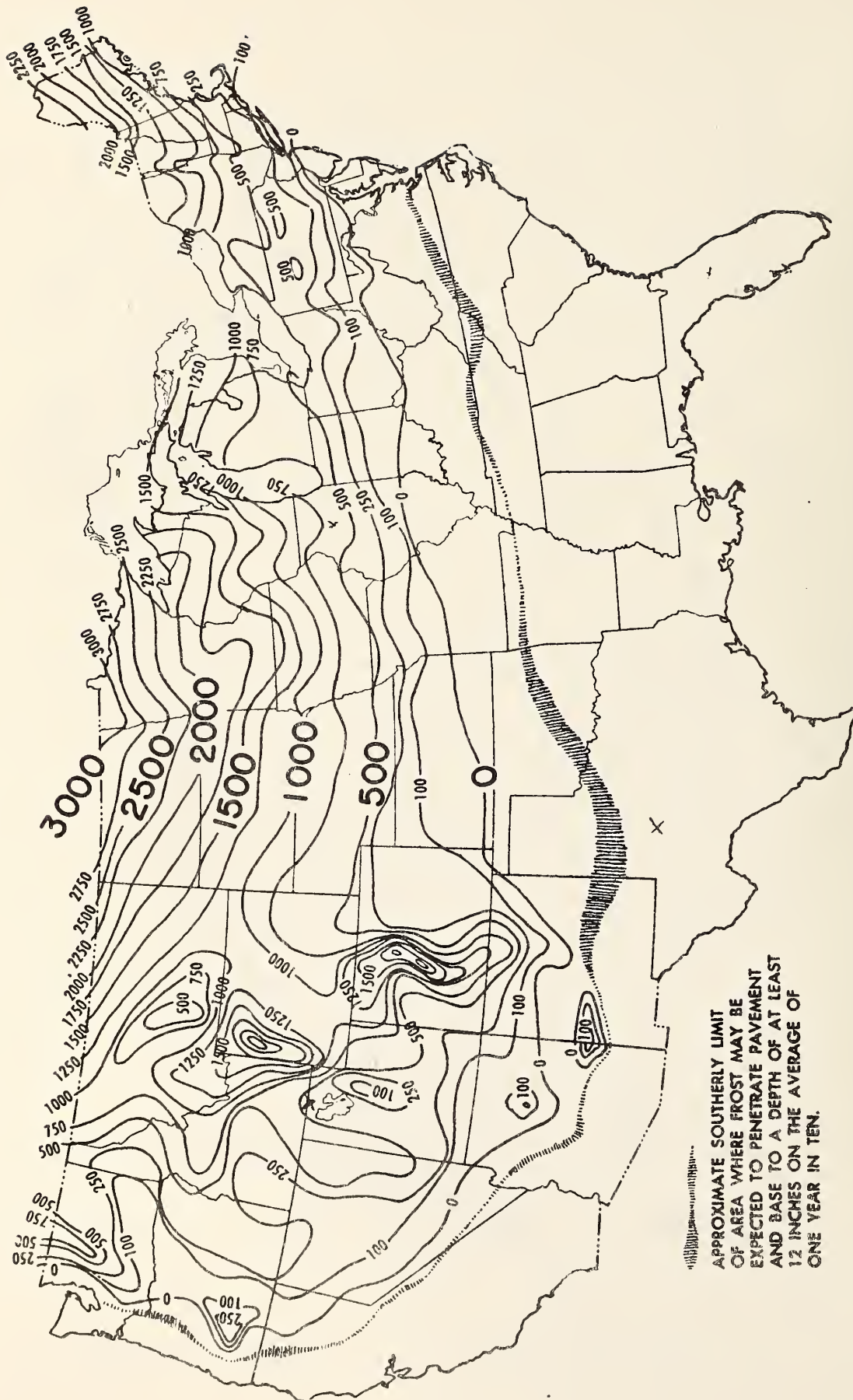
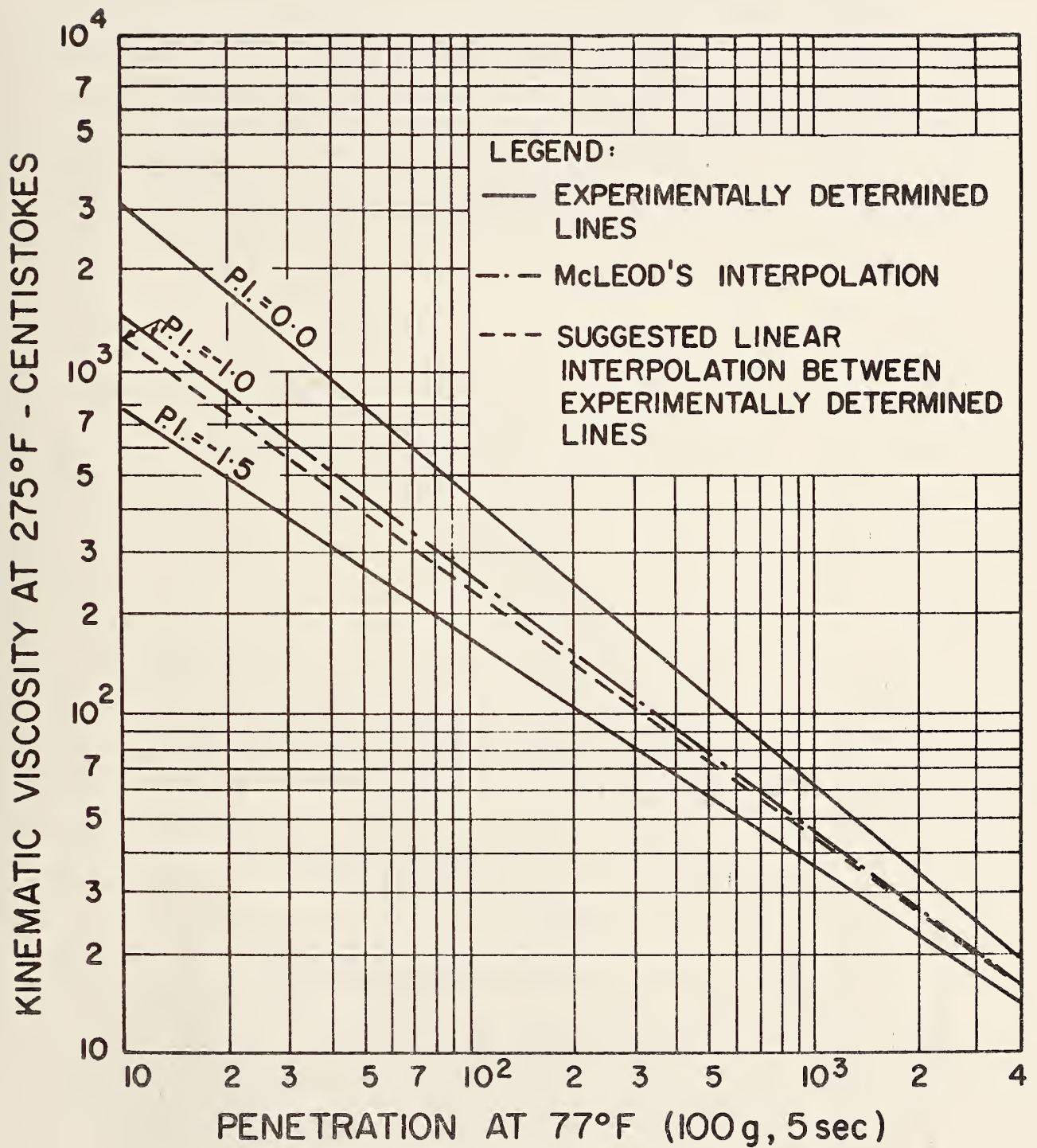


Figure 67. Freezing Index Map of the United States.



$$^{\circ}\text{C} = 0.5554 (^{\circ}\text{F} - 32)$$

Figure 68. McLeod's chart for estimating the P.I. of an asphalt cement.

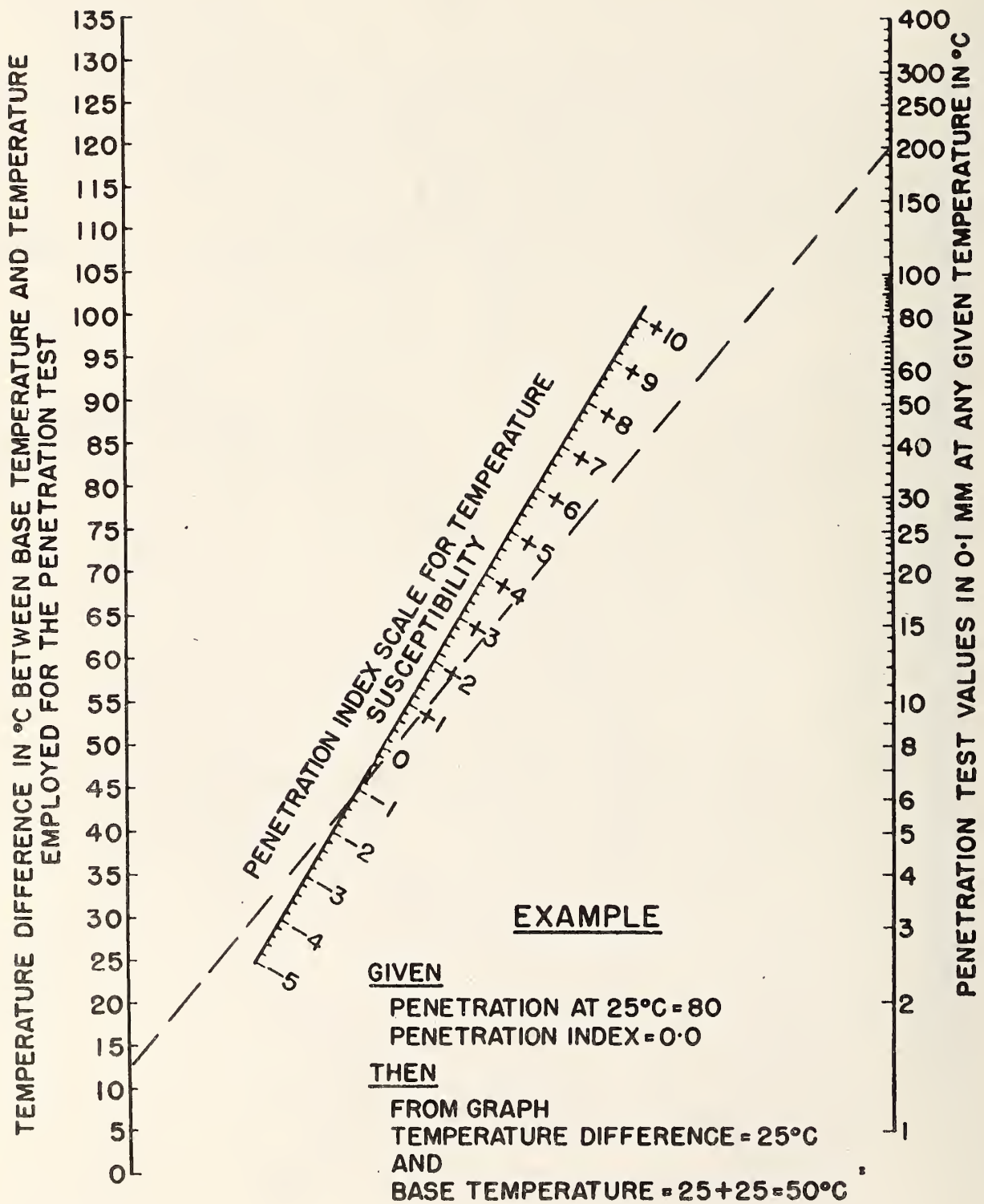


Figure 69. Suggested modification of Heukelom's version of Pfeiffer's and Van Doormal's Nomograph for relationship between penetration, penetration index and base temperature. (After McLeod)

REFERENCES

1. Rauhut, J. B., J. C. O'Quin and W. R. Hudson, "Sensitivity Analysis of FHWA Structural Model VESYS IIM, Vol. 1, Preparatory and Related Studies," Report No. FHWA-RD-76-23, March 1976.
2. Kenis, W. J. "Predictive Design Procedures - A Design Method for Flexible Pavements Using the VESYS Structural Subsystem," Proceedings, Fourth International Conference, Structural Design of Asphalt Pavements, Volume I, August 1977.
3. Proceedings from a Conference on Utilization of Graded Aggregate Base Materials in Flexible Pavements, held March 25-26, 1974 in Oakbrook, Illinois, published by the National Crushed Stone Association, National Sand and Gravel Association and the National Slab Association.
4. Kalcheff, I. V. and R. G. Hicks, "A Test Procedure for Determining the Resilient Properties of Granular Materials," Journal of Testing and Evaluation, Vol. I, No. 6, ASTM, 1973.
5. Finn, F. N., C. Saraf and R. Kulkarni, "Development of Pavement Structural Subsystems," Final Report NCHRP 1-10B, July 1976.
6. Shahin, M. Y., "Prediction of Low-Temperature and Thermal-Fatigue Cracking of Bituminous Pavements," University of Texas, PhD Dissertation, August 1972.
7. Shahin, M. Y., "Design System for Minimizing Asphalt Concrete Thermal Cracking," Proceedings, Fourth International Conference on Structural Design of Asphalt Pavements, August 1977.
8. Hajek, J. J., "A Comprehensive System for Estimation of Low-Temperature Cracking Frequency of Flexible Pavements," The Transport Group, Department of Civil Engineering, University of Waterloo, Waterloo, Canada, July 1971.
9. Haas, R. C. G., "A Method for Designing Asphalt Pavements to Minimize Low-Temperature Shrinkage Cracking," Research Report 73-1, The Asphalt Institute, January 1973.

10. Novak, E. C., Jr., "Evaluation of a Model for Predicting Transverse Cracking for Flexible Pavements," Research Division Michigan Highway Commission, February 1976.
11. Darter, M. I., E. J. Barenberg and J. S. Sarvan, "Maintenance-Free Life of Heavily Trafficked Flexible Pavements, a paper presented at the 55th Annual Meeting of the Transportation Research Board, January 1976.
12. Little, R. J., L. J. McKenzie and P. G. Dierstein, "The Rehabilitated AASHO Test Road, Part I - Materials and Construction," Interim Report IHR-28, Illinois Department of Transportation, July 1973.
13. "The AASHO Road Test - Report 5 - Pavement Research," Highway Research Board Special Report 61E, 1962.
14. Kallas, B. F., "Asphalt Pavement Temperatures, College Park, Maryland," Highway Research Record 150, 1968.
15. Straub, A. L., H. B. Schenk Jr., and F. E. Przybycien, "Bituminous Pavement Temperature Related to Climate," Highway Research Record 256, 1968.
16. Manz, G. P., "A Study of Temperature Variation in Hot-Mix Asphalt Base, Surface Course and Subgrade," Highway Research Record 150, 1968.
17. Long, R. E., "Relationships Between Control Tests for Asphalt Stabilized Materials," Texas A&M University, PhD Dissertation, May 1971.
18. Ruth, B. E., "Evaluation of Flexible Pavement Systems to Determine Low Temperature Cracking Potential," Report to Florida Department of Transportation from Engineering and Industrial Experiment Station, College of Engineering, University of Florida, August 1975.
19. Witczak, M. W., "Design of Full-Depth Airfield Pavement," Proceedings, Third International Conference on the Structural Design of Asphalt Pavements, 1972.
20. Haliburton, T. A., "Subgrade Moisture Variations," Final Report, Oklahoma Research Program, Project 64-01-3, School of Civil Engineering, Oklahoma State University, August 1970.

21. Dempsey, B. J. "Climatic Effects on Airport Pavement Systems State of the Art," Final Report FAA-RD-75-196, U. S. Army Engineer Waterways Experiment Station, June 1976.
22. Bergan, A. T., and C. L. Monismith, "Characterization of Subgrade Soils in Cold Regions for Pavement Design Purposes," Highway Research Record 431, 1973.
23. Cumberledge, G., Cominsky, R. J. and Bhajandas, A. C., "Moisture Variation Beneath Highway Pavements and the Associated Changes in Subgrade Support," Commonwealth of Pennsylvania, Department of Transportation, 1973.
24. Winfrey, R., and Others, "Economics of the Maximum Limits of Motor Vehicle Dimensions and Weights," Volume 1, Report No. FHWA-RD-73-69, September 1968.
25. Whiteside, R. E., T. Y. Chu, J. C. Cosby, R. L. Whitaker, and R. Winfrey, "Changes in Legal Vehicle Weights and Dimensions, Some Economic Effects on Highways," NCHRP Report 141, 1973.
26. Rauhut, J. B., W. J. Kenis and W. R. Hudson, "Improved Techniques for Prediction of Fatigue Life for Asphalt Concrete Pavements," Transportation Research Record 602, 1976.
27. Van Dijk, W., "Practical Fatigue Characterization of Bituminous Mixes," Paper presented at 1975 Annual Meeting of AAPT, Phoenix, February 1975.
28. Kingham, R. I., "Failure Criteria Developed From AASHTO Road Test Data," Proceedings, Third International Conference on the Structural Design of Asphalt Pavements, London, 1972.
29. "Development of New Design Criteria for Asphalt Concrete Overlays of Flexible Pavements," Austin Research Engineers, Volume 1, Report No. FHWA-RD-75-75, June 1975.
30. Schonfeld, R., "Construction of a Full-Scale Road Experiment as Part of a Unit-Price Contract," Department of Highways, Ontario-Report No. RR119, December 1966.
31. Phang, W. A., "Four Years Experience at the Brampton Test Road," Department of Highways, Ontario Report No. RR153, October 1969.

32. Phang, W. A., "The Effects of Seasonal Strength Variation on the Performance of Selected Base Materials," Department of Highways, Ontario-Report No. IR 39, April 1971.
33. Haas, R. C. G., N. I. Kumel and J. Morris, "Brampton Test Road: An Application of Layer Analysis to Pavement Design," University of Waterloo, Ministry of Transportation and Communications Report No. RR182, November 1972.
34. Kallas, B. F., "The Brampton, Ontario Experimental Base Project," Interim Report, Summary of Asphalt Institute Laboratory Test Results, February 1967.
35. Kallas, B. F., "The Brampton, Ontario Experimental Base Project," Supplement to February 1967 Interim Report, Summary of Asphalt Institute Test Results, September 1967.
36. Morris, J., "The Prediction of Permanent Deformation in Asphalt Concrete Pavements," The Transport Group, Department of Civil Engineering, University of Waterloo, Ontario, Canada, September 1973.
37. Anderson, D. I., J. C. McBride and D. E. Peterson, "Field Verification of the VESYS IIM Structural Subsystem in Utah," Proceedings, Fourth International Conference, Structural Design of Asphalt Pavements, Volume 1, August 1977.
38. Sharma, J., L. L. Smith and B. E. Ruth, "Implementation and Verification of Flexible Pavement Design Methodology," Proceedings, Fourth International Conference, Structural Design of Asphalt Pavements, Volume 1, August 1977.
39. Written data collected previously by Texas Transportation Institute and furnished ARE for this project.
40. Austin Research Engineers Inc, "Asphalt Concrete Overlays of Flexible Pavements, Volume 1 - Development of New Design Criteria, FHWA Report No. FHWA-RD-75-75, August 1975.
41. A statistical summary of current bid data for all highway projects in the State of Texas.
42. Means Cost Data, 1977.

43. McLean, D. B., and C. L. Monismith, "Estimation of Permanent Deformation in Asphalt Concrete Layers Due to Repeated Traffic Loading," Transportation Research Record 510, 1974.
44. Morris, Jack, "The Prediction of Permanent Deformation in Asphalt Concrete Pavements," The Transport Group, Department of Civil Engineering, University of Waterloo, Waterloo, Ontario, Canada, September, 1973.
45. Kenis, W. J., and M. G. Sharma, "Prediction of Rutting and Development of Test Procedures for Permanent Deformation in Asphalt Pavements," paper prepared for presentation in the symposium entitled "Deformation Characteristics of Pavement Sections" held during the 55th Annual Meeting of the TRB, January 1976.
46. Chisolm, E. E. and F. C. Townsend, "Behaviorial Characteristics of Gravelly Sand and Crushed Limestone For Pavement Design," Report No. FAA-RD-75-177, U. S. Army Waterways Experiment Station, September 1976.
47. Raymond, G. P., "Research on Rail Support Improvement," Paper presented at Session 73, Transportation Research Board, January 1977.
48. Monismith, C. L., N. Ogawa and C. R. Freeme, "Permanent Deformation Characteristics of Subgrade Soils in Repeated Loading," draft of a prepared paper.
49. Townsend, F. C., and E. E. Chisolm, "Plastic and Resilient Properties of Heavy Clay Under Repetitive Loadings," Report No. FAA-RD-76-107, U. S. Army Engineer Waterways Experiment Station, Soils and Pavements Laboratory, November 1976.
50. Sharma, J., L. L. Smith and B. E. Ruth, "Implementation and Verification of Flexible Pavement Design Methodology," paper prepared for presentation at the Fourth International Conference on Structural Design of Asphalt Pavements, October 1976.
51. M. G. Sharma, "Prediction of Rutting and the Development of Test Procedures for Permanent Deformation in Asphalt Pavements," paper prepared for presentation at the 55th Annual Transportation Research Board, January 1976.

52. Brown, S. F., A. K. F. Lashine and A. F. L. Hyde, "Repeated Load Triaxial Testing of a Silty Clay," *Geotechnique* 25, No. 1, 95-114, 1975.
53. Fromm, H. J., Phang, W. A., "A Study of Transverse Cracking of Bituminous Pavements," Department of Transportation and Communications, Ontario, Report No. RR176, January 1972.

TE662.A3
no. FHWA-RD-
77-116

U.S

BORROWER

John DeBate

Form DOT F 1720.2
FORMERLY FORM DOT F

FEDERALLY COORDINATED PROGRAM OF HIGHWAY RESEARCH AND DEVELOPMENT (FCP)

The Offices of Research and Development of the Federal Highway Administration are responsible for a broad program of research with resources including its own staff, contract programs, and a Federal-Aid program which is conducted by or through the State highway departments and which also finances the National Cooperative Highway Research Program managed by the Transportation Research Board. The Federally Coordinated Program of Highway Research and Development (FCP) is a carefully selected group of projects aimed at urgent, national problems, which concentrates these resources on these problems to obtain timely solutions. Virtually all of the available funds and staff resources are a part of the FCP, together with as much of the Federal-aid research funds of the States and the NCHRP resources as the States agree to devote to these projects.*

FCP Category Descriptions

1. Improved Highway Design and Operation for Safety

Safety R&D addresses problems connected with the responsibilities of the Federal Highway Administration under the Highway Safety Act and includes investigation of appropriate design standards, roadside hardware, signing, and physical and scientific data for the formulation of improved-safety regulations.

2. Reduction of Traffic Congestion and Improved Operational Efficiency

Traffic R&D is concerned with increasing the operational efficiency of existing highways by advancing technology, by improving designs for existing as well as new facilities, and by keeping the demand-capacity relationship in better balance through traffic management techniques such as bus and carpool preferential treatment, motorist information, and rerouting of traffic.

3. Environmental Considerations in Highway Design, Location, Construction, and Operation

Environmental R&D is directed toward identifying and evaluating highway elements which affect the quality of the human environment. The ultimate goals are reduction of adverse highway and traffic impacts, and protection and enhancement of the environment.

4. Improved Materials Utilization and Durability

Materials R&D is concerned with expanding the knowledge of materials properties and technology to fully utilize available naturally occurring materials, to develop extender or substitute materials for materials in short supply, and to devise procedures for converting industrial and other wastes into useful highway products. These activities are all directed toward the common goals of lowering the cost of highway construction and extending the period of maintenance-free operation.

5. Improved Design to Reduce Costs, Extend Life Expectancy, and Insure Structural Safety

Structural R&D is concerned with furthering the latest technological advances in structural designs, fabrication processes, and construction techniques, to provide safe, efficient highways at reasonable cost.

6. Prototype Development and Implementation of Research

This category is concerned with developing and transferring research and technology into practice, or, as it has been commonly identified, "technology transfer."

7. Improved Technology for Highway Maintenance

Maintenance R&D objectives include the development and application of new technology to improve management, to augment the utilization of resources, and to increase operational efficiency and safety in the maintenance of highway facilities.

* The complete 7-volume official statement of the FCP is available from the National Technical Information Service (NTIS), Springfield, Virginia 22161 (Order No. PB 242057, price \$45 postpaid). Single copies of the introductory volume are obtainable without charge from Program Analysis (HRD-2), Offices of Research and Development, Federal Highway Administration, Washington, D.C. 20590.

DOT LIBRARY



00055701

